

For Reference

NOT TO BE TAKEN FROM THIS ROOM

For Reference

NOT TO BE TAKEN FROM THIS ROOM

Ex LIBRIS
UNIVERSITATIS
ALBERTAENSIS





Digitized by the Internet Archive
in 2019 with funding from
University of Alberta Libraries

<https://archive.org/details/James1963>

112
63
29

THE UNIVERSITY OF ALBERTA

AN EXPERIMENTAL DETERMINATION OF
STRESS CONCENTRATIONS AROUND CIRCULAR HOLES IN
CYLINDRICAL PRESSURE VESSELS

by

TRENT A. JAMES, B. Sc. (Alberta)

A THESIS

SUBMITTED TO THE FACULTY OF GRADUATE STUDIES
IN PARTIAL FULFILMENT OF THE REQUIREMENTS
FOR THE DEGREE OF
MASTER OF SCIENCE

DEPARTMENT OF MECHANICAL ENGINEERING

EDMONTON, ALBERTA

FEBRUARY, 1963.

UNIVERSITY OF ALBERTA
FACULTY OF GRADUATE STUDIES

The undersigned certify that they have read, and recommend to the Faculty of Graduate Studies for acceptance, a thesis entitled, "An Experimental Determination of Stress Concentrations Around Circular Holes in Cylindrical Pressure Vessels", submitted by Trent A. James in partial fulfilment of the requirements for the degree of Master of Science.

ABSTRACT

The purpose of the experimental work in this thesis is to observe the increase in stress introduced by an unreinforced circular hole in the wall of a cylinder subjected to internal pressure. From the stresses determined using wire resistance strain gauges, a set of curves showing stress concentration factors around the hole are presented.

The results of this investigation indicate that the critical stress due to the hole is not always at the point round by proceeding in the axial direction from the hole, and that flat plate theory is not a good basis for analysis unless the diameter of the hole is very small compared to the diameter of the cylinder.

Experimental consideration of the stresses near the hole showed that the disturbed area around the hole is of a local character, although not as small as commonly assumed.

ACKNOWLEDGMENTS

The author wishes to extend his thanks and appreciation to Dr. G. Ford for supervising this thesis.

Thanks are also due to the staff of the Department of Mechanical Engineering for all the assistance and encouragement given during the execution of this investigation.

The author takes this opportunity to express his gratitude to his wife, Jean, for her co-operation during the preparation and typing of this report.

NOTATION


σ_{θ}	=	Hoop Stress
σ_z	=	Longitudinal Stress
σ_r	=	Radial Stress
E	=	Modulus of Elasticity
μ	=	Poisson's Ratio
e_{θ}	=	Hoop Strain
e_z	=	Longitudinal Strain
e_r	=	Radial Strain
P	=	Pressure inside cylinder
a	=	internal radius of cylinder
b	=	external radius of cylinder
Stress Concentration Factor	=	$\frac{\text{Stress Tangential to Hole}}{\text{Hoop Stress in Undisturbed Area of Cylinder}}$
Points A and B	=	

TABLE OF CONTENTS

CHAPTER	PAGE
1. INTRODUCTION.....	1
2. OBJECT AND SCOPE.....	7
3. THEORY.....	9
4. TEST SPECIMENS.....	16
5. APPARATUS AND INSTRUMENTATION.....	25
6. EXPERIMENTAL PROCEDURE.....	31
7. EXPERIMENTAL RESULTS AND DISCUSSION...	33
Poisson's Ratio.....	33
Strain-Pressure Diagrams.....	46
Stress and Strain Approaching Point A.....	89
Stress and Strain Approaching Point B.....	116
Stress Concentration Factor Curves.....	141
8. CONCLUSIONS.....	150
9. BIBLIOGRAPHY.....	152
 APPENDIX	
A. Typical Calculation.....	154

LIST OF TABLES

TABLE		PAGE
1	Poisson's Ratios.....	53
2	Typical Calculation of Stress Approaching Point A.....	157
3	Typical Calculation of Stress Approaching Point B.....	158

LIST OF FIGURES

FIGURE		PAGE
1.	Deflections as Calculated by Vainberg and Siniavskii.....	6
2.	Test Cylinder Dimensions.....	19
3.	View of Pipe Support Used to Pull Plug Into Hole.....	20
4.	Drawing of 1/4 inch Plug.....	21
5.	Drawing of 1/2 inch Plug.....	22
6.	Drawing of 3/4 inch Plug.....	23
7.	Close-up of 3/4 inch Plug.....	24
8.	General View of Test Equipment.....	27
9.	Pressure Gauge Calibration Curve.....	28
10.	View of Gauges Around the Hole.....	29
11.	View of Test Cylinder.....	30
12.	Positioning of Control Gauges 1/8 inch Wall Thickness.....	35
13.	Axial Strain vs. Hoop Strain 1/8 inch Wall Thickness.....	36
14.	Positioning of Control Gauges 1/4 inch Wall Thickness.....	37

FIGURE	PAGE
15., 16. Axial Strain vs. Hoop Strain 1/4 inch Wall	
Thickness.....	38, 39
17. Positioning of Gauges 3/8 inch Wall	
Thickness.....	40
18., 19. Axial Strain vs. Hoop Strain 3/8 inch Wall	
Thickness.....	41, 42
20. Positioning of Gauges 1/2 inch Wall	
Thickness.....	43
21., 22. Axial Strain vs. Hoop Strain 1/2 inch Wall	
Thickness.....	44, 45
23. Positioning of Gauges 1/8 inch Wall Thickness	
1/4 inch Hole.....	47
24.-26. Strain vs. Pressure 1/8 inch Wall Thickness	
1/4 inch Hole.....	48-50
27. Positioning of Gauges 1/8 inch Wall Thickness	
1/2 inch Hole.....	51
28., 29. Strain vs. Pressure 1/8 inch Wall Thickness	
1/2 inch Hole.....	52-53
30. Positioning of Gauges 1/8 inch Wall Thickness	
3/4 inch Hole.....	54

FIGURE	PAGE
31.-34. Strain vs. Pressure 1/8 inch Wall Thickness	
3/4 inch Hole.....	55-58
35. Positioning of Gauges 1/4 inch Wall Thickness	
1/4 inch Hole.....	59
36.-38. Strain vs. Pressure 1/4 inch Wall Thickness	
1/4 inch Hole.....	60-62
39. Positioning of Gauges 1/4 inch Wall Thickness	
1/2 inch Hole.....	63
40., 41. Strain vs. Pressure 1/4 inch Wall Thickness	
1/2 inch Hole.....	64-65
42. Positioning of Gauges 1/4 inch Wall Thickness	
3/4 inch Hole.....	66
43., 44. Strain vs. Pressure 1/4 inch Wall Thickness	
3/4 inch Hole.....	67-68
45. Positioning of Gauges 3/8 inch Wall Thickness	
1/4 inch Hole.....	69
46., 47. Strain vs. Pressure 3/8 inch Wall Thickness	
1/4 inch Hole.....	70, 71
48. Positioning of Gauges 3/8 inch Wall Thickness	
1/2 inch Hole.....	72

FIGURE	PAGE
49., 50	Strain vs. Pressure $3/8$ inch Wall Thickness
	$1/2$ inch Hole..... 73, 74
51.	Positioning of Gauges $3/8$ inch Wall Thickness
	$3/4$ inch Hole..... 75
52.-54.	Strain vs. Pressure $3/8$ inch Wall Thickness
	$3/4$ inch Hole..... 76-78
55.	Positioning of Gauges $1/2$ inch Wall Thickness
	$1/4$ inch Hole..... 79
56., 57.	Strain vs. Pressure $1/2$ inch Wall Thickness
	$1/4$ inch Hole..... 80, 81
58.	Positioning of Gauges $1/2$ inch Wall Thickness
	$1/2$ inch Hole..... 82
59., 60.	Strain vs. Pressure $1/2$ inch Wall Thickness
	$1/2$ inch Hole..... 83-85
61.	Positioning of Gauges $1/2$ inch Wall Thickness
	$3/4$ inch Hole..... 86
62., 63.	Strain vs. Pressure $1/2$ inch Wall Thickness
	$3/4$ inch Hole..... 87, 88
64.	Strains Approaching Point A $1/8$ inch Wall
	Thickness $1/4$ inch Hole.... 92

FIGURE		PAGE
65.	Strains Approaching Point A $1/8$ inch Wall Thickness $1/2$ inch Hole.....	93
66.	Strains Approaching Point A $1/8$ inch Wall Thickness $3/4$ inch Hole.....	94
67.	Strains Approaching Point A $1/4$ inch Wall Thickness $1/4$ inch Hole.....	95
68.	Strains Approaching Point A $1/4$ inch Wall Thickness $1/2$ inch Hole.....	96
69.	Strains Approaching Point A $1/4$ inch Wall Thickness $3/4$ inch Hole.....	97
70.	Strains Approaching Point A $3/8$ inch Wall Thickness $1/4$ inch Hole.....	98
71.	Strains Approaching Point A $3/8$ inch Wall Thickness $1/2$ inch Hole.....	99
72.	Strains Approaching Point A $3/8$ inch Wall Thickness $3/4$ inch Hole.....	100
73.	Strains Approaching Point A $1/2$ inch Wall Thickness $1/4$ inch Hole.....	101
74.	Strains Approaching Point A $1/2$ inch Wall Thickness $1/2$ inch Hole.....	102

FIGURE		PAGE
75.	Strains Approaching Point A $1/2$ inch Wall Thickness $3/4$ inch Hole.....	103
76.	Stress Approaching Point A $1/8$ inch Wall Thickness $1/4$ inch Hole.....	104
77.	Stress Approaching Point A $1/8$ inch Wall Thickness $1/2$ inch Hole.....	105
78.	Stress Approaching Point A $1/8$ inch Wall Thickness $3/4$ inch Hole.....	106
79.	Stress Approaching Point A $1/4$ inch Wall Thickness $1/4$ inch Hole.....	107
80.	Stress Approaching Point A $1/4$ inch Wall Thickness $1/2$ inch Hole.....	108
81.	Stress Approaching Point A $1/4$ inch Wall Thickness $3/4$ inch Hole.....	109
82.	Stress Approaching Point A $3/8$ inch Wall Thickness $1/4$ inch Hole.....	110
83.	Stress Approaching Point A $3/8$ inch Wall Thickness $1/2$ inch Hole.....	111
84.	Stress Approaching Point A $3/8$ inch Wall Thickness $3/4$ inch Hole.....	112

FIGURE		PAGE
85.	Stress Approaching Point A $1/2$ inch Wall Thickness $1/4$ inch Hole.....	113
86.	Stress Approaching Point A $1/2$ inch Wall Thickness $1/2$ inch Hole.....	114
87.	Stress Approaching Point A $1/2$ inch Wall Thickness $3/4$ inch Hole.....	115
88.	Strains Approaching Point B $1/8$ inch Wall Thickness $1/4$ inch Hole.....	117
89.	Strains Approaching Point B $1/8$ inch Wall Thickness $1/2$ inch Hole.....	118
90.	Strains Approaching Point B $1/8$ inch Wall Thickness $3/4$ inch Hole.....	119
91.	Strains Approaching Point B $1/4$ inch Wall Thickness $1/4$ inch Hole.....	120
92.	Strains Approaching Point B $1/4$ inch Wall Thickness $1/2$ inch Hole.....	121
93.	Strains Approaching Point B $1/4$ inch Wall Thickness $3/4$ inch Hole.....	122
94.	Strains Approaching Point B $3/8$ inch Wall Thickness $1/4$ inch Hole.....	123

FIGURE		PAGE
95.	Strains Approaching Point B $\frac{3}{8}$ inch Wall	
	Thickness $\frac{1}{2}$ inch Hole....	124
96.	Strains Approaching Point B $\frac{3}{8}$ inch Wall	
	Thickness $\frac{3}{4}$ inch Hole....	125
97.	Strains Approaching Point B $\frac{1}{2}$ inch Wall	
	Thickness $\frac{1}{4}$ inch Hole....	126
98.	Strains Approaching Point B $\frac{1}{2}$ inch Wall	
	Thickness $\frac{1}{2}$ inch Hole....	127
99.	Strains Approaching Point B $\frac{1}{2}$ inch Wall	
	Thickness $\frac{3}{4}$ inch Hole....	128
100.	Stress Approaching Point B $\frac{1}{8}$ inch Wall	
	Thickness $\frac{1}{4}$ inch Hole....	129
101.	Stress Approaching Point B $\frac{1}{8}$ inch Wall	
	Thickness $\frac{1}{2}$ inch Hole....	130
102.	Stress Approaching Point B $\frac{1}{8}$ inch Wall	
	Thickness $\frac{3}{4}$ inch Hole....	131
103.	Stress Approaching Point B $\frac{1}{4}$ inch Wall	
	Thickness $\frac{1}{4}$ inch Hole....	132
104.	Stress Approaching Point B $\frac{1}{4}$ inch Wall	
	Thickness $\frac{1}{2}$ inch Hole....	133

FIGURE		PAGE
105.	Stress Approaching Point B $1/4$ inch Wall	
	Thickness $3/4$ inch Hole.....	134
106.	Stress Approaching Point B $3/8$ inch Wall	
	Thickness $1/4$ inch Hole.....	135
107.	Stress Approaching Point B $3/8$ inch Wall	
	Thickness $1/2$ inch Hole.....	136
108.	Stress Approaching Point B $3/8$ inch Wall	
	Thickness $3/4$ inch Hole.....	137
109.	Stress Approaching Point B $1/2$ inch Wall	
	Thickness $1/4$ inch Hole.....	138
110.	Stress Approaching Point B $1/2$ inch Wall	
	Thickness $1/2$ inch Hole.....	139
111.	Stress Approaching Point B $1/2$ inch Wall	
	Thickness $3/4$ inch Hole.....	140
112.	Stress Concentration Factors at Point A.....	143
113.	Stress Concentration Factors at Point B.....	144
114.	Theoretical Stress Concentration Factors at	
	Point B.....	147

CHAPTER 1

INTRODUCTION

The problem of stress distribution around holes in cylinders has been the subject of a comparatively small number of papers. The solution of the problem for circular holes in large plates under tension or compression first obtained by G. Kirsch in 1898 is treated by S. P. Timoshenko and J. N. Goodier¹. This solution is applicable to cylindrical shells with holes, provided the diameter of the hole is very small compared to the bore of the cylinder and the wall thickness is small compared to the diameter of the cylinder. In this case the variation of hoop stress in the radial direction and the effect of curvature may be neglected, so that all points on the middle surface of the cylinder are assumed to have the same radial deflection. The problem may then be considered as two dimensional and the stress field around the hole the same as around a circular hole in an infinite plate under biaxial tension.

One of the first attempts which allows for a curvature effect in a thin cylinder subjected to direct loadings was given by A. I. Lurie² in 1947. Unfortunately this article

was in a Russian publication which could not be obtained. However, a short résumé of the work in this paper was given in a publication by D. S. Houghton³. Lurie, in his analysis of circular holes in curved shells, neglected the displacements tangential to the surface medium when calculating the change in curvature of the shell. The change in curvature was then expressed only by the radial component of the displacement. A solution for the tangential stress around the hole was given which consists of the flat plate solution plus a curvature correction term.

Houghton compared the curvature effect predicted by Lurie with experimental results conducted on unreinforced holes using a photoelastic technique. The cylinder which was tested had a side hole to bore diameter ratio of 0.22 and a wall thickness to diameter ratio of 0.028. For this geometrical configuration flat plate theory was found to have closer agreement with experimental results than calculations using a curvature correction effect as given by Lurie.

The flat plate theory was extended to the analysis of holes in thick cylinders by J. H. Faupel and D. B. Harris⁴ in 1957. Experimental results using both photoelastic and strain

gauge techniques were presented in this paper. The ratio of external to internal diameter of the cylinders tested ranged from 1.5 to 4.0, and the ratio of hole diameter to bore diameter varied from 0.125 to 1.0. The stress concentration factors calculated from experimental results varied between 1.70 and 3.02. These experiments only considered the variation of hoop stress approaching the hole in a direction parallel to the longitudinal axis of the cylinder. A considerable amount of discrepancy was noted between experimental results and theoretical predictions.

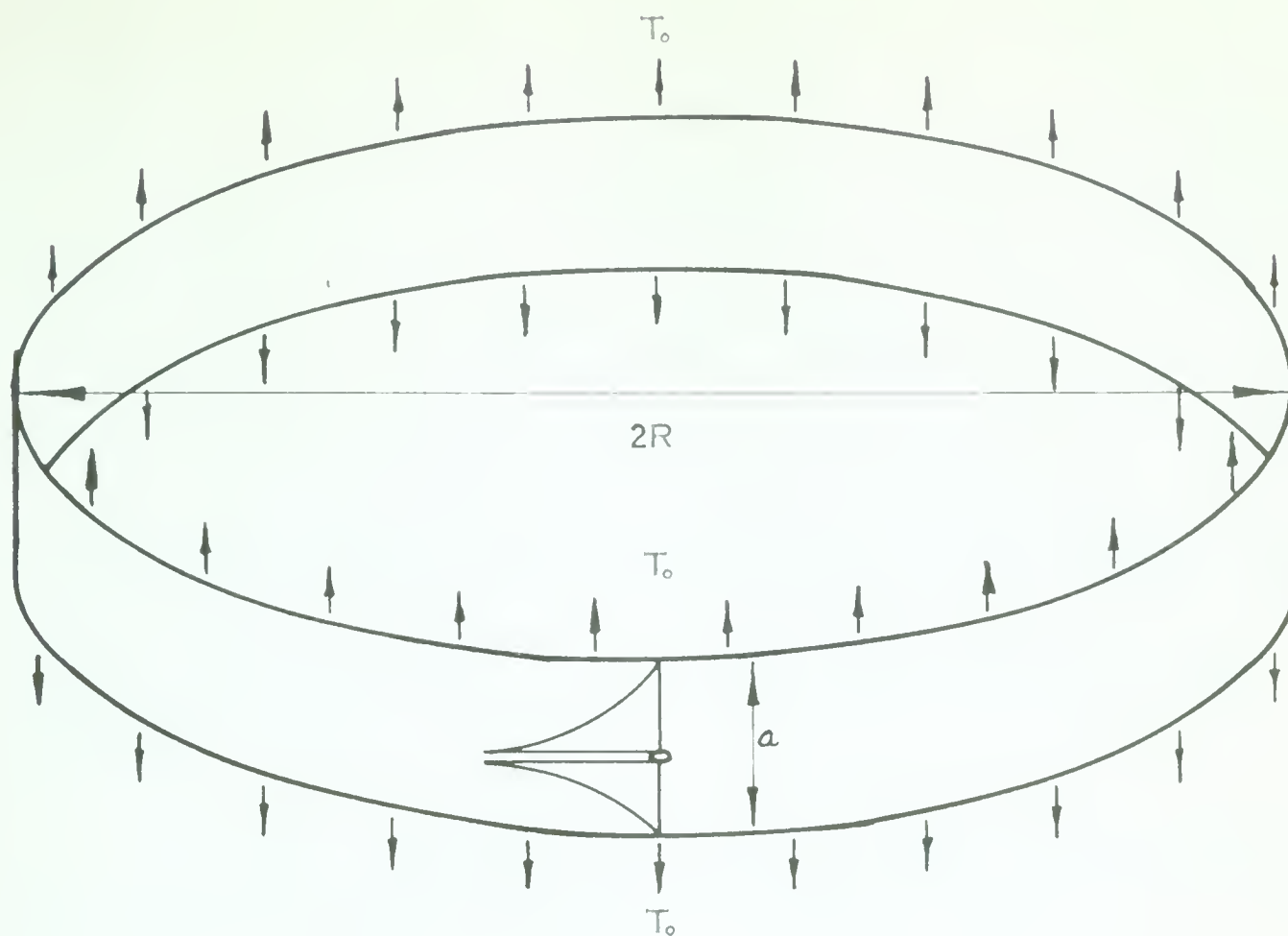
An experimental investigation of the stress produced in a thick-walled cylinder by a radially penetrating hole when loaded by an internal pressure was presented by M. A. Loshkarev⁵ in 1958. This also was a Russian publication which could not be obtained, but a review of the paper⁶ stated that, "The investigations have resulted in establishing that, with increasing wall thickness as well as increasing diameter of the radial hole, the stress concentration also increases. The results presented refer to the case when the pressure acts on the internal surface of the cylinder, and on the radial hole, as well as on the surfaces of the covers closing the cylinder at the ends."

A photoelastic investigation of the stresses near reinforced openings in pressure vessels was conducted by C. E. Taylor and J. W. Schweiker⁷ in 1959. Stresses in the region of cylindrical outlets projecting from thin walled cylindrical and spherical vessels were considered. The vessels were reinforced around the branch pipe connections. This investigation indicated that outlets in spherical shells are less critical than outlets in cylindrical shells of the same dimensions.

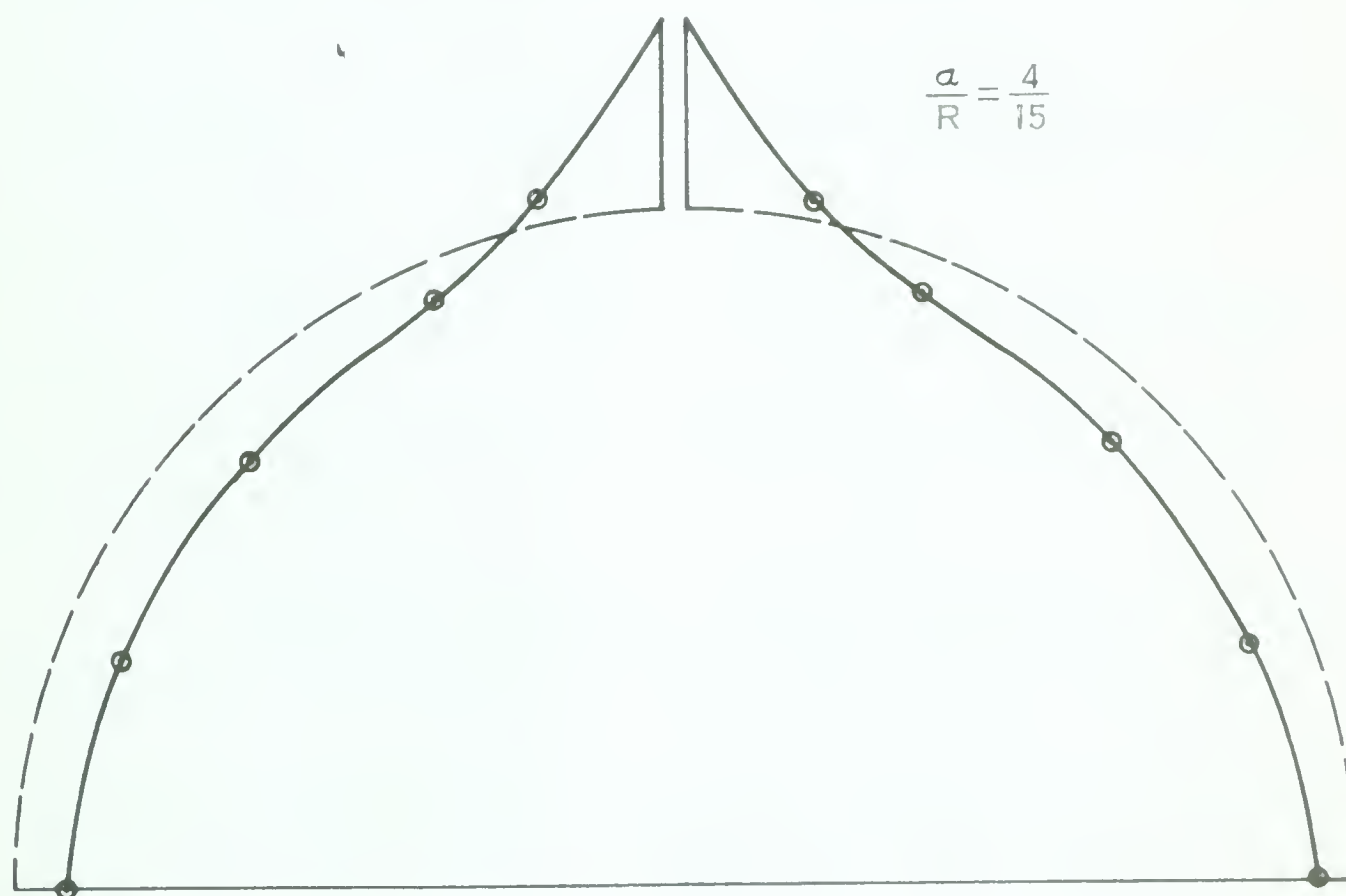
The stress distribution in a shell with a hole of arbitrary shape has been discussed by G. N. Savin⁸ (1961). This is a mathematical analysis of the problem and the solution has been left in differential form. The study considers a membrane state of stress and is not directly applicable to this investigation. Experiments aimed at finding the extent of the region affected by the hole were conducted using rubber discs glued to rubber membranes. For convenient observation these shells were inscribed in their undeformed state with a square net of lines. This work indicated that the disturbed area was of a local character extending not more than one hole diameter from the edge of the hole.

The methods of potential theory were applied to the

analysis of thin shells with holes by D. V. Vainberg and A. L. Siniavskii⁹ (1961). This paper considered specifically the problem of a cylindrical shell with an elliptical hole subjected to a uniform tensile force in the axial direction. A method of computing deflections of the shell was given and the numerical work was executed for a cylinder with a wall thickness to diameter ratio of $1/60$, having an elliptical hole with a minor axis to major axis ratio of $1/2$. The ratio of the major axis of the ellipse to the diameter of the cylinder was $1/30$. Radial deflections of the cylinder due to the presence of the hole calculated using this method were found to extend a considerable distance from the hole, as shown in Fig. 1.



RADIAL DEFLECTIONS IN LONGITUDINAL DIRECTION



RADIAL DEFLECTIONS IN CIRCUMFERENTIAL DIRECTION

DEFLECTIONS AS CALCULATED BY D. V. VAINBERG AND
A. L. SINIAVSKII

FIGURE 1.

CHAPTER 2

OBJECT AND SCOPE

The primary object of this investigation was to observe the increase in stress introduced by an unreinforced circular hole in the wall of a cylinder subjected to internal pressure.

Four cylinders were tested, ranging in dimension from a wall thickness to internal diameter ratio of $1/24$ to $1/6$. This series of tests extended from the "thin cylinder" area through the transition to the "thick cylinder" field. In this case a "thin cylinder" is defined as one which has a wall thickness to internal diameter ratio of less than $1/10$.

Three sizes of hole were tested for each cylinder. In all cylinders the diameter of hole to bore diameter ratios were $1/12$, $1/6$, and $1/4$.

Boundary conditions at the hole consisted of a shear loading around the perimeter of the hole at the cylinder bore due to the force exerted by the plug and a uniform fluid pressure acting on the sides of the hole up to the line of intersection of the O-ring with the cylinder wall.

All strain measurements were taken on the outside surface of the cylinders, and therefore, the results obtained are directly applicable only to stresses on the outside surface of the cylinder near the edge of the hole.

CHAPTER 3

THEORY

The use of strain gauge techniques for experimental investigations reveals the strains sustained by the specimen at the points where the strain gauges are placed. In order to describe the stresses in the specimens, the relations between the components of stress and the components of strain must be found. The expressions for these relationships are developed using Hooke's law and Poisson's effect.

Consider an elemental rectangular parallelepiped from the wall of a cylinder subjected to three stresses σ_θ , σ_z , and σ_r in the hoop, longitudinal and radial directions respectively. The expressions for strain may be written for each one of these stresses separately and superposition used to find the strains due to the combined stresses.

The magnitude of the hoop strain due to σ_θ is given by Hooke's law:
$$e_\theta = \frac{\sigma_\theta}{E}$$
 where E is the modulus of elasticity.

Extension of the element in the hoop direction is

accompanied by lateral contractions in the longitudinal and radial directions: $e_z = -\mu \frac{\sigma_\theta}{E}$ $e_r = -\mu \frac{\sigma_\theta}{E}$

where μ is Poisson's ratio.

The strains due to σ_z and σ_r may be expressed in a similar manner. By superimposing the strains produced by the three stresses, the strains due to the combined stresses are found to be:

$$\begin{aligned} e_\theta &= \frac{1}{E} [\sigma_\theta - \mu(\sigma_z + \sigma_r)] \\ e_z &= \frac{1}{E} [\sigma_z - \mu(\sigma_\theta + \sigma_r)] \dots\dots\dots 1 \\ e_r &= \frac{1}{E} [\sigma_r - \mu(\sigma_\theta + \sigma_z)] \end{aligned}$$

At the outside surface of the cylinder the stress in the radial direction is zero and the expressions for strain reduce to:

$$\begin{aligned} e_\theta &= \frac{1}{E} (\sigma_\theta - \mu\sigma_z) \\ e_z &= \frac{1}{E} (\sigma_z - \mu\sigma_\theta) \dots\dots\dots 2 \\ e_r &= -\frac{\mu}{E} (\sigma_\theta + \sigma_z) \end{aligned}$$

The expressions for hoop stress and longitudinal stress in terms of hoop strain and longitudinal strain at the outside surface are found from Eqns. 2.

$$\begin{aligned} \sigma_\theta &= E \frac{(e_\theta + \mu e_z)}{(1 - \mu^2)} \dots\dots\dots 3 \\ \sigma_z &= E \frac{(e_z + \mu e_\theta)}{(1 - \mu^2)} \end{aligned}$$

Eqns. 3 were used to compute the hoop stress σ_θ and the longitudinal stress σ_z from the observed strains as measured by wire resistance strain gauges.

Similarly the average stresses at the undisturbed surface of the cylinder were derived from Eqns. 3 using the strains measured on the cylinder at a considerable distance from the hole. A check on these stresses was made by calculating them using the thick cylinder theory. This check showed both methods to be in agreement and verified the experimental technique. Thus a comparison of stress near the hole with the stress in the undisturbed area of the cylinder did not depend upon the modulus of elasticity used or the accuracy of theoretical solutions. A numerical value for the modulus of elasticity was used to calculate stresses in the cylinder, however, this number cancelled out when stresses were compared in the calculation of the stress concentration factor.

From Eqns. 3 it is noted that the magnitude of the stress calculated from measured strains is dependent upon Poisson's ratio, μ , for the material tested. Poisson's ratio may be calculated from the relationship between longitudinal strain and hoop strain measured on the undisturbed area of the

cylinder.

The solution for the stress distribution in a hollow cylinder submitted to uniform pressure on the inner and outer surfaces was first derived by Lamé¹⁰ in 1852. From this analysis the hoop stress at the outside surface of a cylinder subjected to internal pressure P is given by:

$$\sigma_{\theta} = \frac{2 a^2 P}{(b^2 - a^2)} \dots\dots\dots 4$$

where a and b are the internal and external radii of the cylinder respectively.

The force exerted by the pressure acting on the ends of the closed cylindrical vessel is balanced by a stress in the longitudinal direction. This stress is assumed to be distributed uniformly through the wall of the cylinder.

From these considerations the longitudinal stress is found to be:

$$\sigma_z = \frac{\pi a^2 P}{\pi b^2 - \pi a^2} = \frac{a^2 P}{b^2 - a^2} \dots\dots\dots 5$$

or 1/2 the hoop stress.

Using $\sigma_{\theta} = 2\sigma_z$ we may calculate strains at the surface in the hoop and longitudinal directions from Eqns. 2.

$$e_{\theta} = \frac{1}{E} (\sigma_{\theta} - \mu \sigma_z) = \frac{\sigma_z}{E} (2 - \mu) \quad \dots\dots\dots 6$$

$$e_z = \frac{1}{E} (\sigma_z - \mu \sigma_{\theta}) = \frac{\sigma_z}{E} (1 - 2\mu)$$

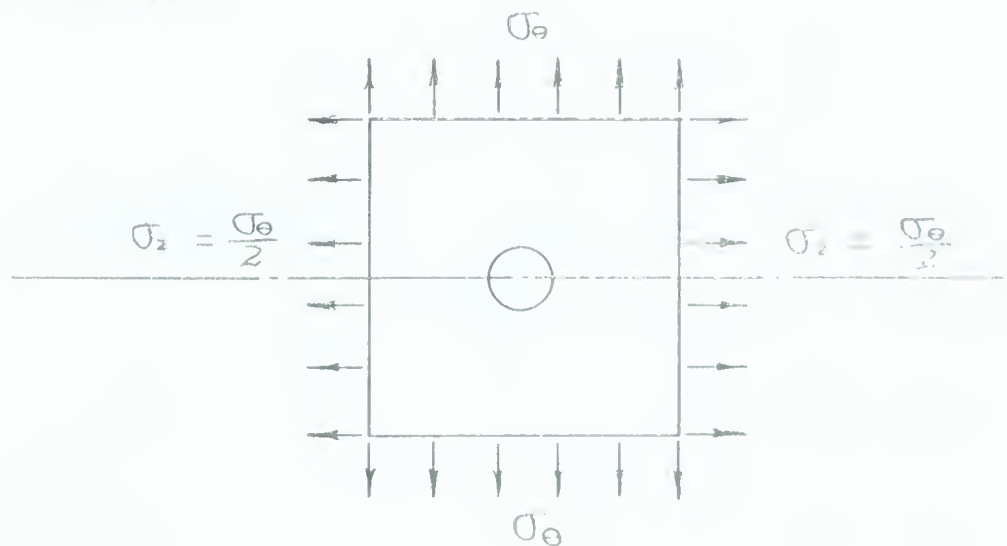
Combining the two above equations we obtain:

$$\frac{e_z}{e_{\theta}} = \frac{1 - 2\mu}{2 - \mu} \quad \dots\dots\dots 7$$

From experimental results the longitudinal strain on the outer surface of the cylinder was plotted vs. hoop strain at the same point. Using the slope of this line, Poisson's ratio was calculated using Eqn. 7.

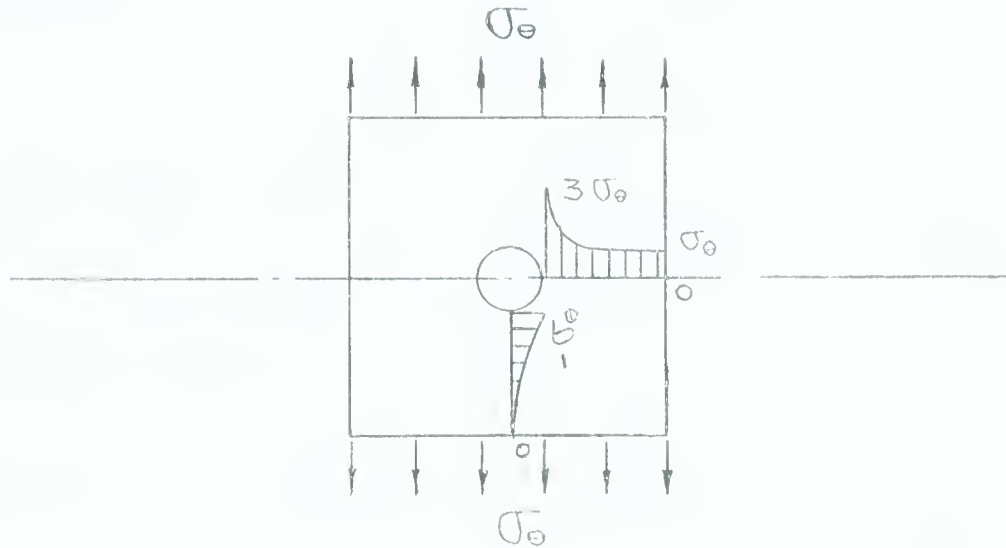
Flat plate theory may be used to solve for the stresses around a circular hole in a cylindrical shell, if the diameter of the hole is very small compared to the diameter of the cylinder.

The drawing below represents a shell submitted to uniform tensions of magnitudes σ_{θ} in the hoop direction and σ_z in the axial direction.



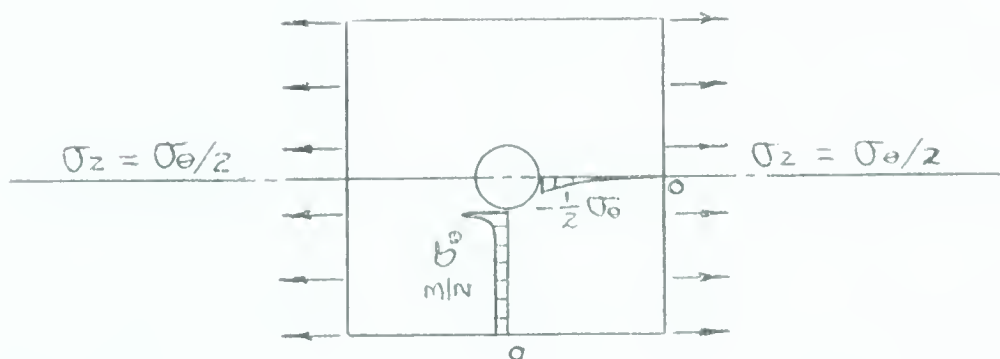
If a small hole is introduced in the middle of the shell the stress distribution will be changed, and may be analyzed by considering the two tensions separately and using superposition to find the effect of the combined stresses.

Using the flat plate solution described by S. P. Timoshenko and J. N. Goodier¹ the stresses due to σ_θ on two cross sections passing through the centre of the hole are as shown below.

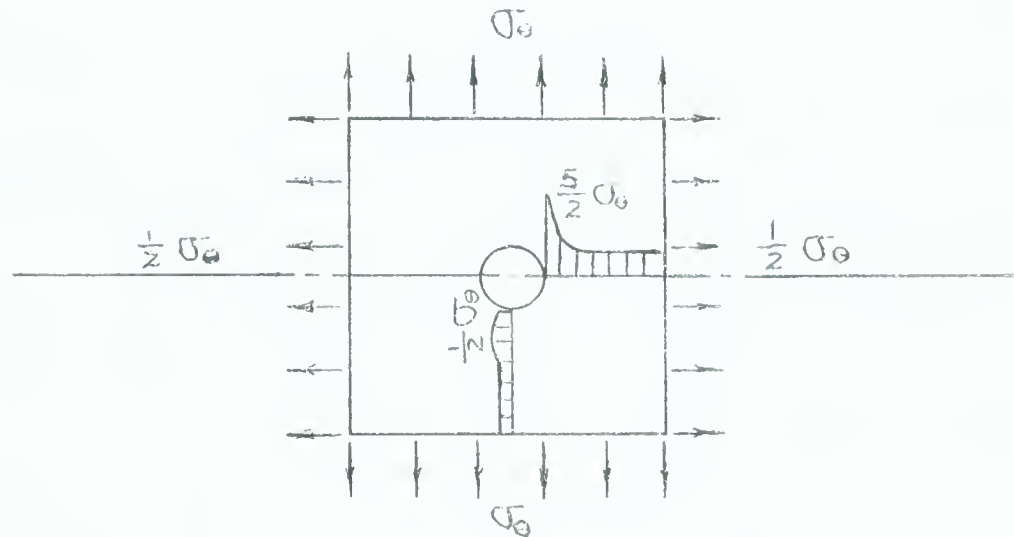


Similarly the stresses around the hole due to

$\sigma_z = \frac{1}{2} \sigma_\theta$ are:



Superimposing the stresses around the hole due to these two tensions the solution for the biaxially loaded plate is:



As shown in the figure the effect of the hole is of a very localized character, the stresses reducing to within 5 percent of the stresses in the undisturbed area at a distance of 2 hole diameters from the edge of the hole.

CHAPTER 4

TEST SPECIMENS

Four cylinders, all with the same internal diameter and progressively increasing wall thicknesses were used for this investigation. All cylinders had a nominal internal diameter of 3 inches with nominal wall thicknesses of 1/8 inch, 1/4 inch, 3/8 inch, and 1/2 inch. The test specimens were 15 inches in length and had plates of sufficient thickness to withstand the pressure applied to the cylinder, welded on both ends. Exact dimensions of the cylinders are shown in Fig. 2.

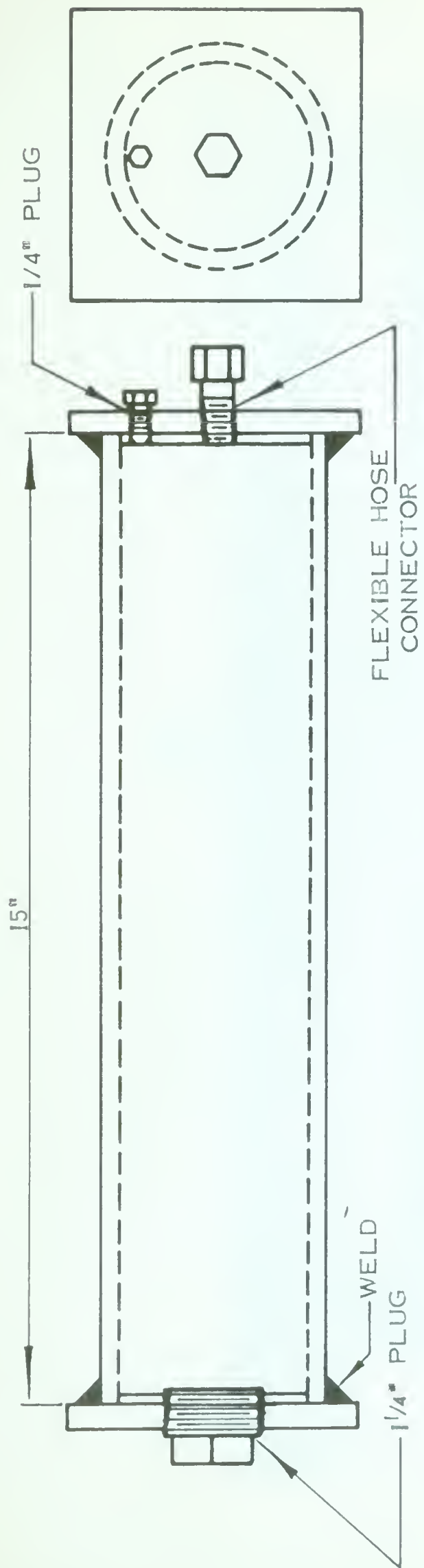
The rough form of the specimens was composed of seamless steel mechanical tubing having a slightly heavier wall thickness than required for the finished cylinder. The mild steel in this tubing was of A.I.S.I. specification MT1015.

The first step in the preparation of the specimens was a stress relieving operation which consisted of heating the cylinders to a temperature of 1000°F. and holding this temperature for a period of half an hour. The heat supply for the oven was then turned off and the cylinders were allowed to cool with the oven.

After each cylinder had been machined and the end plates welded on, a hole was drilled and reamed to 1/4 inch in diameter midway along the length of the cylinder, with the axis of the cylindrical hole intersecting the axis of the cylinder. When this hole had been tested, it was drilled and reamed to 1/2 inch in diameter. Similarly, a 3/4 inch hole was located concentric with the first two. The reaming operation left the holes with a tolerance on the diameter of ± 0.001 inches.

Brass plugs with O-ring seals were used to confine the hydraulic fluid to the inside of the cylinders. Three plugs were made, of 1/4 inch, 1/2 inch, and 3/4 inch diameters. The same plugs were used for all the cylinders tested. Each plug was constructed in such a way as to be inserted from the inside of the cylinder, with a shoulder which came in contact with the inner surface preventing the plug from being pushed through the hole. For the 1/4 inch holes the brass shoulder was allowed to rest against the cylinder, but for the 1/2 inch and 3/4 inch plugs a lead washer was inserted between the plug and the inside surface of the cylinder. The lead washers were moulded to the curvature of the tube by pulling the plug outward with a bolt through a pipe support as shown in Fig. 3. After the lead

washer had been deformed sufficiently, the plug was removed and the washer machined to the diameter of the shoulder of the plug. For a pictorial description of the plugs see Figs. 4 to 7.



TEST CYLINDER DIMENSIONS				
CYLINDER NUMBER	INSIDE DIAMETER INCHES	OUTSIDE DIAMETER INCHES	END PLATE DIMENSIONS INCHES	WELD SIZE INCHES
1	2.978	3.224	4 X 4 X 1/2	1/4
2	3.020	3.479	4 1/2 X 4 1/2 X 5/8	1/2
3	2.993	3.744	5 X 5 X 3/4	5/8
4	2.993	3.993	5 1/2 X 5 1/2 X 1	3/4

FIGURE 2.

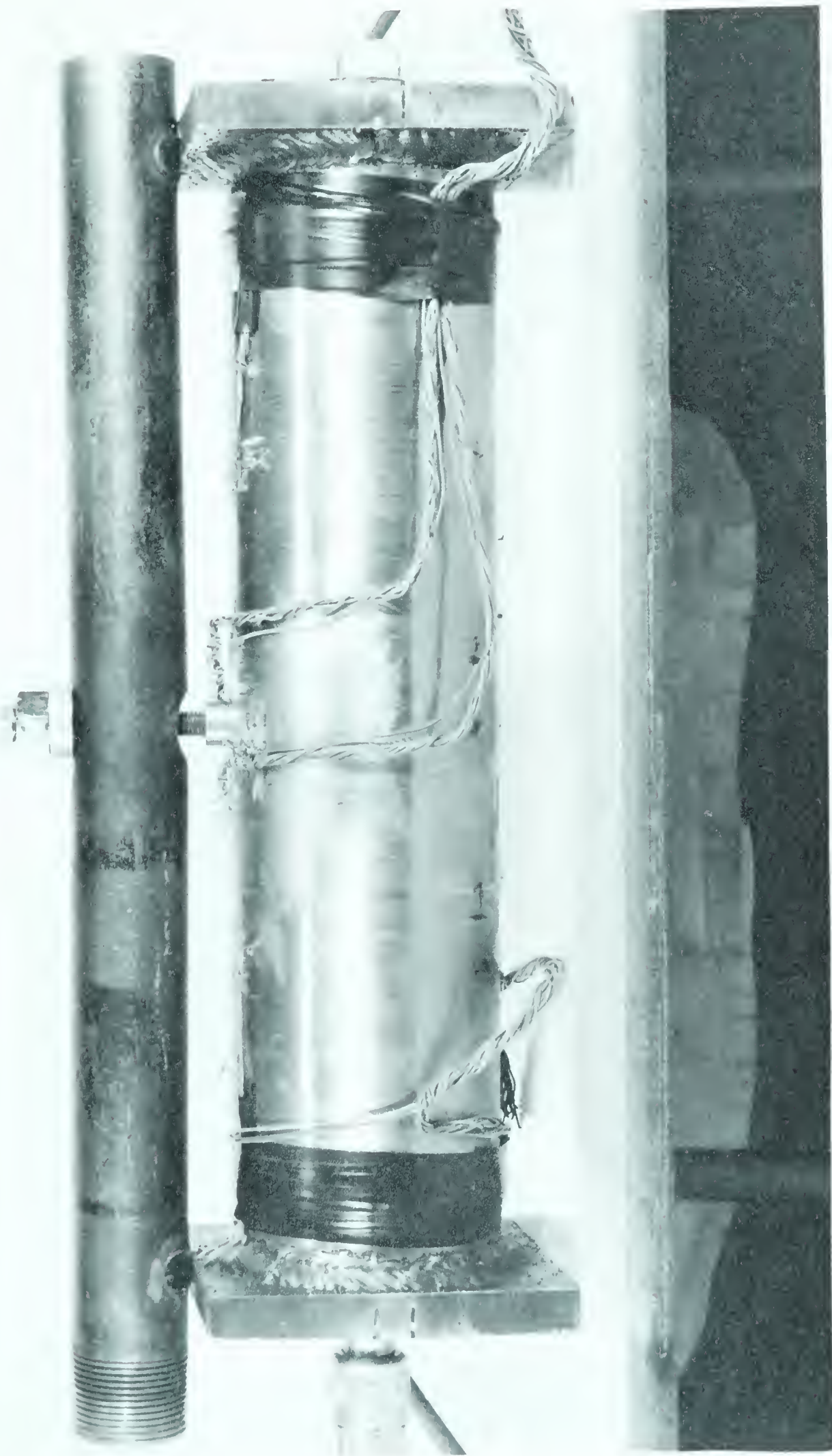


FIGURE 3. VIEW OF PIPE SUPPORT USED TO PULL PLUG INTO PLACE

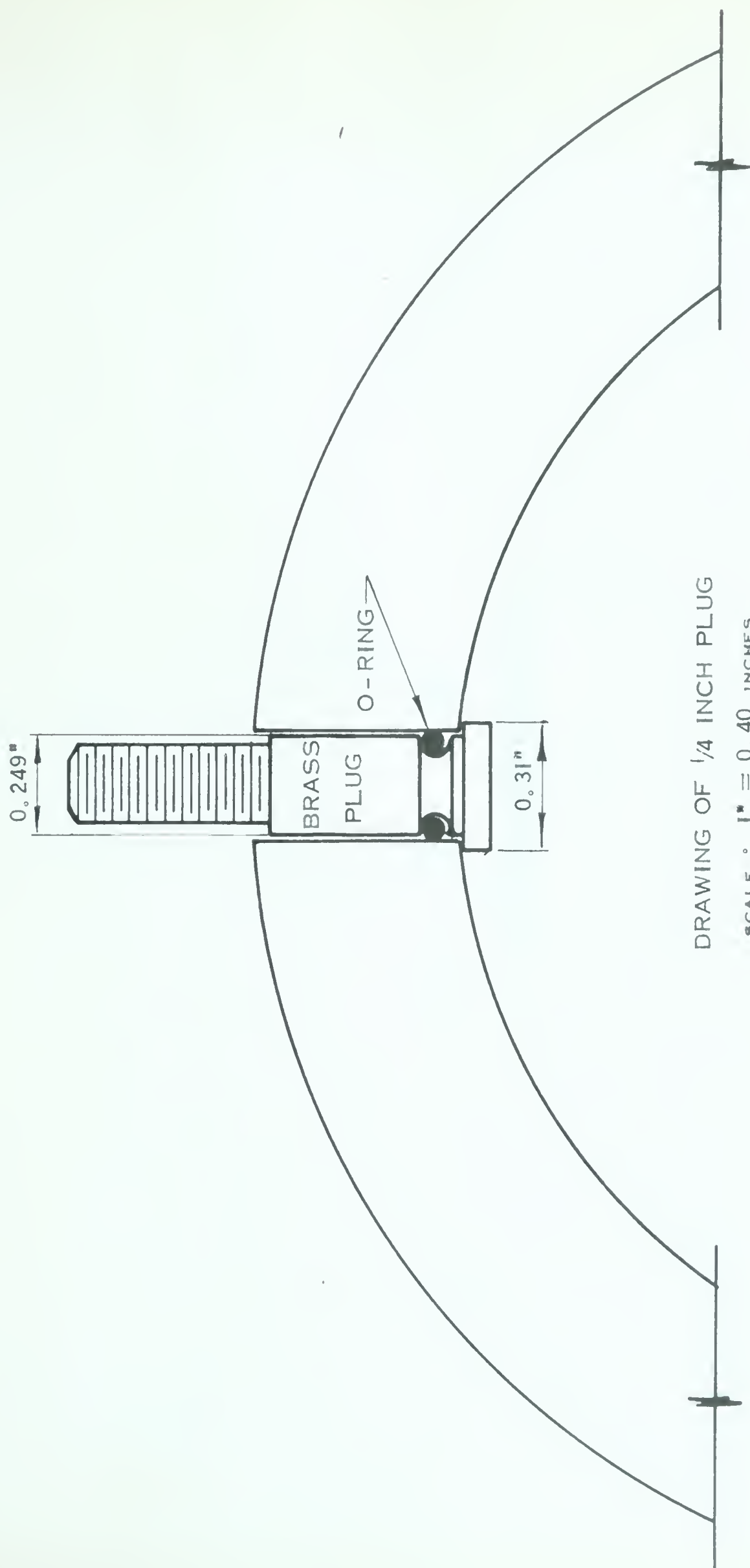
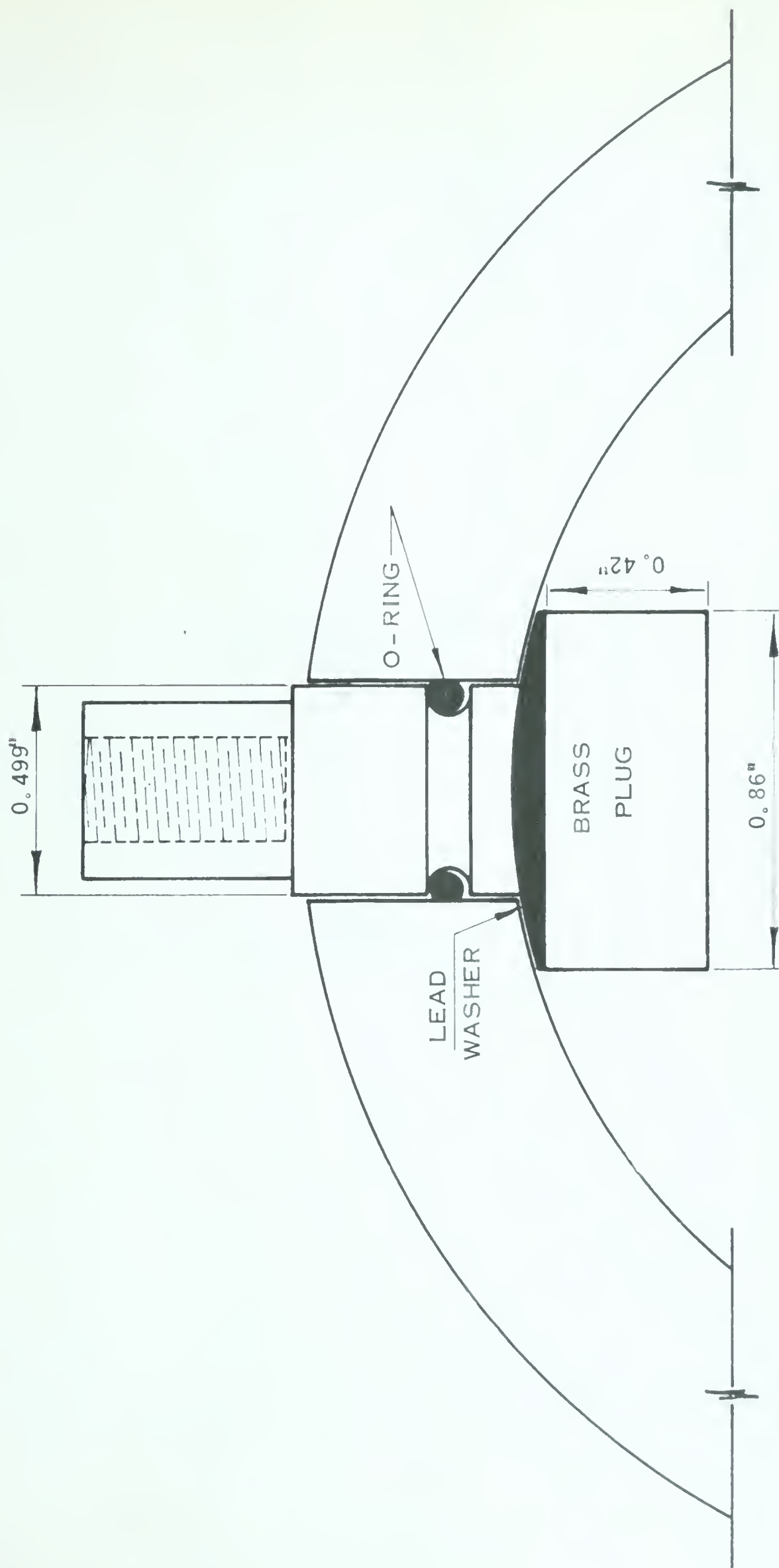


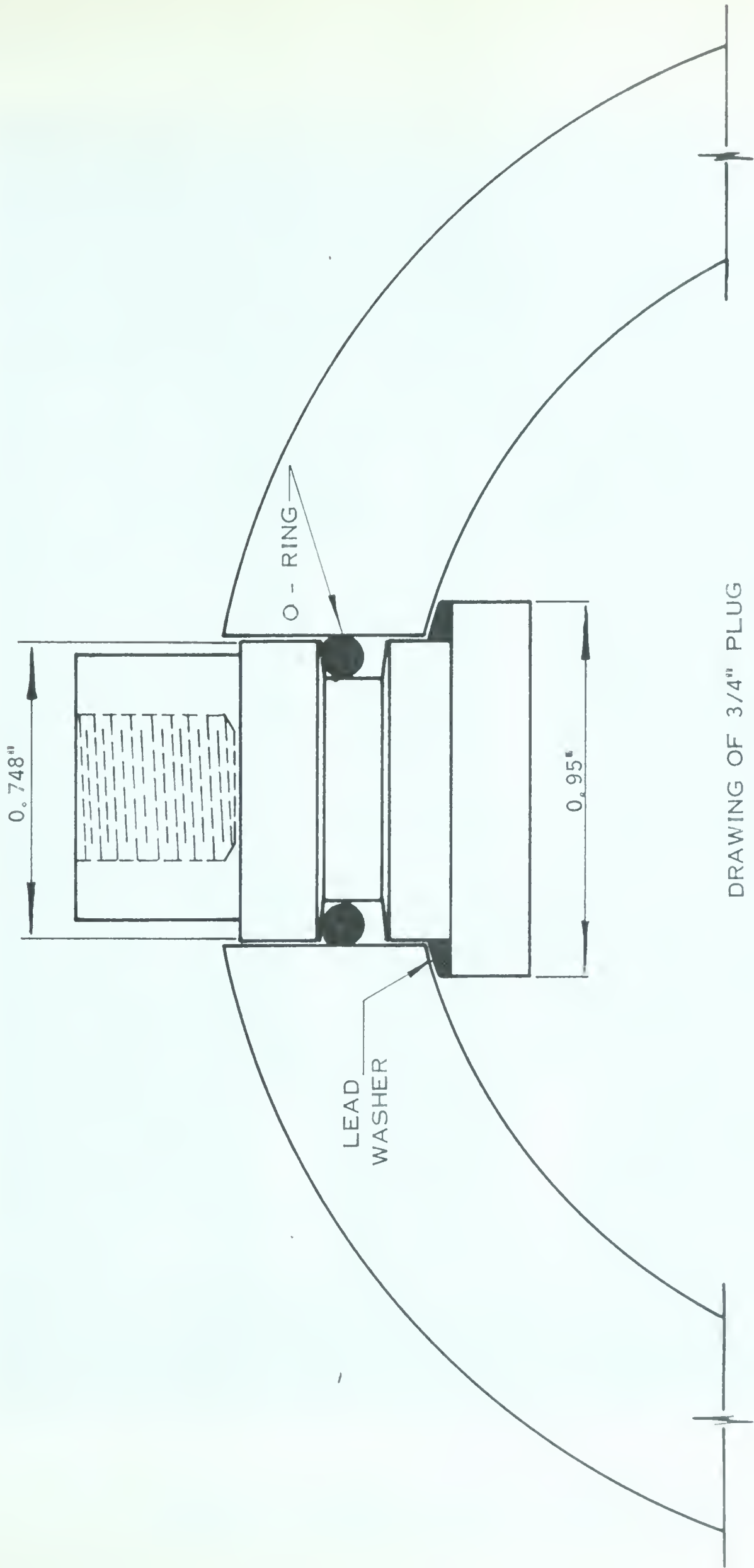
FIGURE 4.



DRAWING OF 1/2 INCH PLUG

SCALE : $1'' = 0.40$ INCHES

FIGURE 5.



DRAWING OF 3/4" PLUG

SCALE : 1" = 0.40 INCHES

FIGURE 6.



FIGURE 7. CLOSE-UP OF 3/4 INCH PLUG

CHAPTER 5

APPARATUS AND INSTRUMENTATION

A general view of the test equipment is shown in Fig. 8.

Pressure was supplied to the inside of the cylinder by hydraulic fluid brought from a "Blackhawk" pressure ram through flexible high pressure hose. The pressure limit of the ram and hose was 10,000 psi., but the pressure gauge used on the ram only had a range up to 5,000 psi., so the pressure of the system was limited to this value. Pressures in the region of 10,000 psi. would have been advantageous for the tests on the cylinders before the holes were drilled, but the lower pressure proved sufficient to give the desired results. A calibration curve for the pressure gauge is shown in Fig. 9.

Strain gauges of the wire resistance type mounted on a thin paper base were used for all strain measurements on the cylinder. Strains on the cylinder surface unaffected by the hole were measured using "Kyowa K-22-1" gauges of 10.5 mm. gauge length. Positioning of these control gauges is shown in Figs. 12, 14, 17, and 20. "Kyowa K-19-1" gauges of 3 mm. gauge length

were placed in four directions around the holes as shown in Fig. 10. A view of the test cylinder with all gauges in place is given in Fig. 11. All the strain gauges were connected to a "Baldwin" switching box and read by means of a "Baldwin" Strain Indicator, Type NA. A "Baldwin" Switching and Balancing Unit was used for some of the earlier tests of the series, but the results were not as consistent as those obtained using the ordinary switching box, so its use was discontinued for the latter tests.

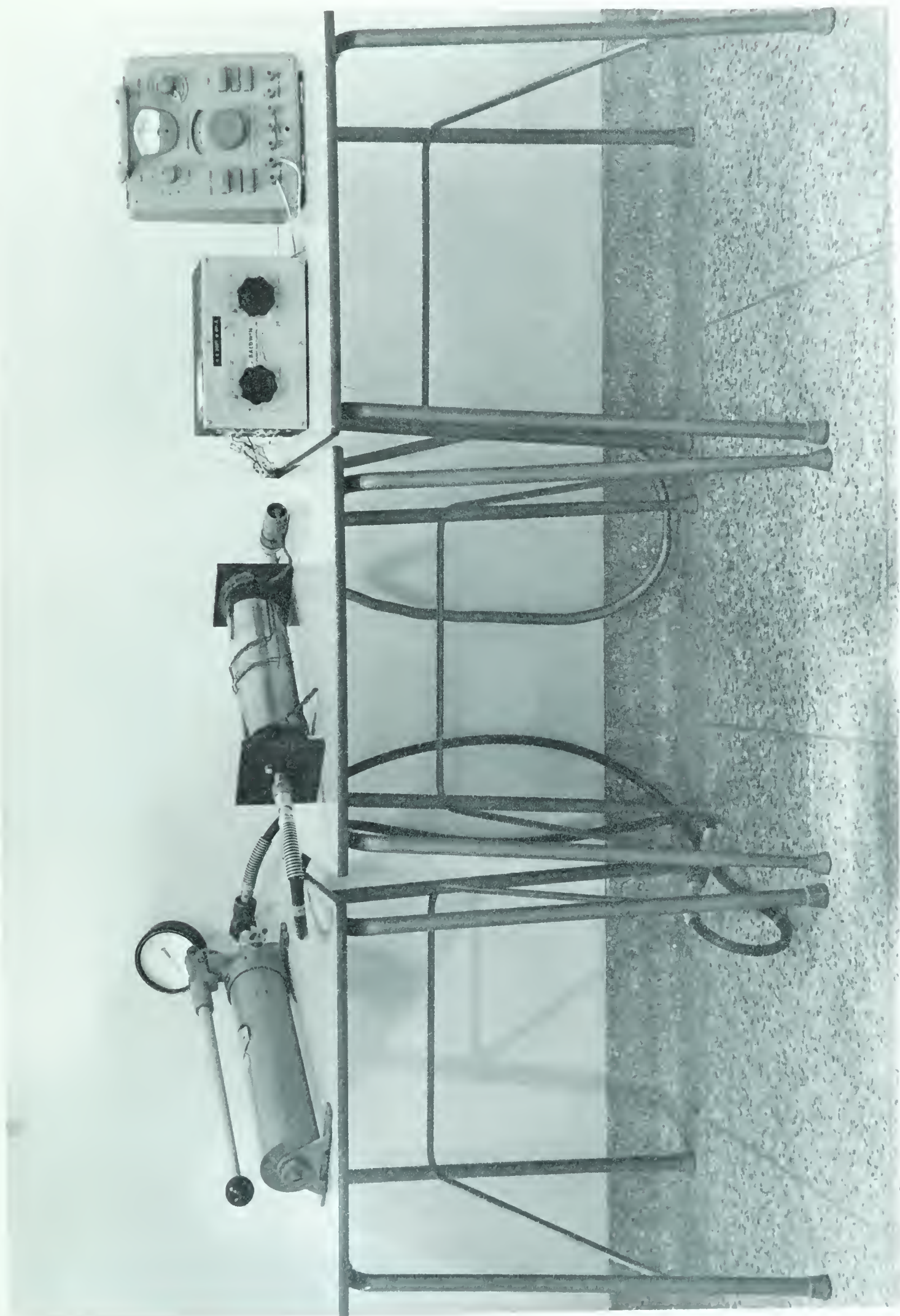


FIGURE 8. GENERAL VIEW OF TEST EQUIPMENT

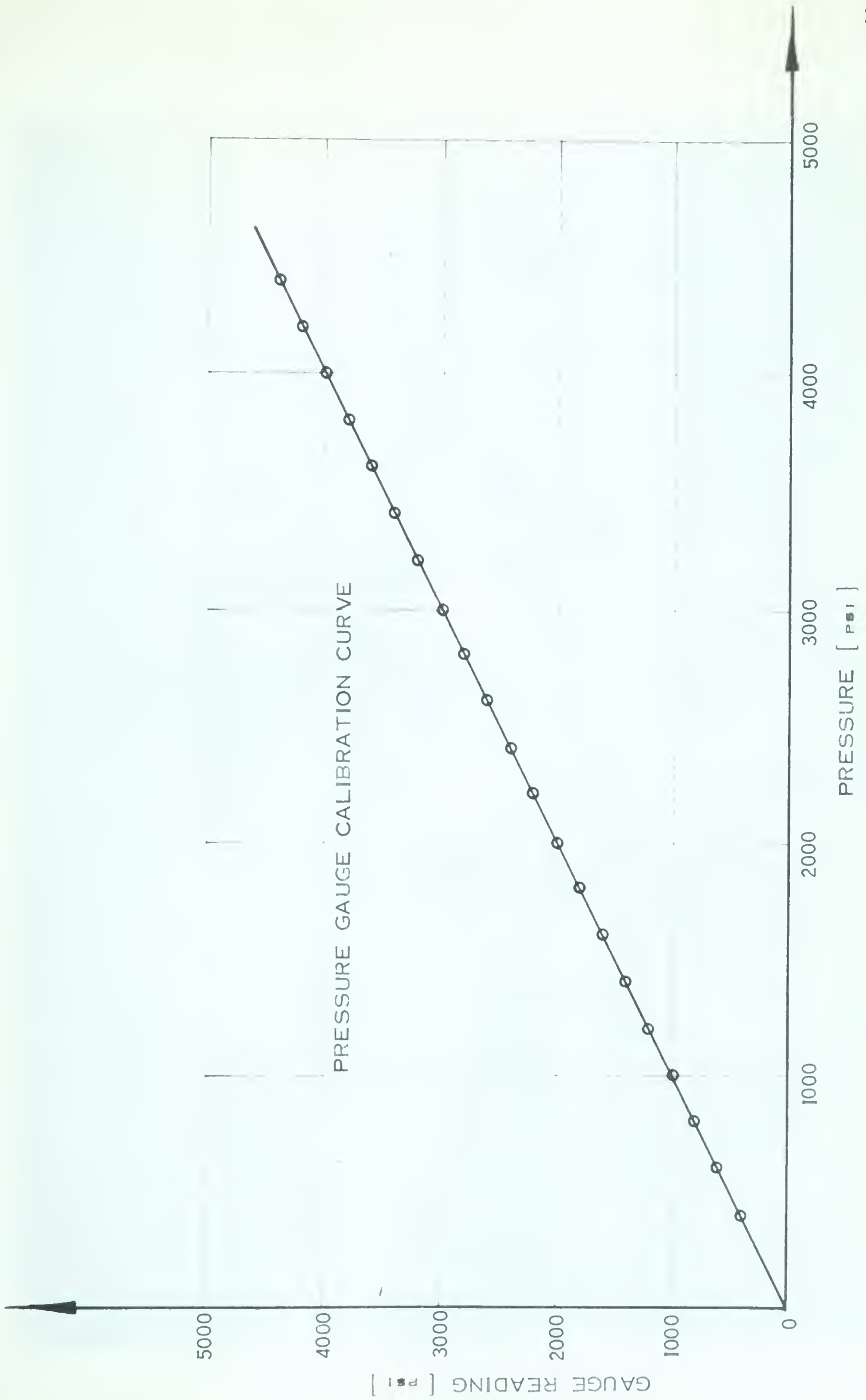


FIGURE 9.



FIGURE 10. VIEW OF GAUGES AROUND HOLE

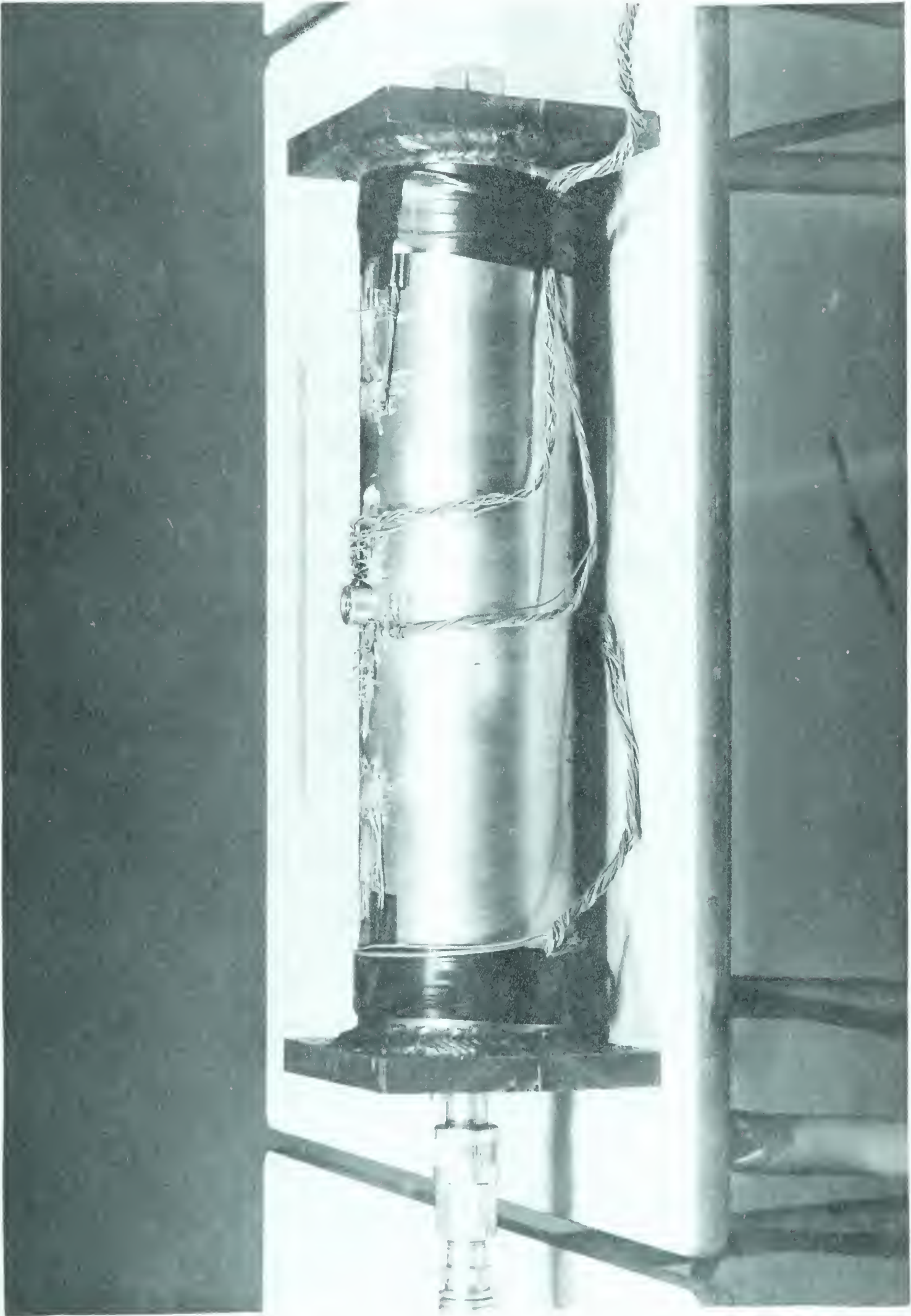


FIGURE II. VIEW OF TEST CYLINDER

CHAPTER 6

EXPERIMENTAL PROCEDURE

After each specimen had been fabricated, control gauges were glued on the outside of the cylinder and at least three tests were run on the vessel before the first hole was drilled. Strain readings were taken at intervals as the pressure was applied and the initial reading of the gauges at zero pressure was checked after the test was completed. A set of readings was rejected if the gauges did not return to their initial readings after all load was removed.

Two of the control gauges at the centre of the cylinder were then removed and the 1/4 inch hole was drilled in the same place that the two gauges had previously been positioned. Using this technique it was possible to compare stresses within a small area before and after drilling the hole.

When the hole had been drilled, strain gauges were mounted around it and the 1/4 inch plug was placed in position. The pressure inside the cylinder was pumped to a pre-determined value and held at that pressure while all the gauges were read, then increased to the next level. This procedure was repeated

until the maximum load was reached, then the pressure was reduced to zero and the zero readings were checked. At least three tests which gave consistent results were averaged.

Stresses near the hole were computed before reaming the hole to the next larger size. Appendix A describes the method in which the strain readings were converted to stresses. If the stresses derived did not appear to be correct the test was re-run, or in some cases the strain gauges were replaced.

When it was established that the results from the tests around the 1/4 inch hole were satisfactory, the strain gauges were removed and the hole was drilled and reamed to 1/2 inch in diameter. Gauges were then placed around this hole and a procedure similar to that used for the 1/4 inch hole was followed. The largest hole was tested in the same manner.

CHAPTER 7

EXPERIMENTAL RESULTS AND DISCUSSION

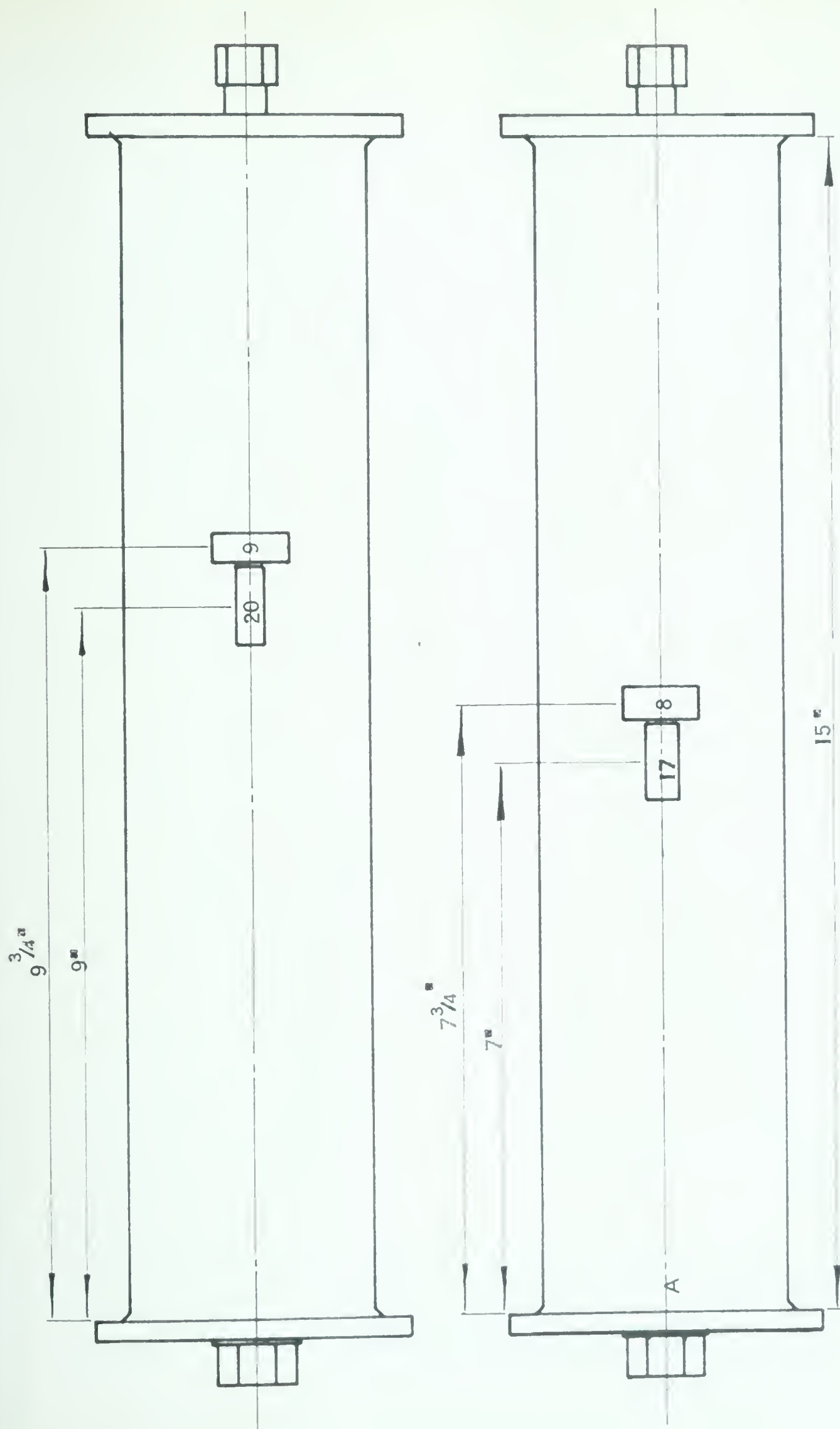
7.1 Poisson's Ratio

Strain gauge readings of axial strain vs. hoop strain are shown in Figs. 13 to 22. The numbers on the lines refer to the gauge numbers as noted on the drawings preceeding the diagrams. Using the slope of the lines, Poisson's ratio was computed using Eqn. 7. Table 1 below gives the values of Poisson's ratio as calculated from the curves of Figs. 13 to 22.

TABLE 1 POISSON'S RATIO

CYLINDER WALL THICKNESS	GAUGE NUMBERS	POISSON'S RATIO
1/8"	9 & 20	0.266
"	8 & 17	0.274
1/4"	1 & 2	0.274
"	3 & 4	0.273
"	5 & 6	0.253
"	7 & 8	0.269
"	9 & 10	0.249
"	11 & 12	0.273
3/8"	1 & 2	0.286
"	3 & 4	0.276
"	5 & 6	0.280
"	7 & 8	0.270
"	9 & 10	0.260
"	11 & 12	0.272
1/2"	1 & 2	0.246
"	3 & 4	0.279
"	5 & 6	0.269
"	7 & 8	0.252
"	9 & 10	0.248
"	11 & 12	0.235

It is seen from this table that the apparent Poisson's ratio varied considerably for different points on the cylinders. A weighted mean value for Poisson's ratio of 0.27 was used in subsequent calculations for all the test specimens.



POSITIONING OF CONTROL GAUGES
1/8 INCH WALL THICKNESS

FIGURE 12.

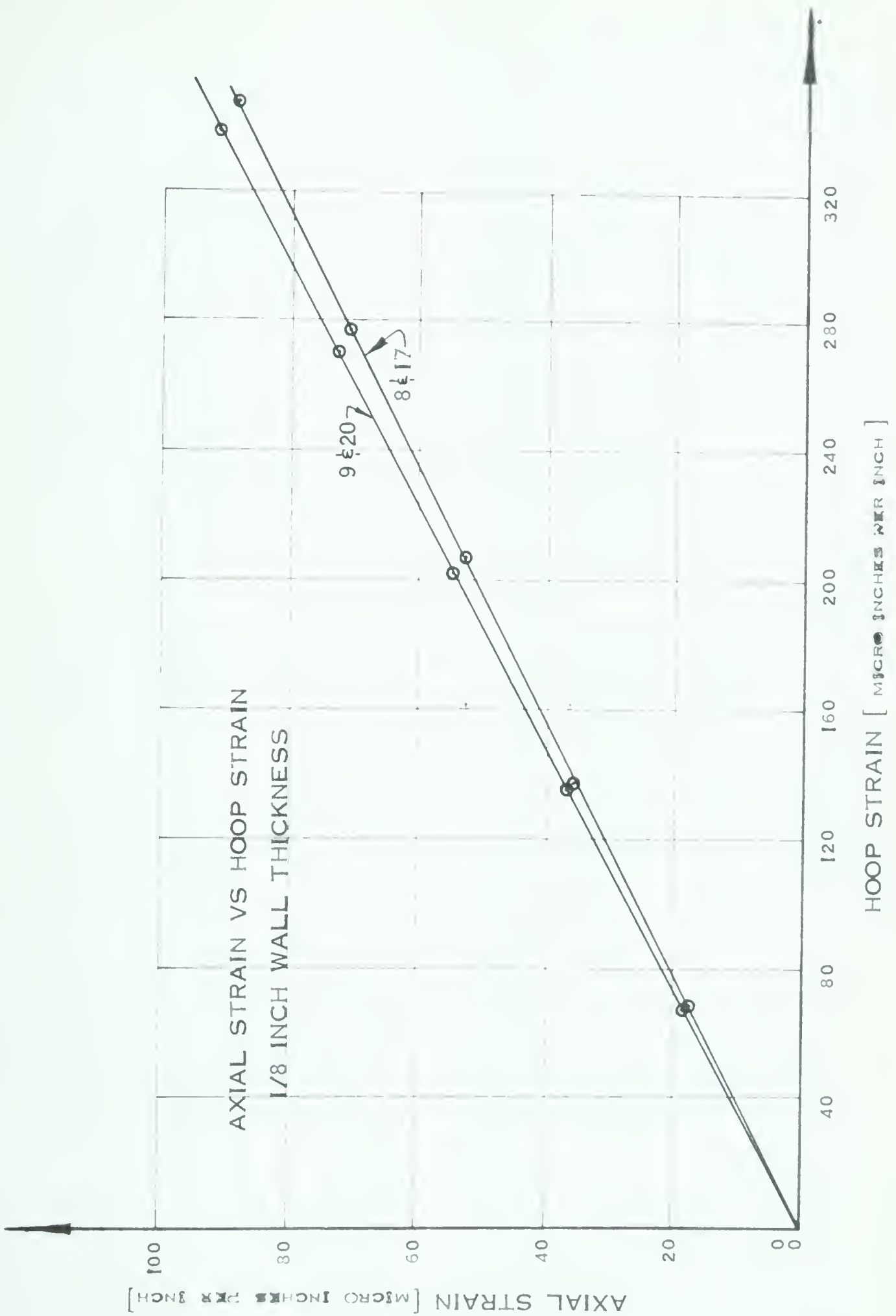
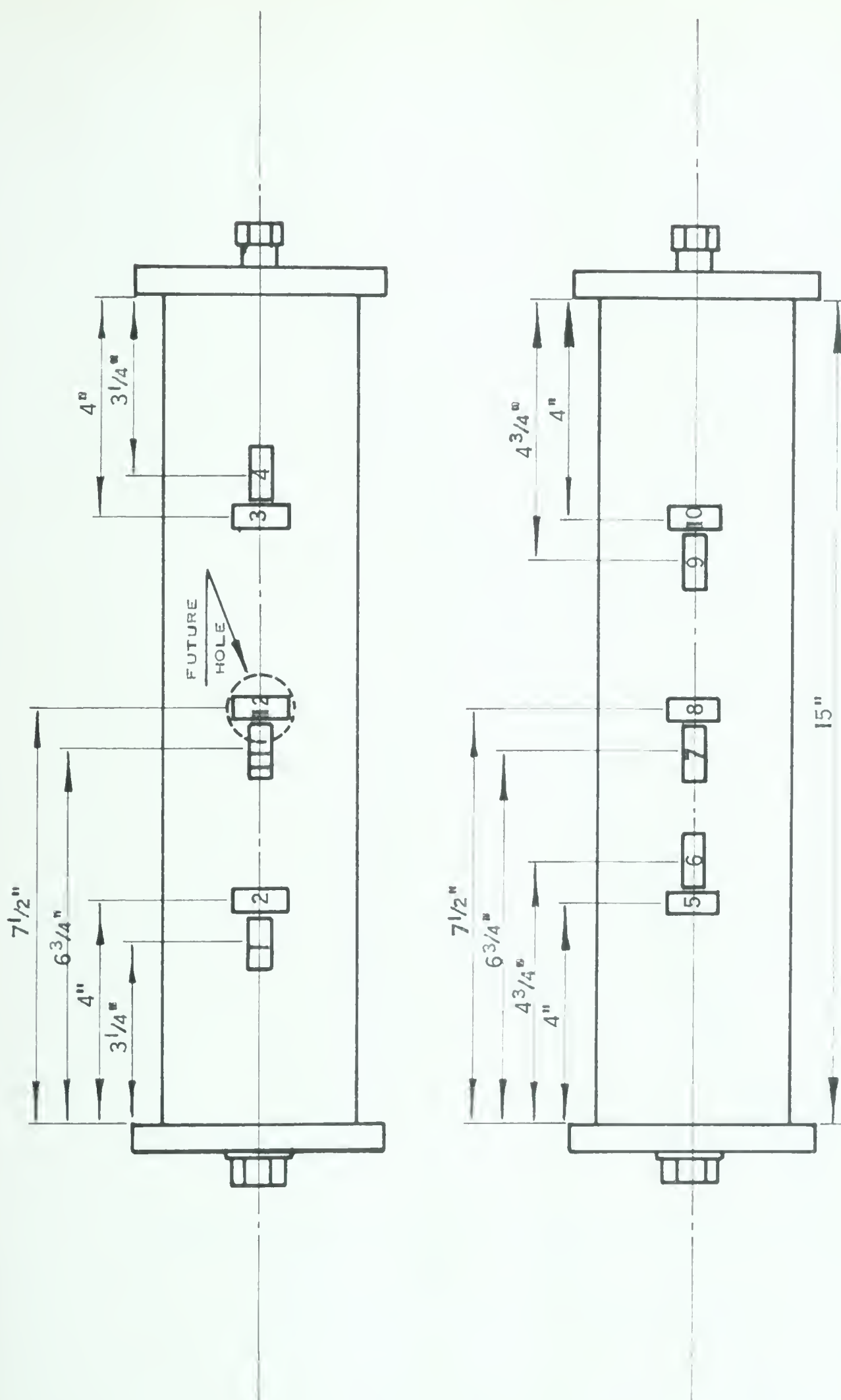


FIGURE 13.



POSITIONING OF CONTROL GAUGES
1/4 INCH WALL THICKNESS

FIGURE 14.

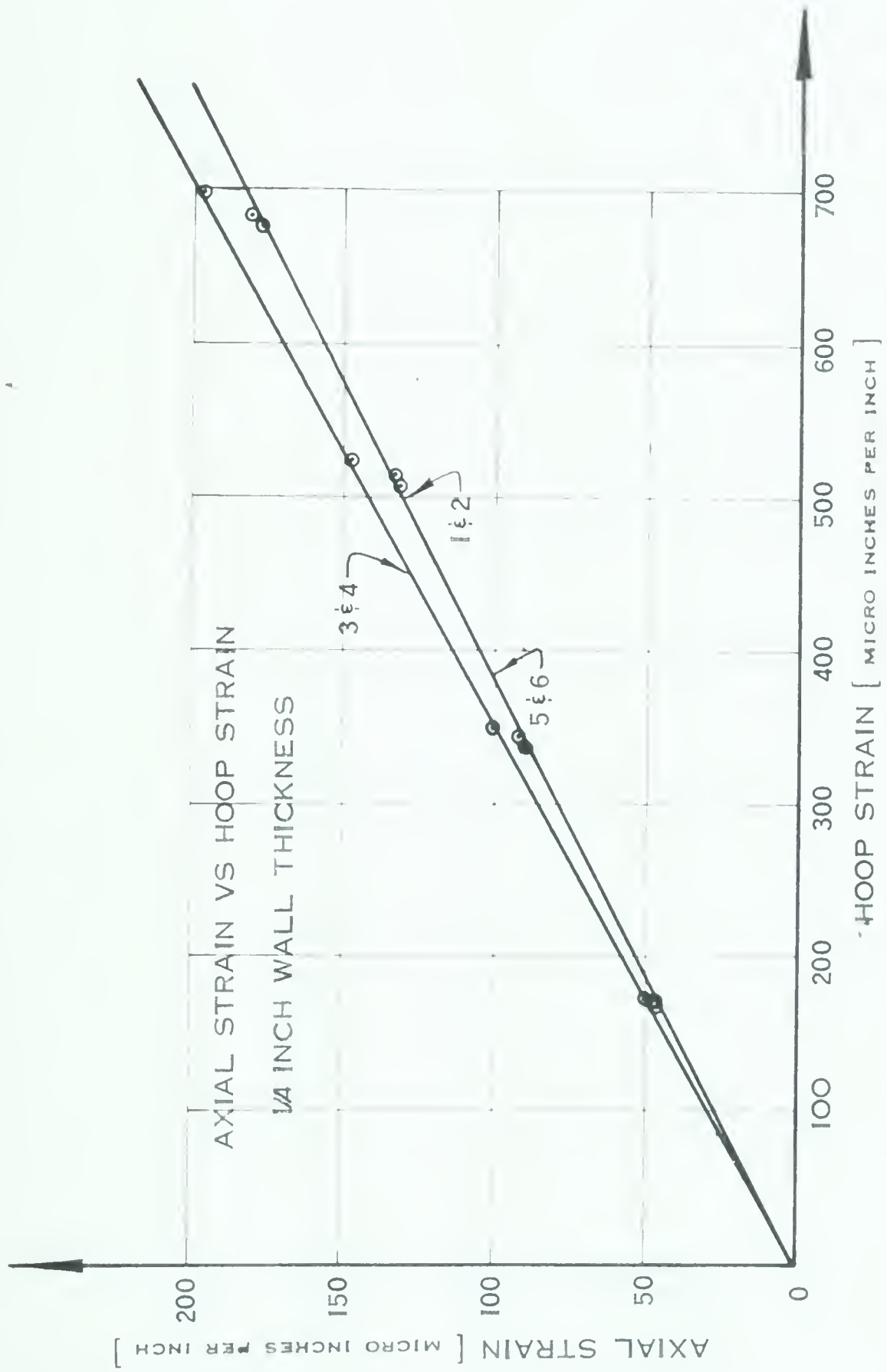


FIGURE 15.

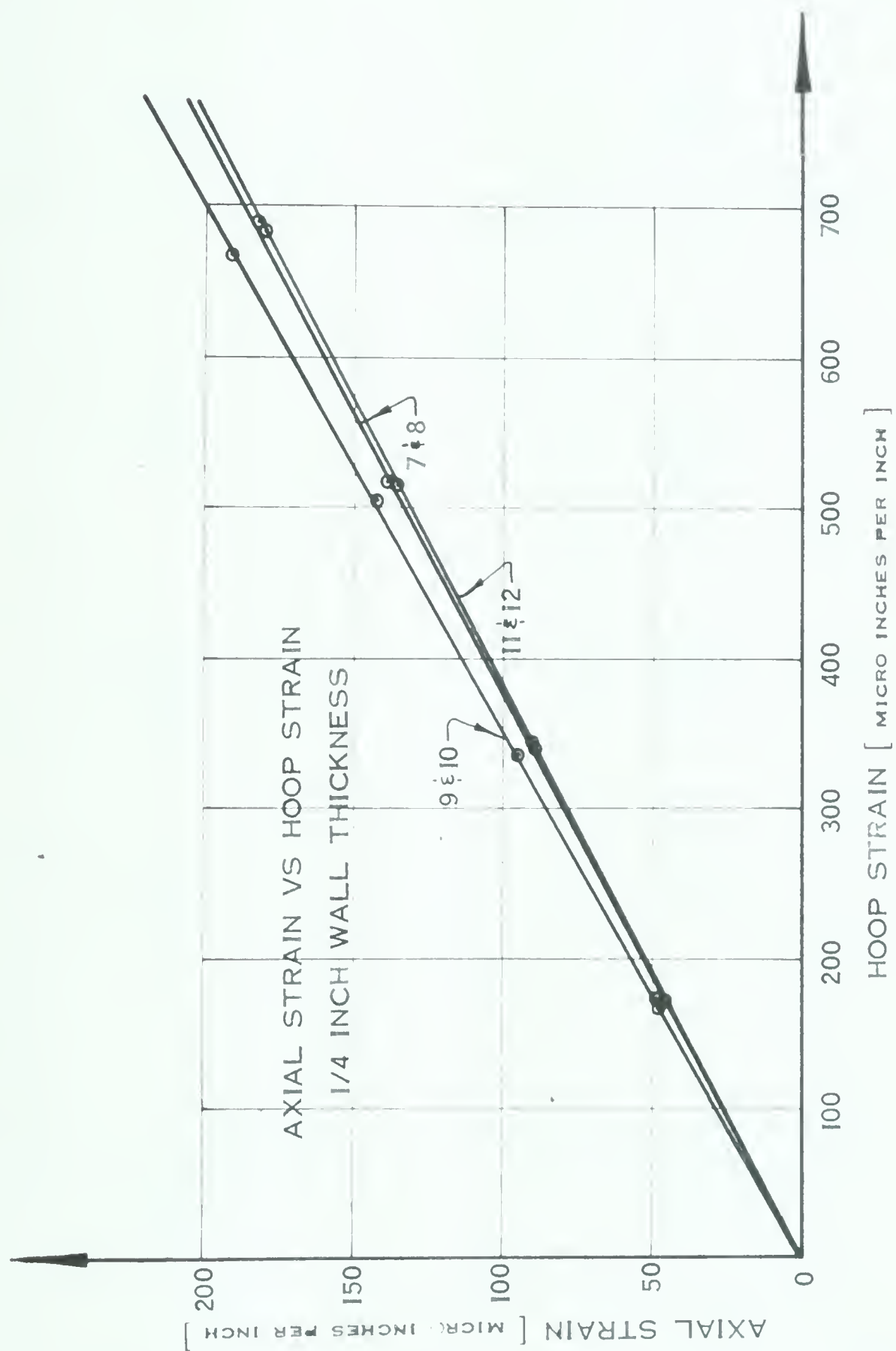
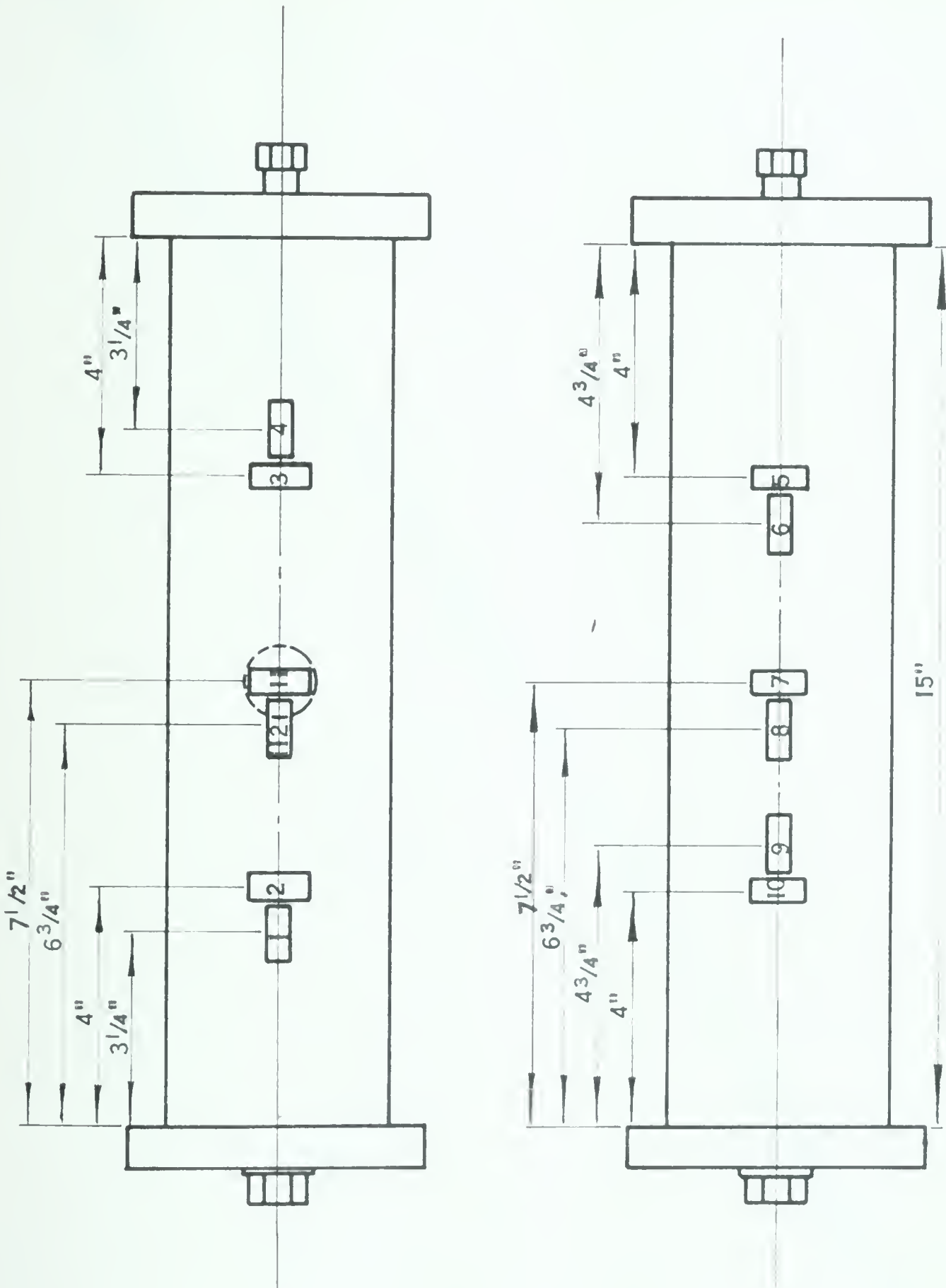


FIGURE 16.



POSITIONING OF CONTROL GAUGES
3/8 INCH WALL THICKNESS
FIGURE 17.

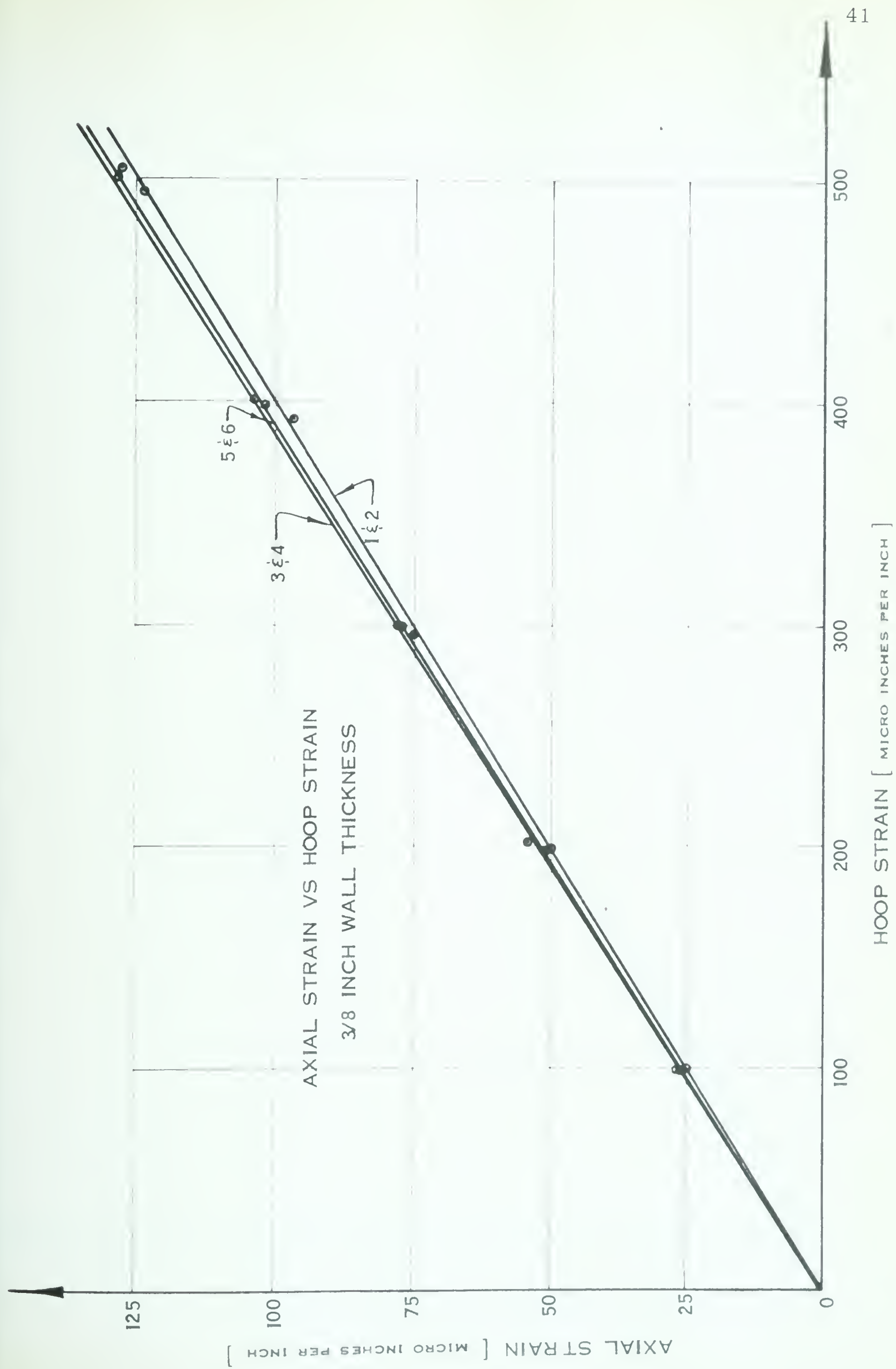


FIGURE 18.

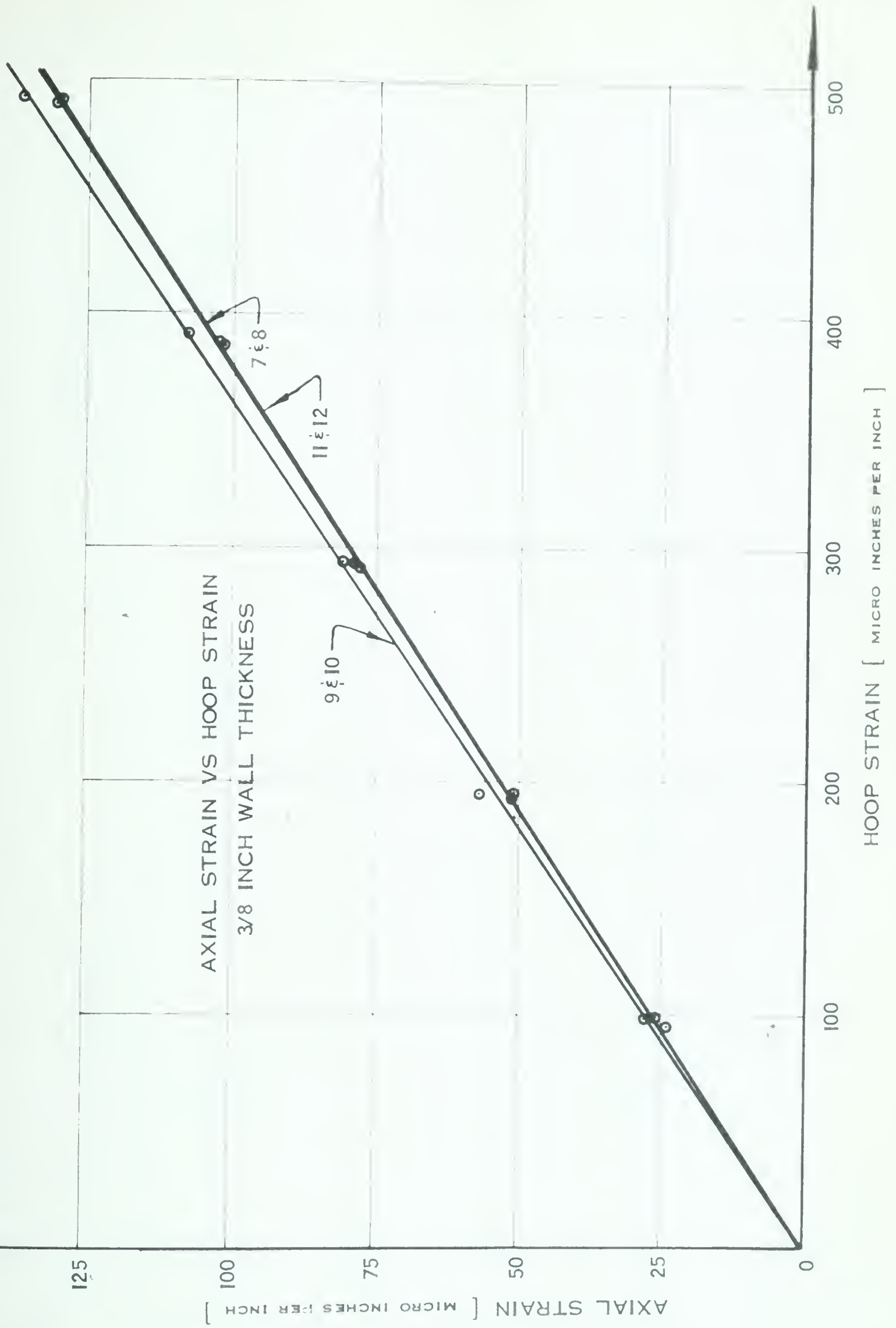
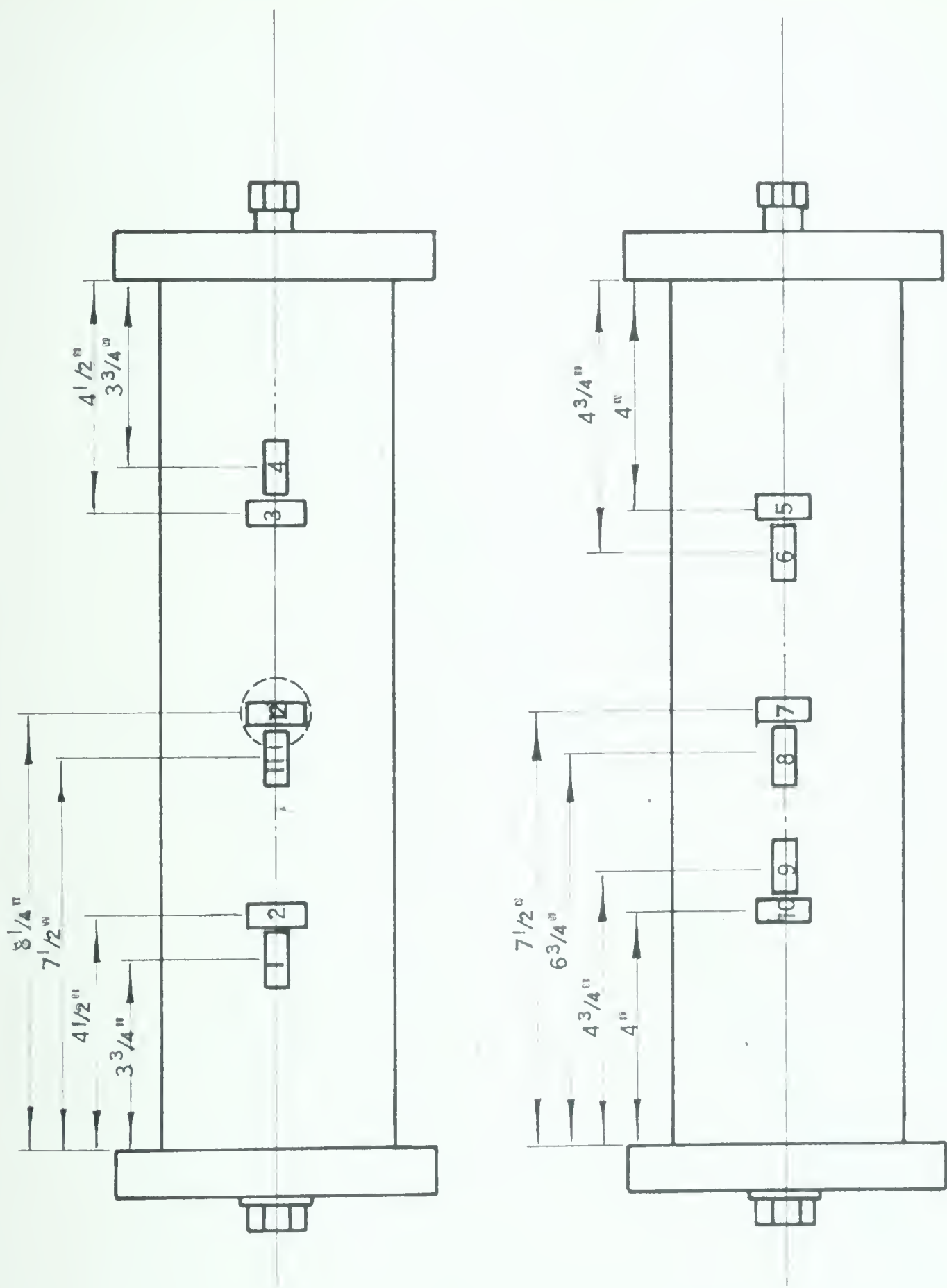


FIGURE 19.



POSITIONING OF CONTROL GAUGES
1/2 INCH WALL THICKNESS

FIGURE 20.

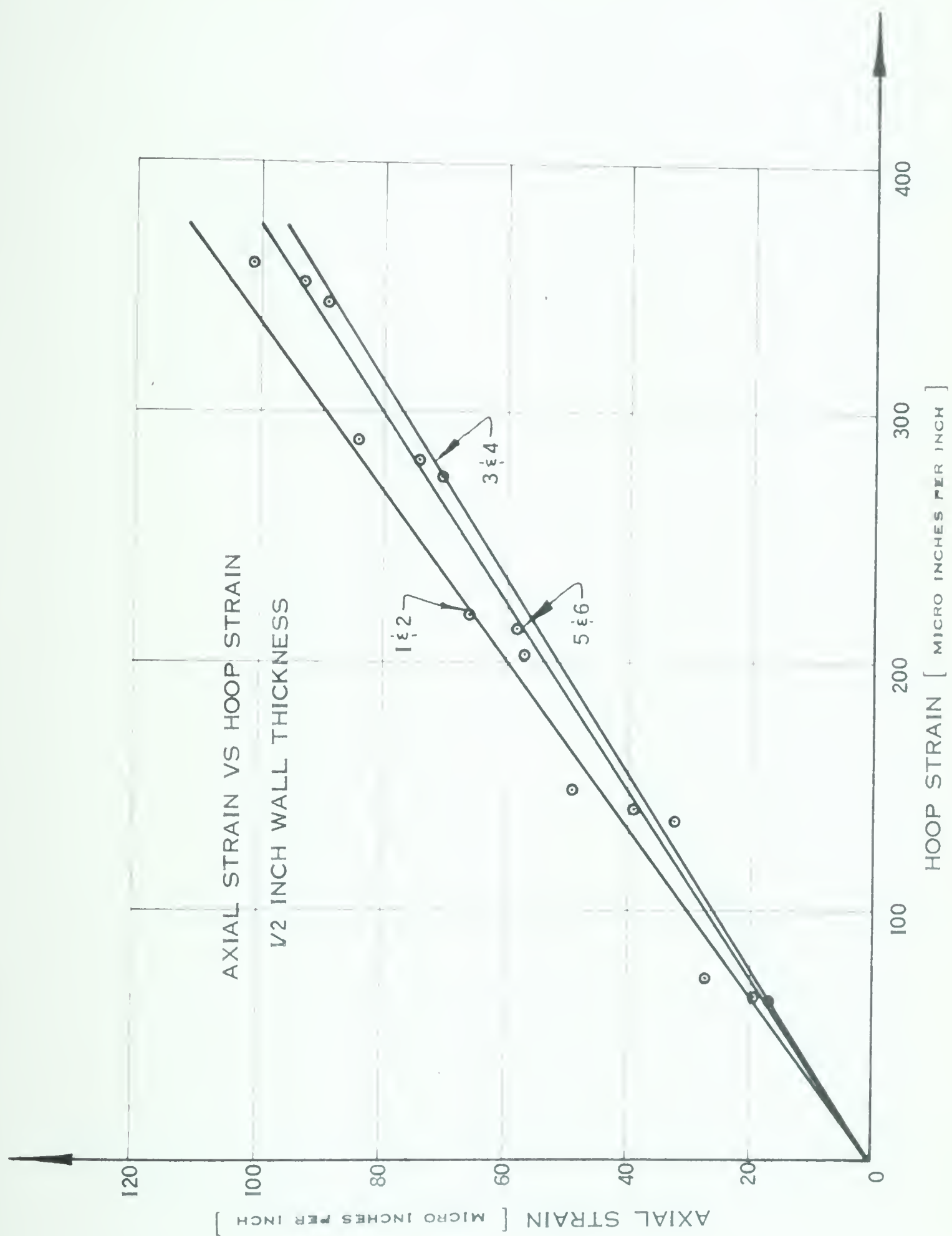


FIGURE 21.

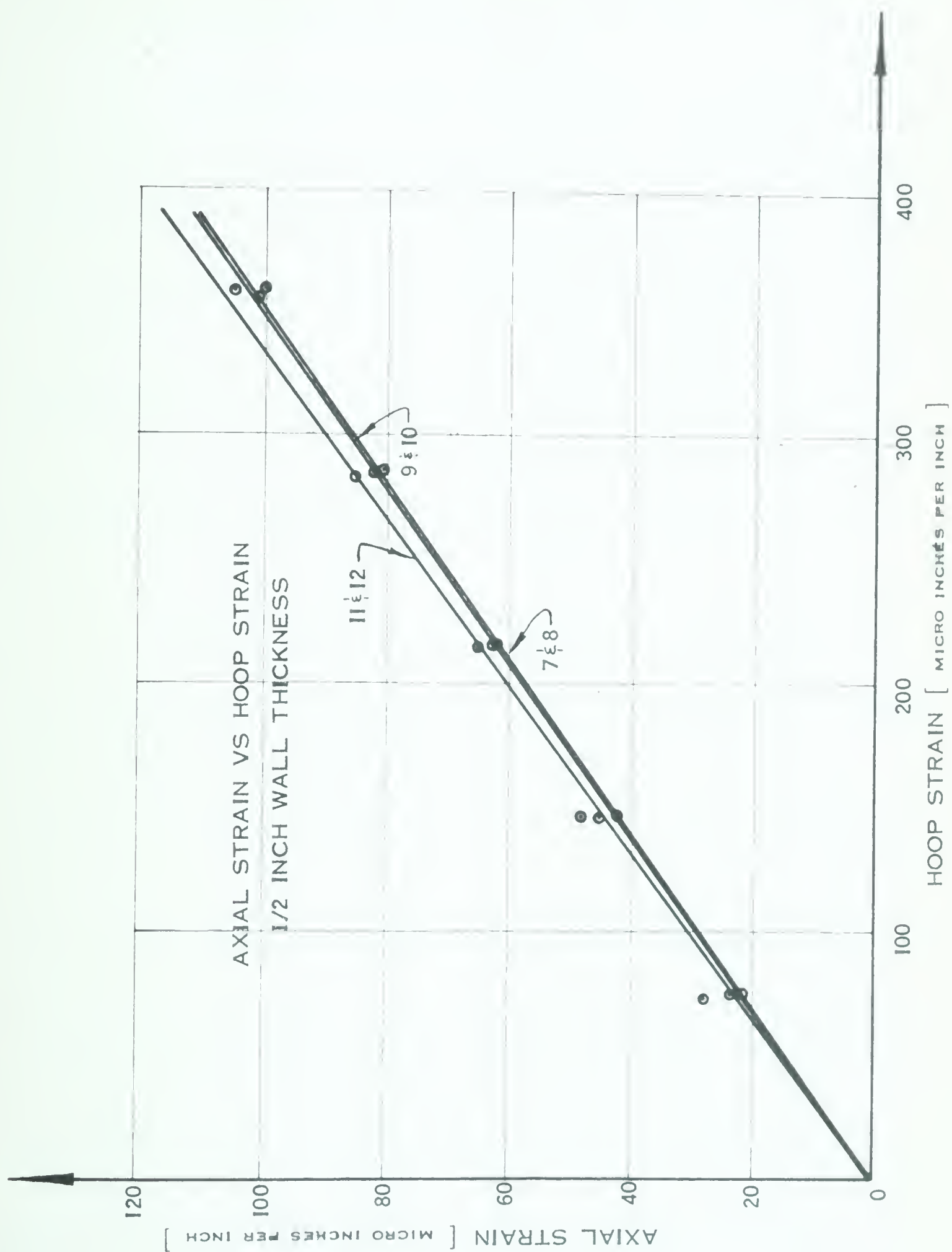


FIGURE 22.

7.2 Strain-Pressure Diagrams

The purpose of the strain-pressure diagrams was to find the most accurate relationship between strain at the outside surface of the cylinder and pressure within the cylinder. The test specimens were stressed within the elastic range, so a comparison of stresses near the hole with those in the undisturbed area at any particular pressure gave the required stress concentration factor. To derive the stresses at that pressure it was necessary to find the true strains around the hole.

Rather than use the strain gauge readings for one specific pressure, the strains read from each gauge were plotted vs. pressure and the best-fit straight lines drawn for these results. The strains found from these lines at one specific pressure were used to calculate the stresses around the hole. The plots of strain vs. pressure also provided a check on the experimental equipment. The diagrams of strain vs. pressure for the gauges together with the drawings showing the positioning of the gauges relative to the holes, are given in Figs. 23 to 63. The number within the circle at the end of each line refers to the gauge number as noted in the drawing preceding the strain-pressure diagram.

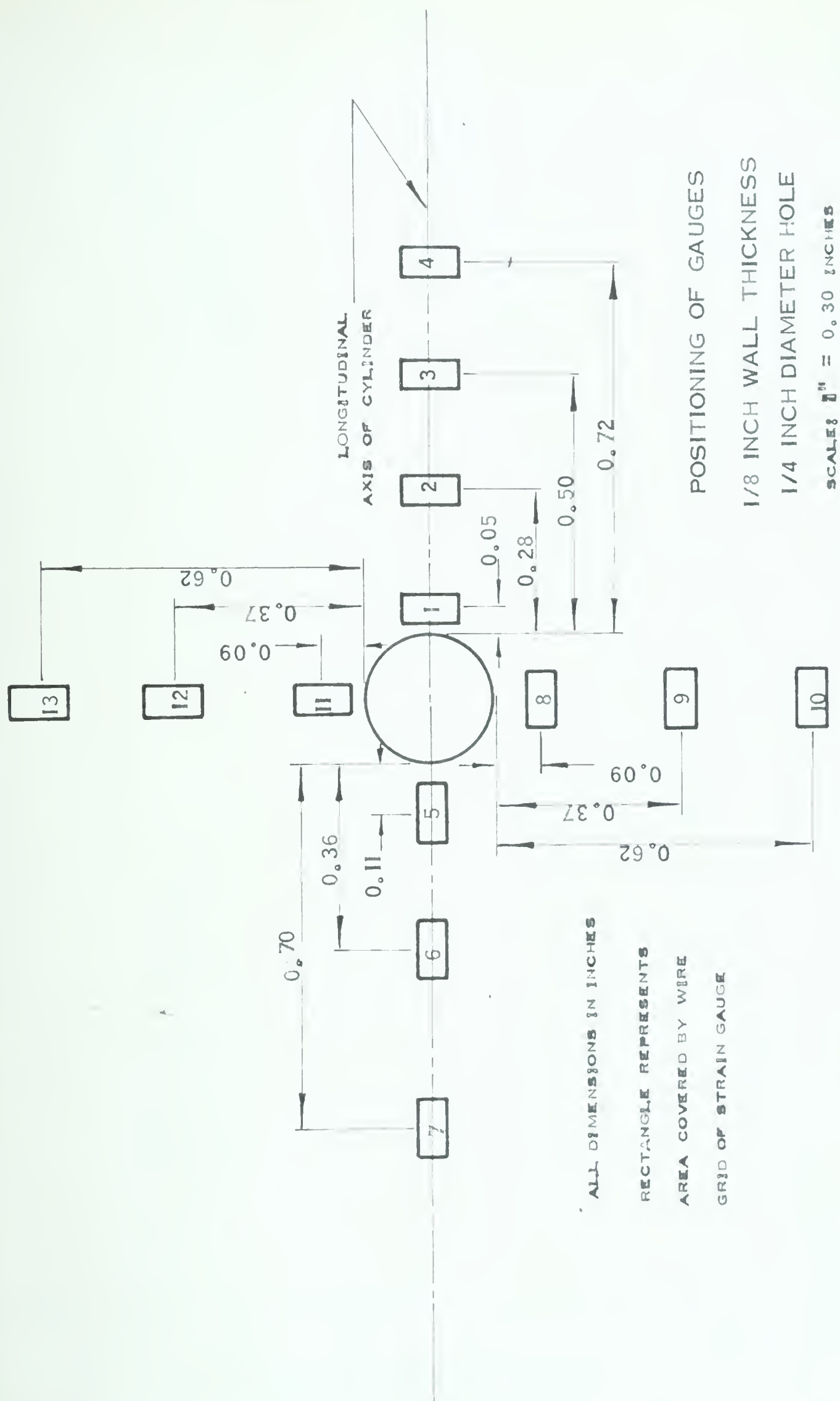


FIGURE 23.

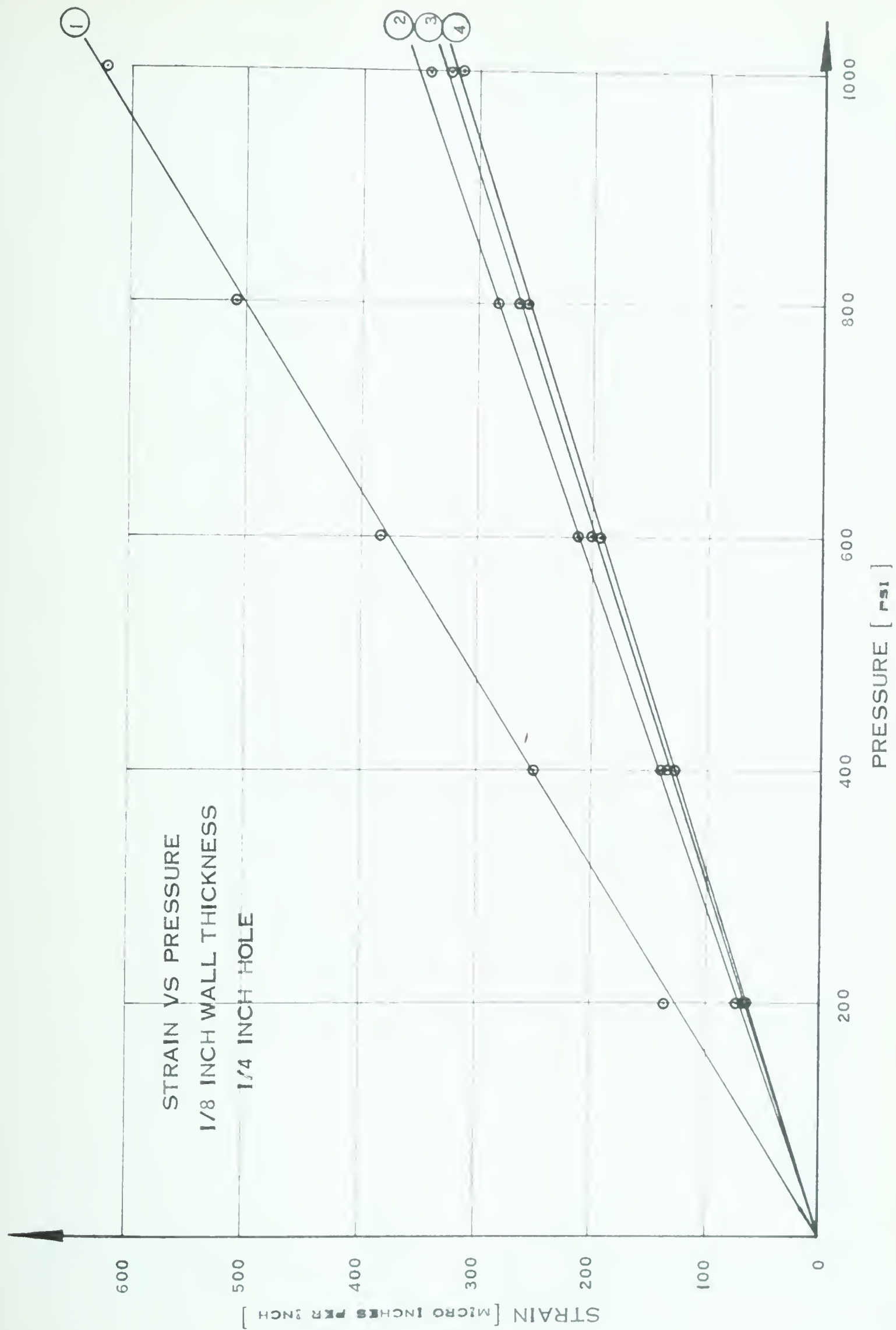


FIGURE 24.

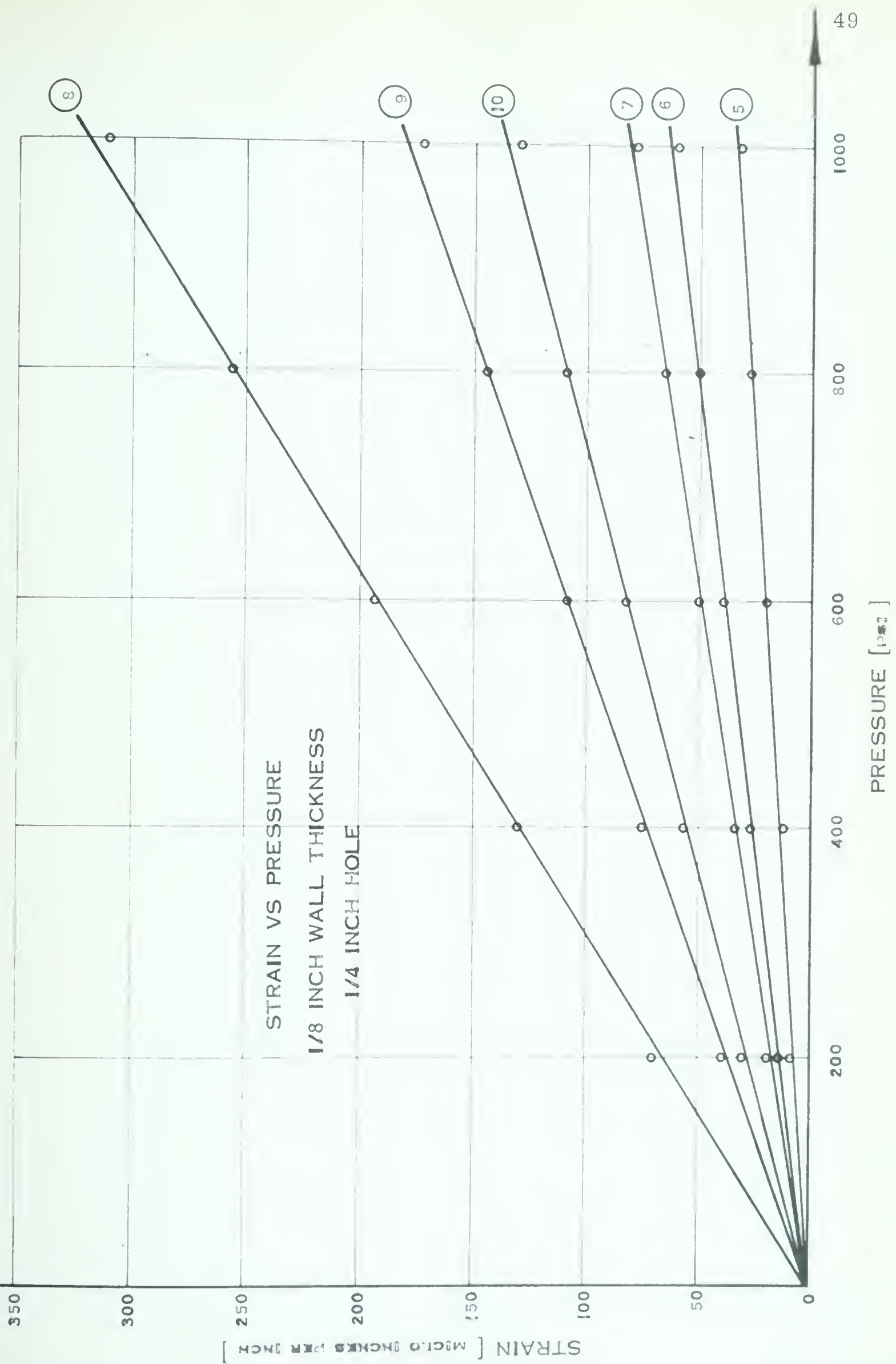


FIGURE 25.

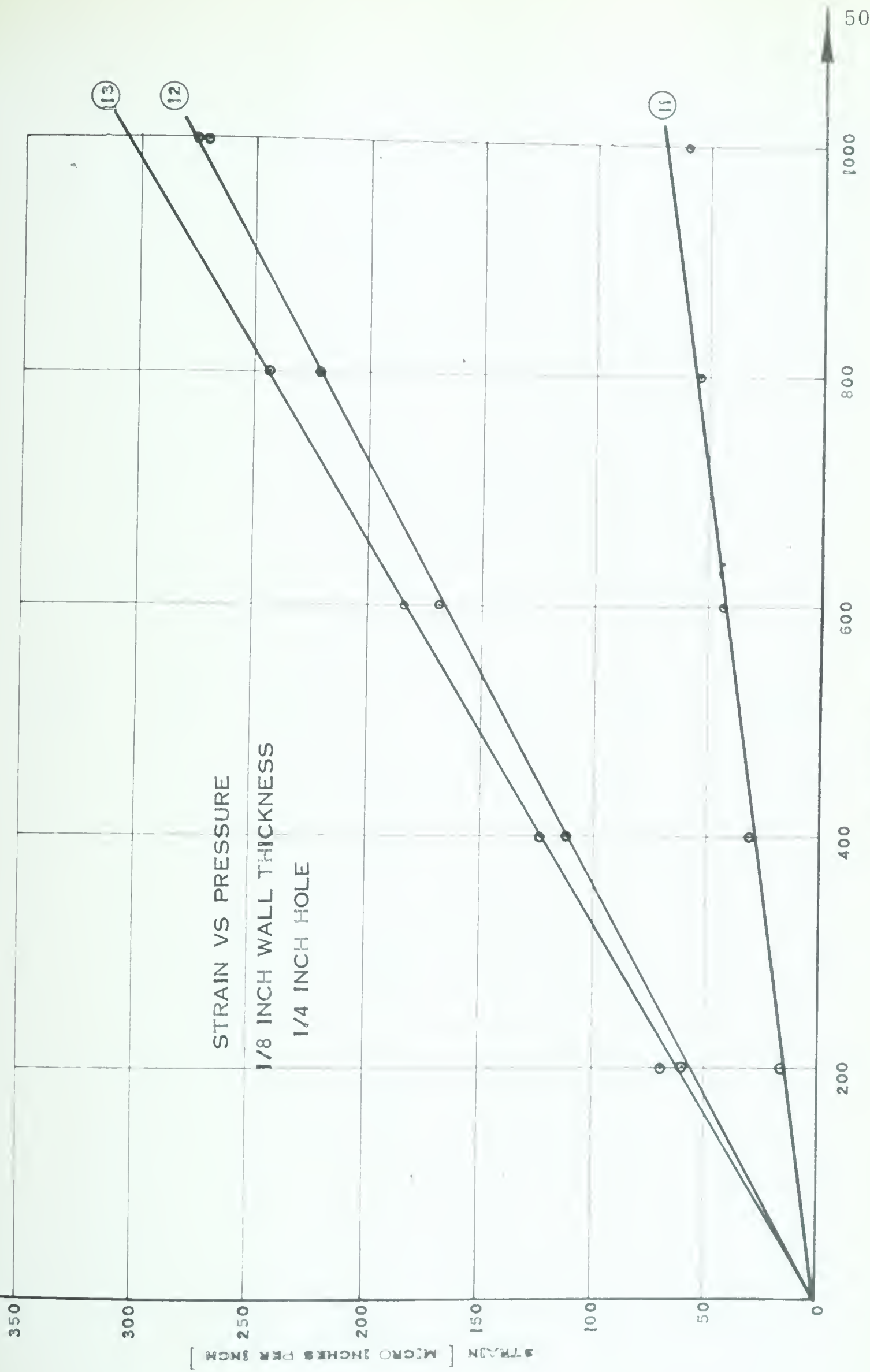


FIGURE 26.

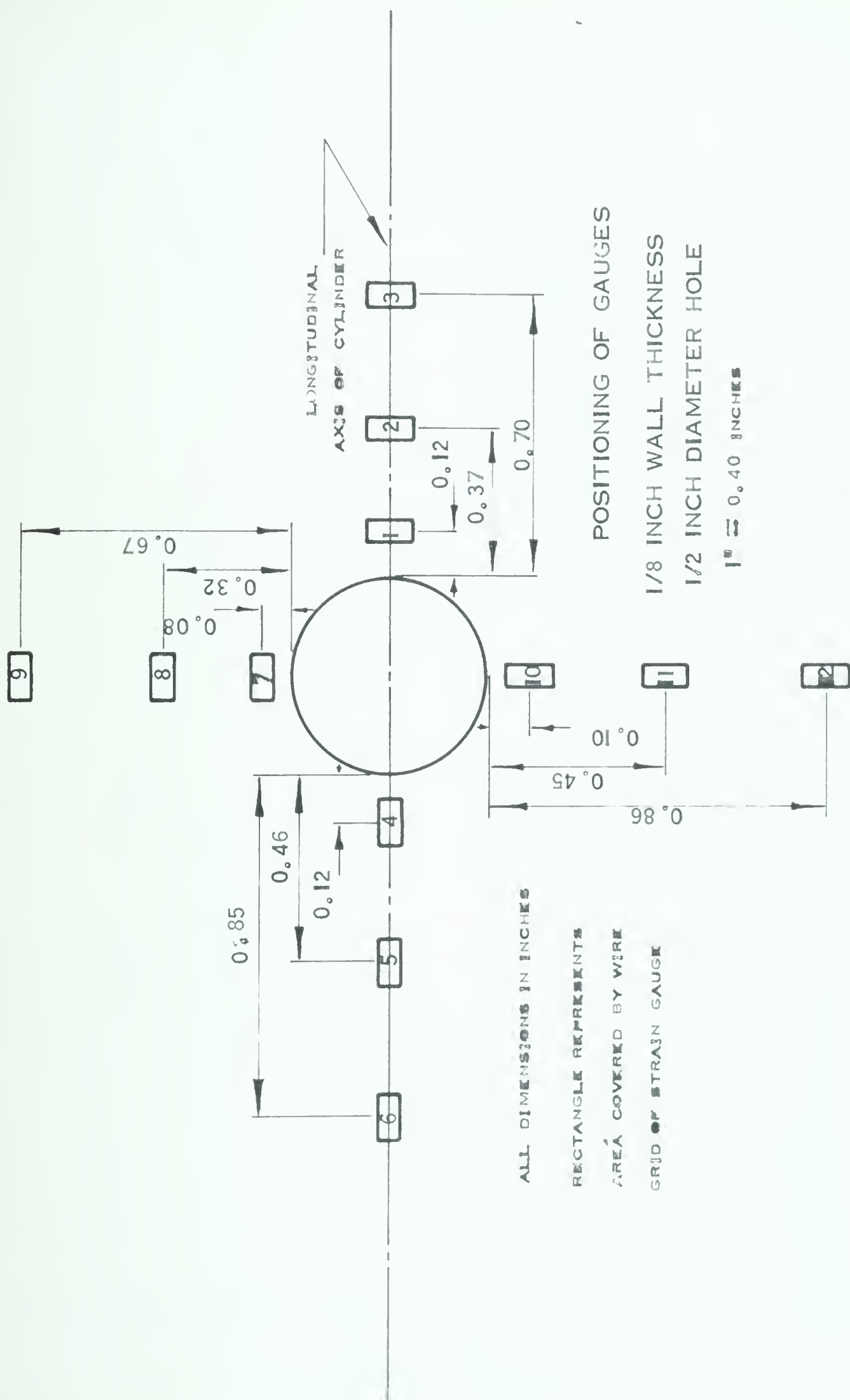


FIGURE 27.

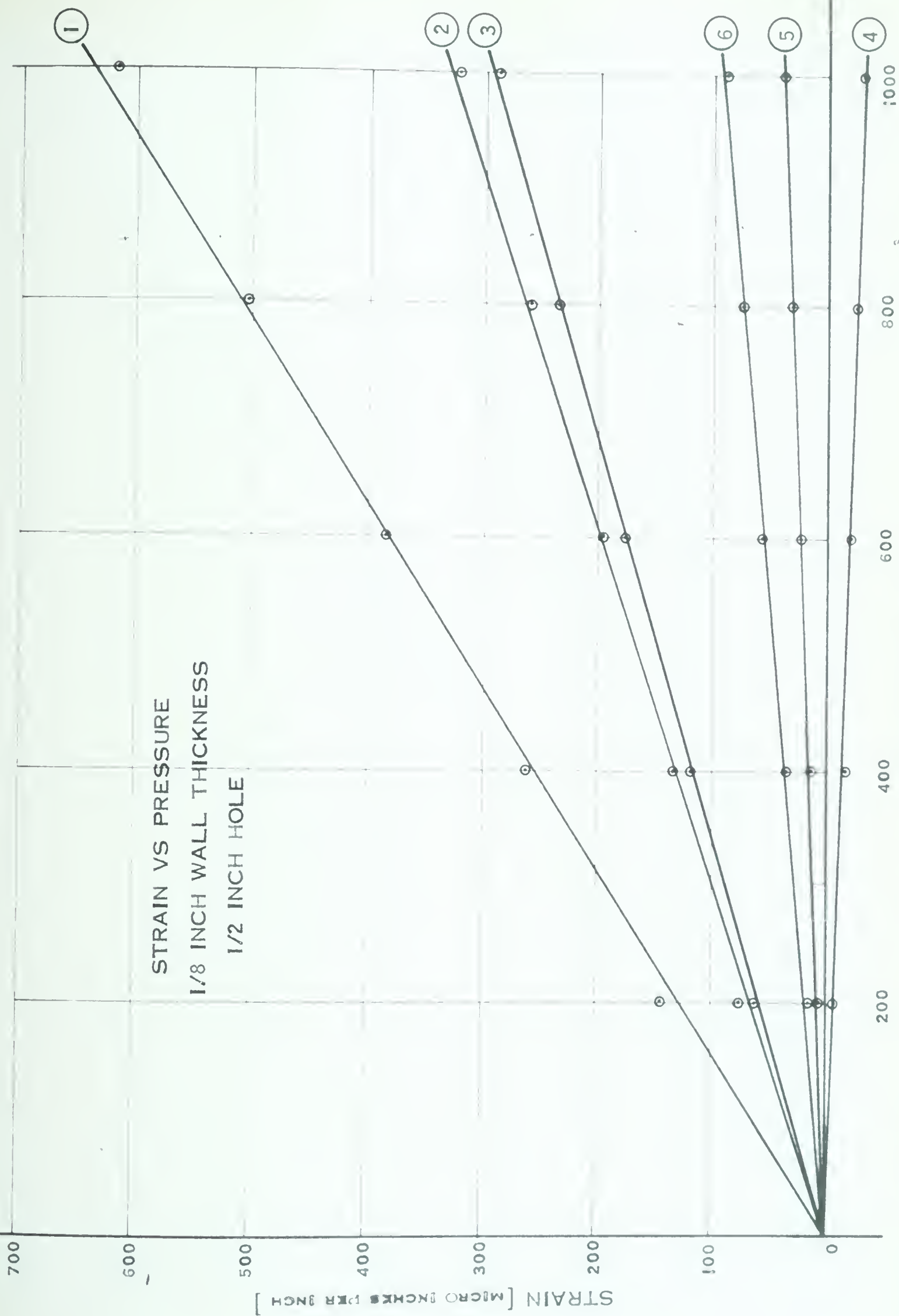


FIGURE 28.

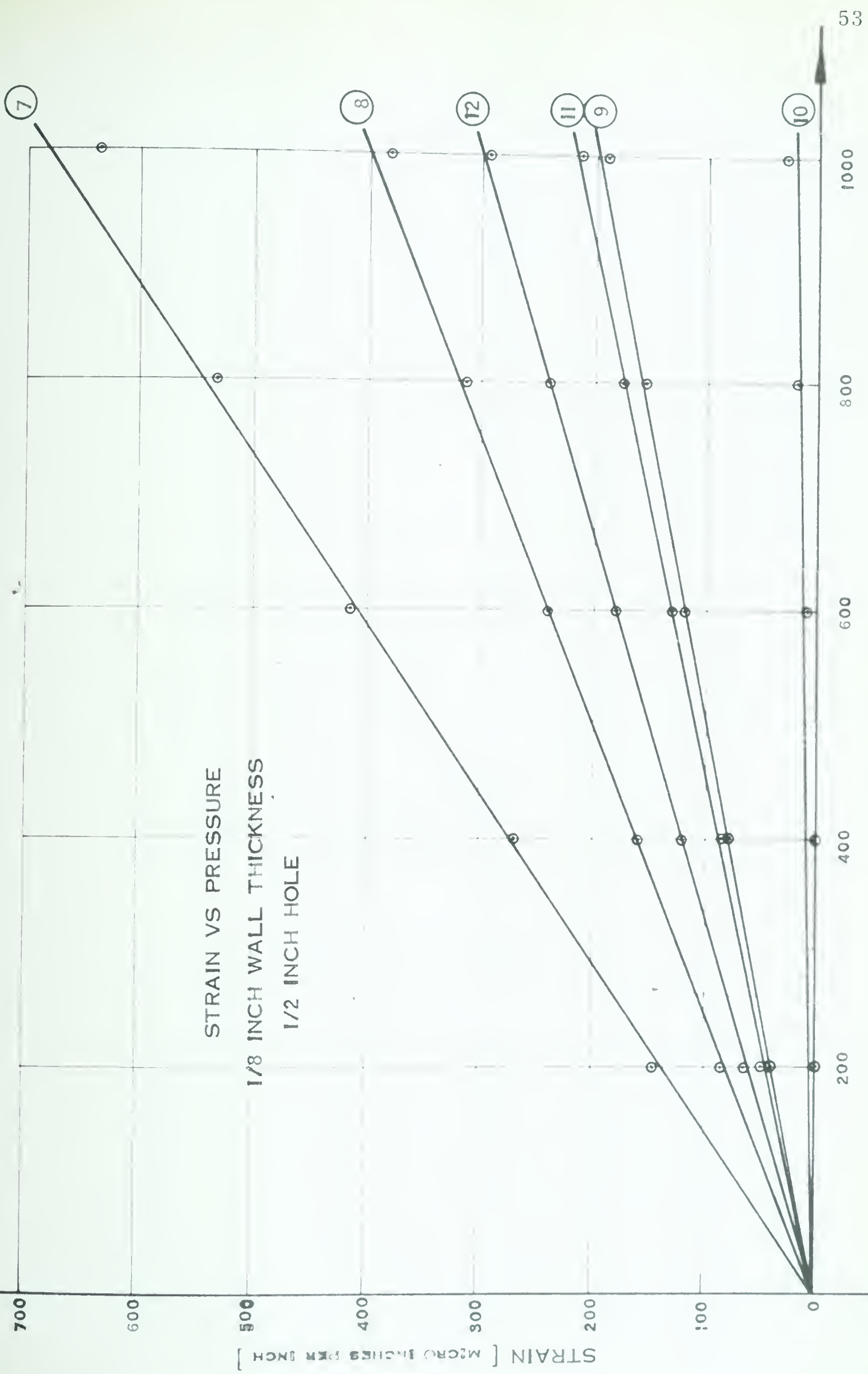


FIGURE 29.

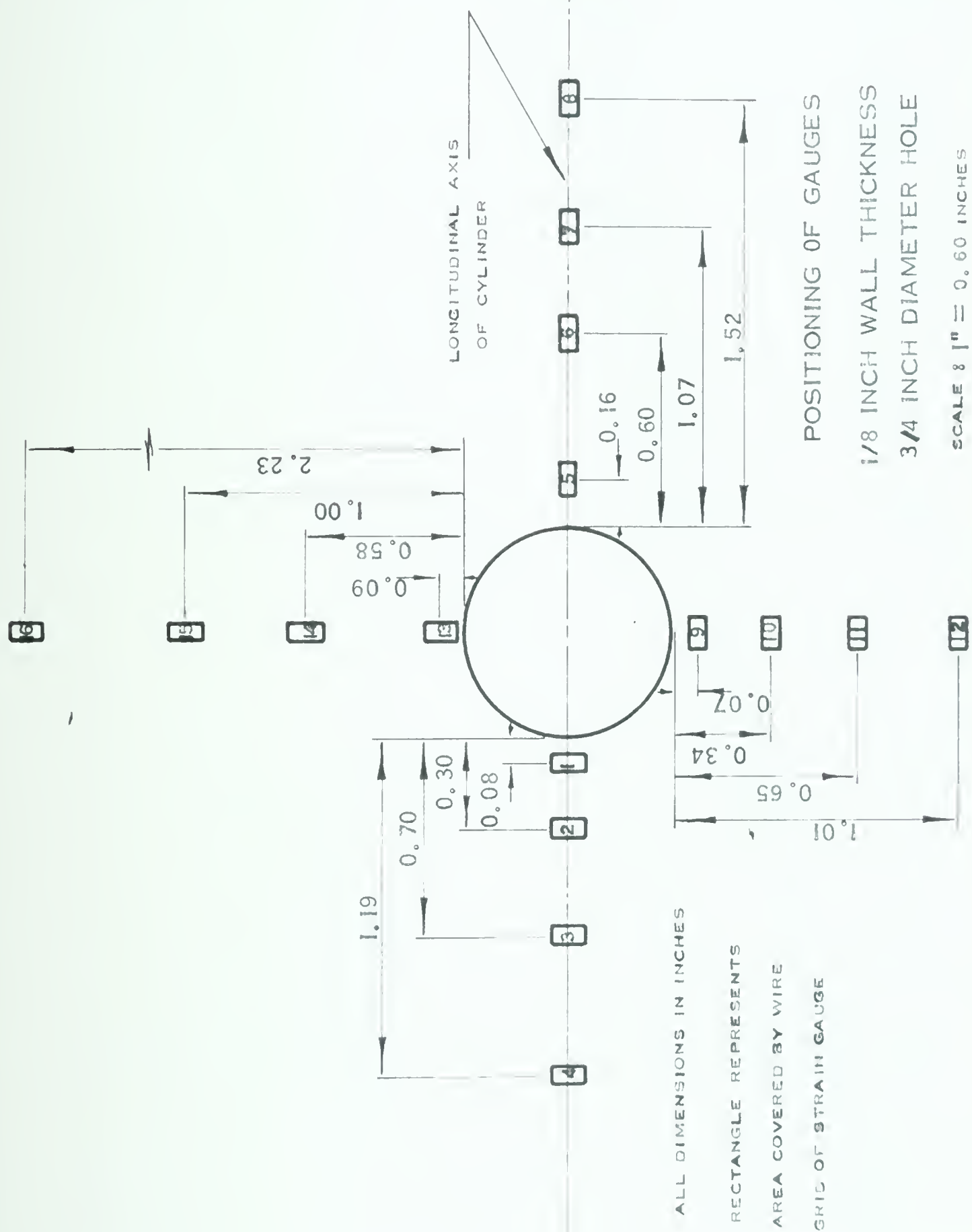


FIGURE 30.

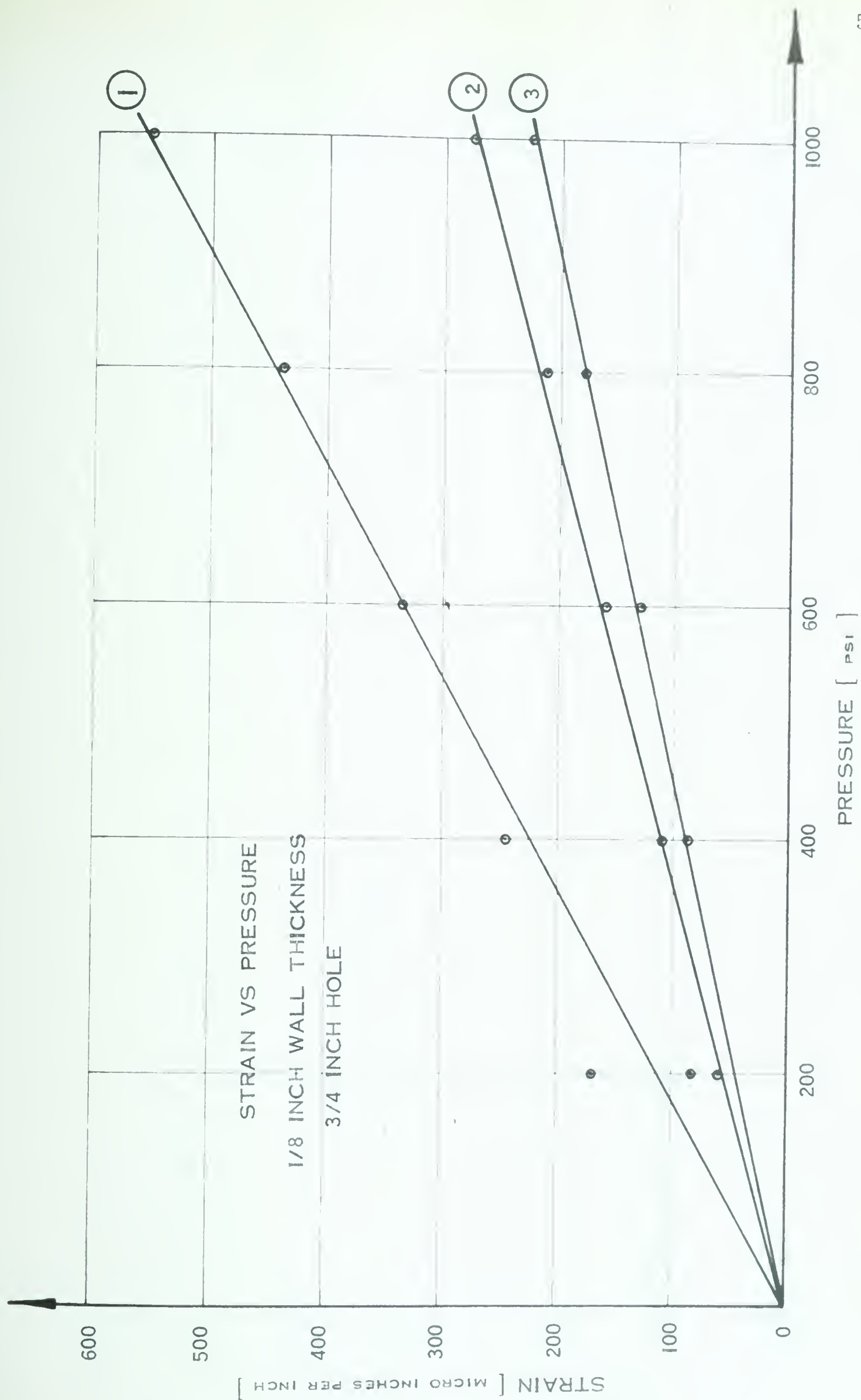


FIGURE 31.

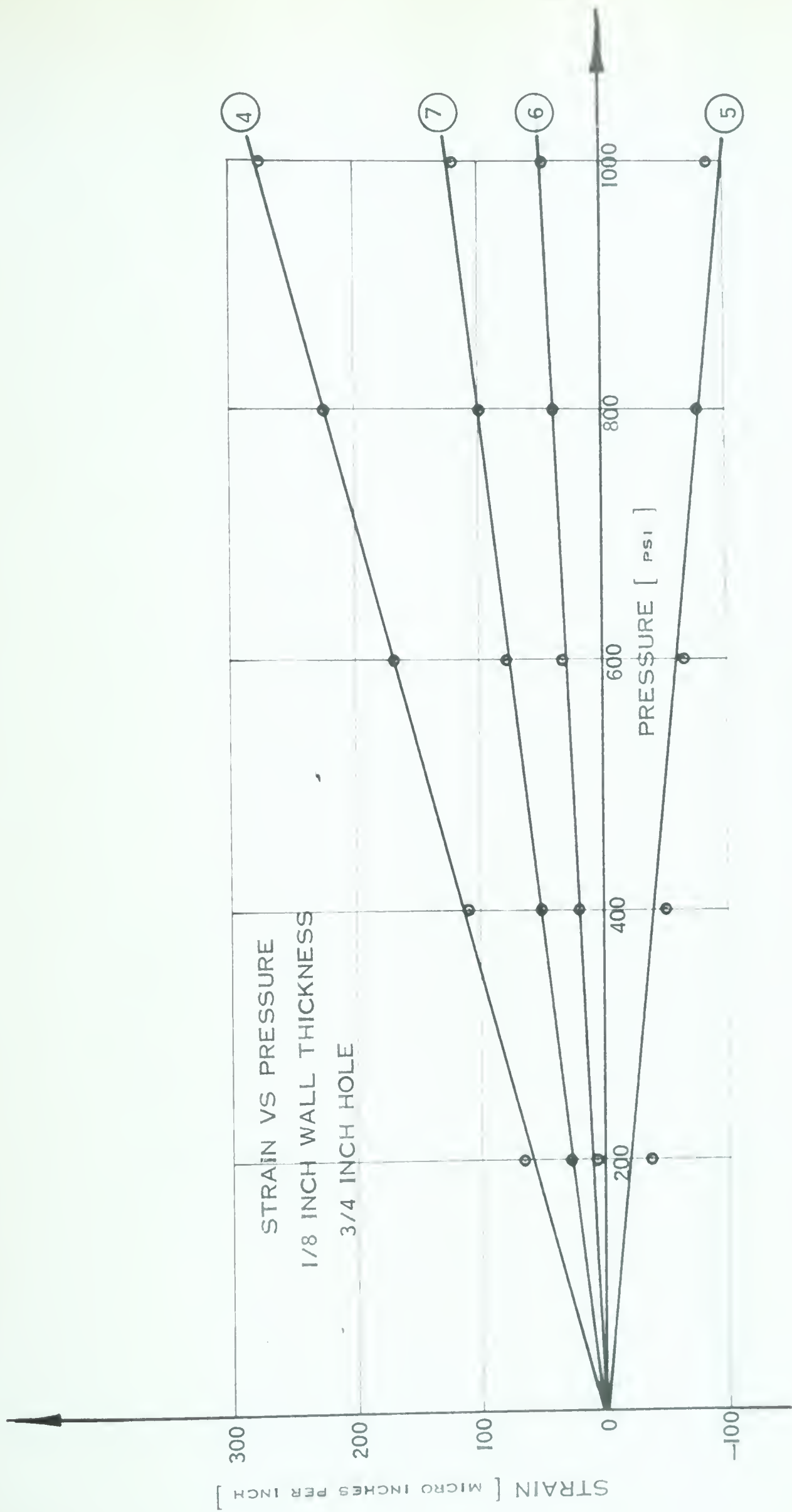


FIGURE 32.

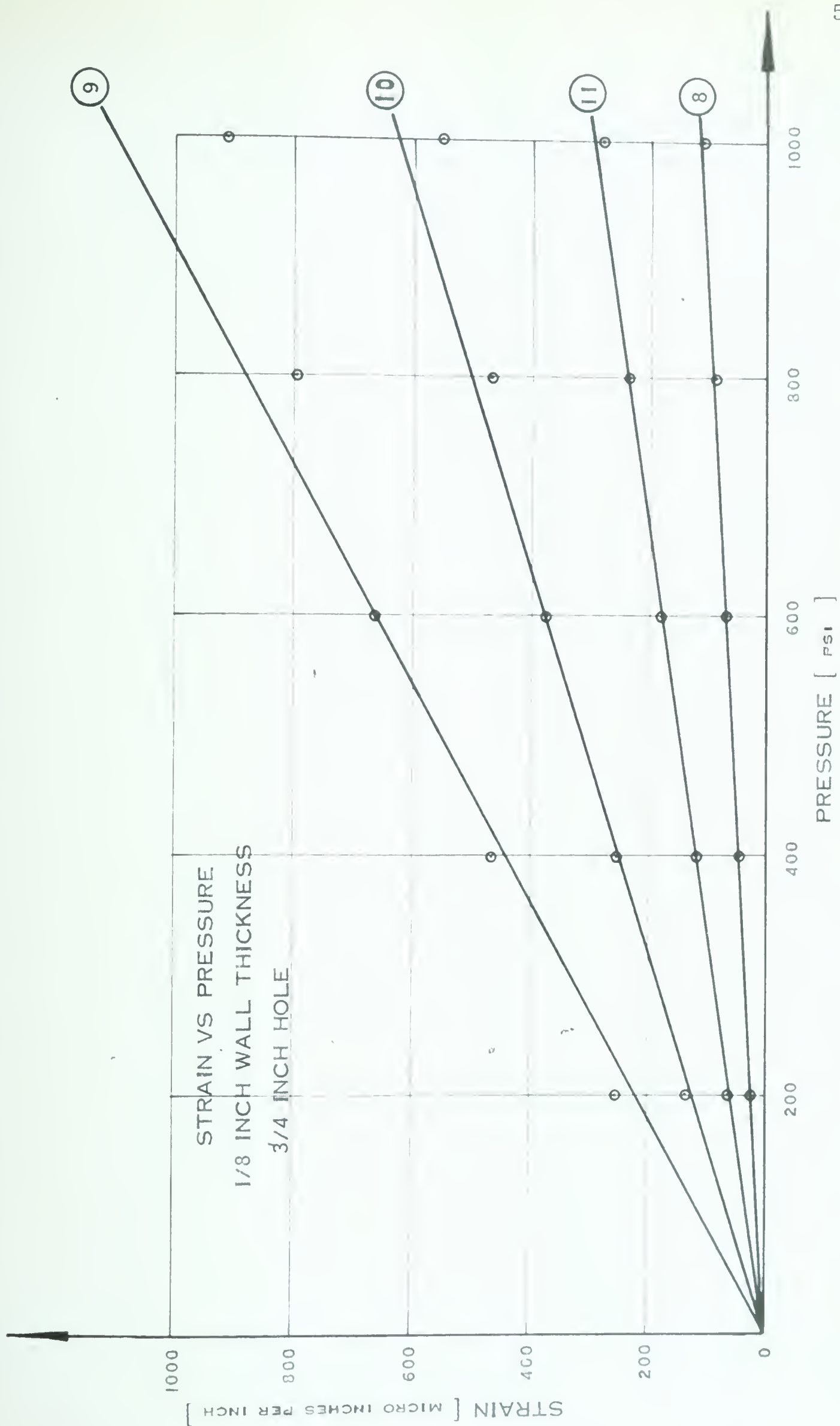


FIGURE 33.

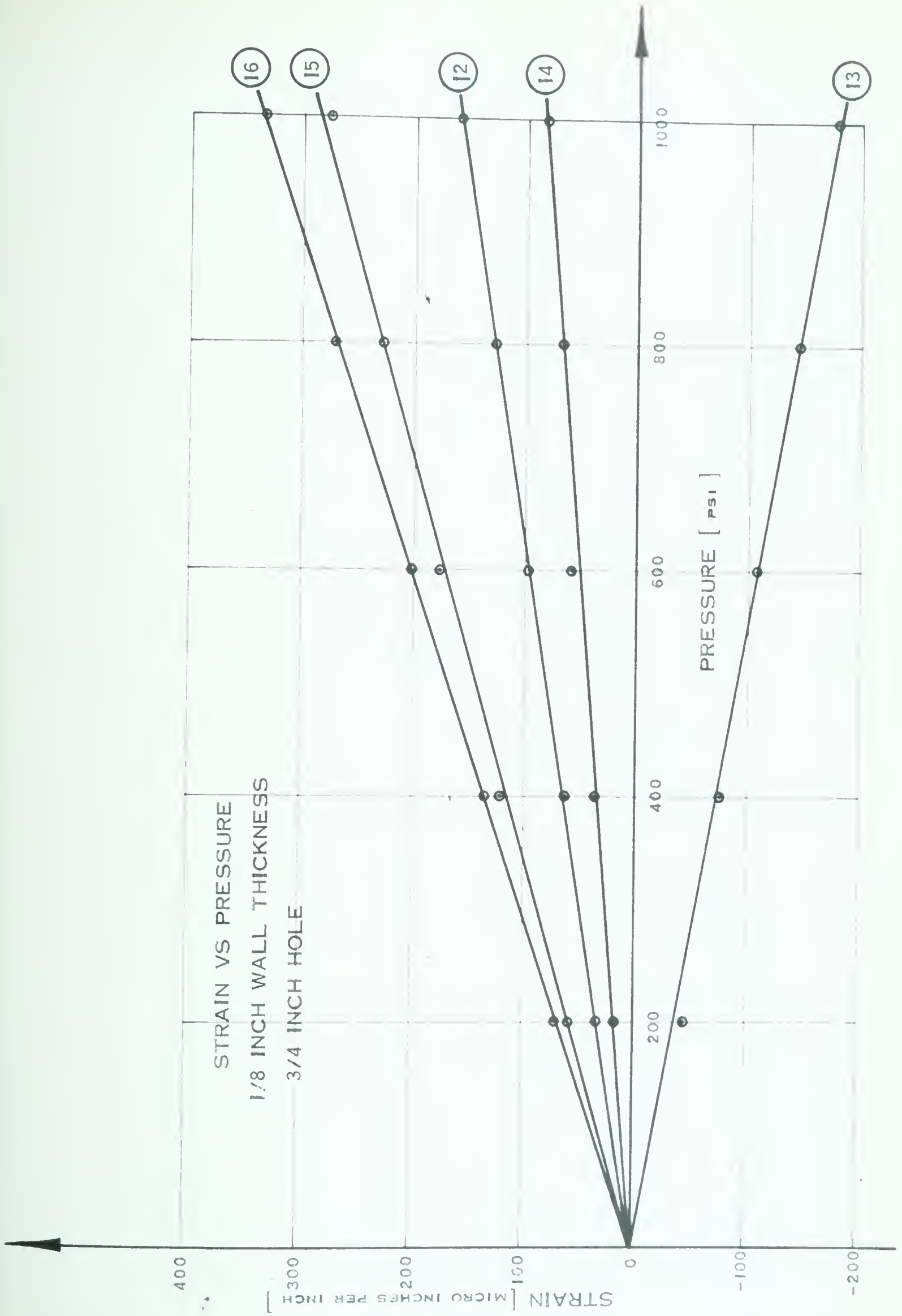


FIGURE 34.

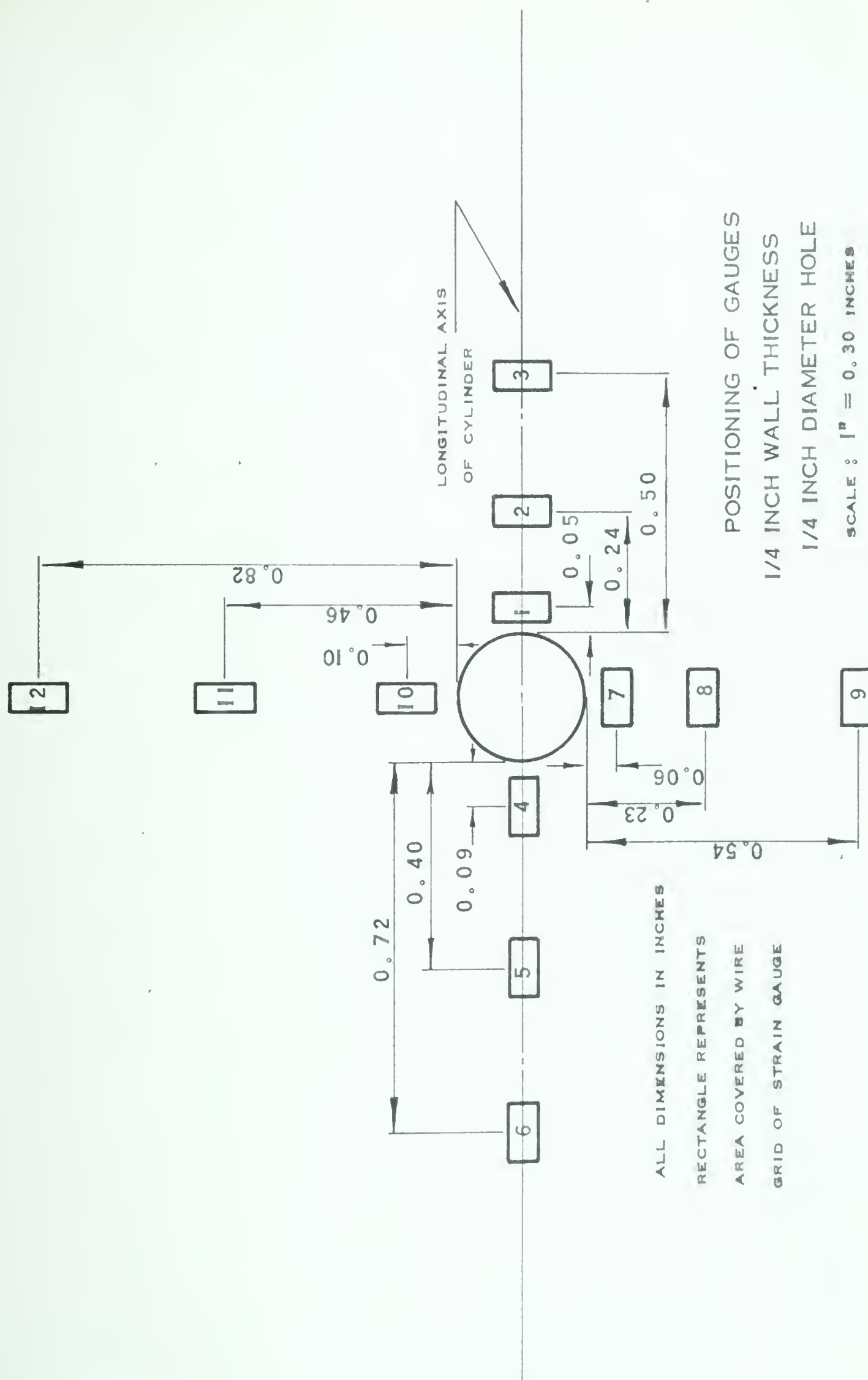


FIGURE 35.

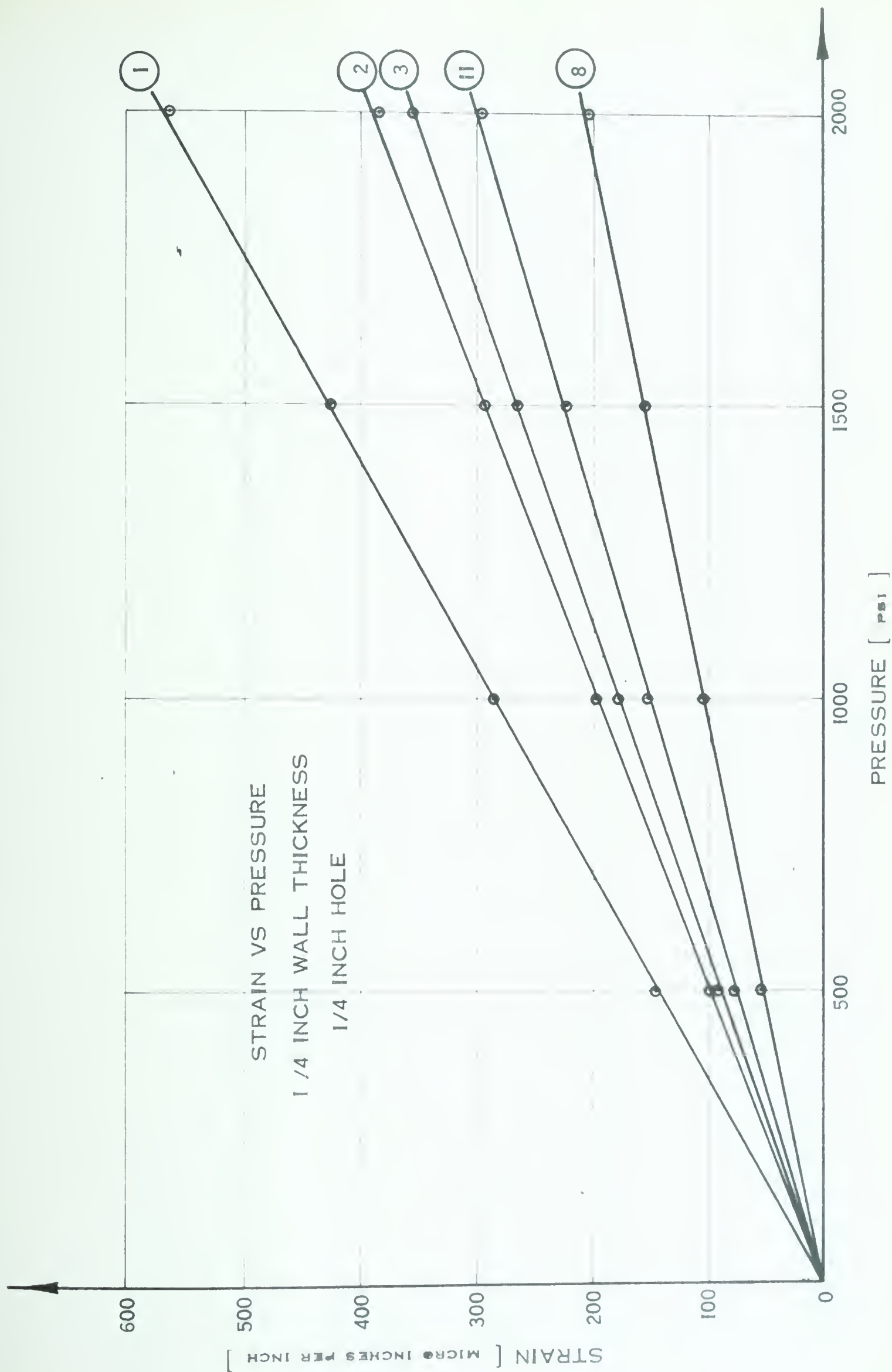


FIGURE 36.

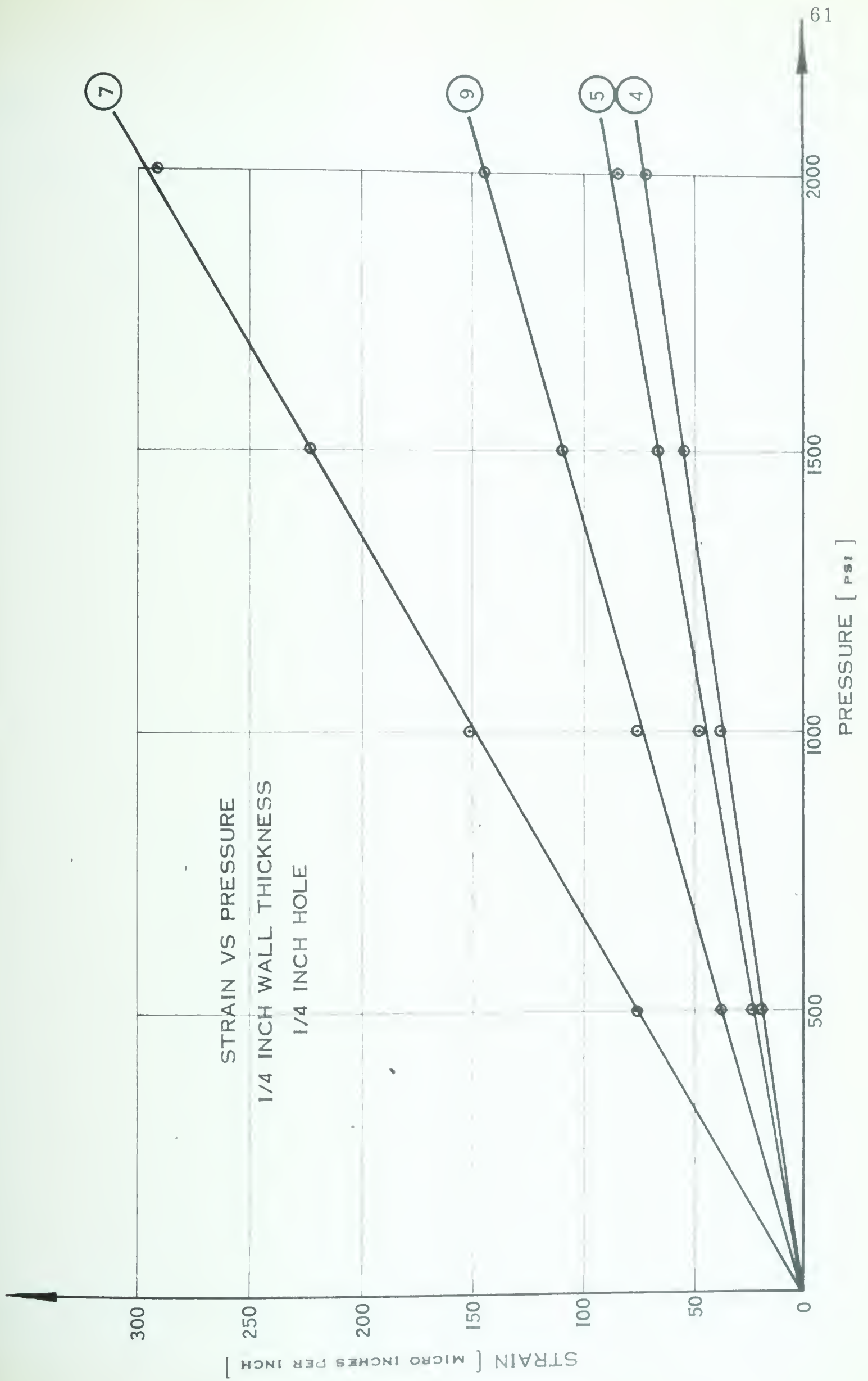


FIGURE 37.

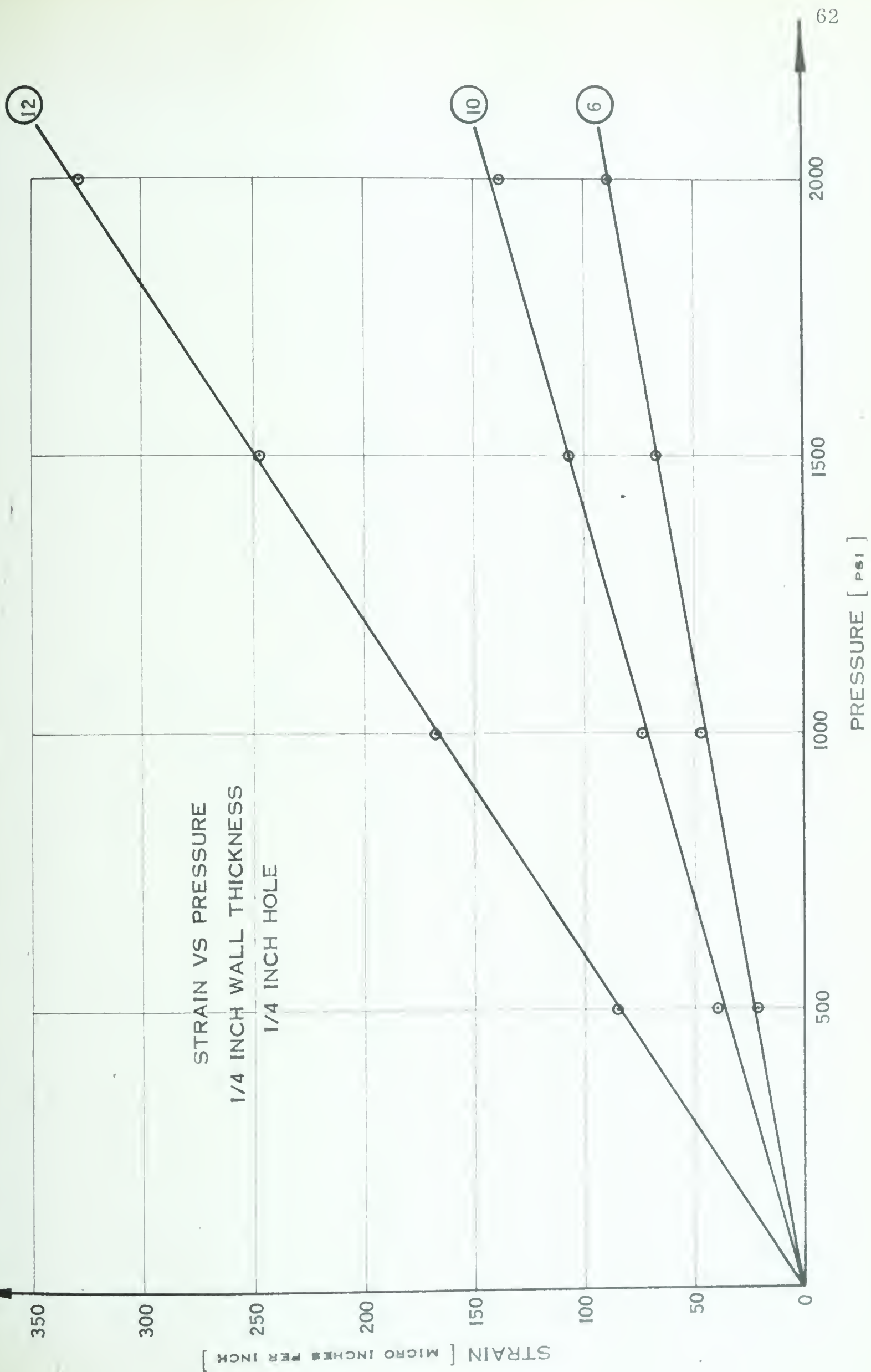


FIGURE 38.

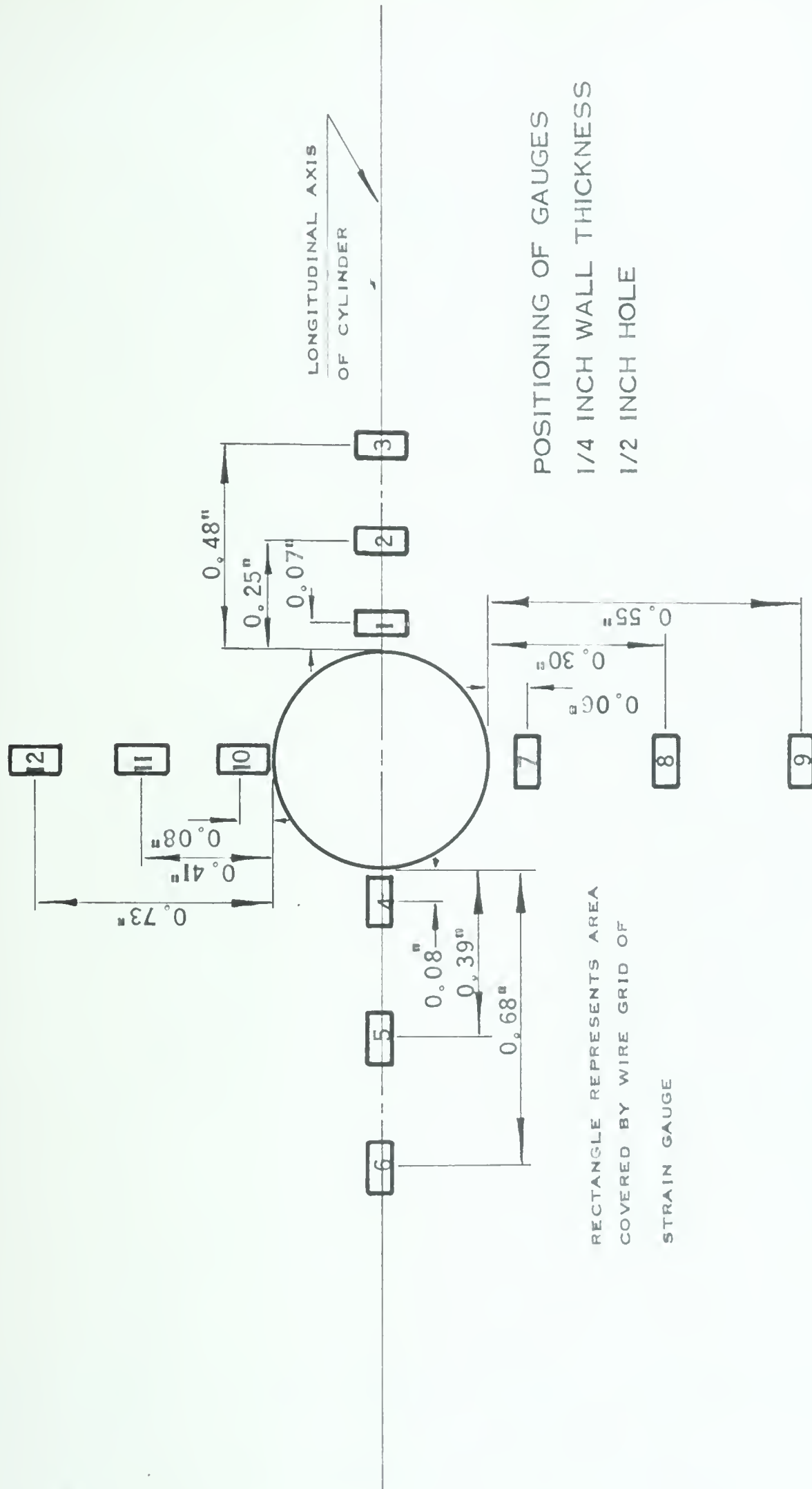


FIGURE 39.

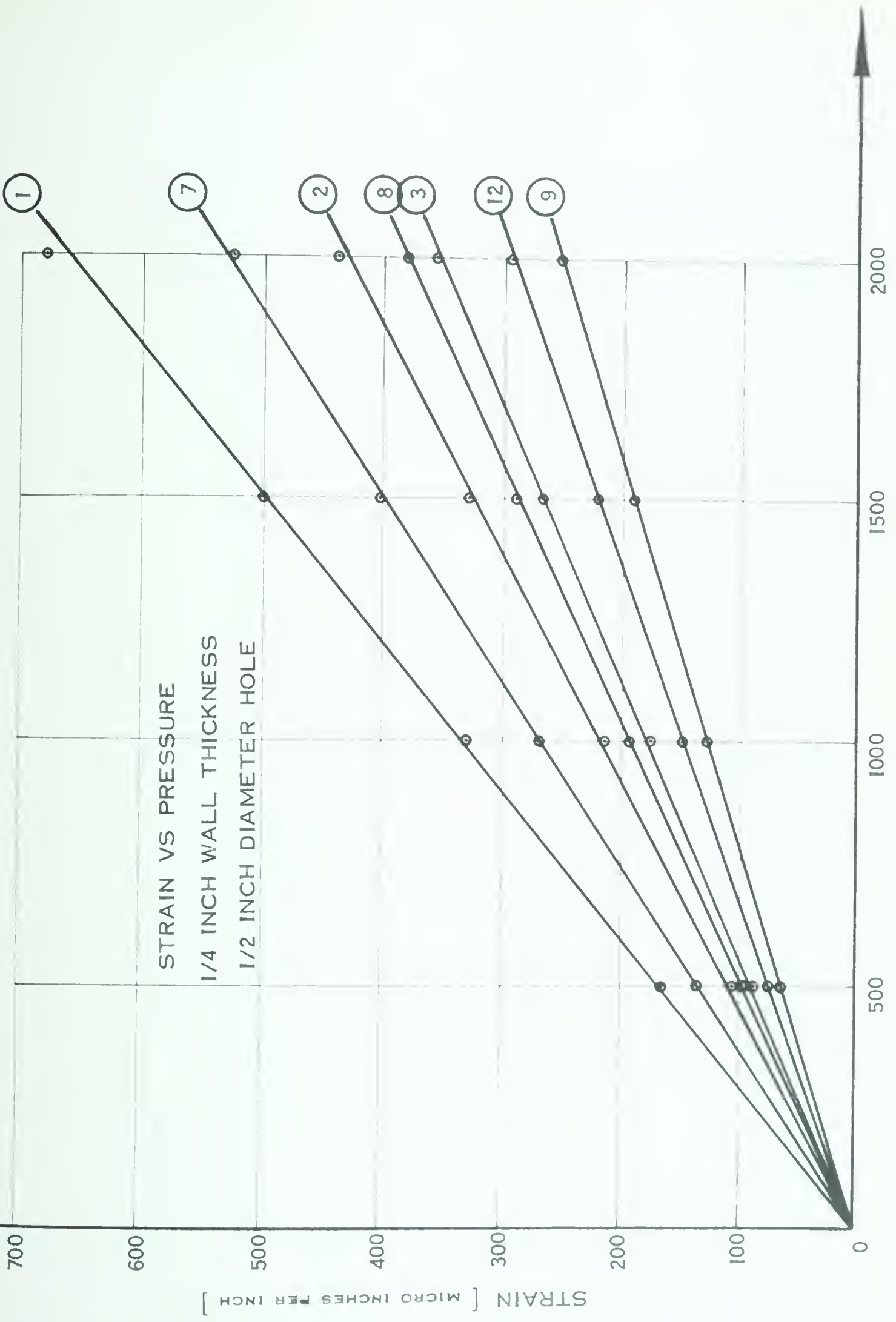


FIGURE 40.

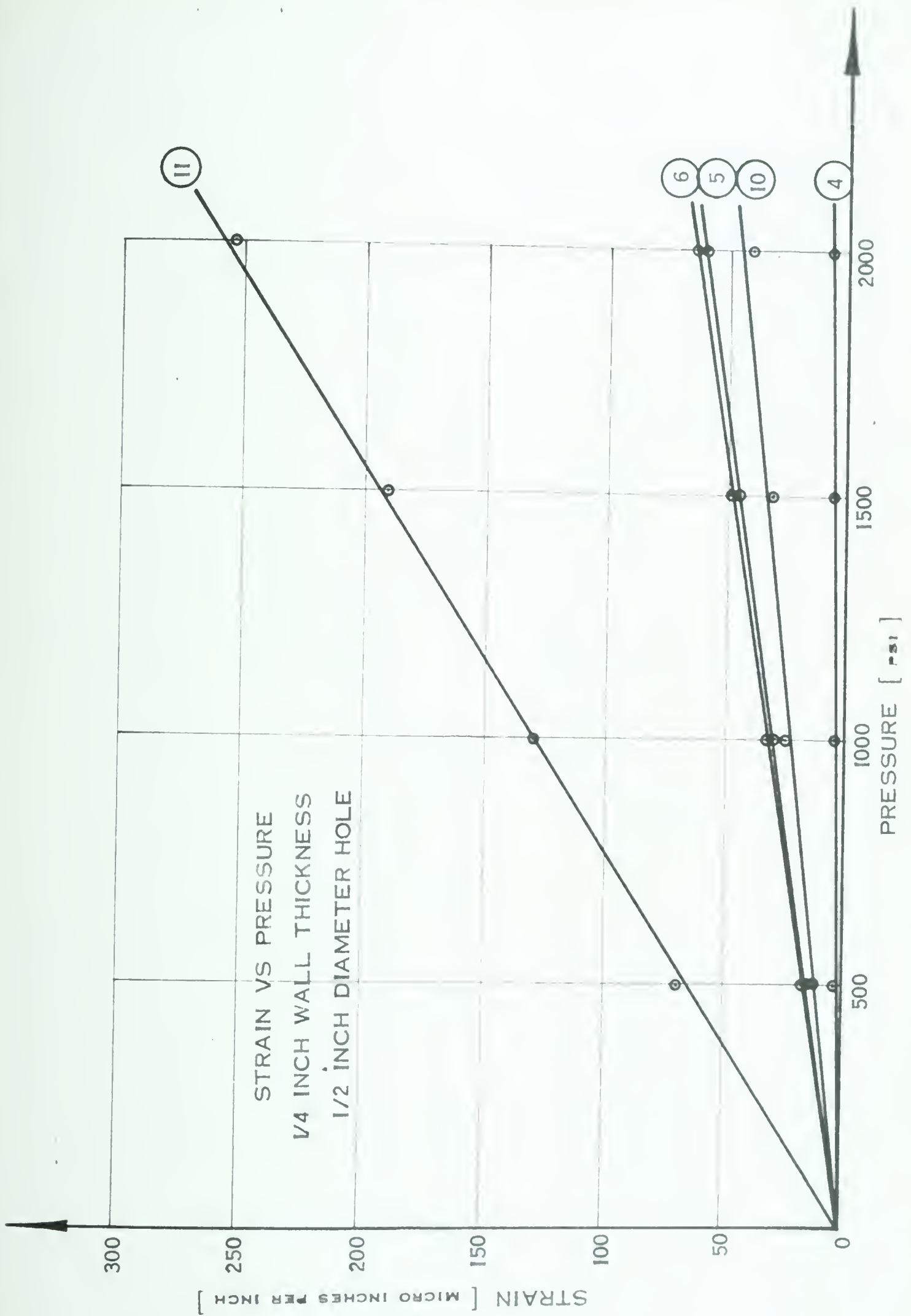


FIGURE 41.

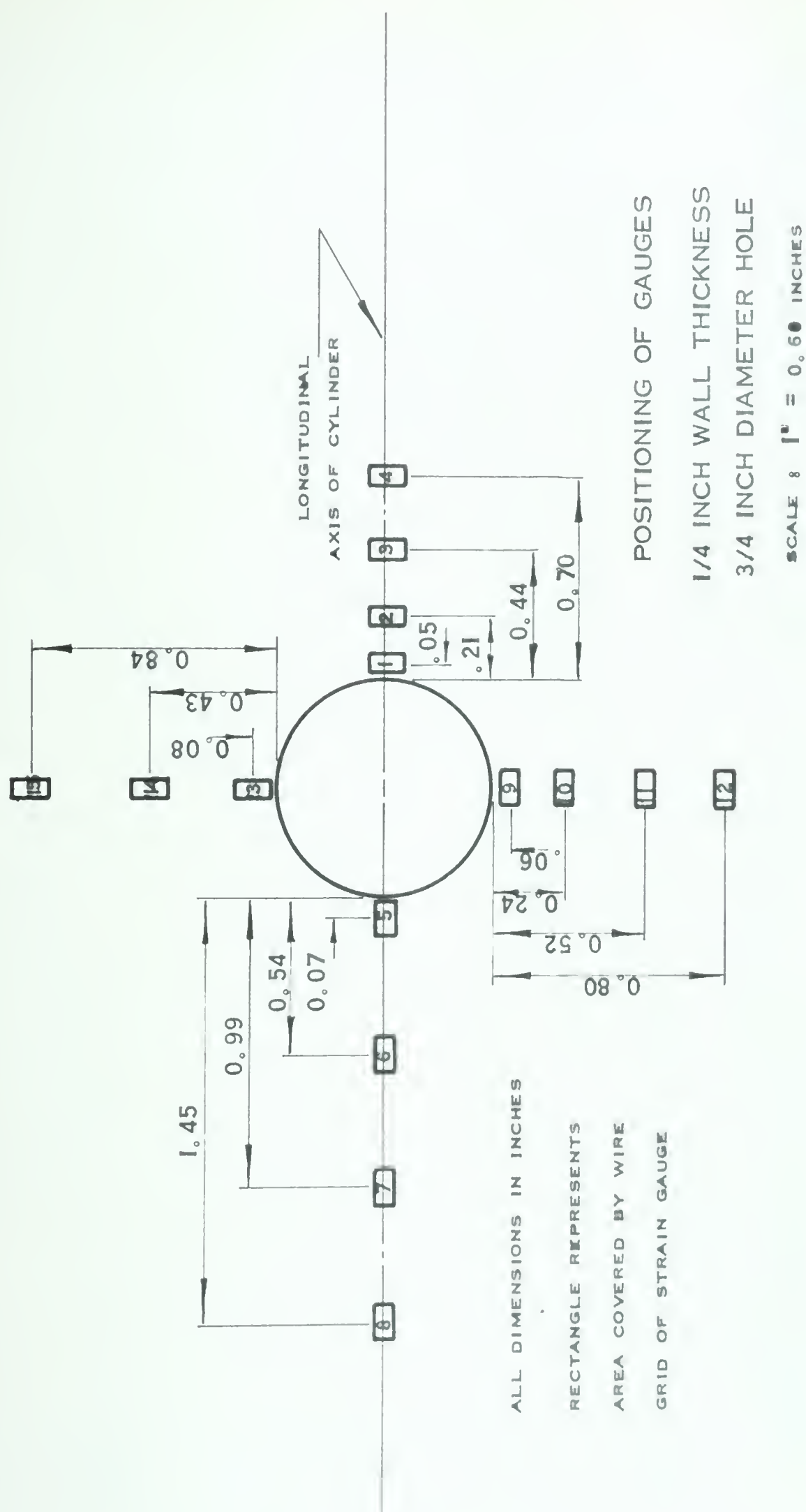


FIGURE 42.

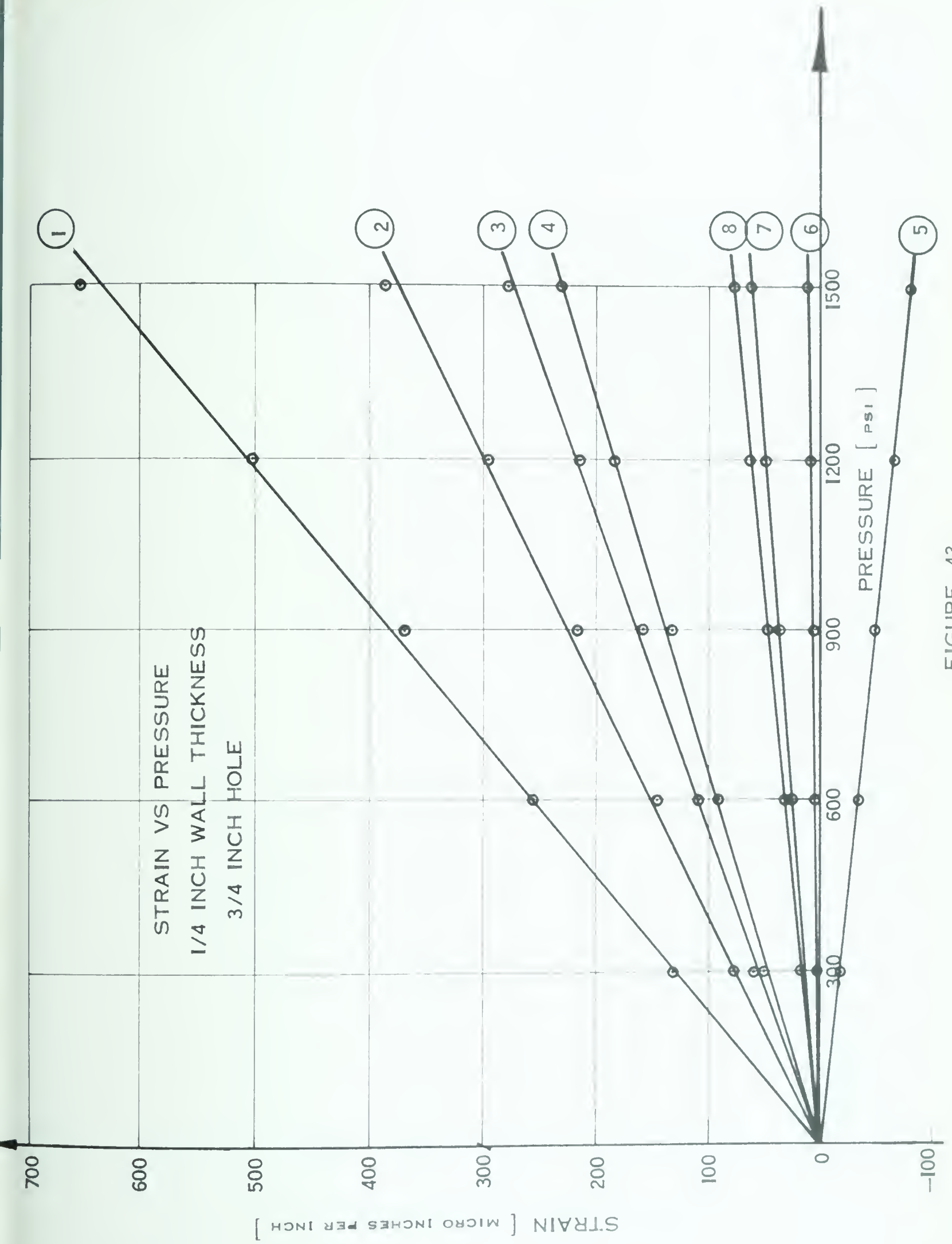


FIGURE 43.

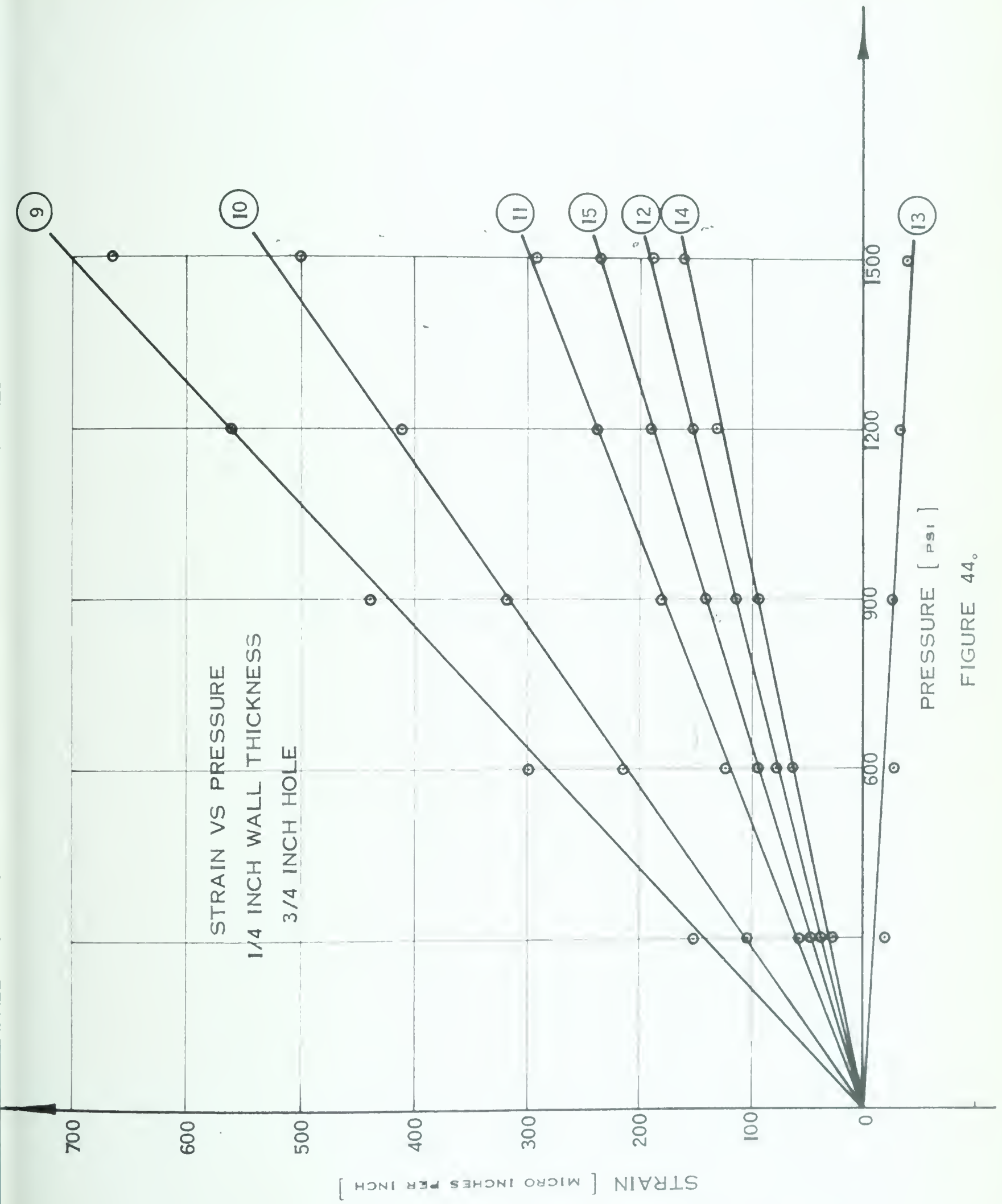


FIGURE 44.

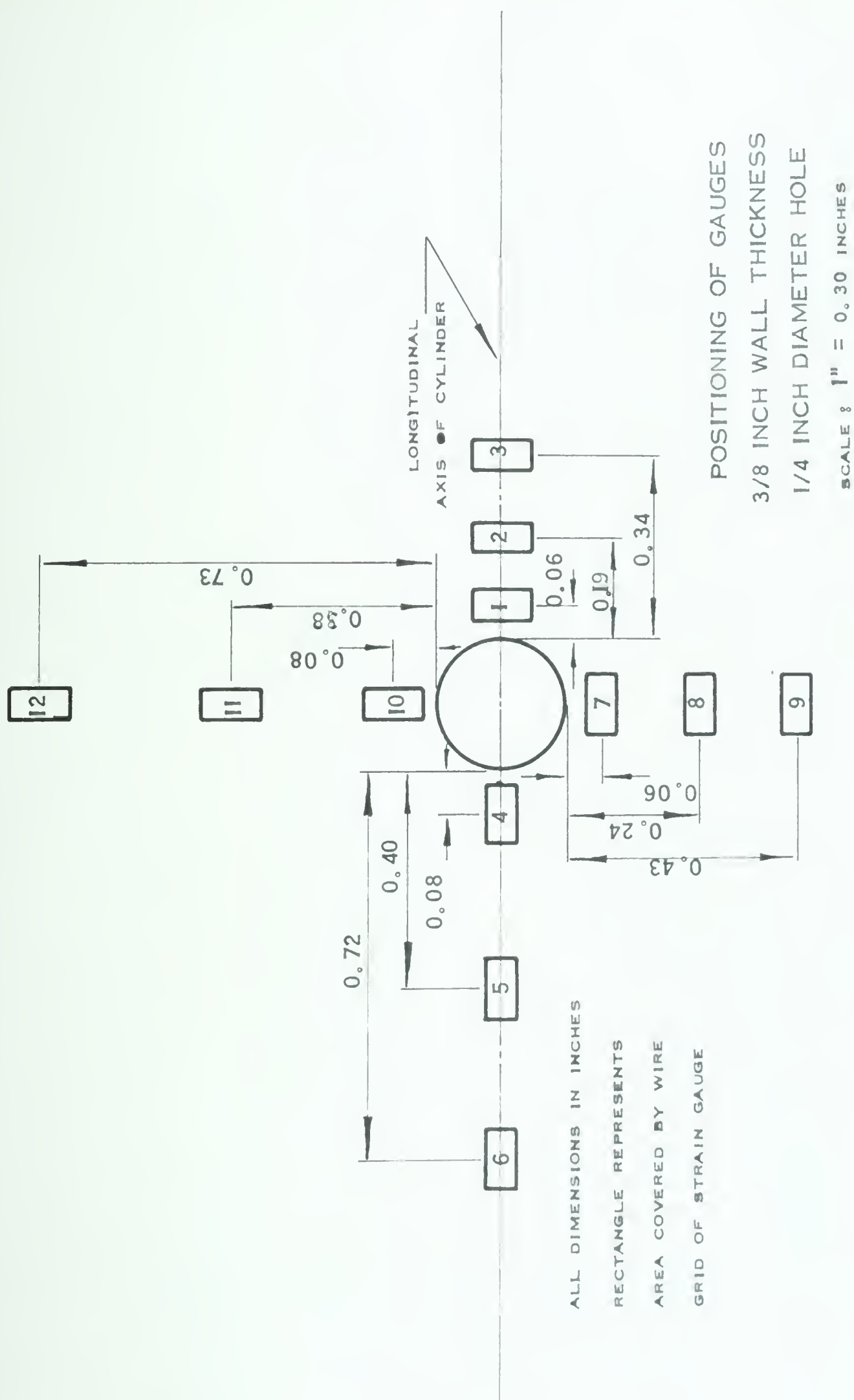


FIGURE 45.

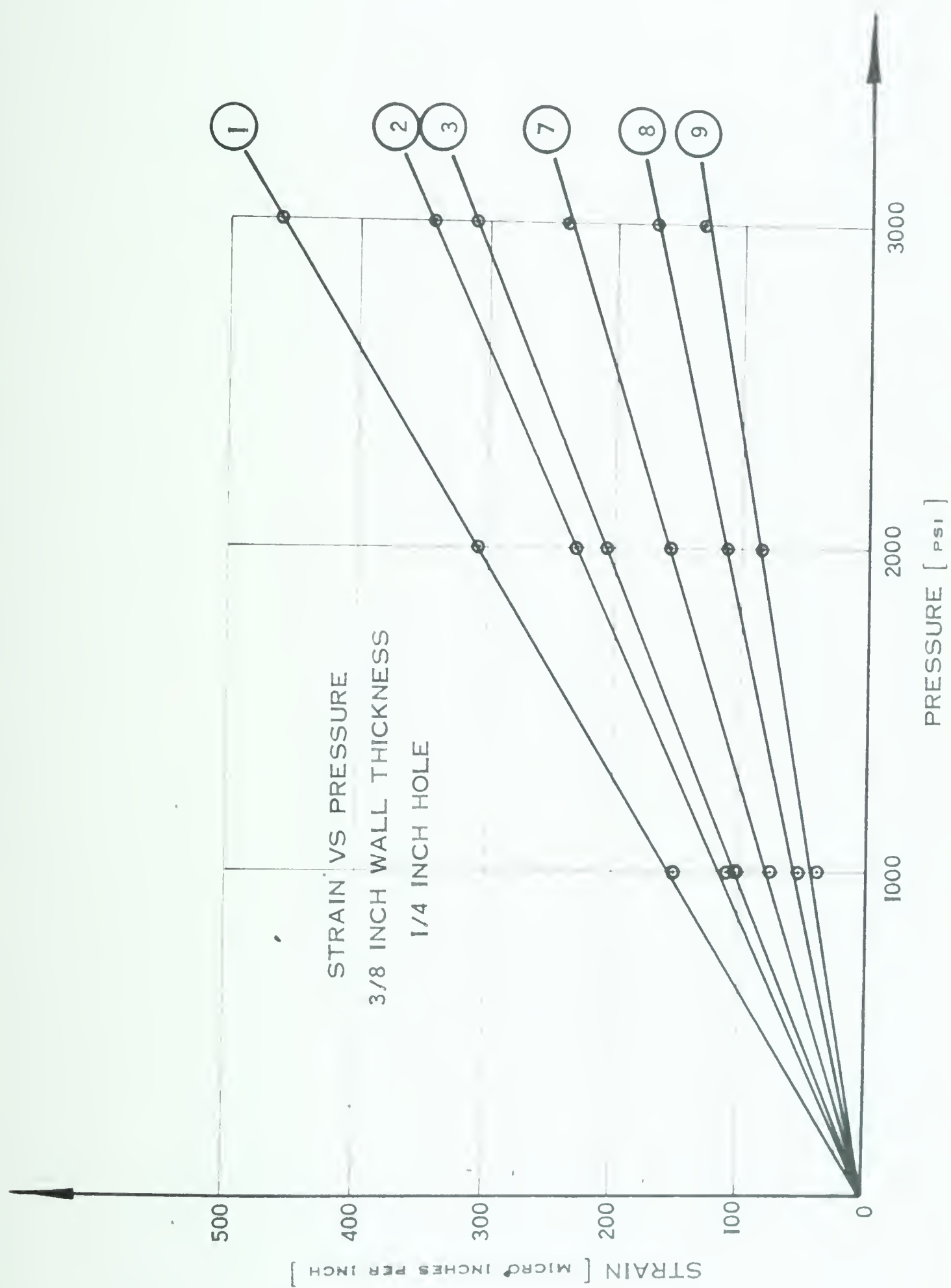


FIGURE 46.

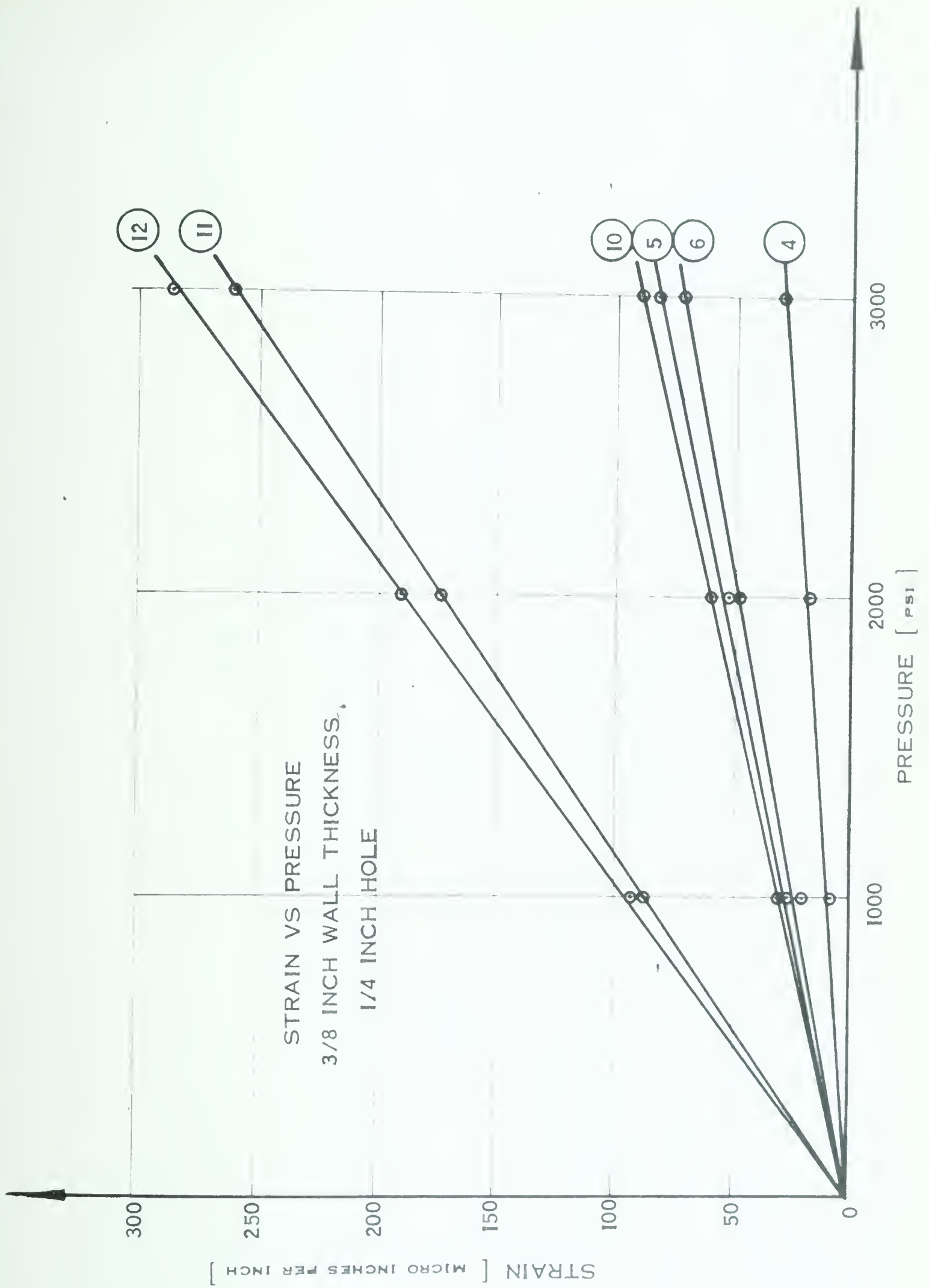


FIGURE 47.

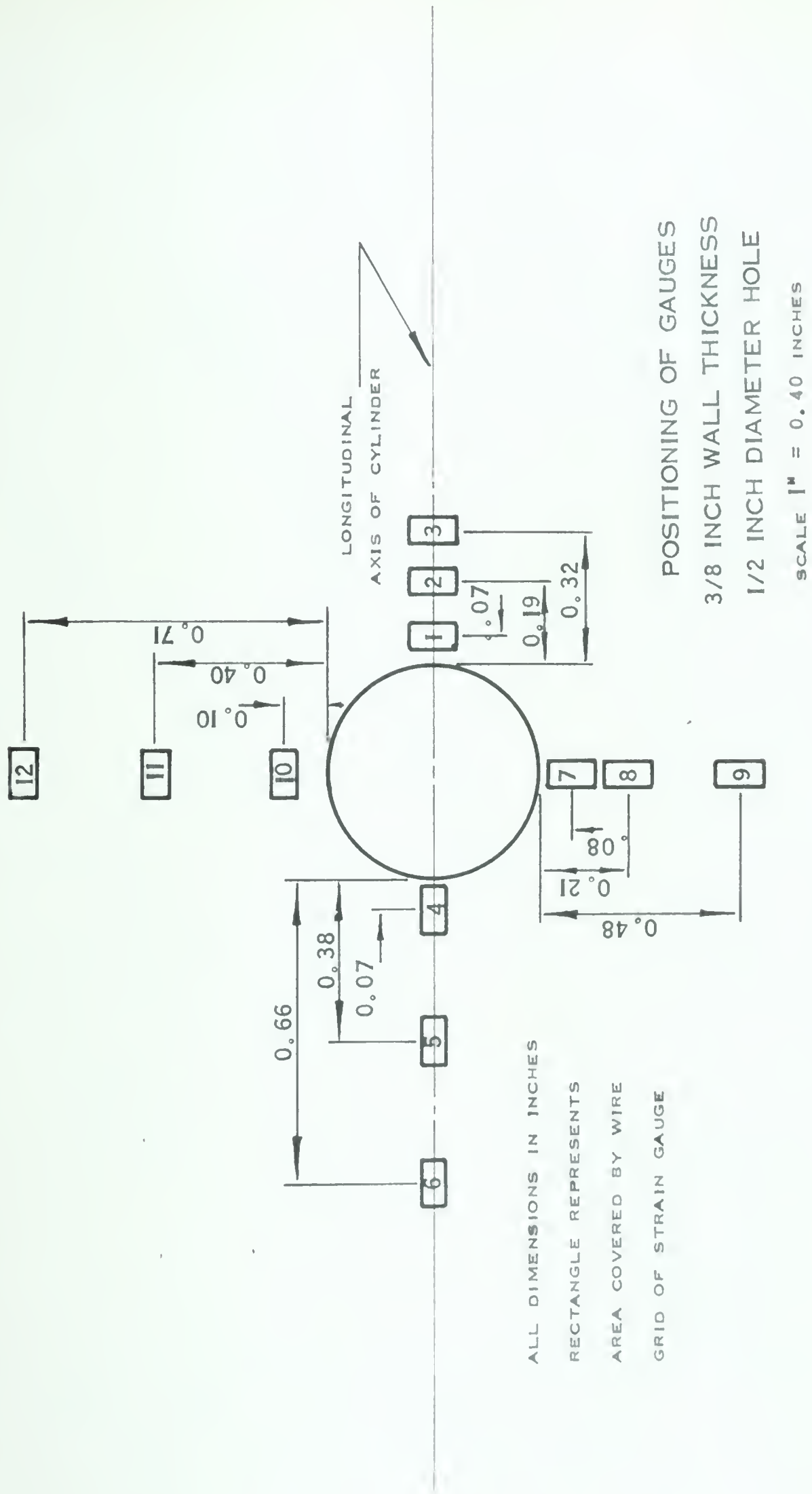


FIGURE 48.

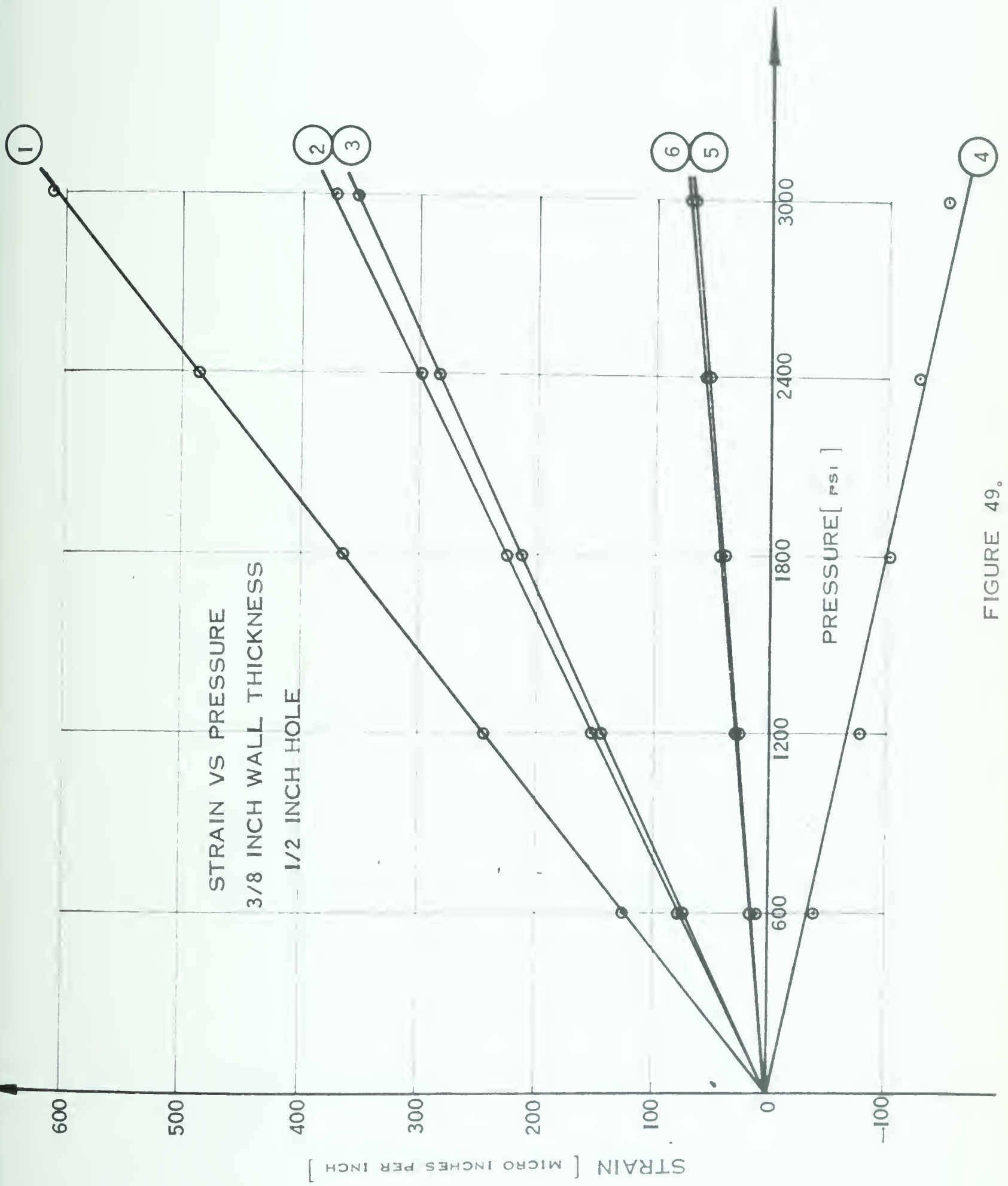


FIGURE 49.

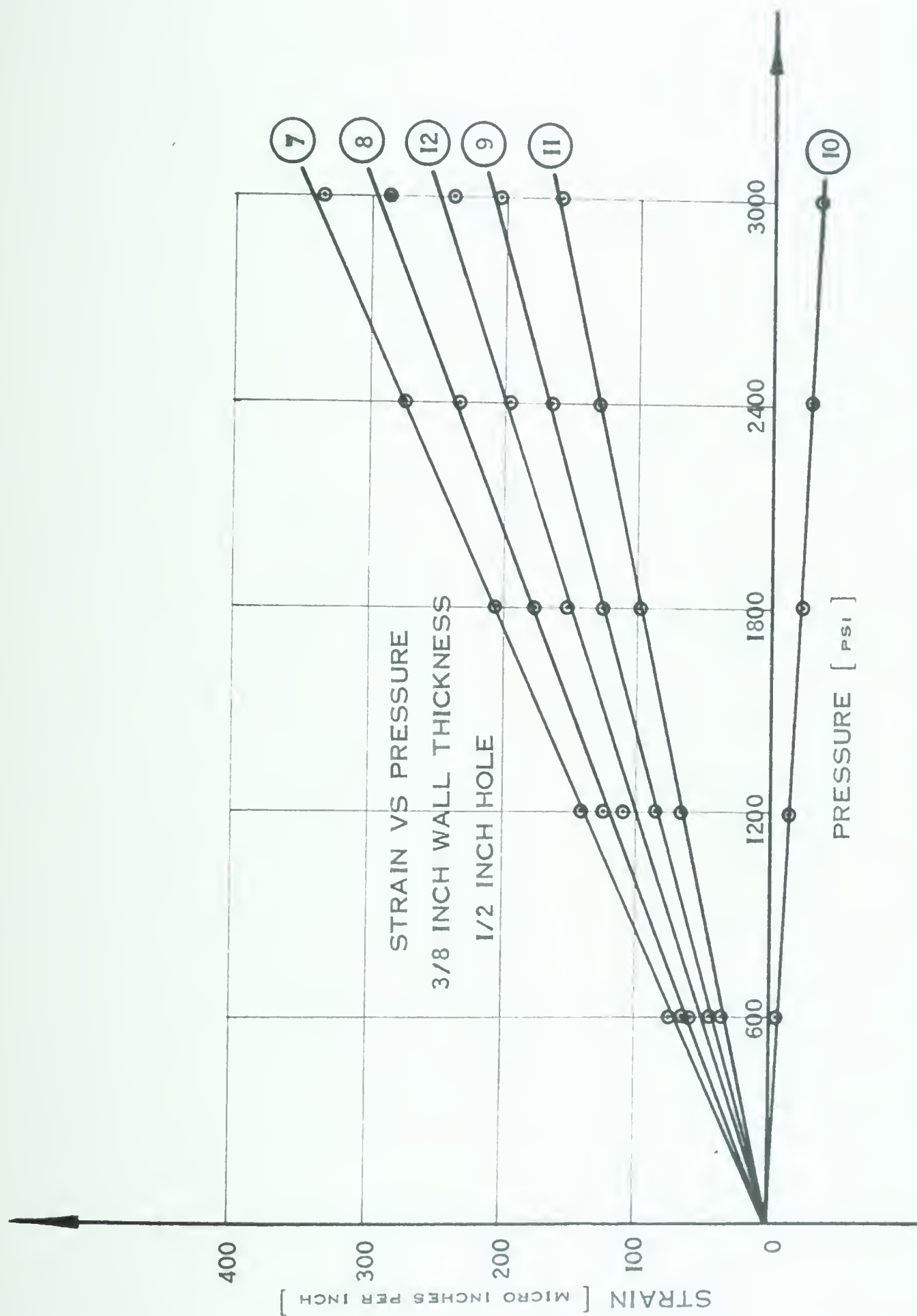


FIGURE 50.

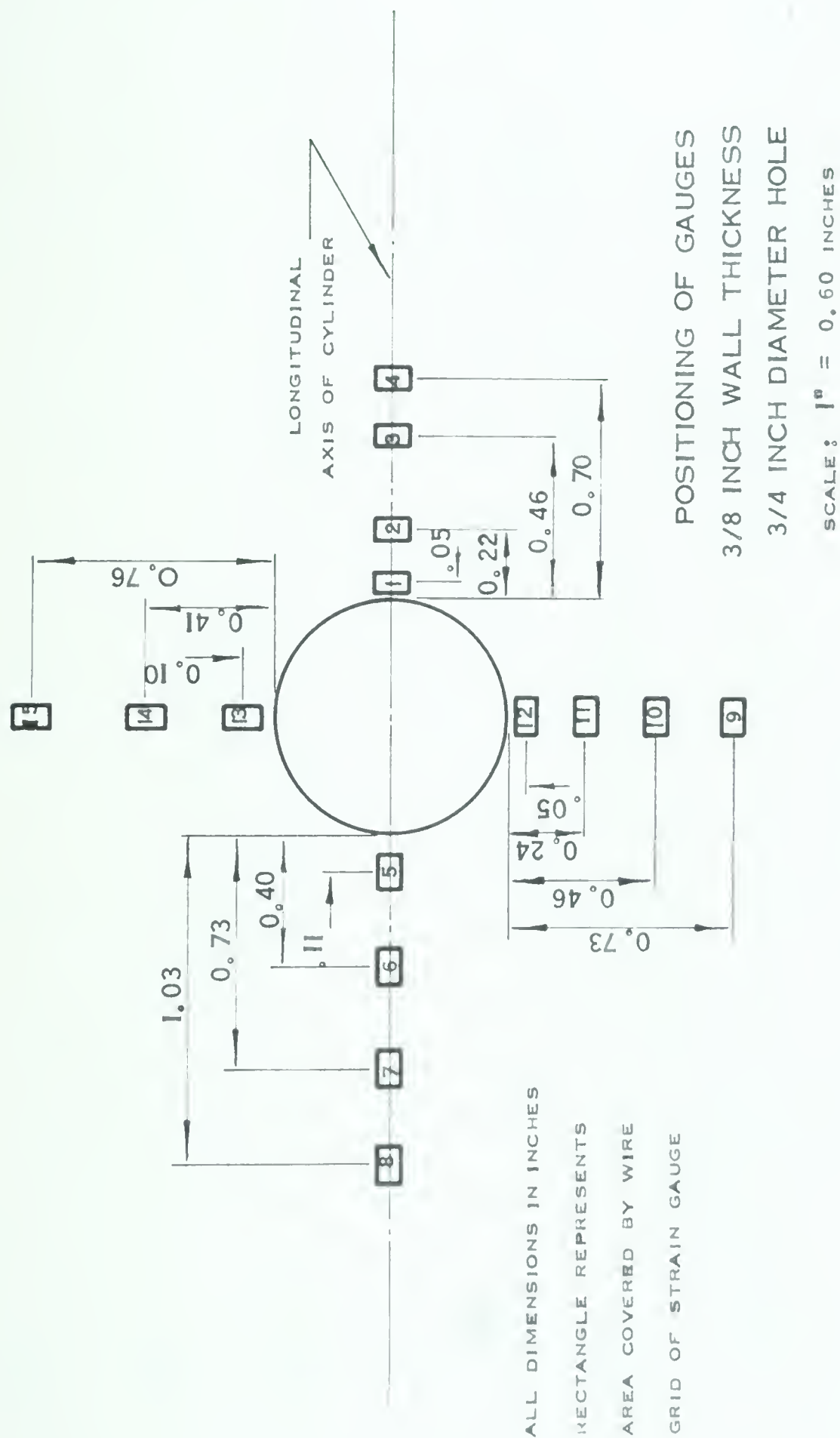


FIGURE 51.

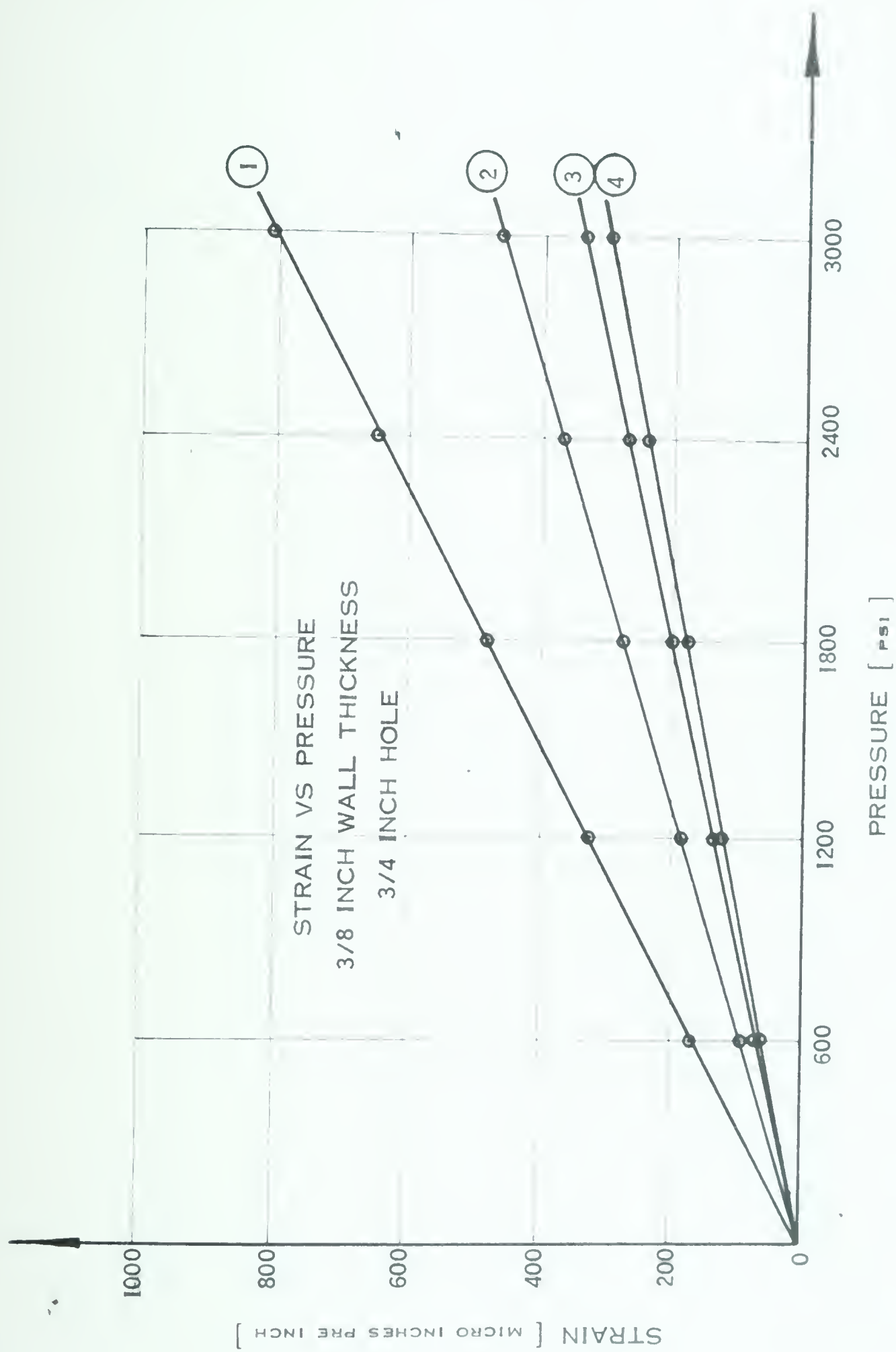


FIGURE 52.

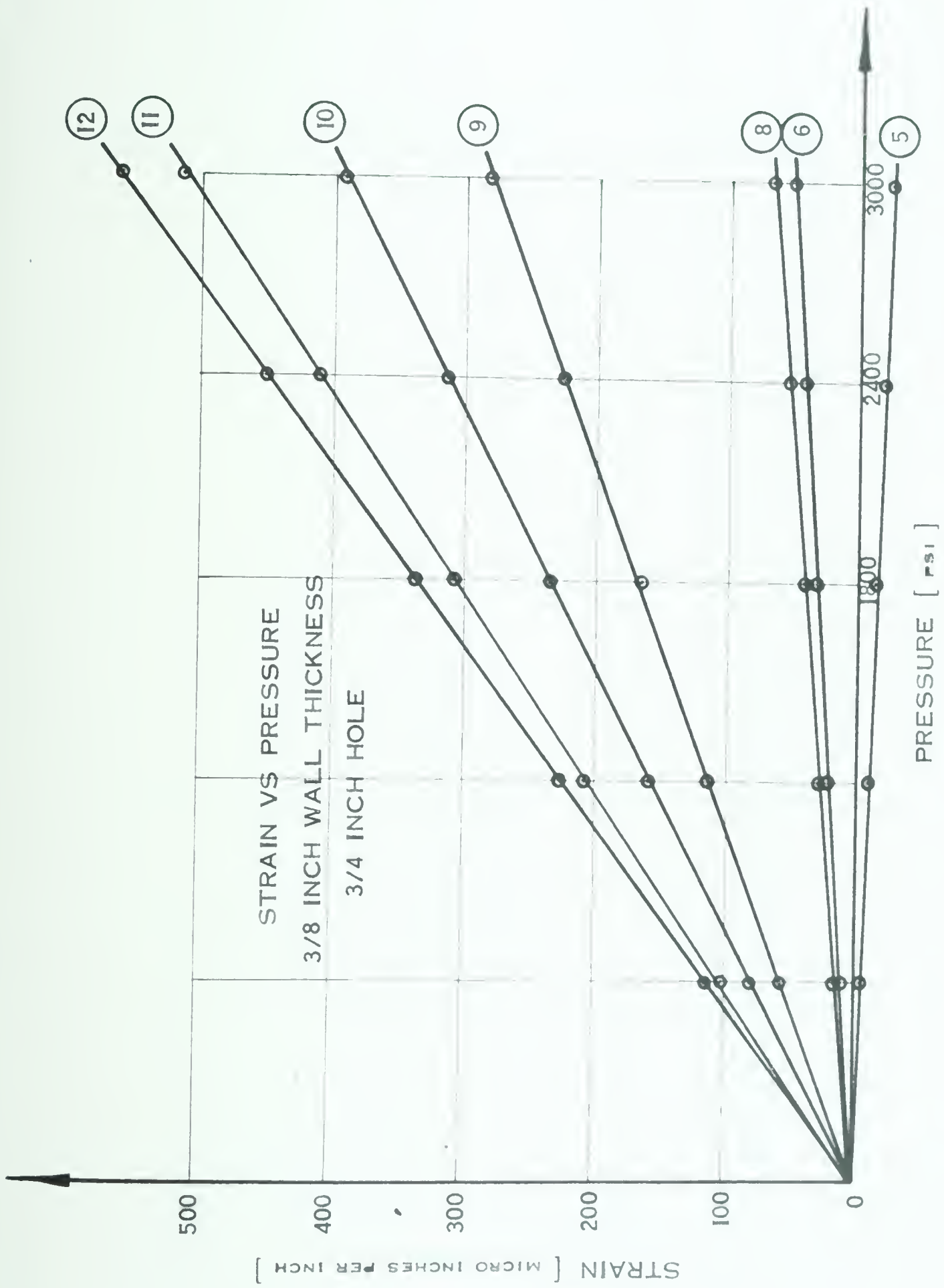


FIGURE 53.

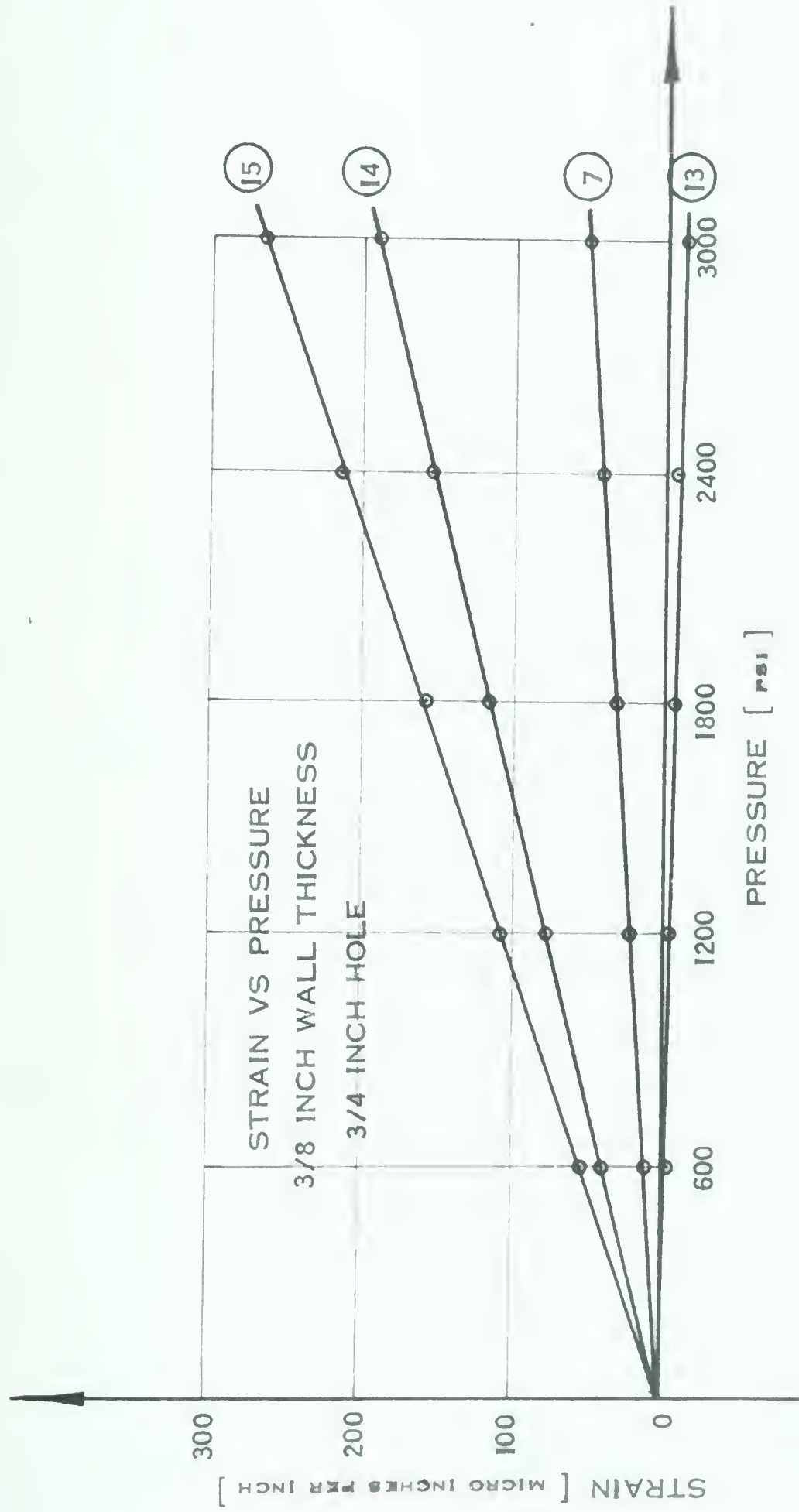


FIGURE 54.

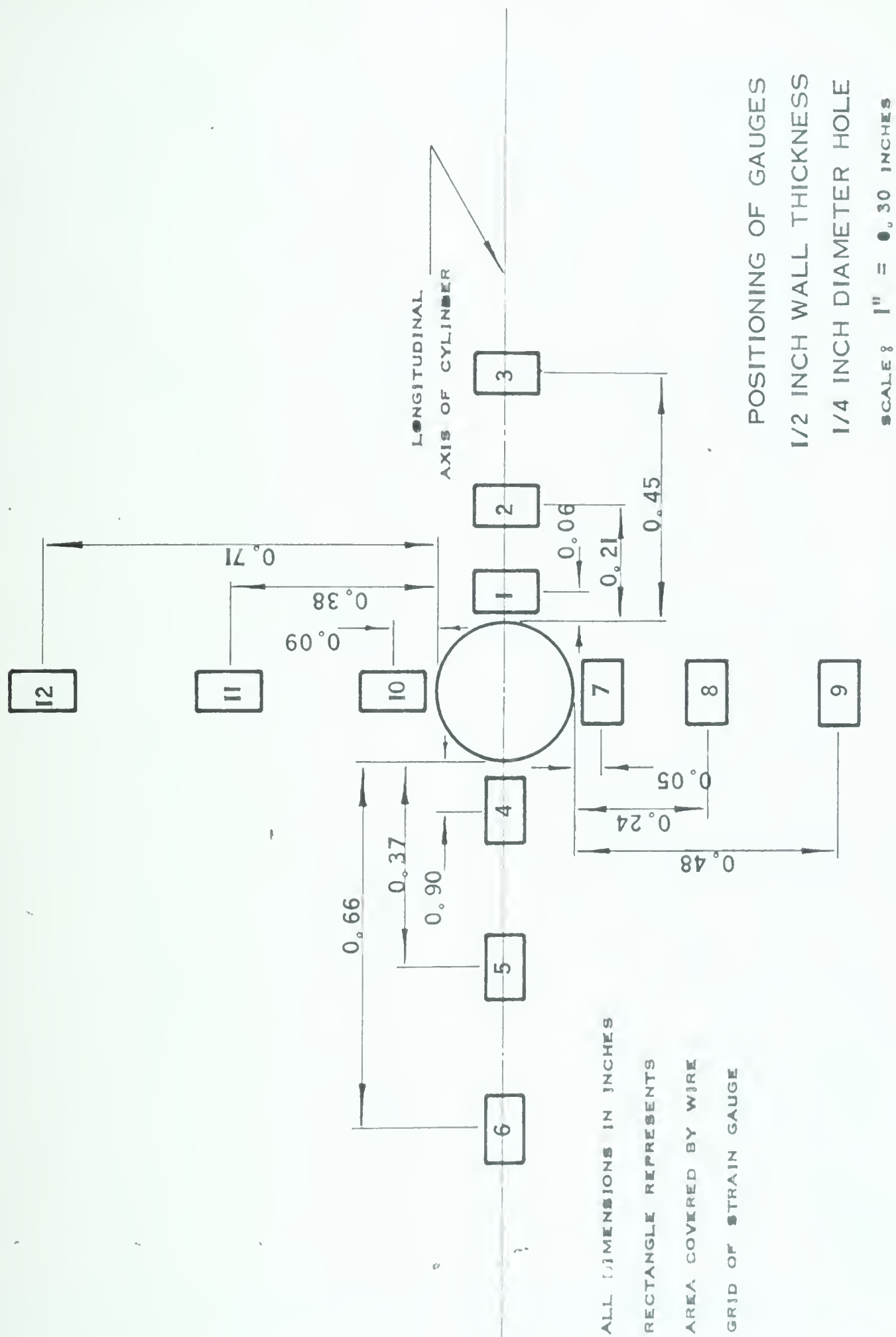


FIGURE 55.

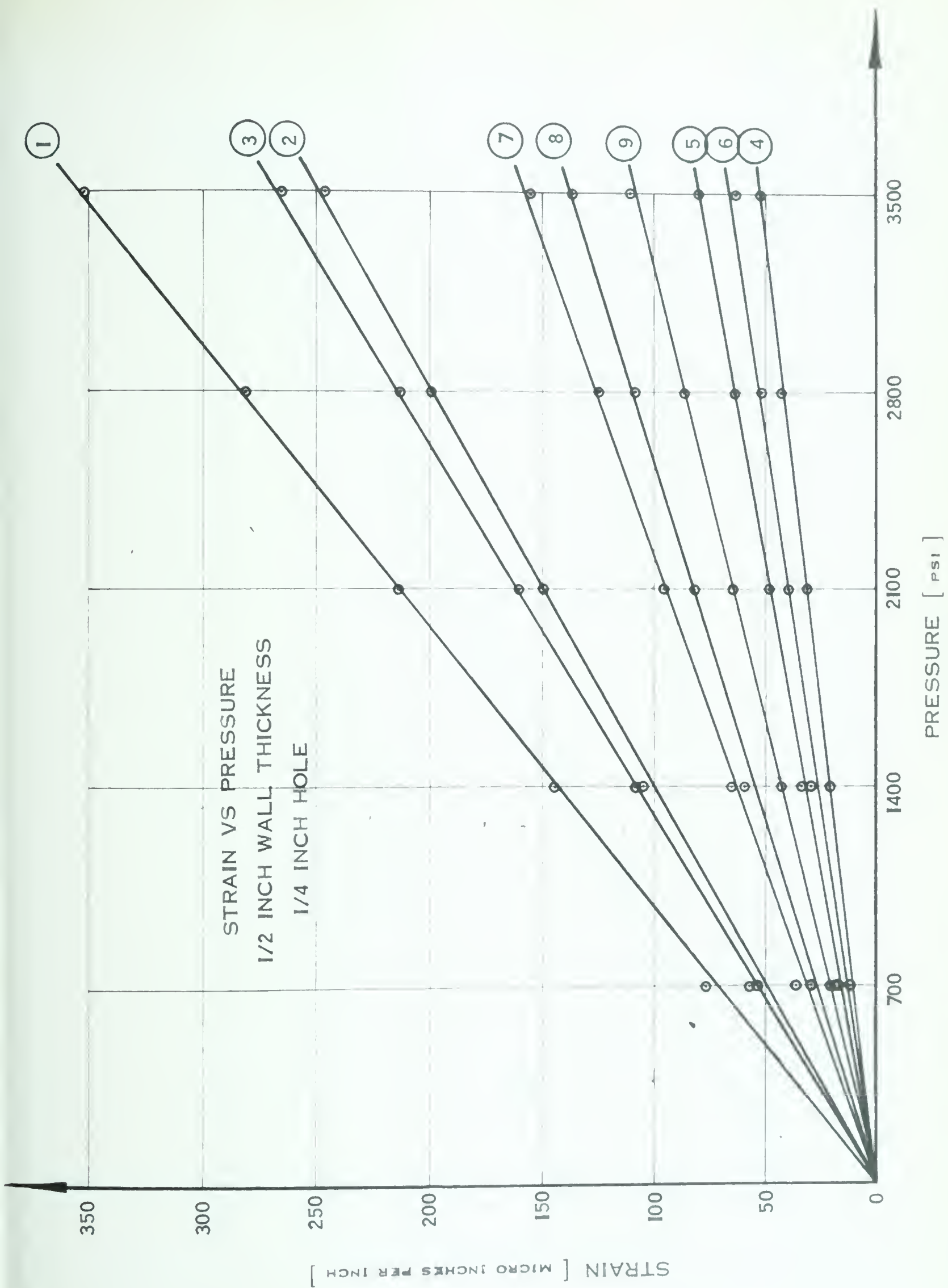


FIGURE 56.

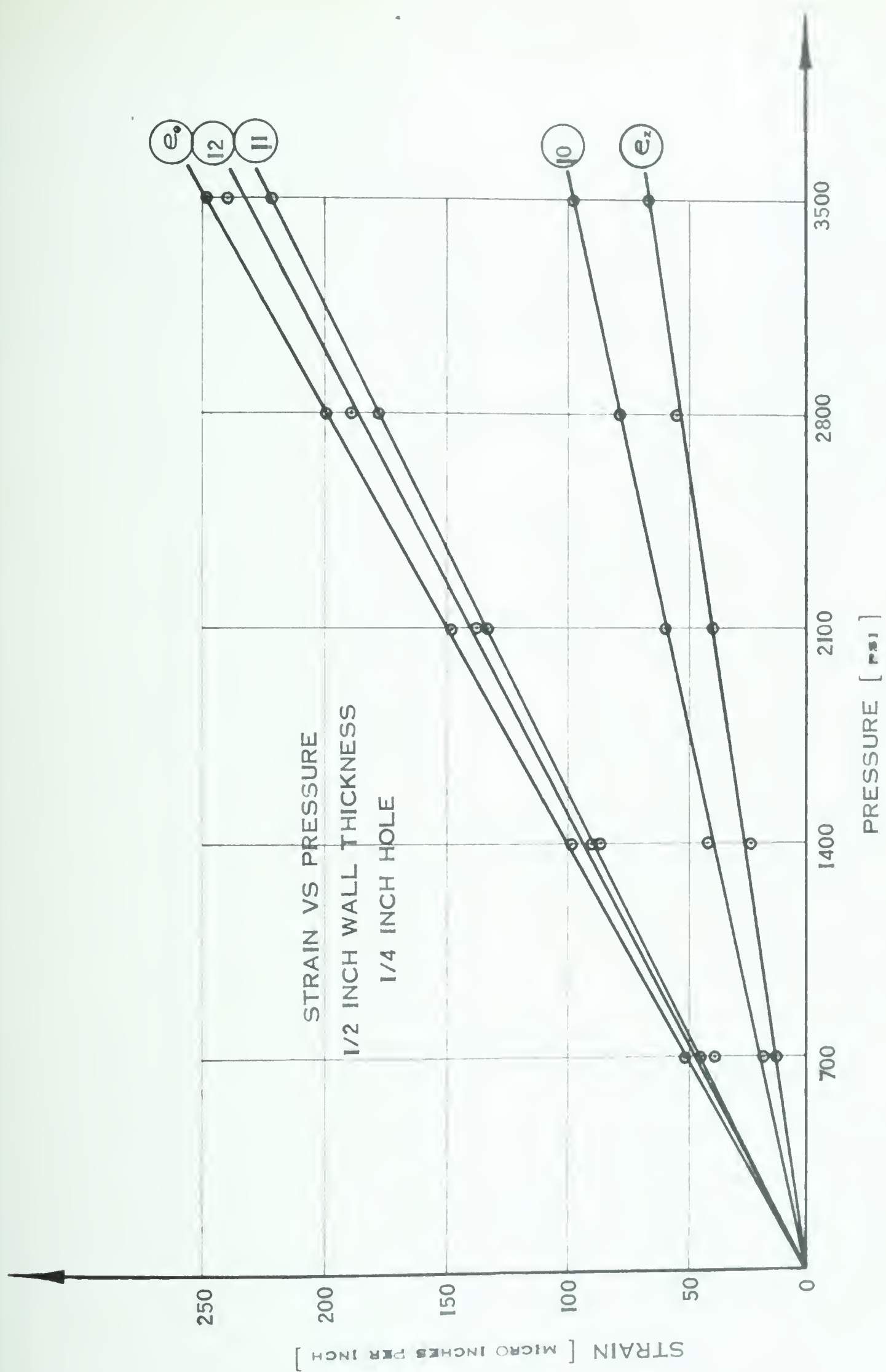


FIGURE 57.

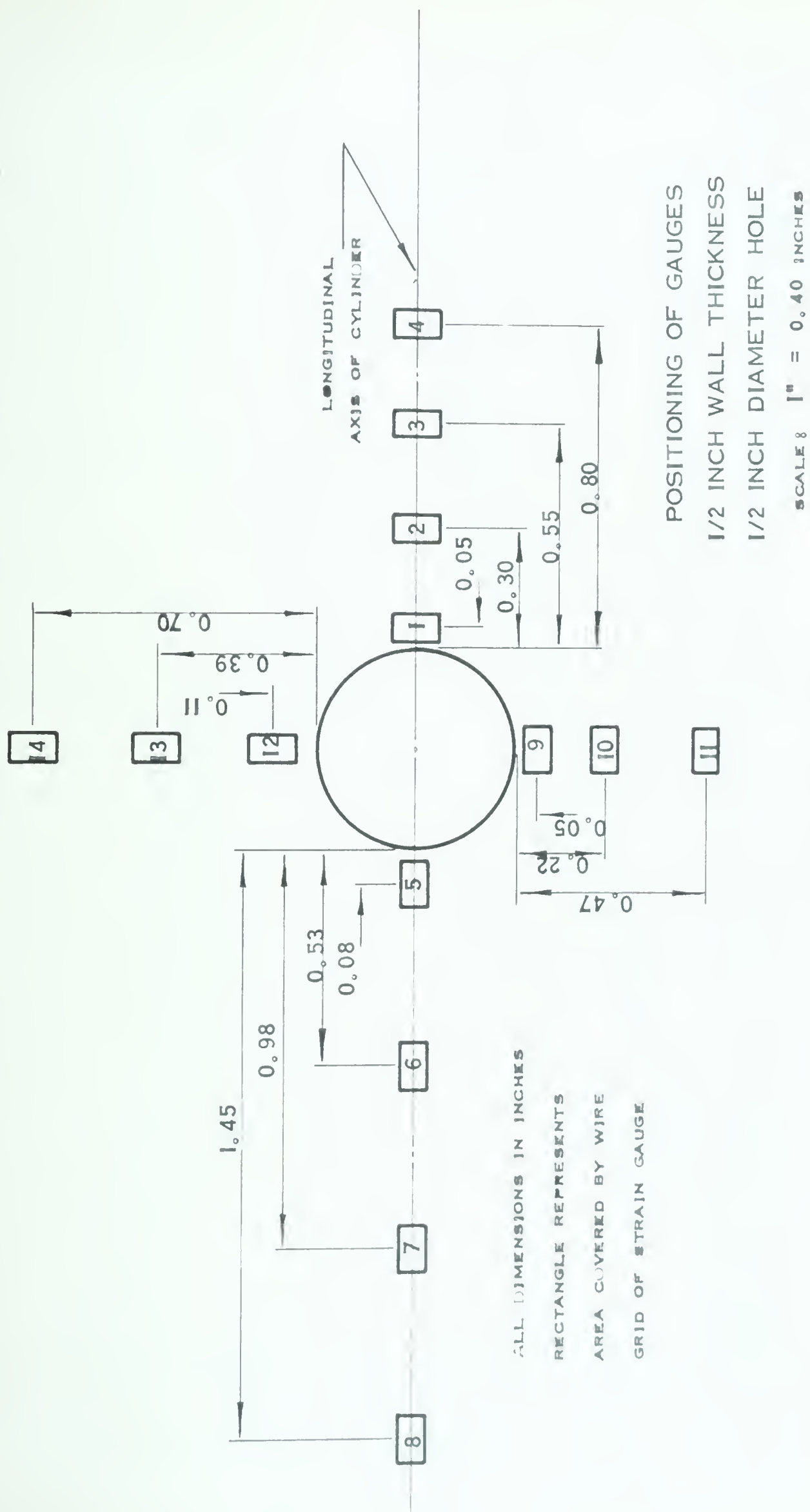


FIGURE 58.

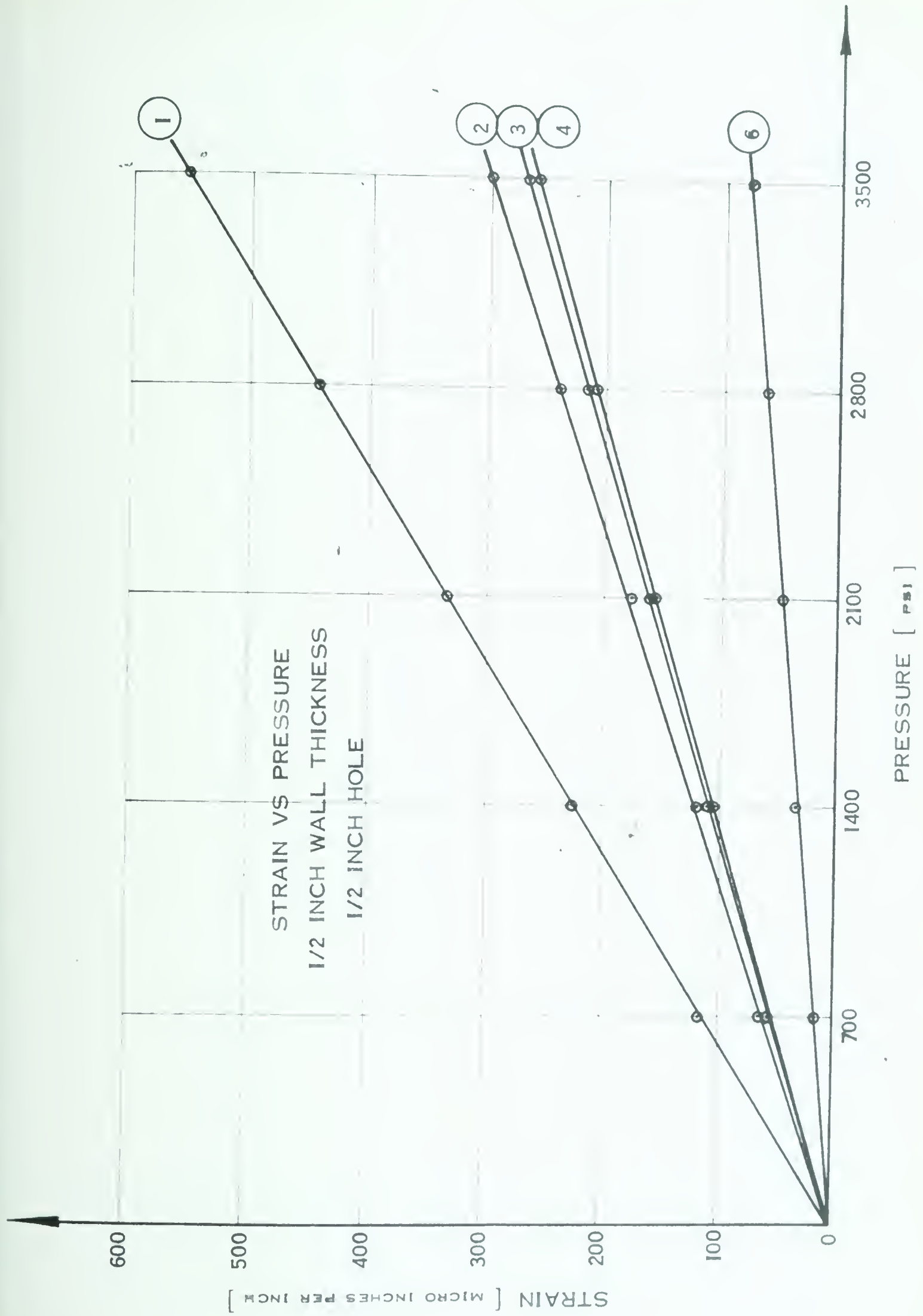


FIGURE 59.

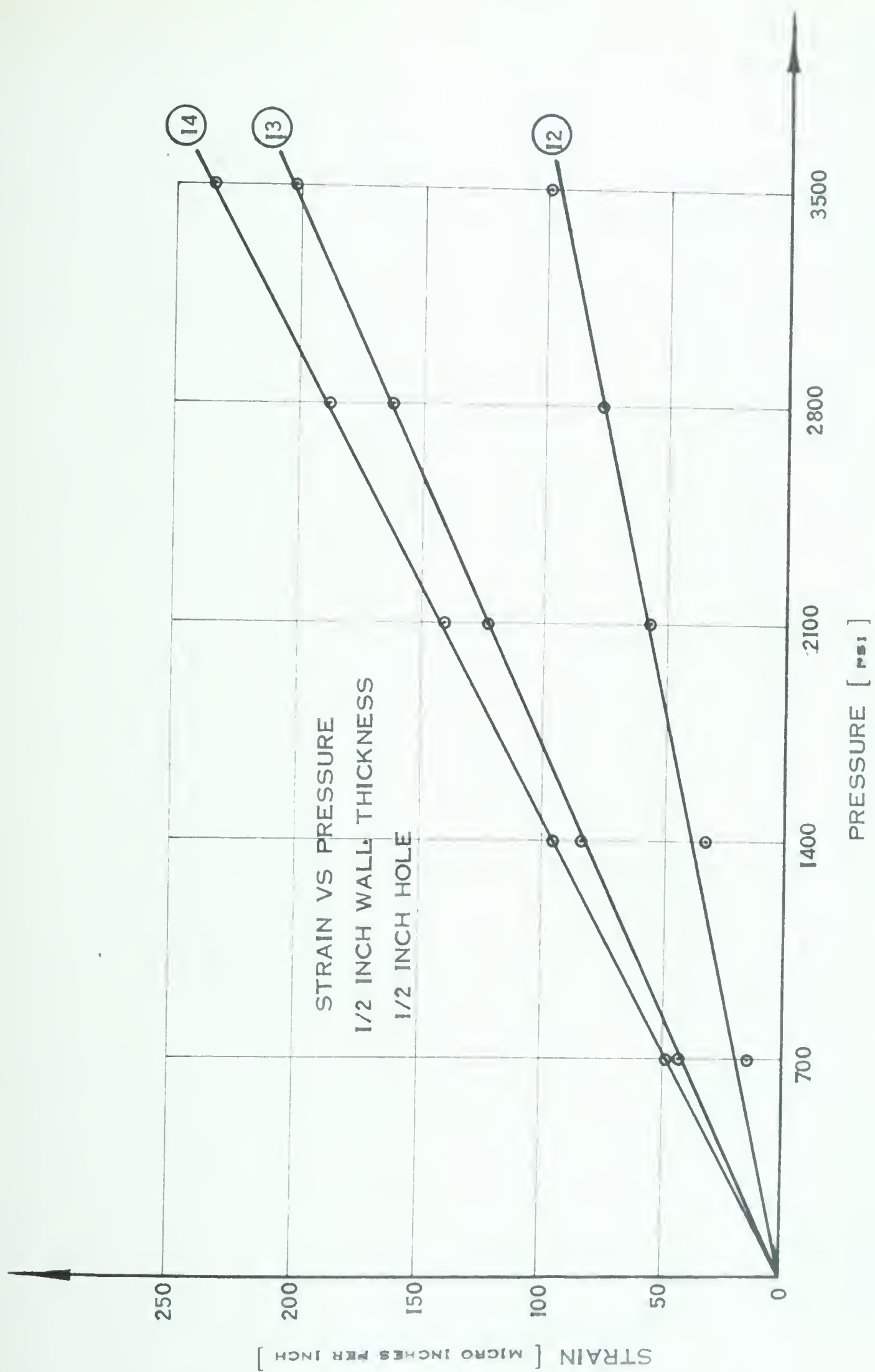


FIGURE 60.

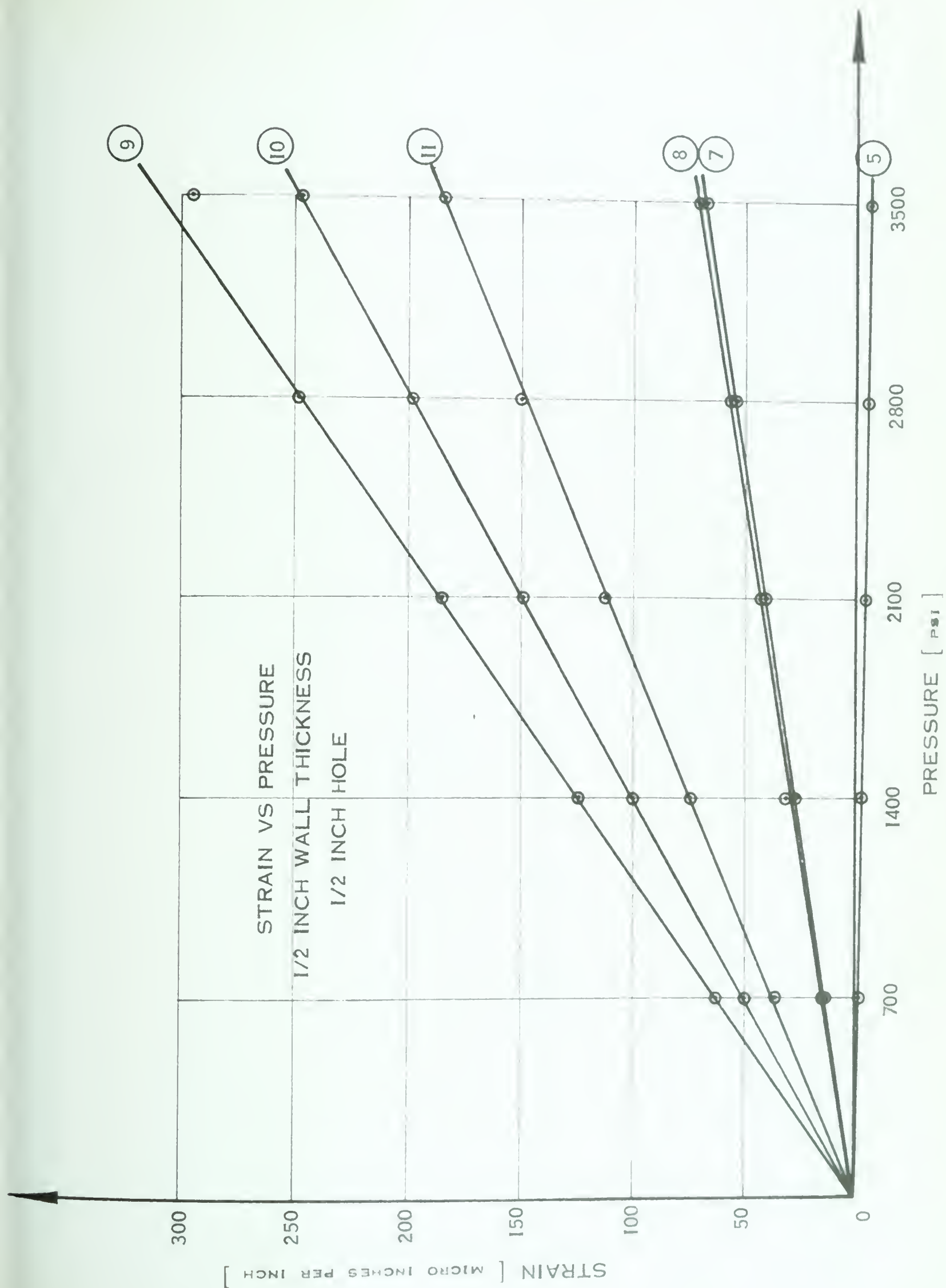


FIGURE 60A.

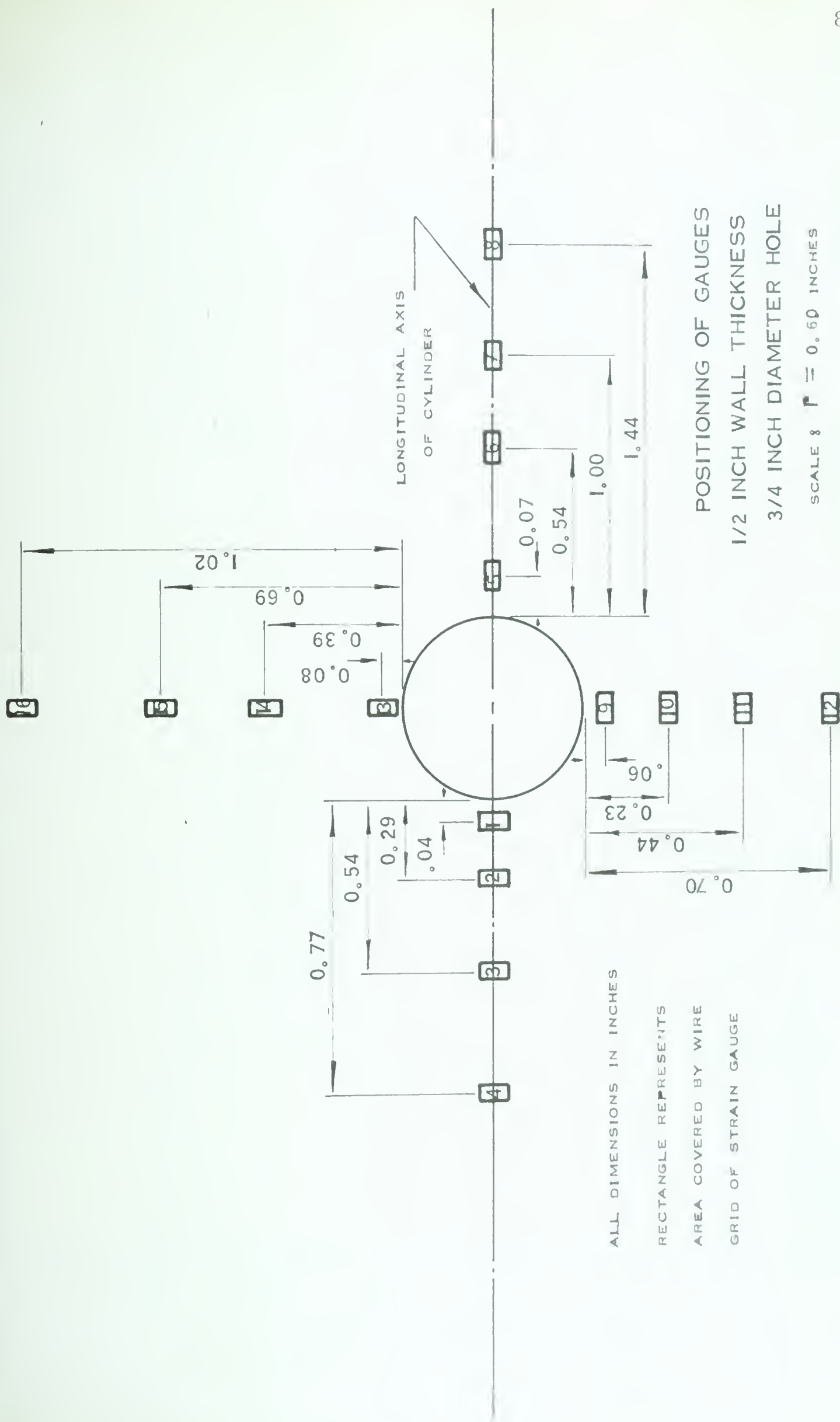


FIGURE 61.

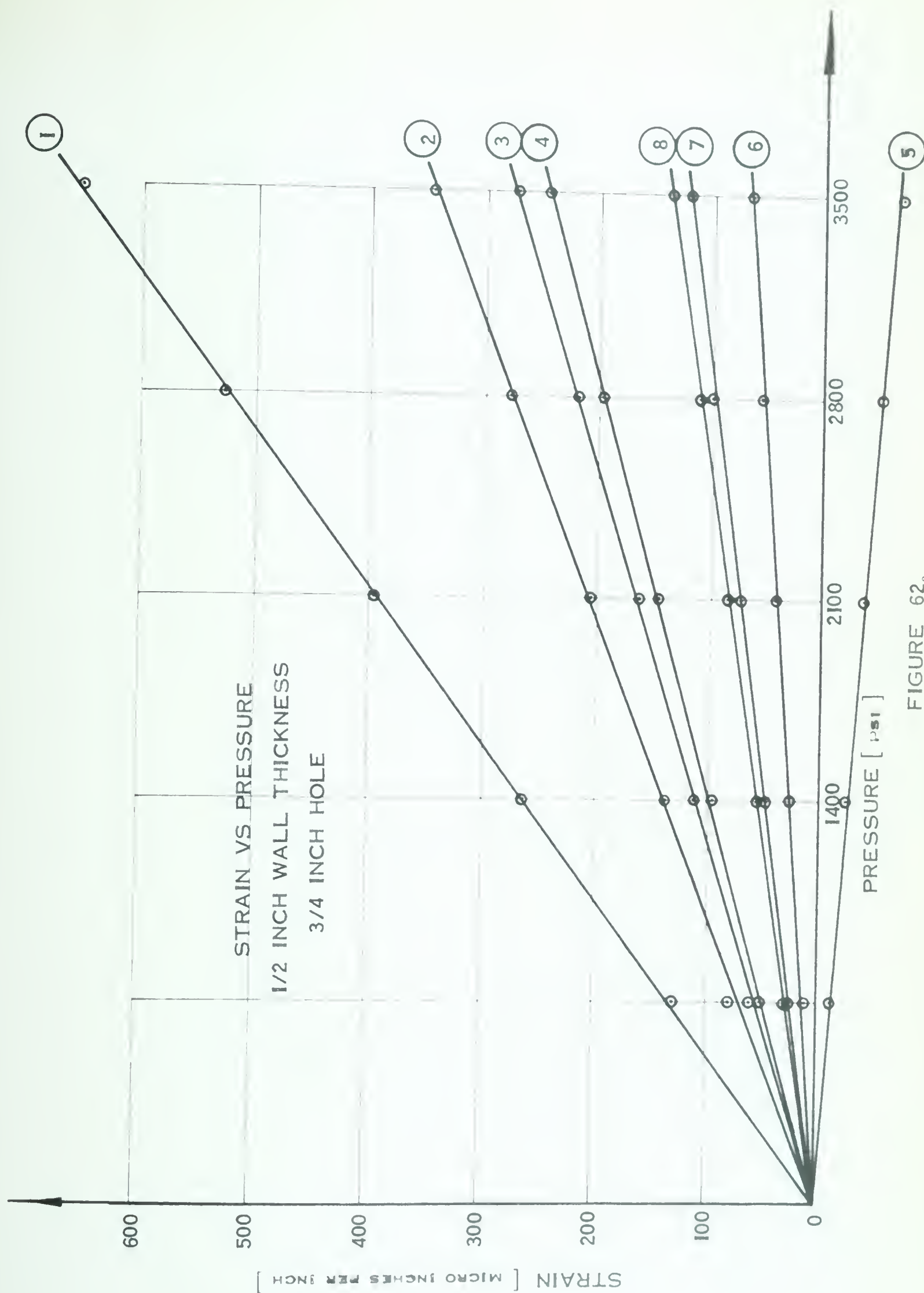


FIGURE 62.

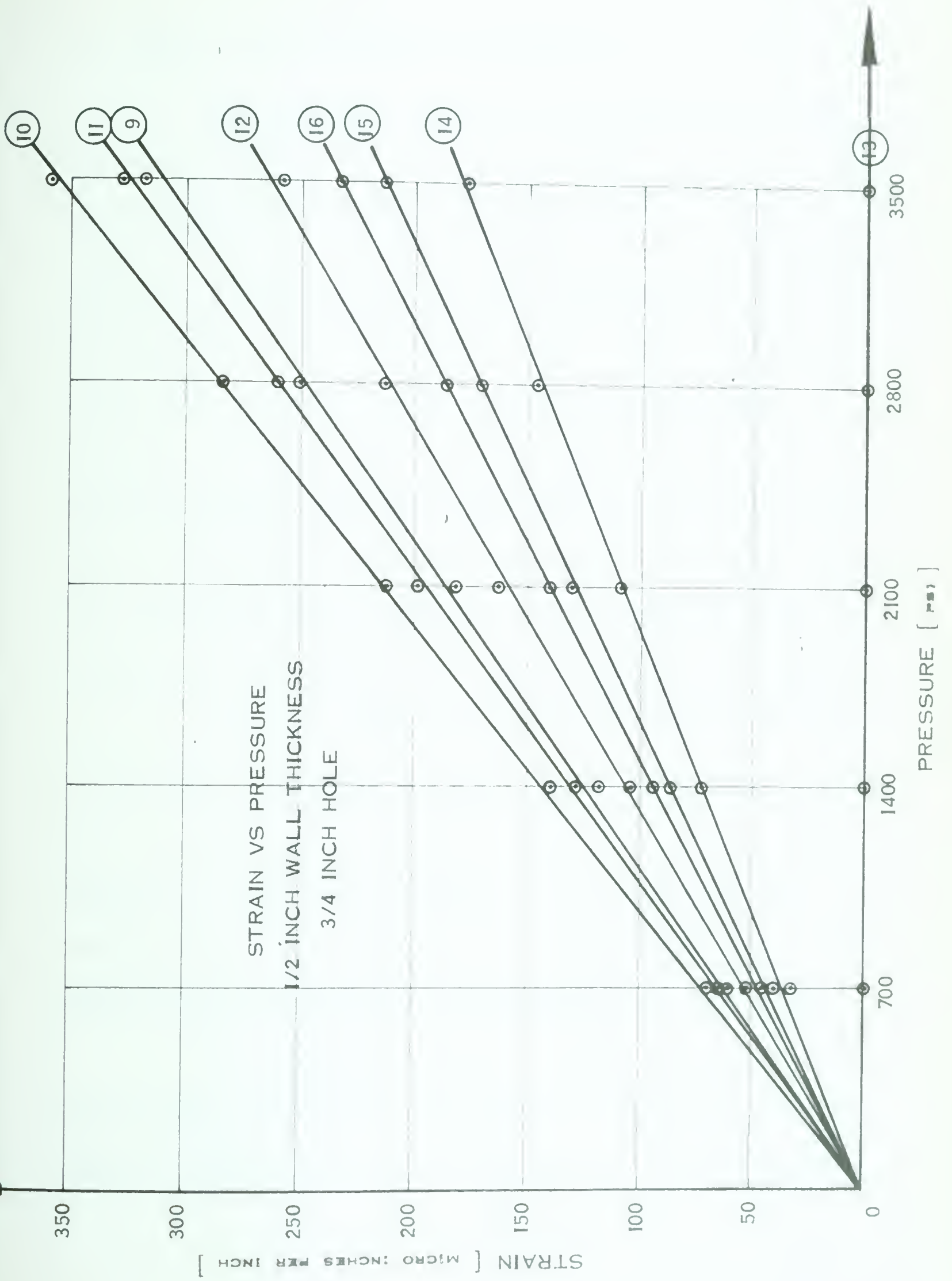


FIGURE 63.

7.3 Stress and Strain Approaching Point A

The diagrams of strain vs. distance from the edge of the hole approaching point A are shown in Figs. 64 to 75. The values of strain at the edge of the hole obtained by extending the curves are of questionable accuracy, especially for the 1/4 inch diameter holes. The points where strains were measured were not as close to the edge of the hole as would have been desirable. This occurred because the gauges, although the smallest available, were still large compared to the size of the hole. The problem of physical dimensions also prevented the use of a sufficient number of gauges in the area affected by the hole to provide a clear picture of the strain pattern in that region.

A further misrepresentation was introduced through the fact that the readings obtained from the strain gauges, which were the average strains over the length of the gauges, were plotted as if they were the strains at the points where the centres of the wire grids were placed. However, the inaccuracy caused by this approximation was insignificant in most cases.

The diagrams of stress vs. distance from the edge of the hole approaching point A are shown in Figs. 76 to 87. The method of obtaining the stress diagrams from the strain diagrams

is described in Appendix A.

The first observation to be made from these diagrams is that the disturbed area is of a local character. The stress decreases to within five percent of the stress in the undisturbed region at a distance of less than one and one half hole diameters from the edge of the hole in all cases, and for the larger holes at a distance of less than one hole diameter from the opening. This would seem to be contradictory to the theoretical work of Vainberg and Siniavskii which indicated that a much larger area was affected. However, it must be noted that their analysis considered deflections of the shell in the radial direction due to an axial load only, whereas this investigation has considered the stresses tangential to the surface of the cylinder due to an internal pressure.

The general form of the stress distribution is similar for all the holes tested, although the stress perpendicular to the boundary as shown in Figs. 78 and 83 did not increase as rapidly as in the remainder of the tests. This may have been caused by an eccentric loading due to the plug exerting a force on the side of the hole. The stress tangential to the hole showed an oscillating effect in the thin cylinder, and in the thicker cylinders

with large holes, that is, the hoop stress at a short distance from the hole dropped to a value lower than that in the undisturbed region. The work of Vainberg and Siniavskii showed an oscillating effect for the deflection of shells under axial load.

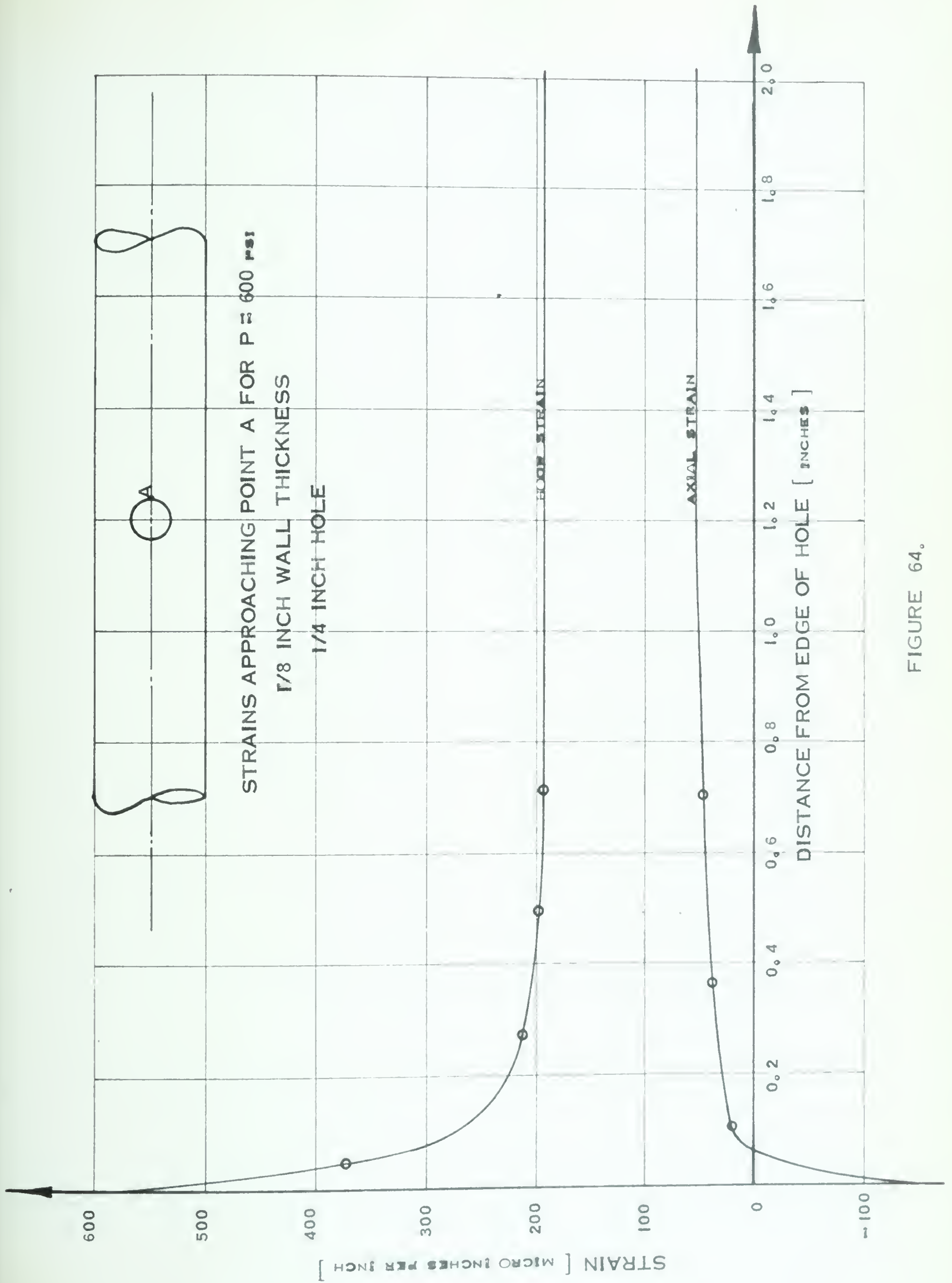


FIGURE 64.

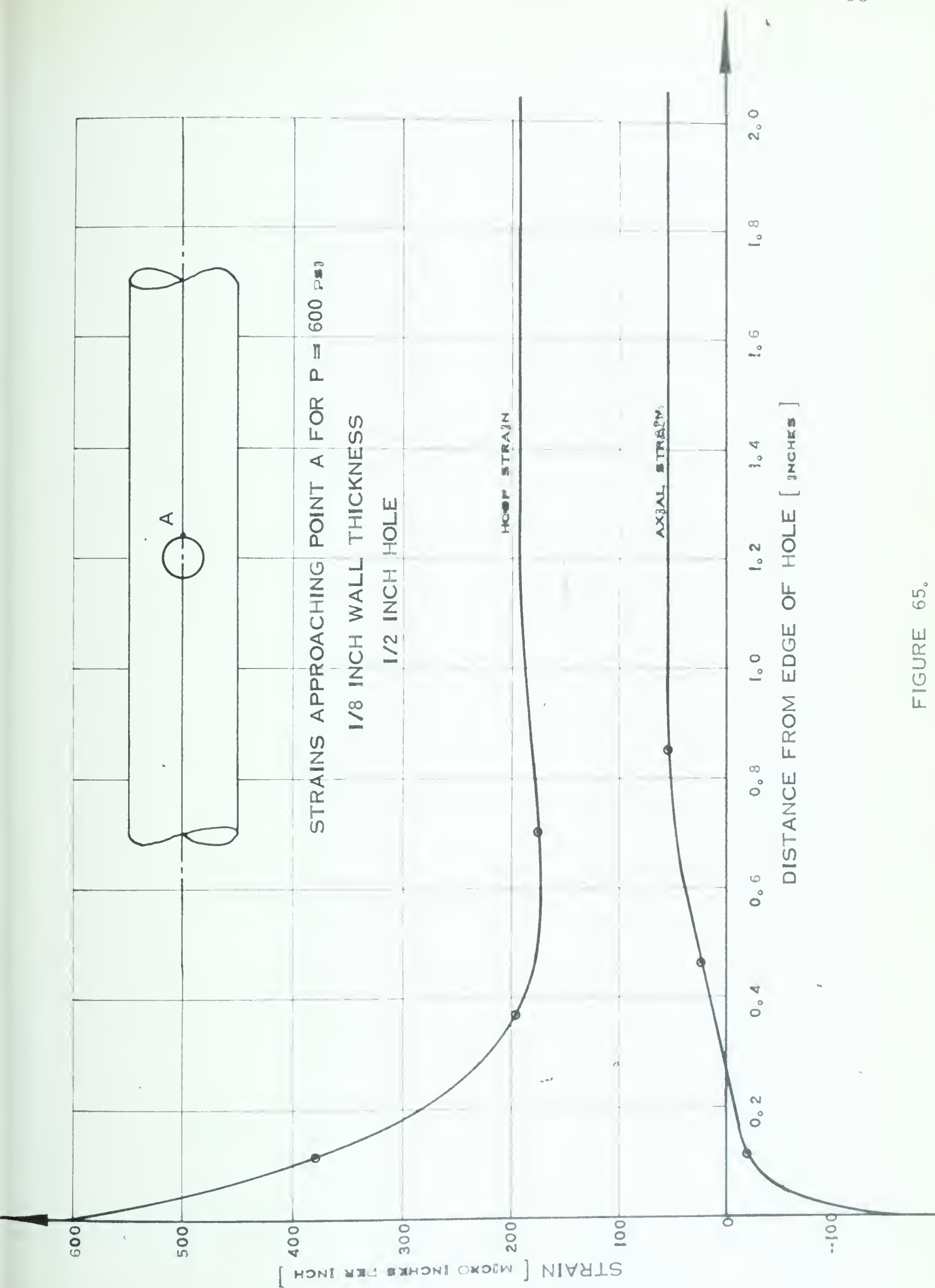


FIGURE 65.

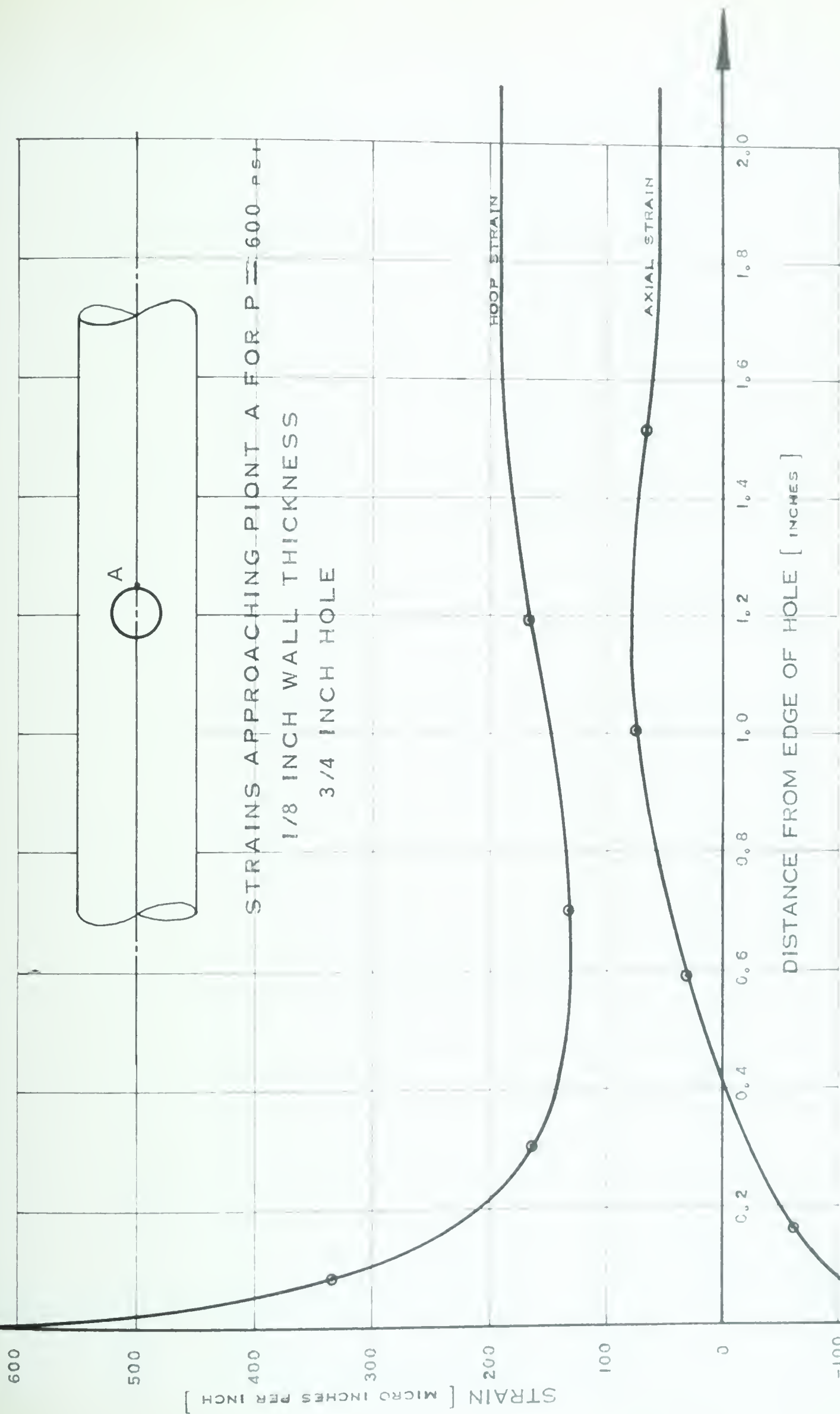


FIGURE 66.

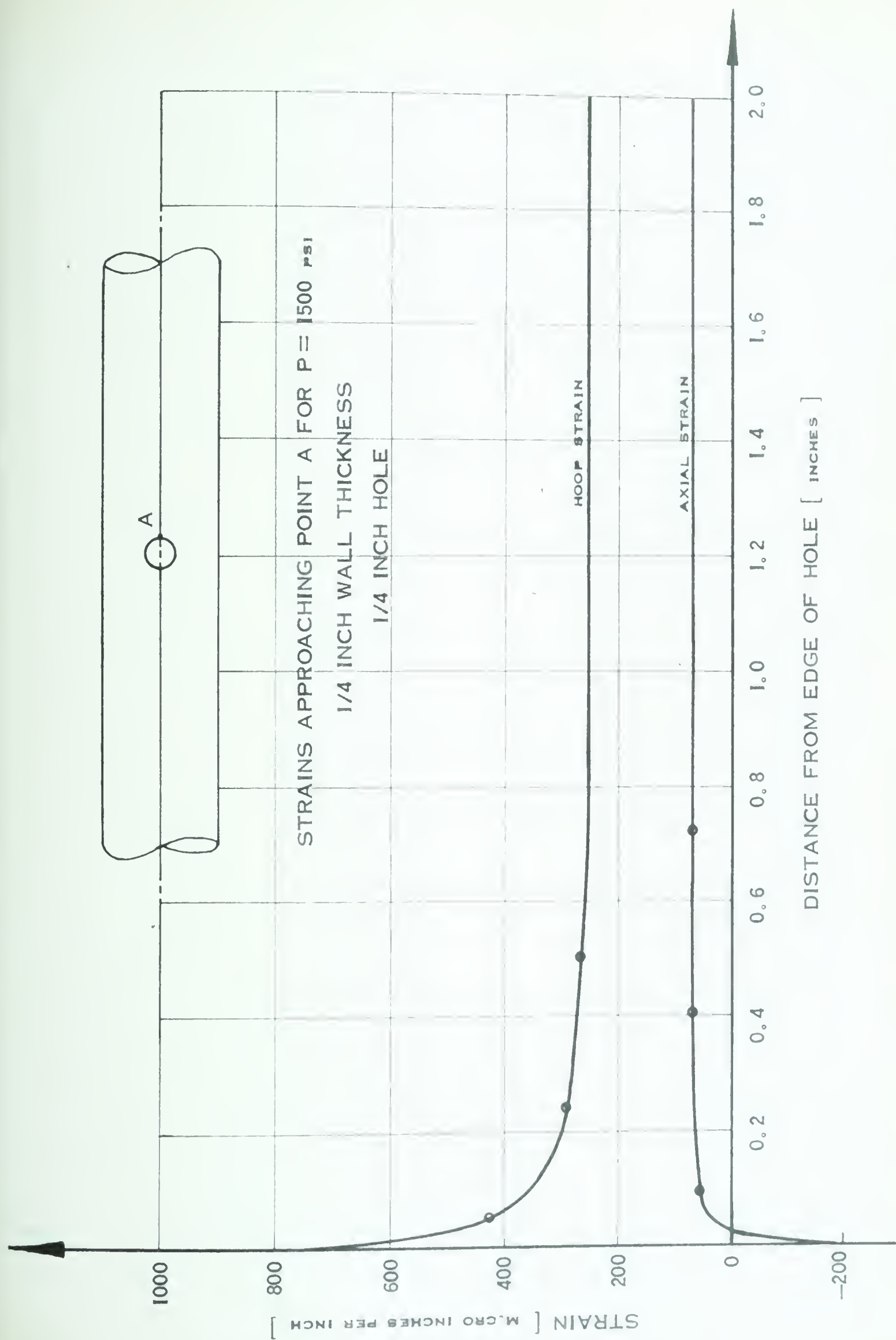


FIGURE 67.

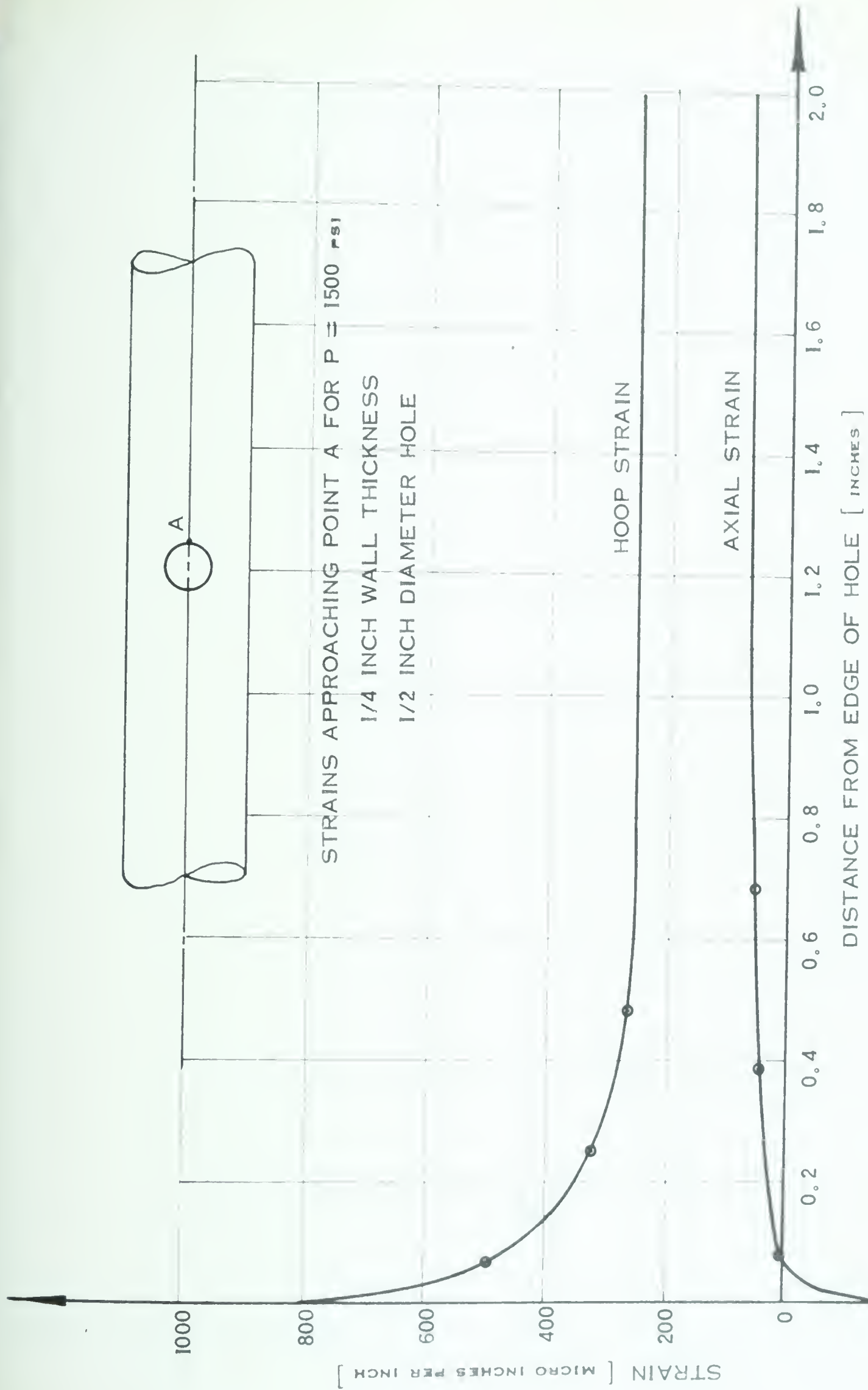


FIGURE 68.

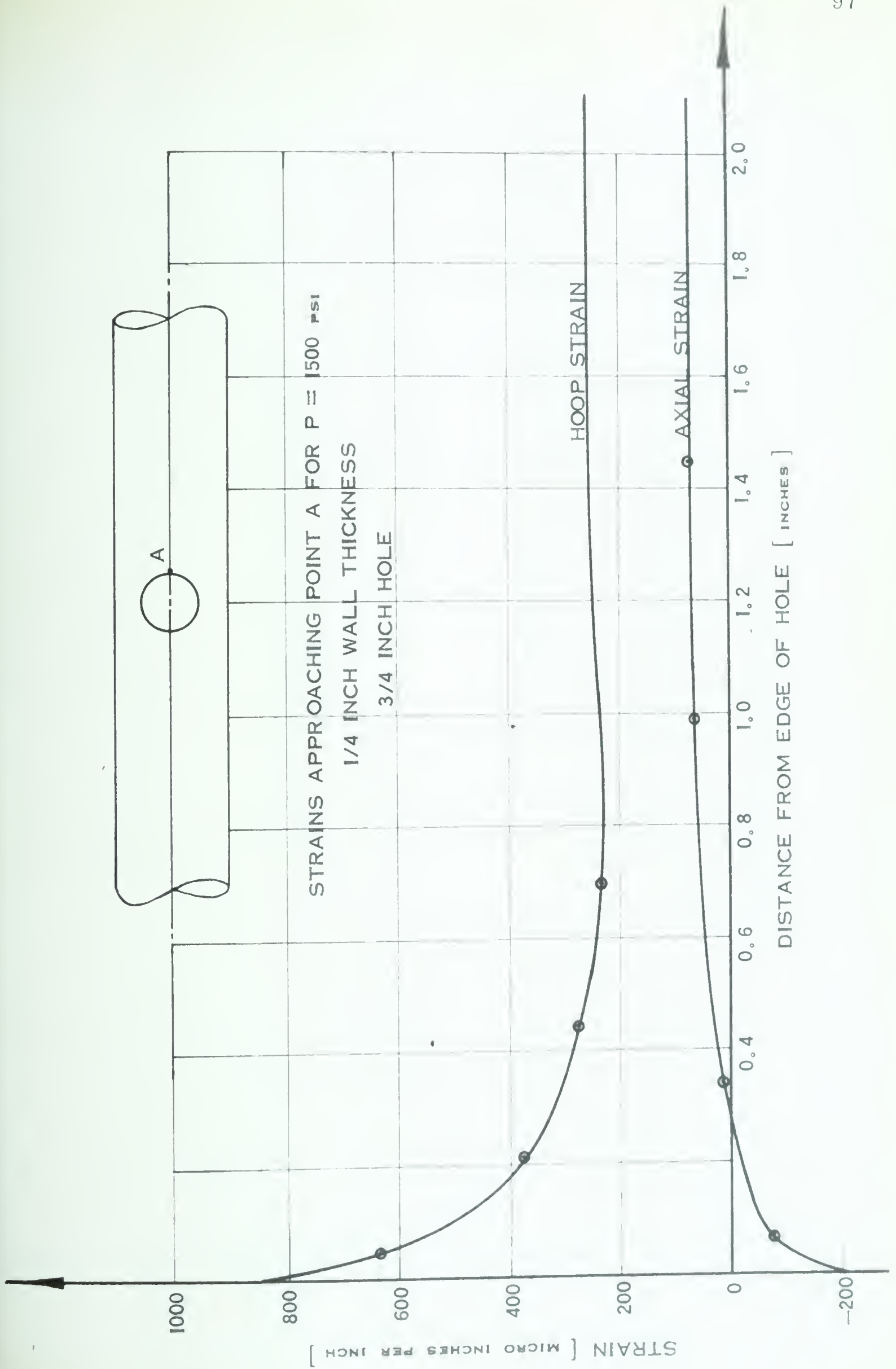


FIGURE 69.

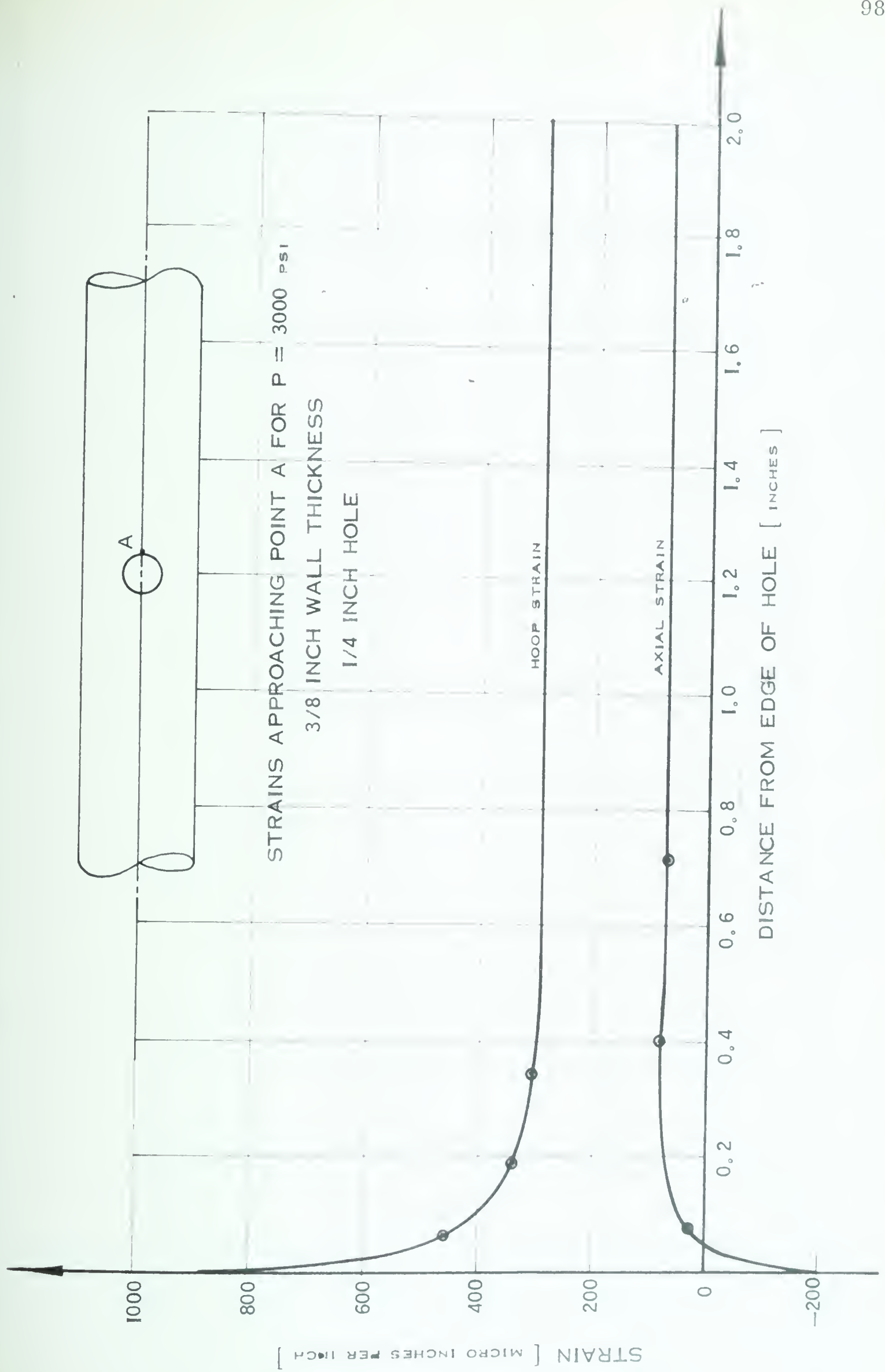


FIGURE 70.

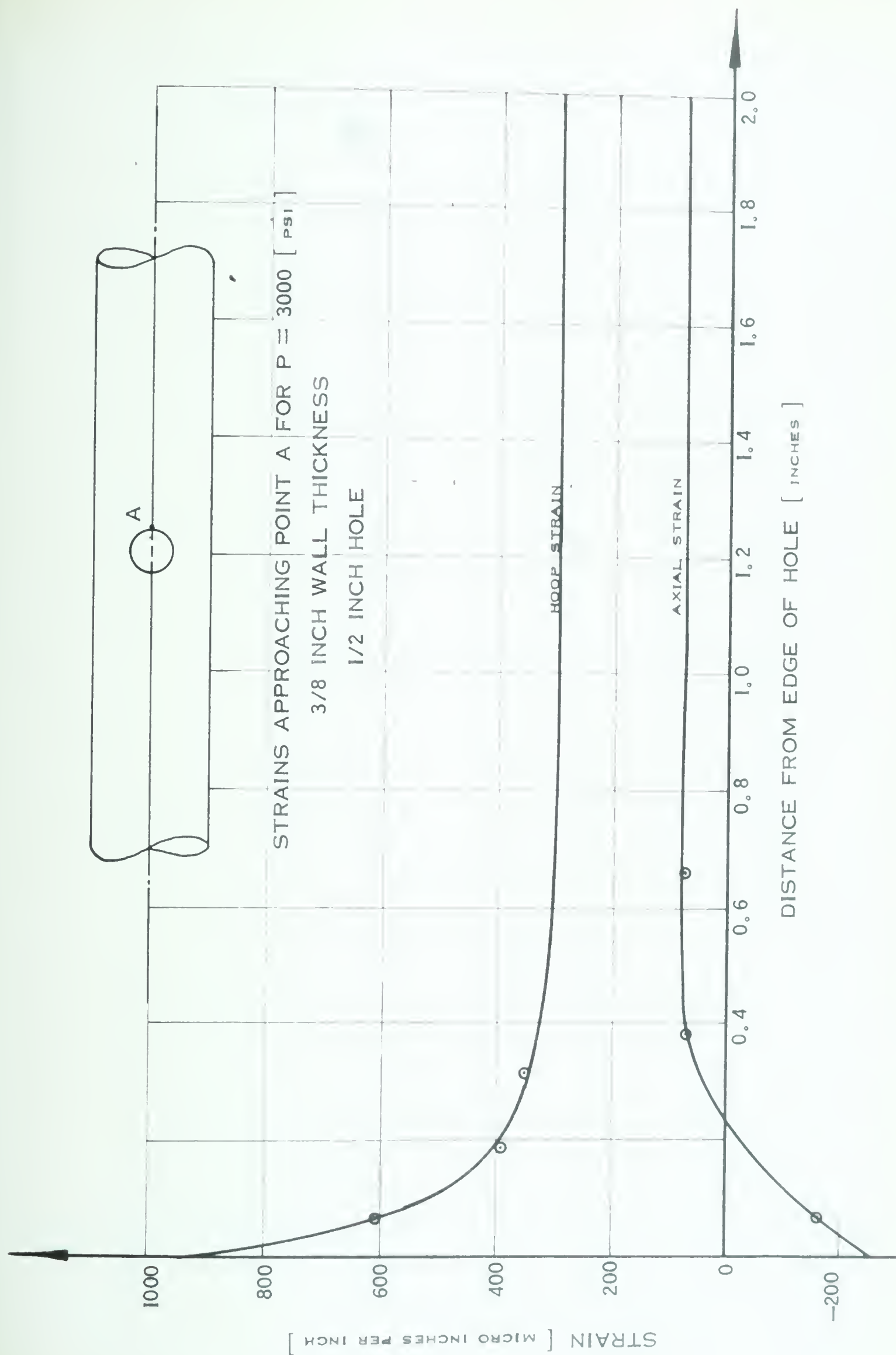


FIGURE 7I.

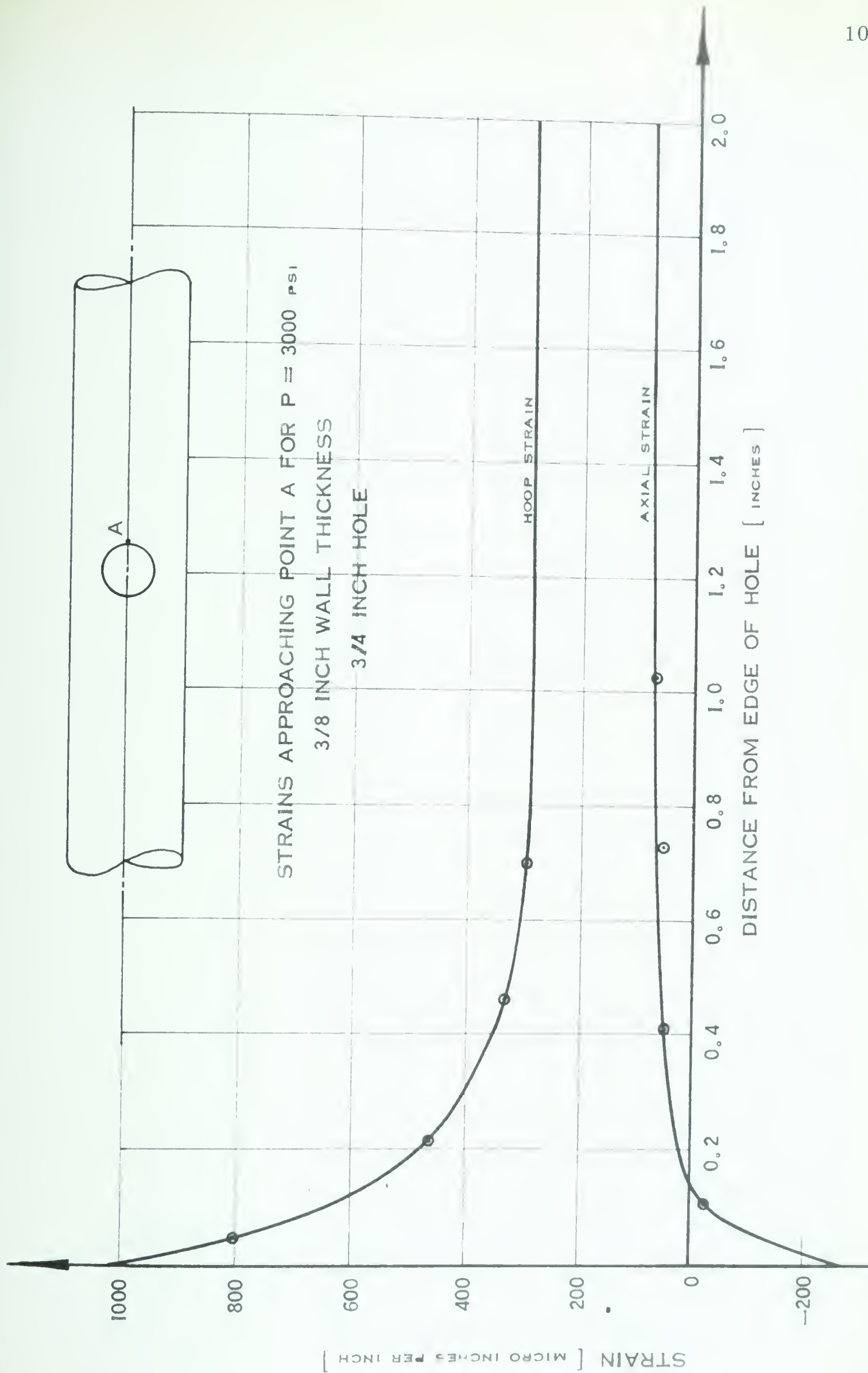


FIGURE 72.

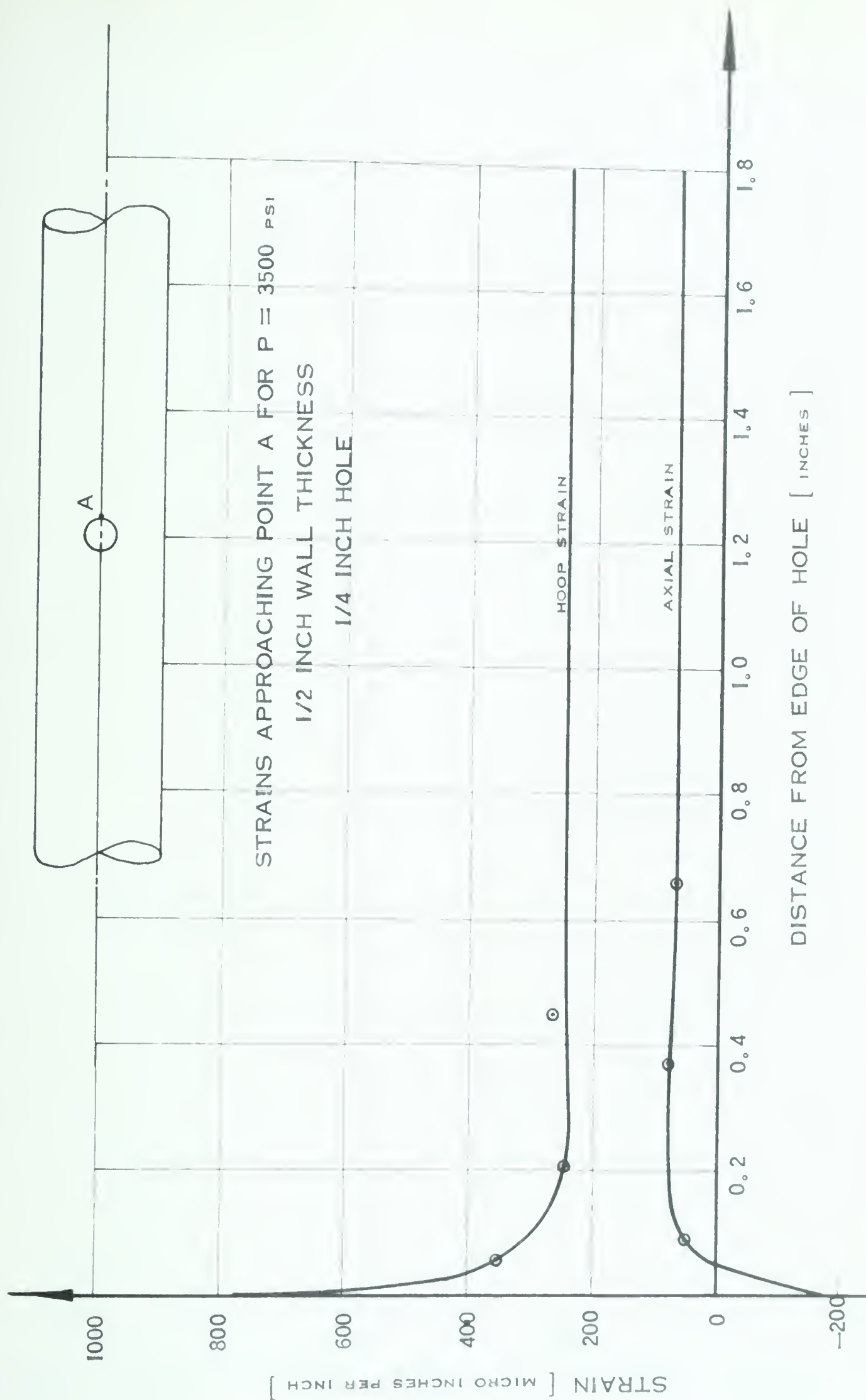


FIGURE 73.

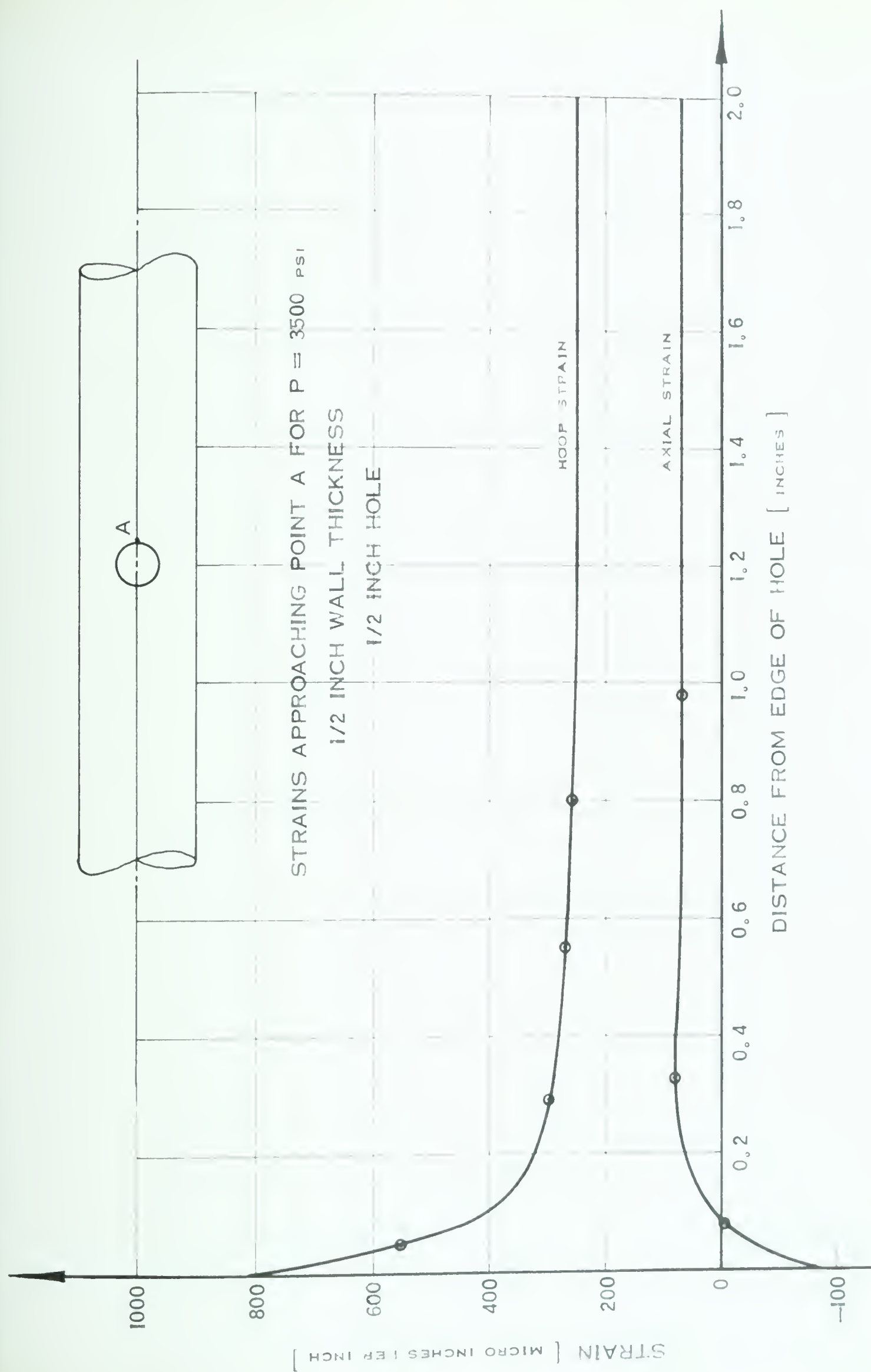


FIGURE 74.

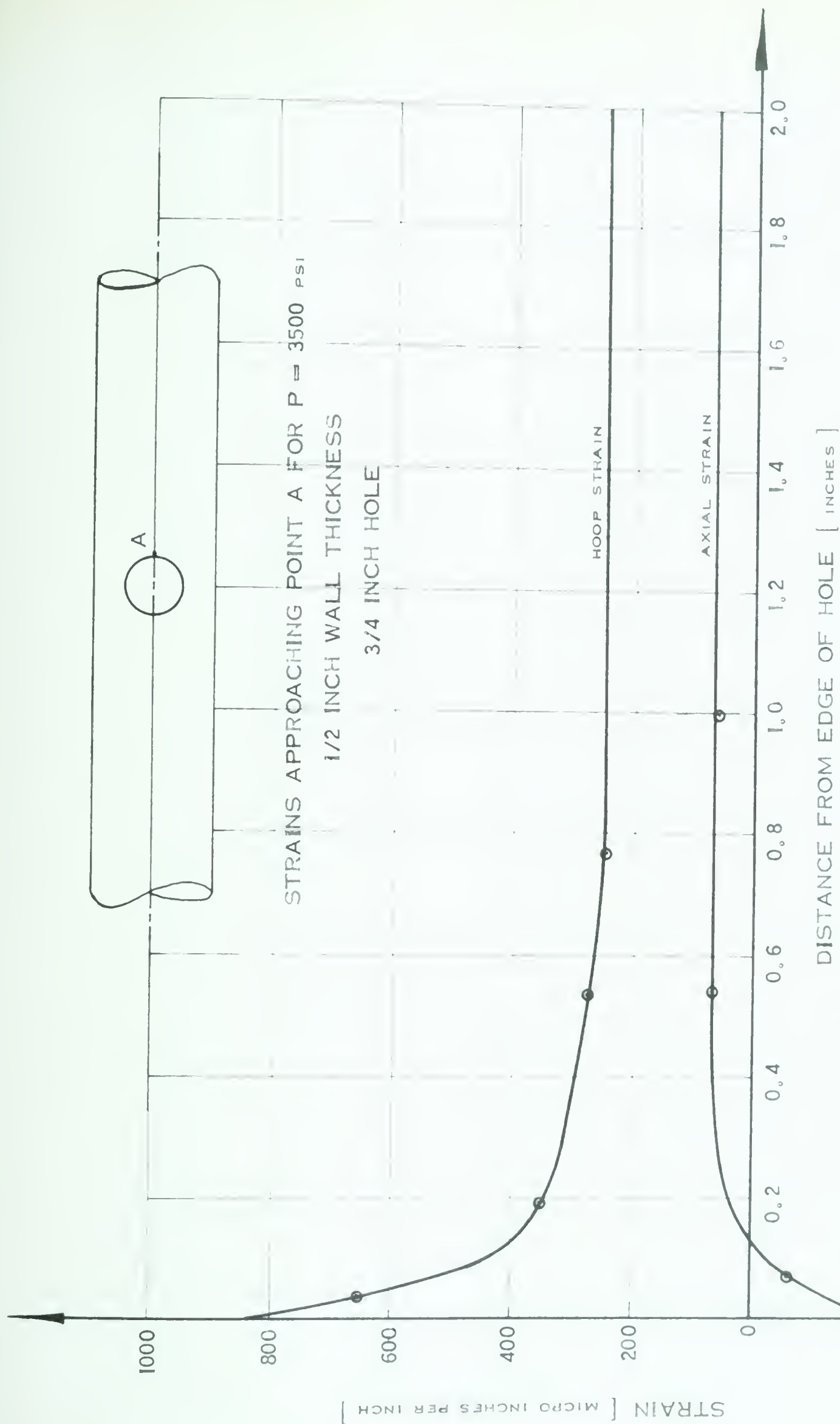


FIGURE 75.

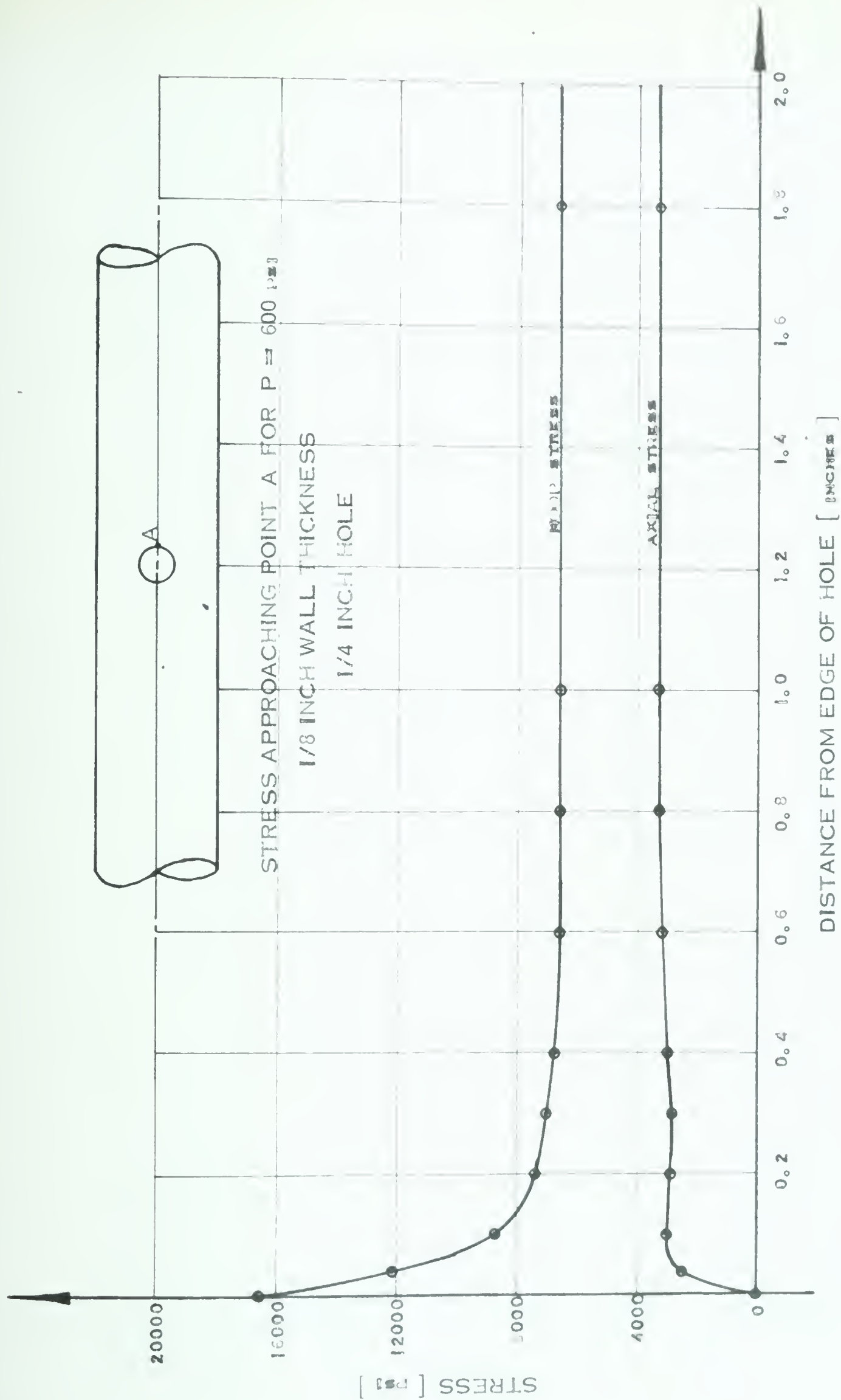


FIGURE 76.

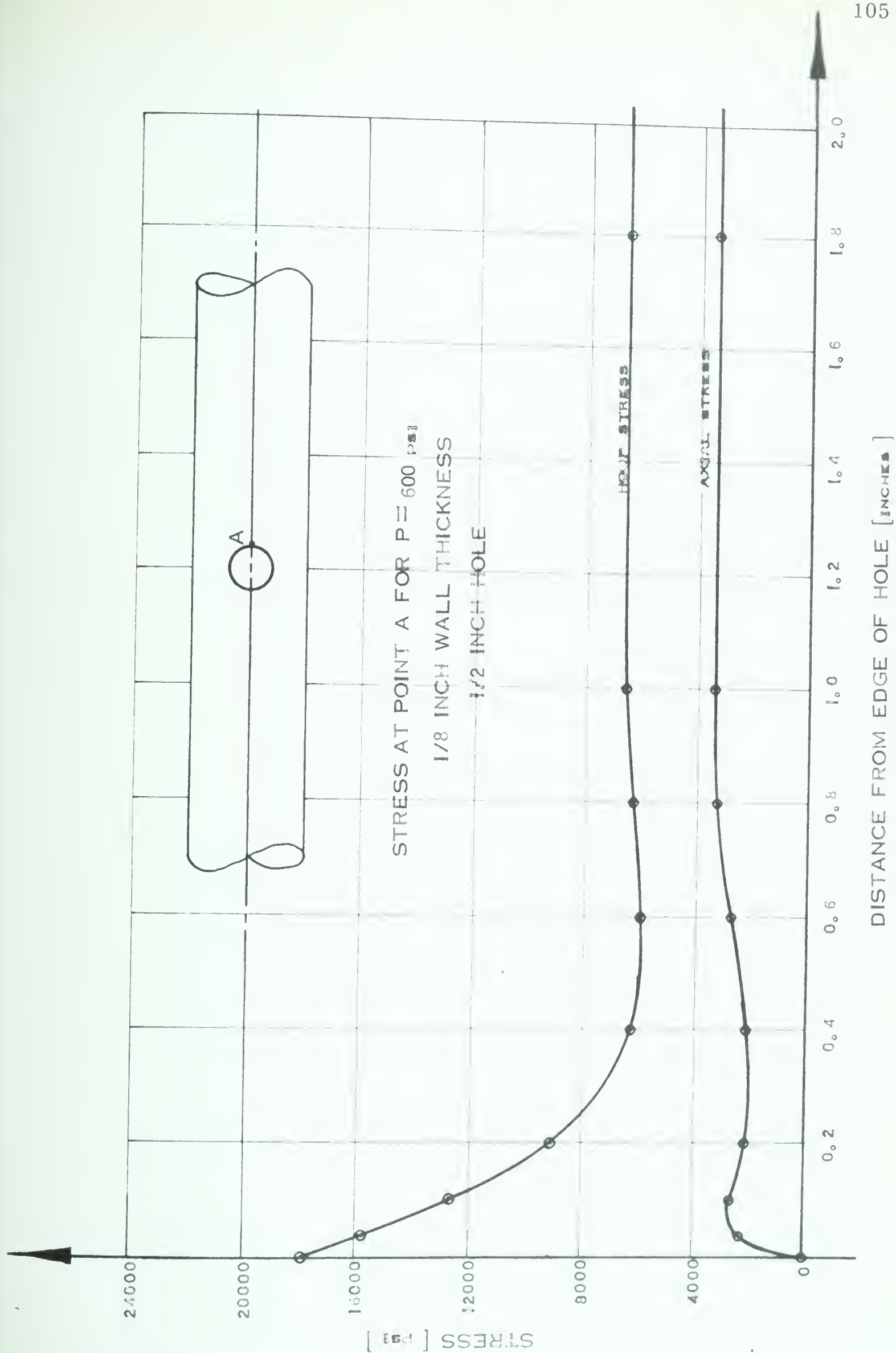


FIGURE 77.

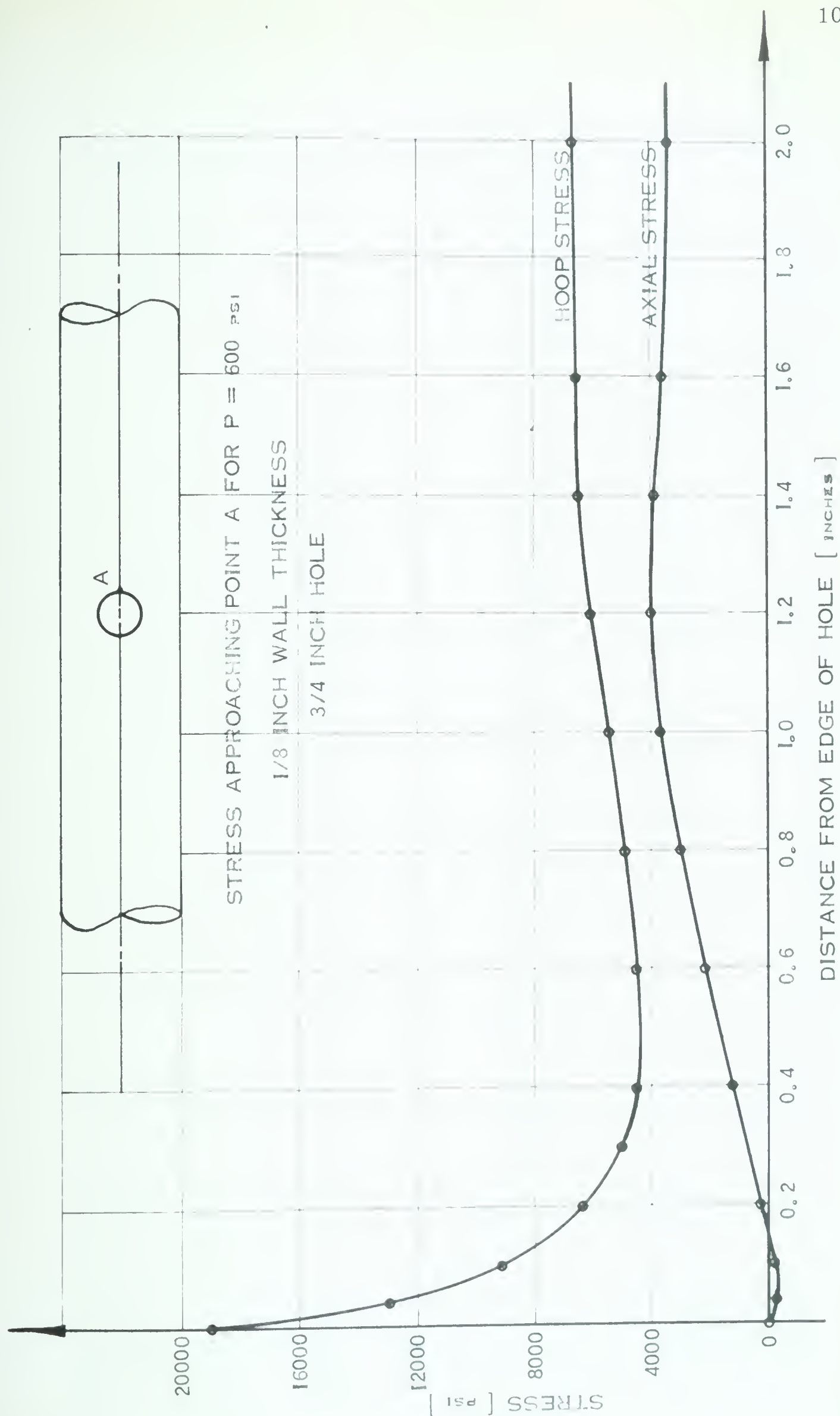


FIGURE 78.

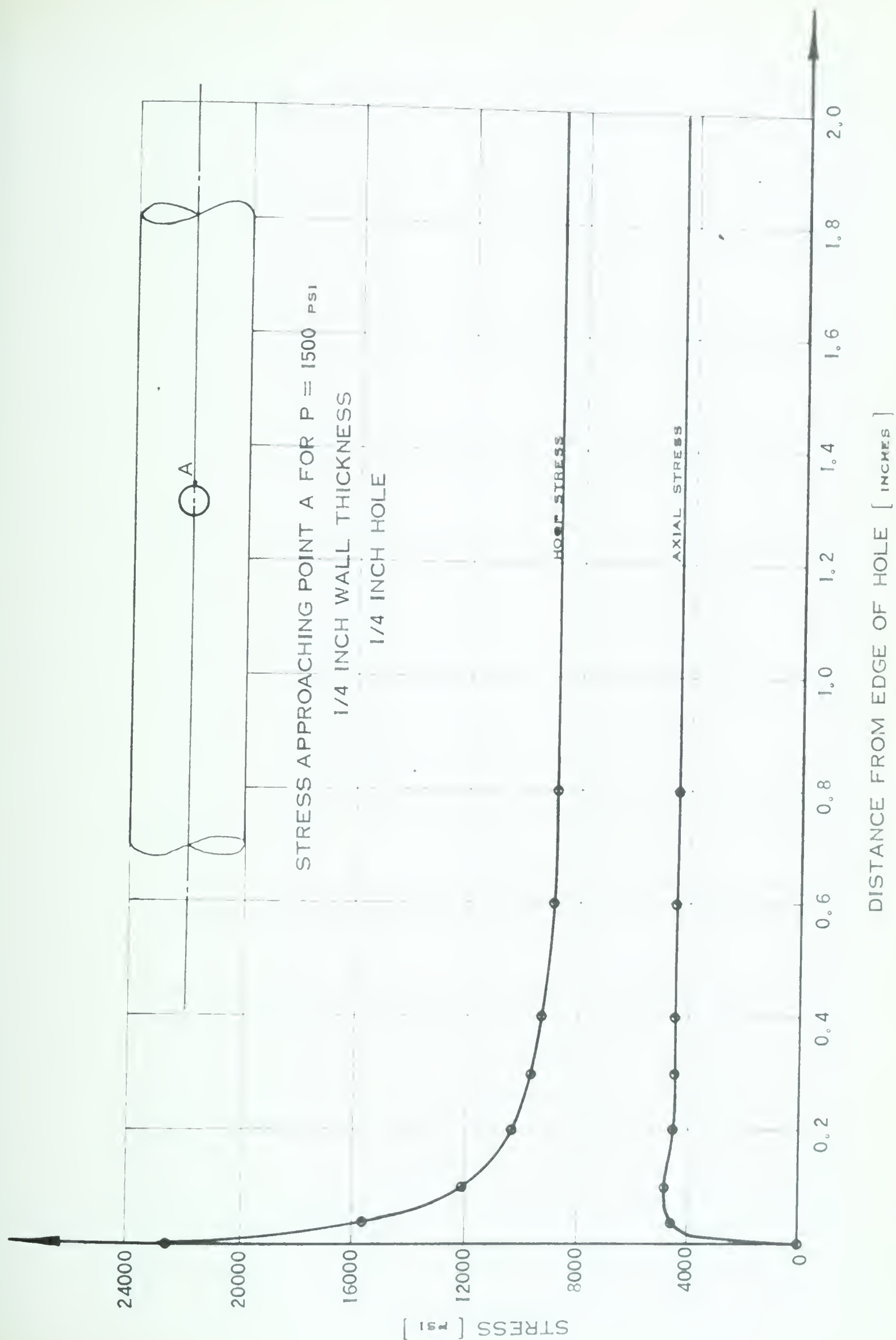


FIGURE 79.

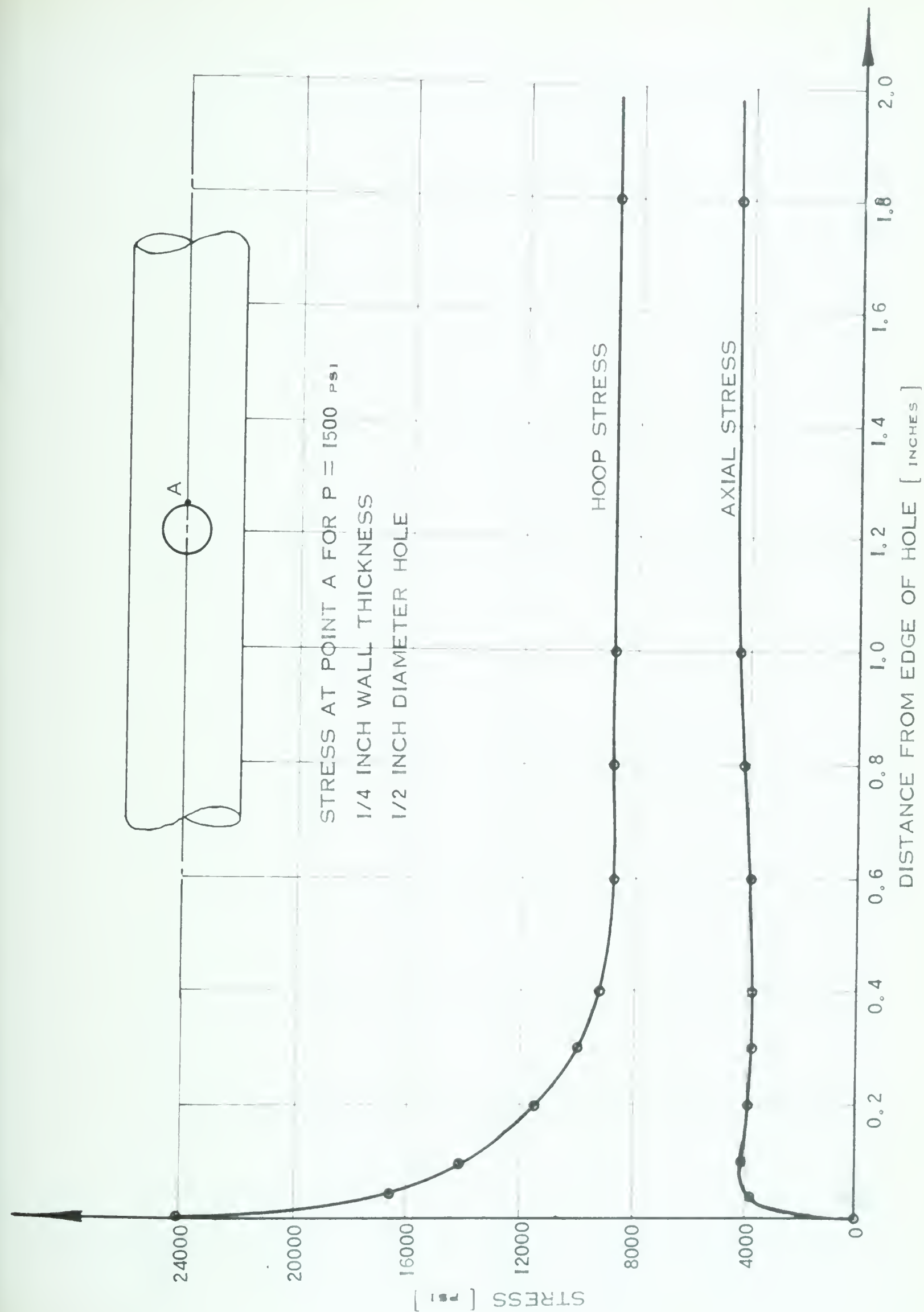


FIGURE 80.

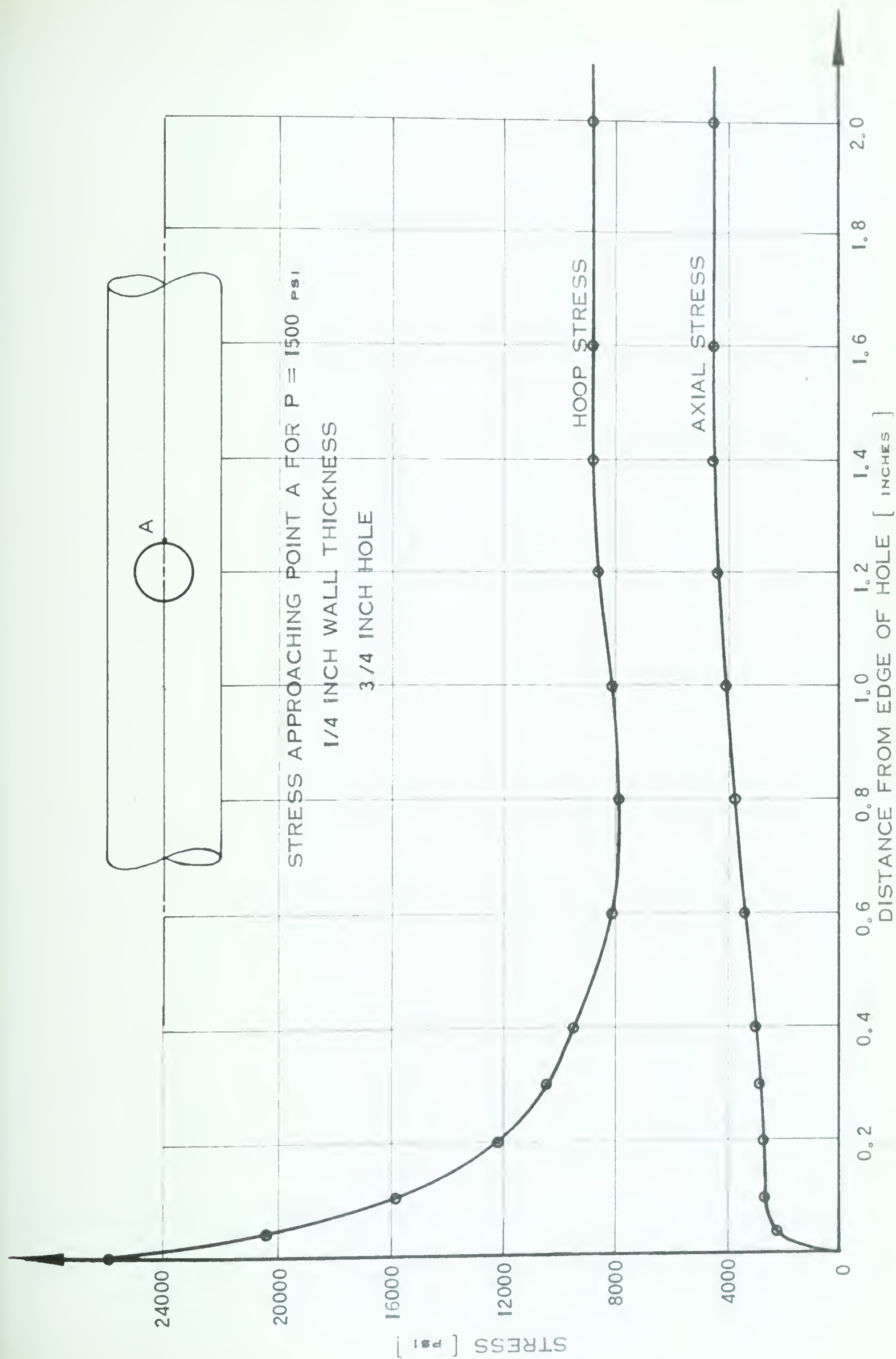


FIGURE 81.

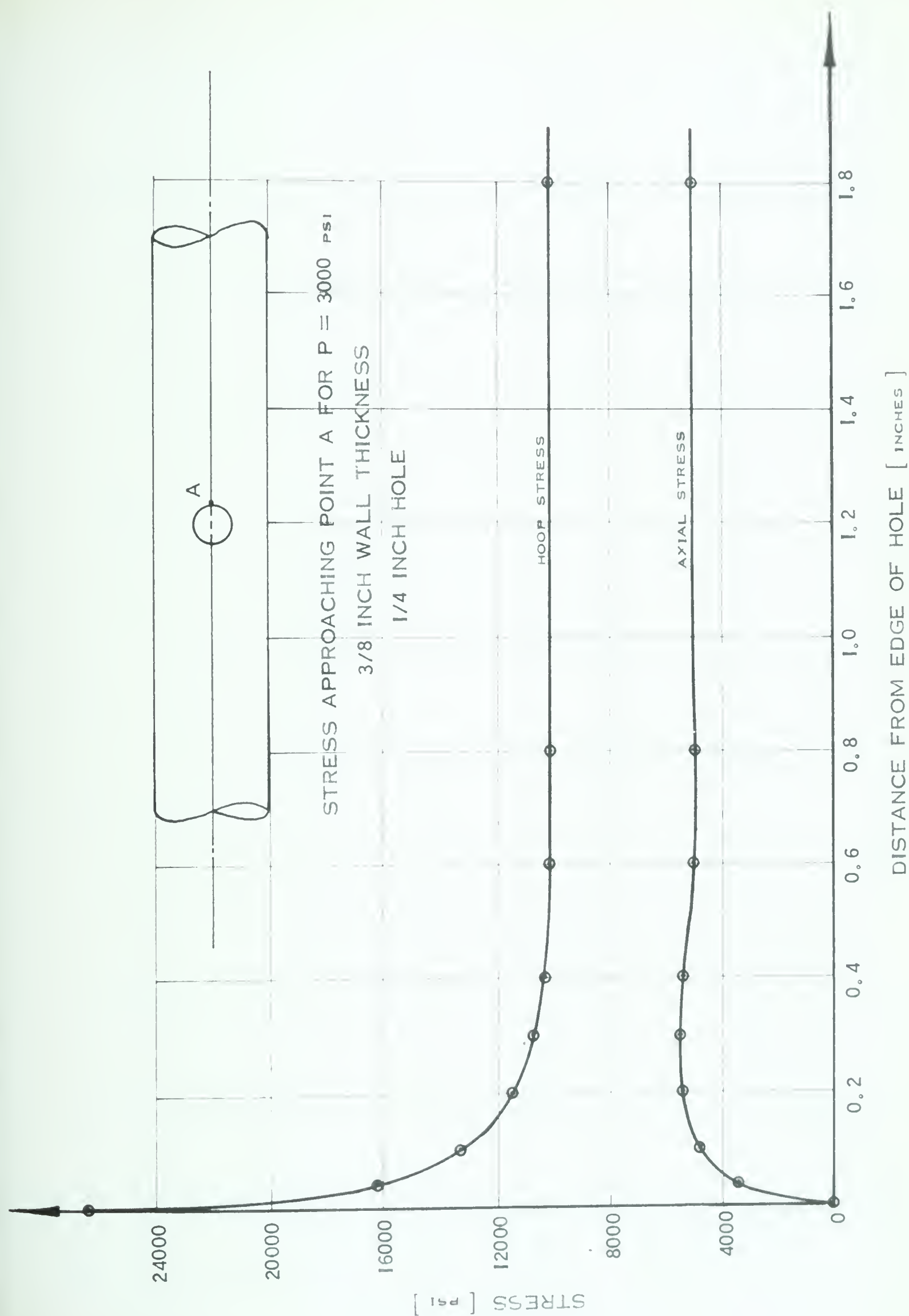


FIGURE 82.

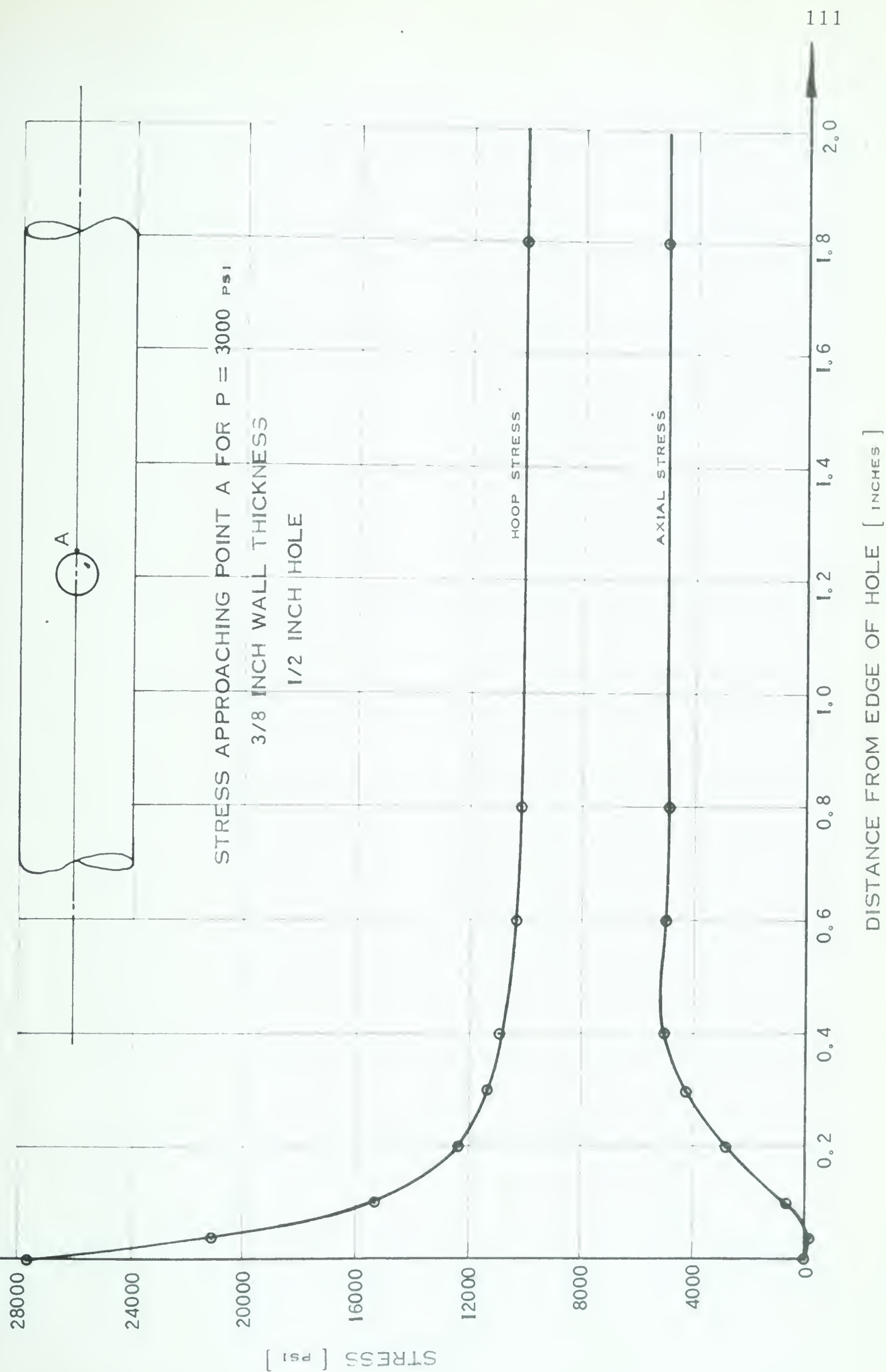


FIGURE 83.

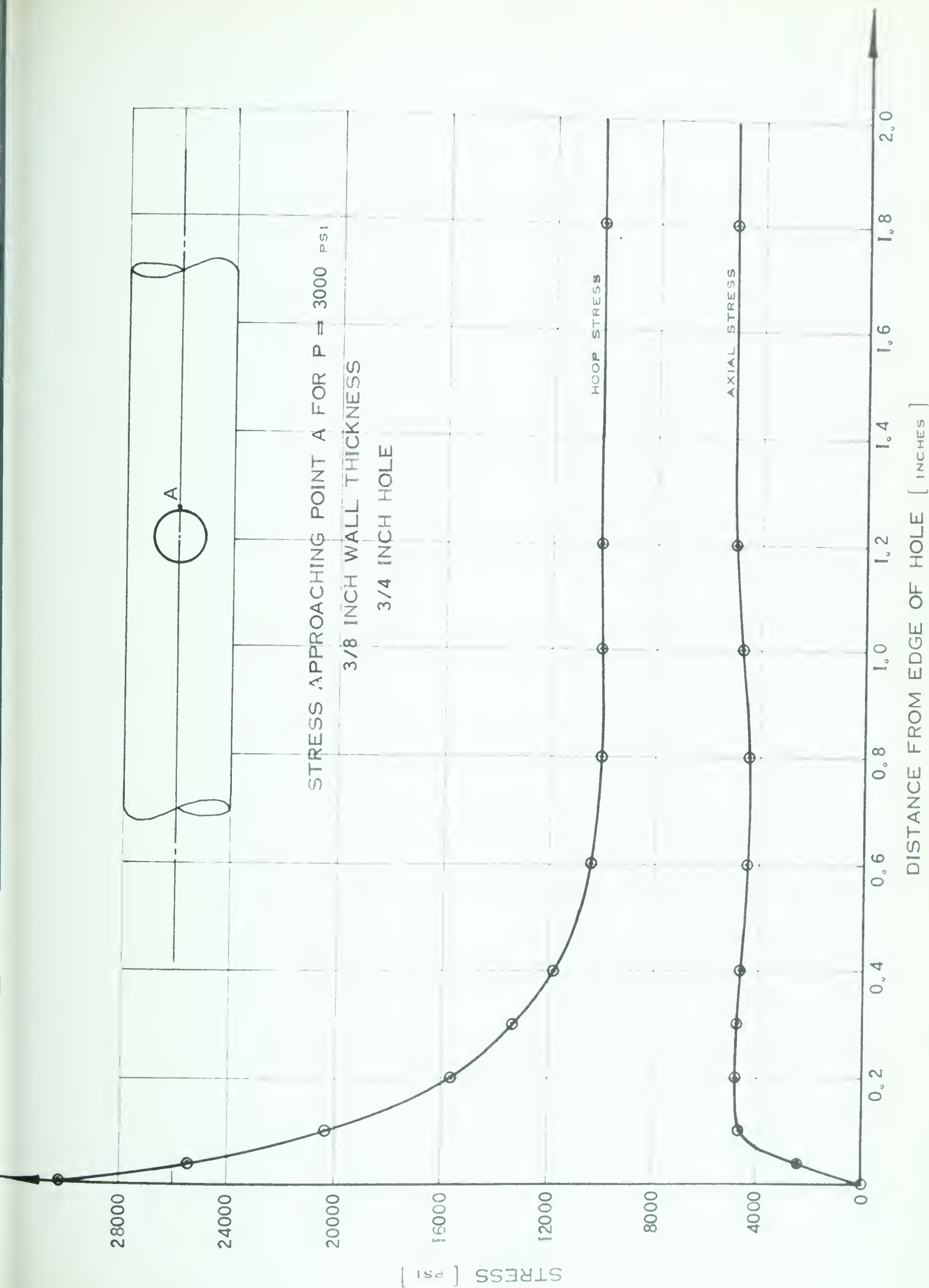


FIGURE 84.

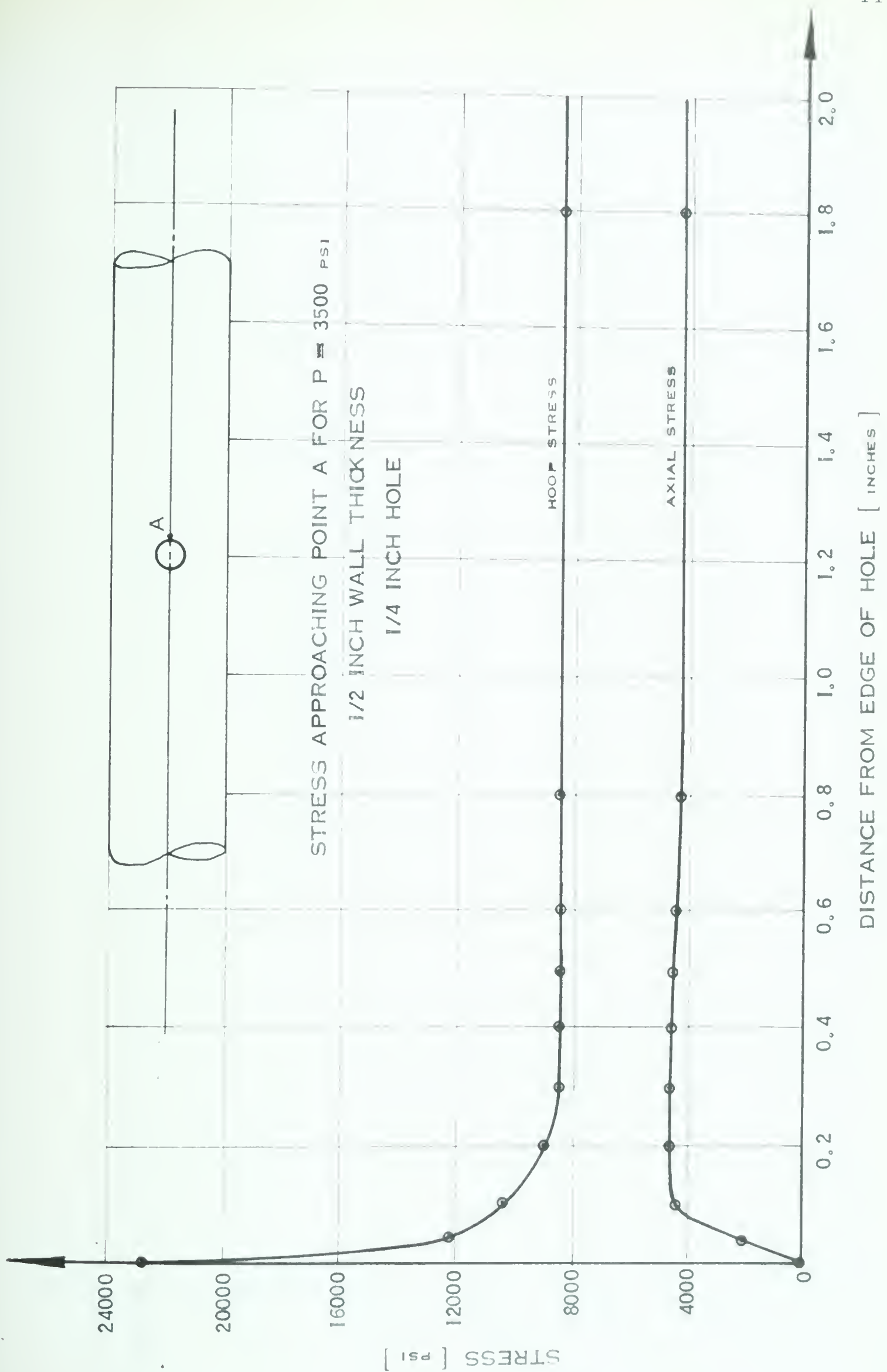


FIGURE 85.

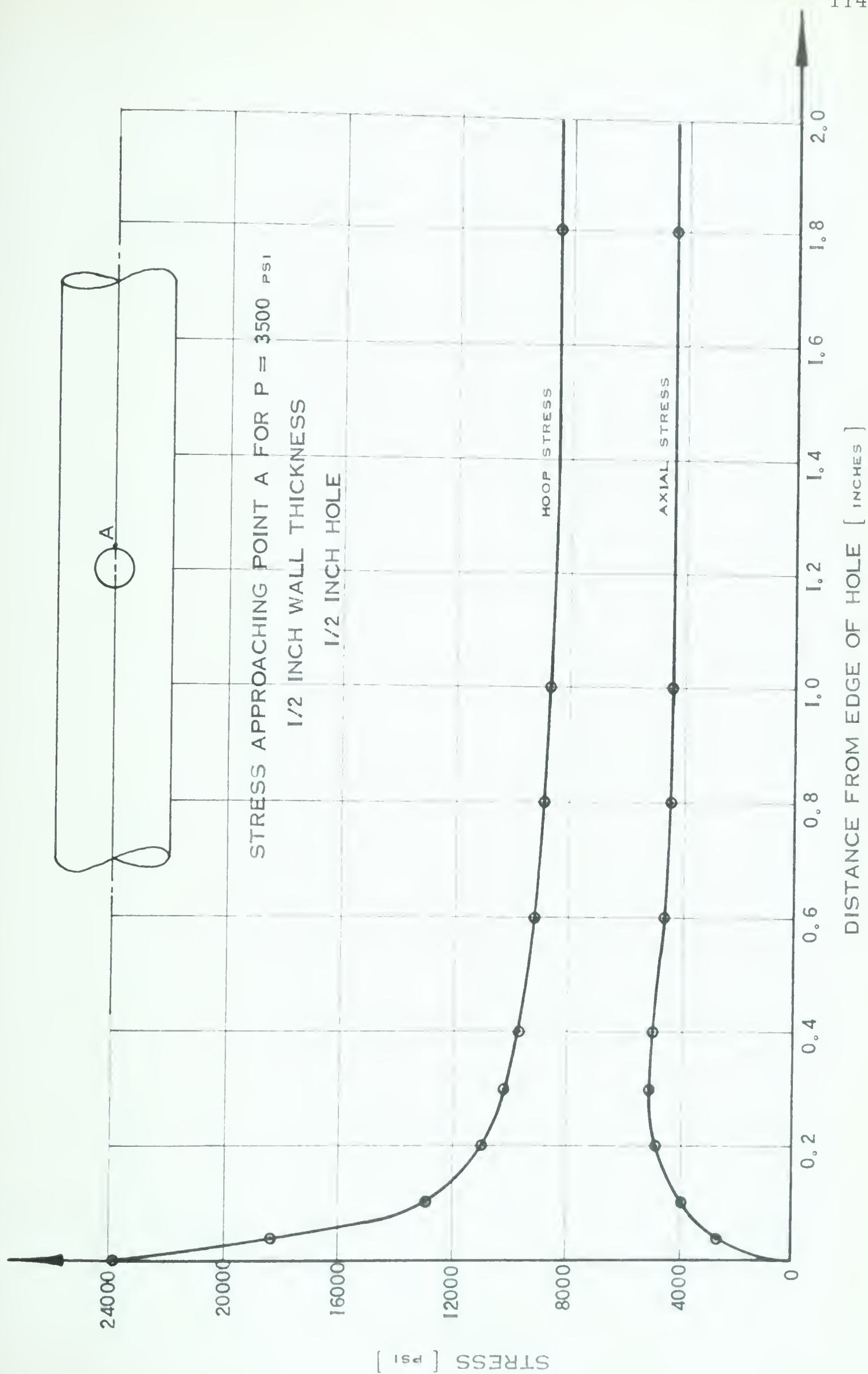


FIGURE 86.

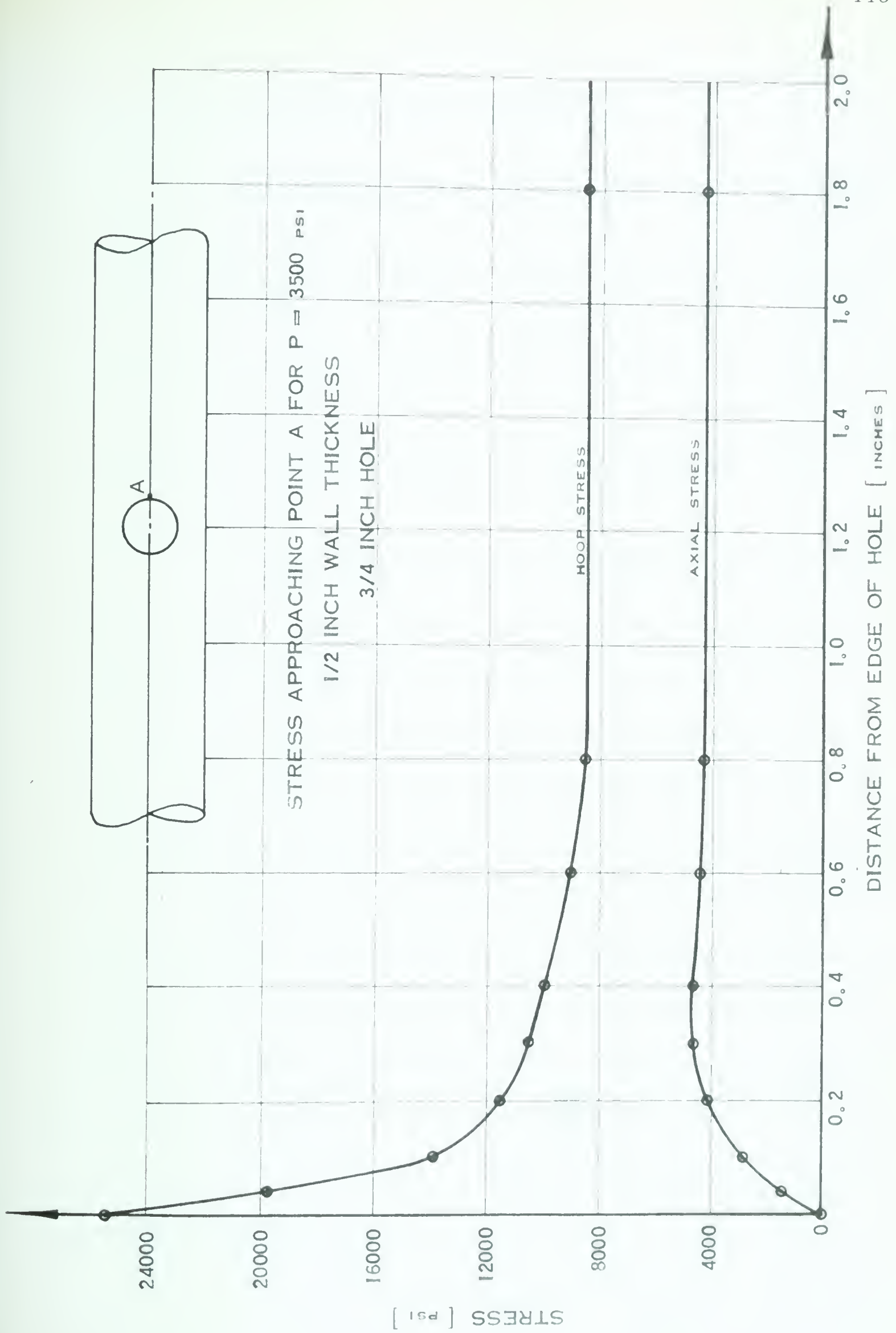


FIGURE 87.

7.4 Stress and Strain Approaching Point B

The diagrams of strain vs. distance from the edge of the hole approaching point B are shown in Figs. 88 to 99. The problem of physical dimensions mentioned for point A also applies for point B, although the strain did not increase as sharply near the edge of the hole at this point. If future investigations are endeavored, it would be advisable to use specimens of much larger dimensions.

The diagrams of stress vs. distance from the edge of the hole approaching point B are shown in Figs. 100 to 111. From these diagrams it is noted that the stress does not decrease as rapidly in this direction as does the stress approaching point A. In the most extreme cases the stress does not reduce to within five percent of the stress in the undisturbed area at a distance of less than four hole diameters from the edge of the hole, and in none of the configurations tested is the stress within this limit at a distance of less than one and one half hole diameters from the boundary. However, the magnitude of the stress tangential to the hole approaching point B was in most cases not as great as at point A. It, therefore, was not the governing stress.

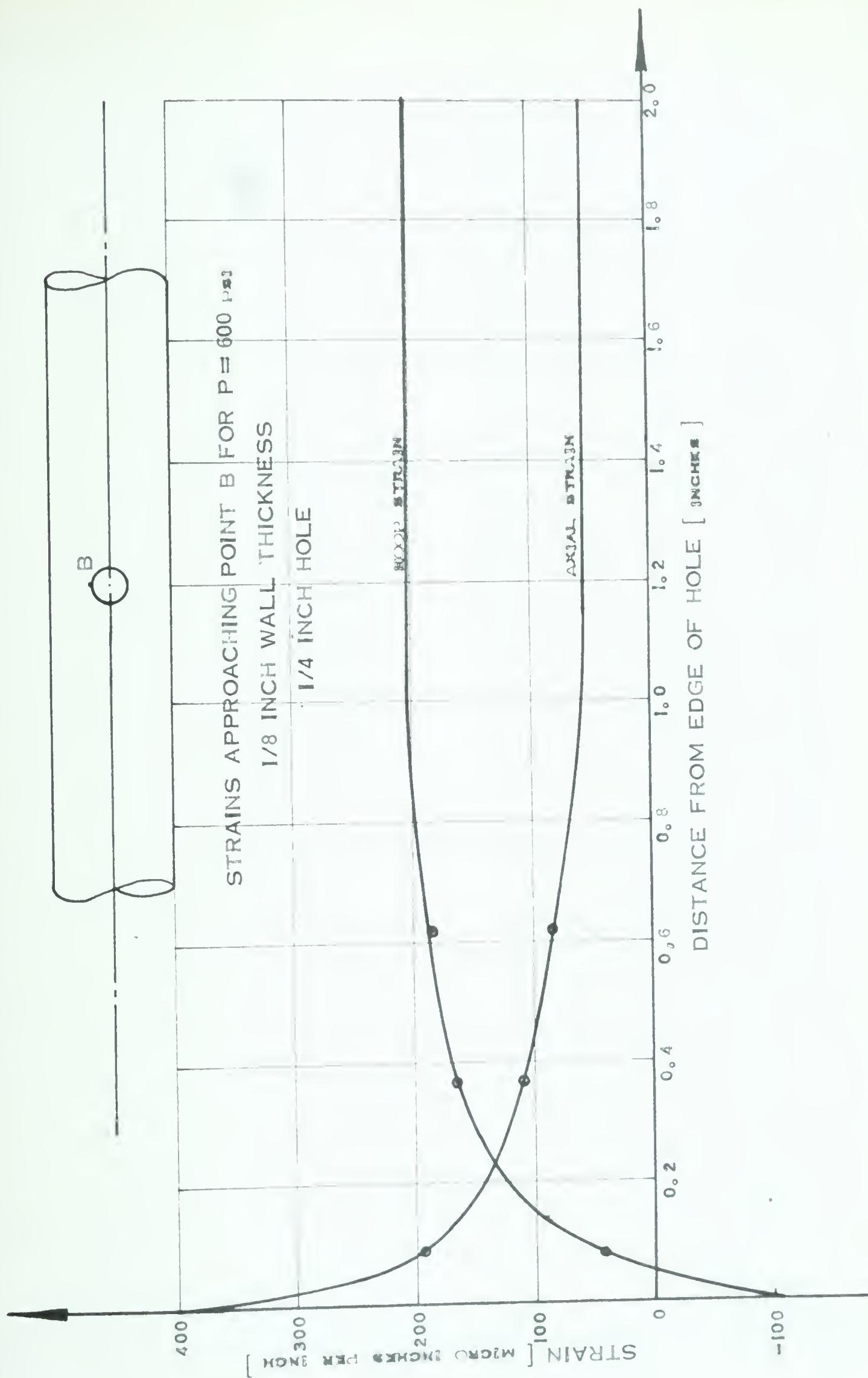


FIGURE 88.

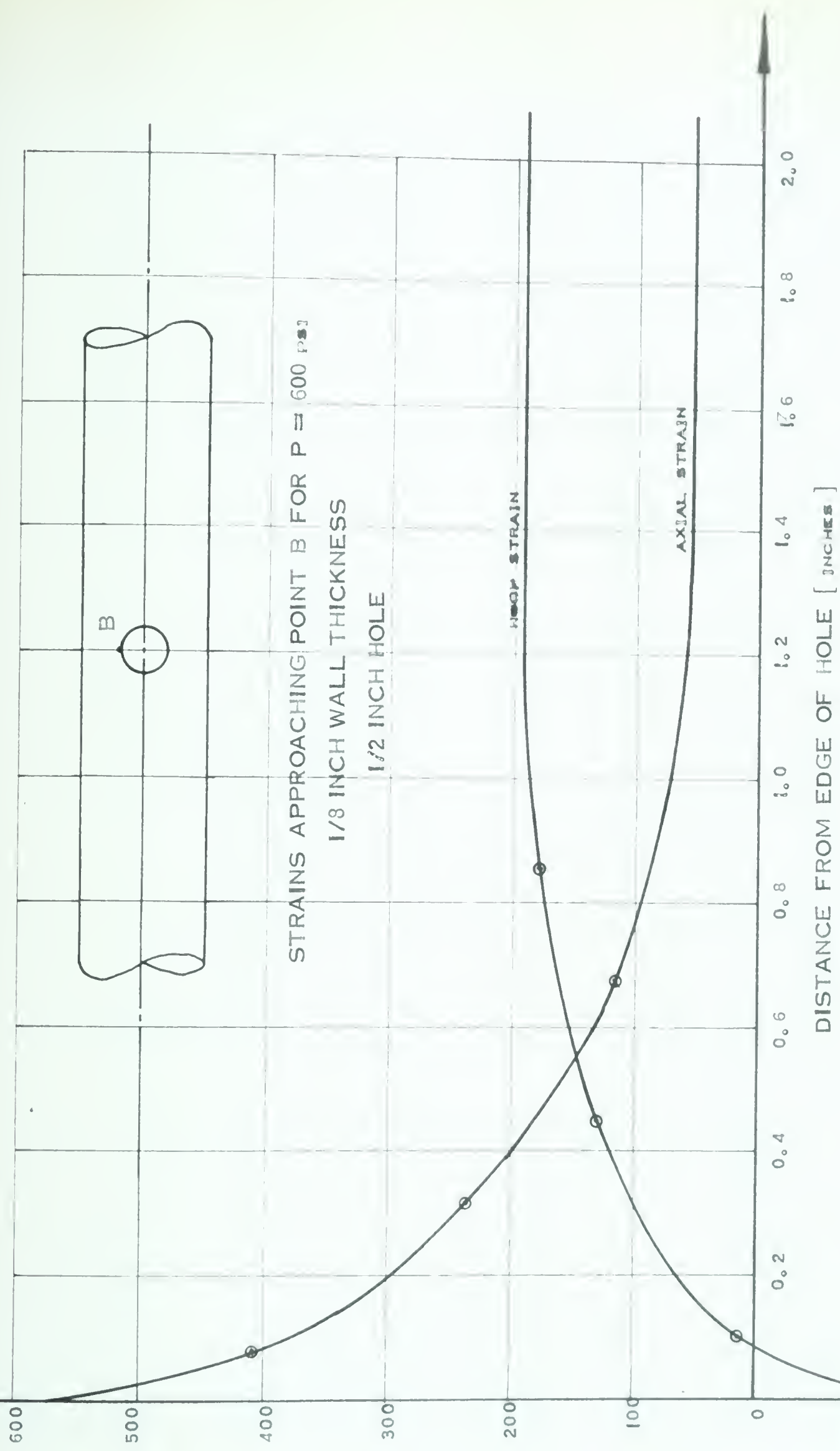


FIGURE 89.

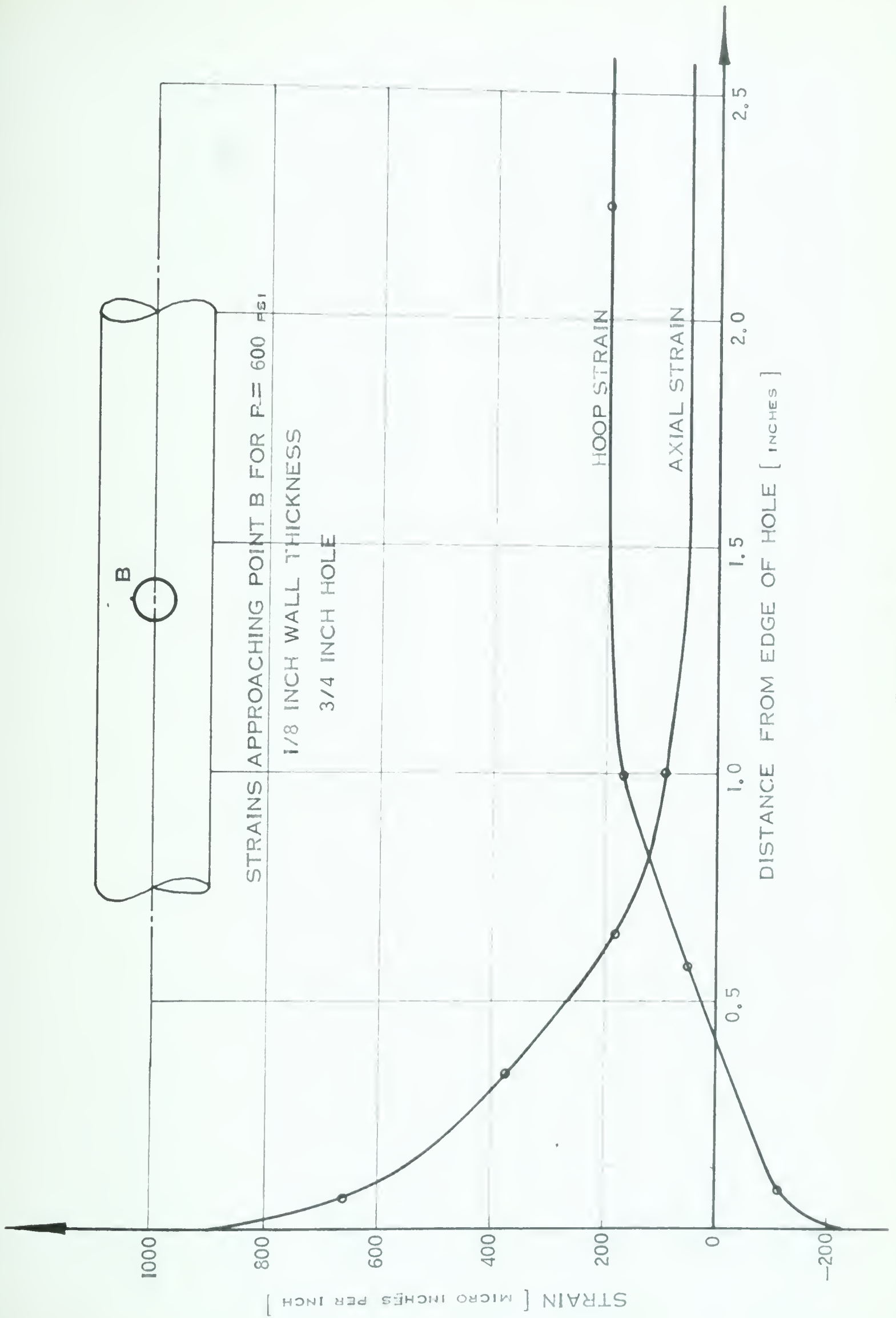


FIGURE 90.

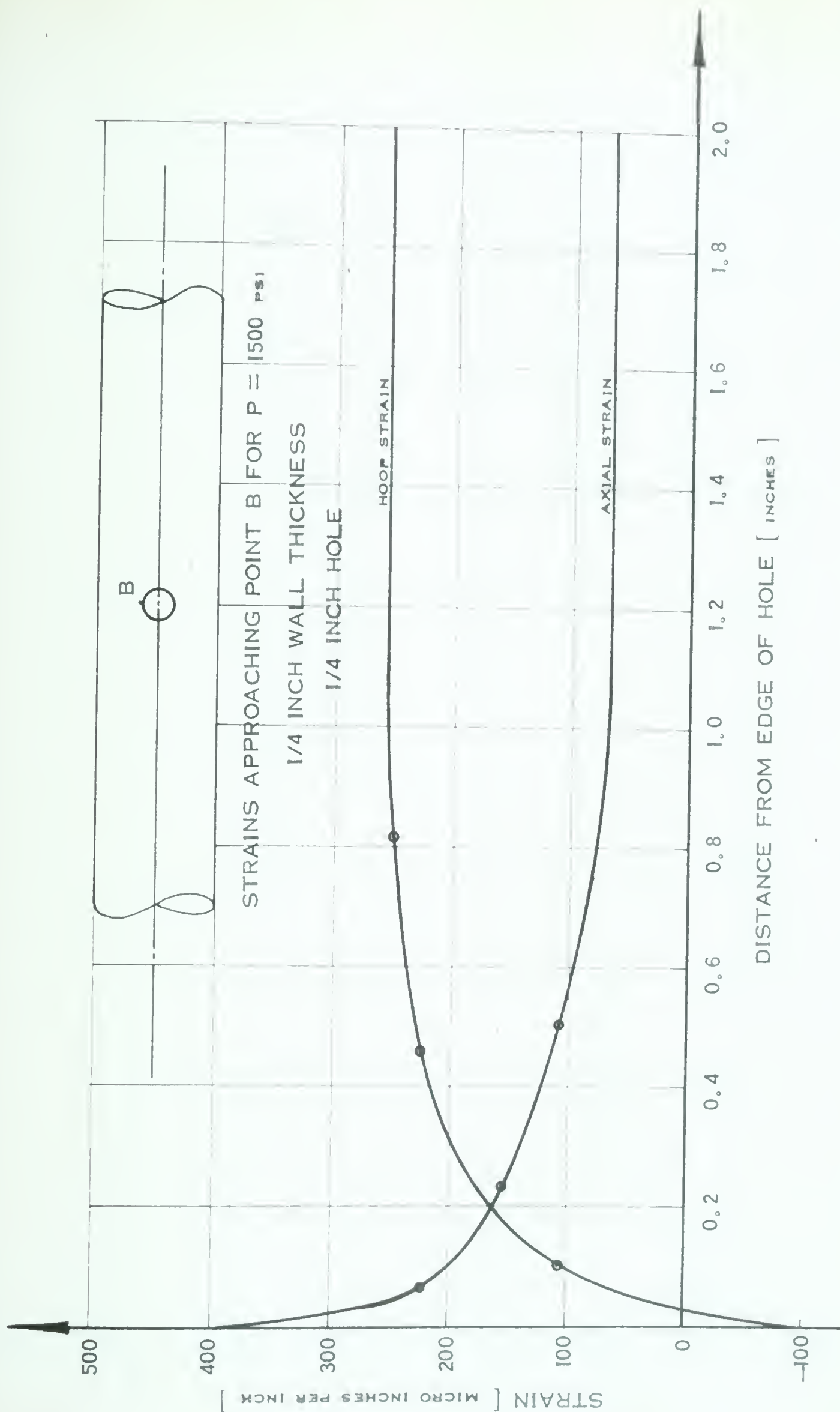


FIGURE 91.

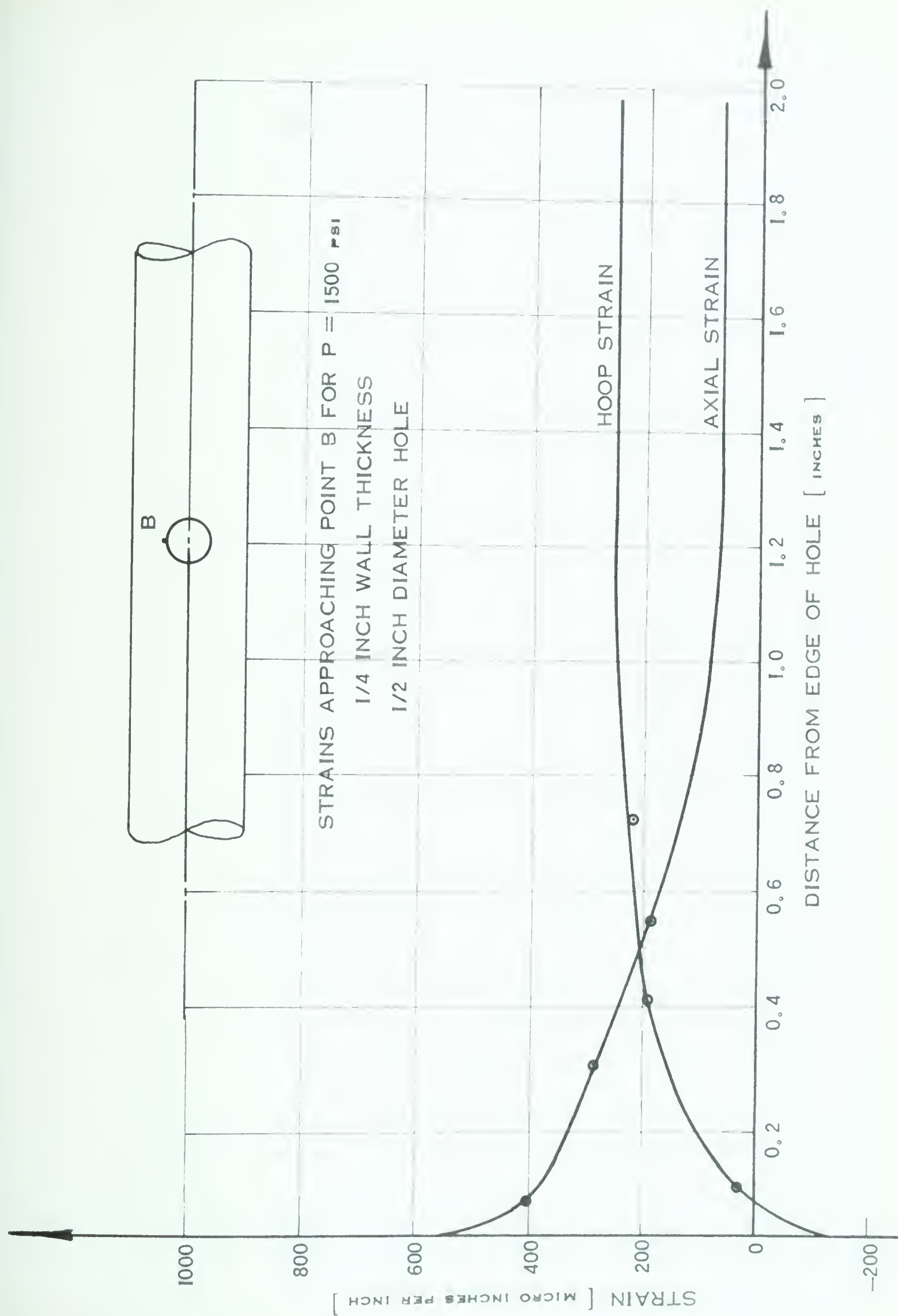


FIGURE 92.

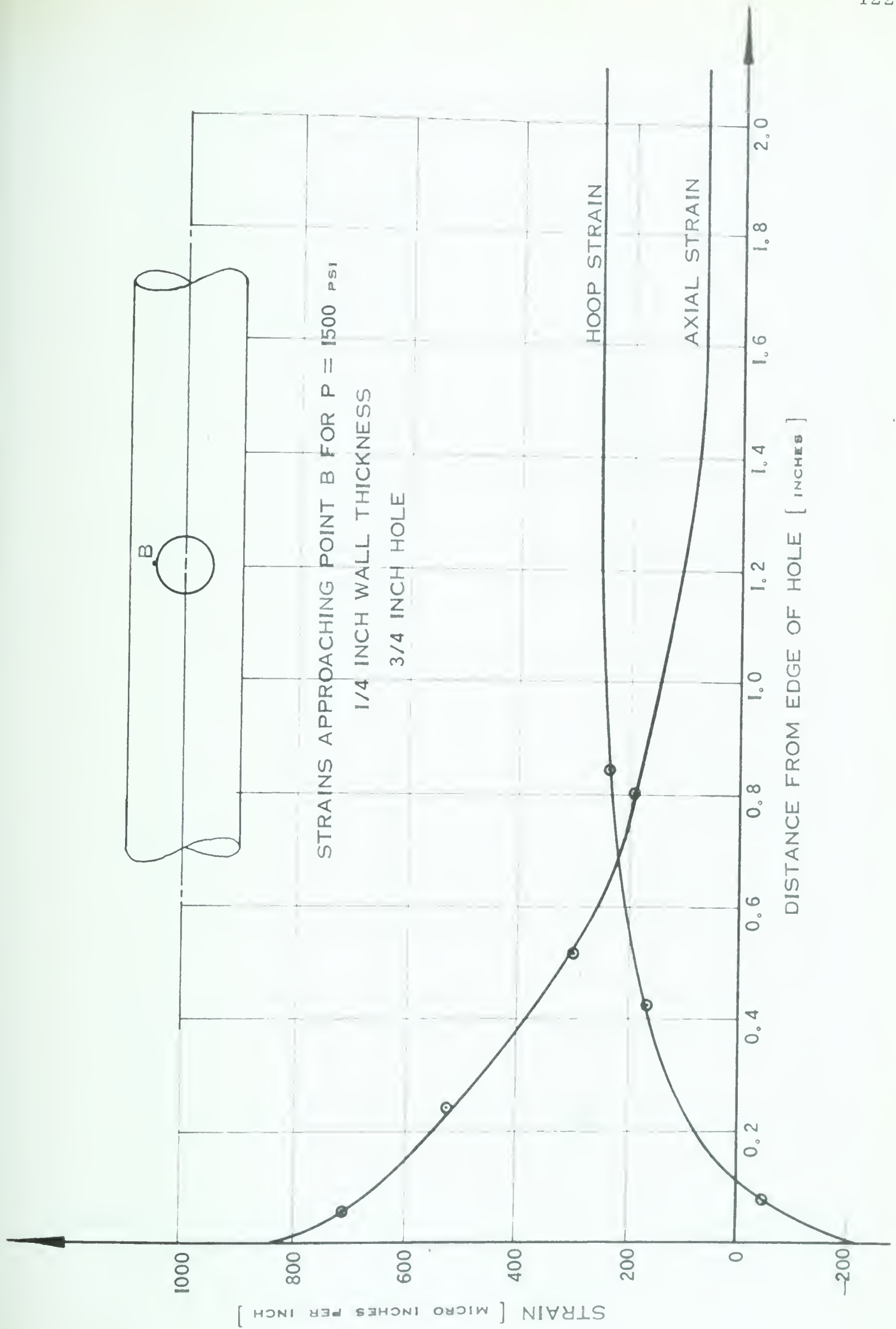


FIGURE 93.

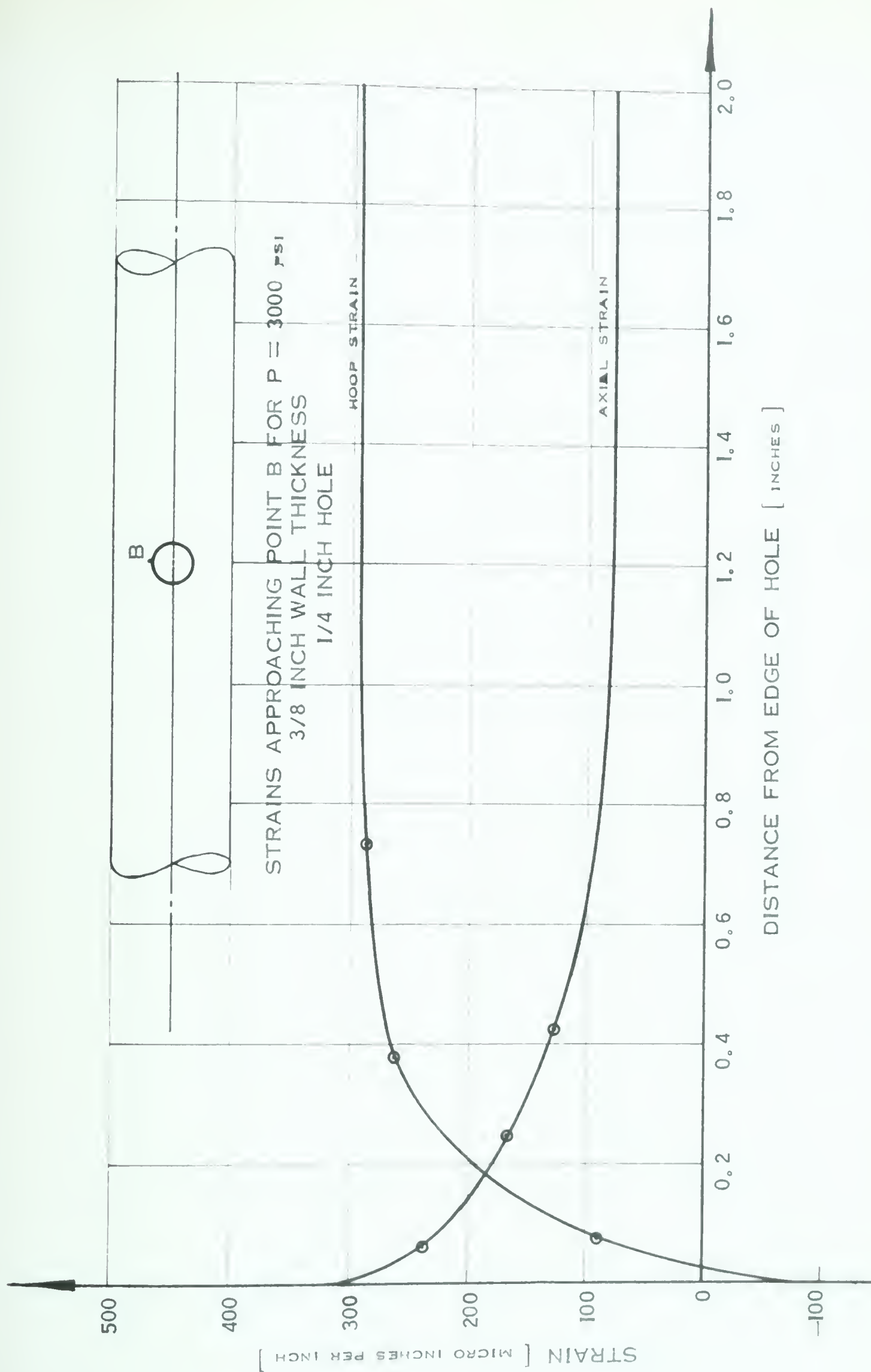


FIGURE 94.

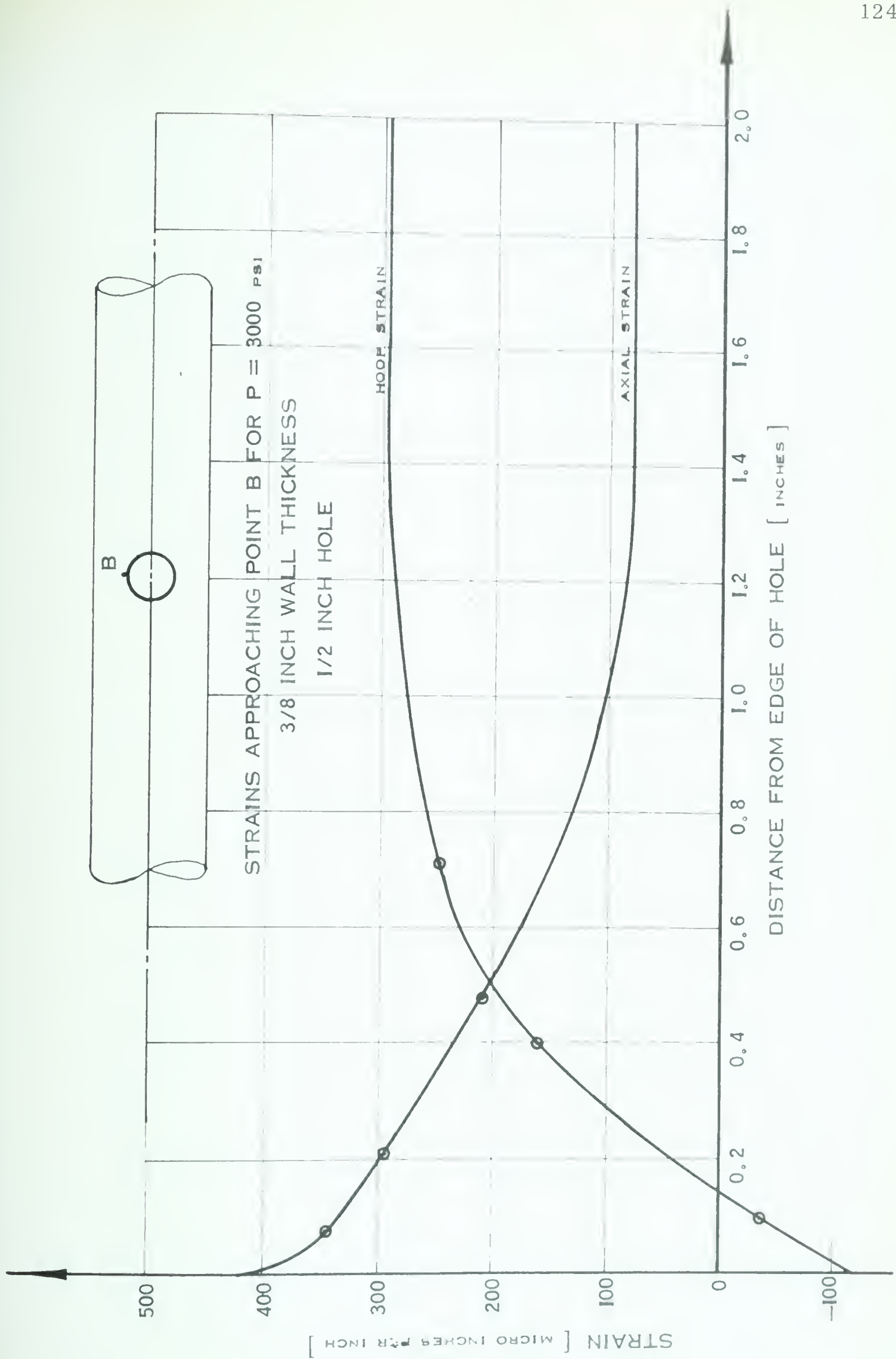


FIGURE 95.

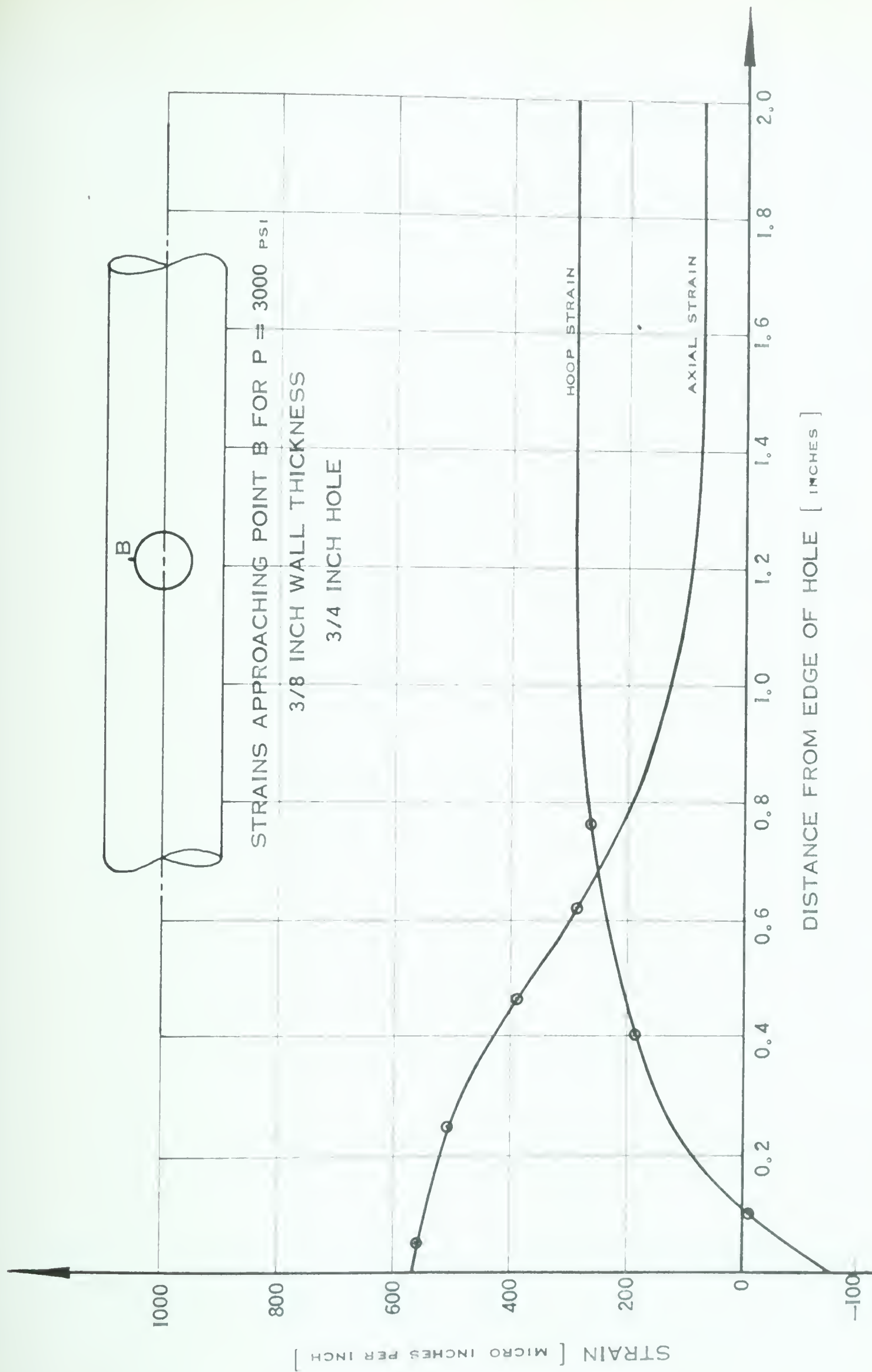


FIGURE 96.

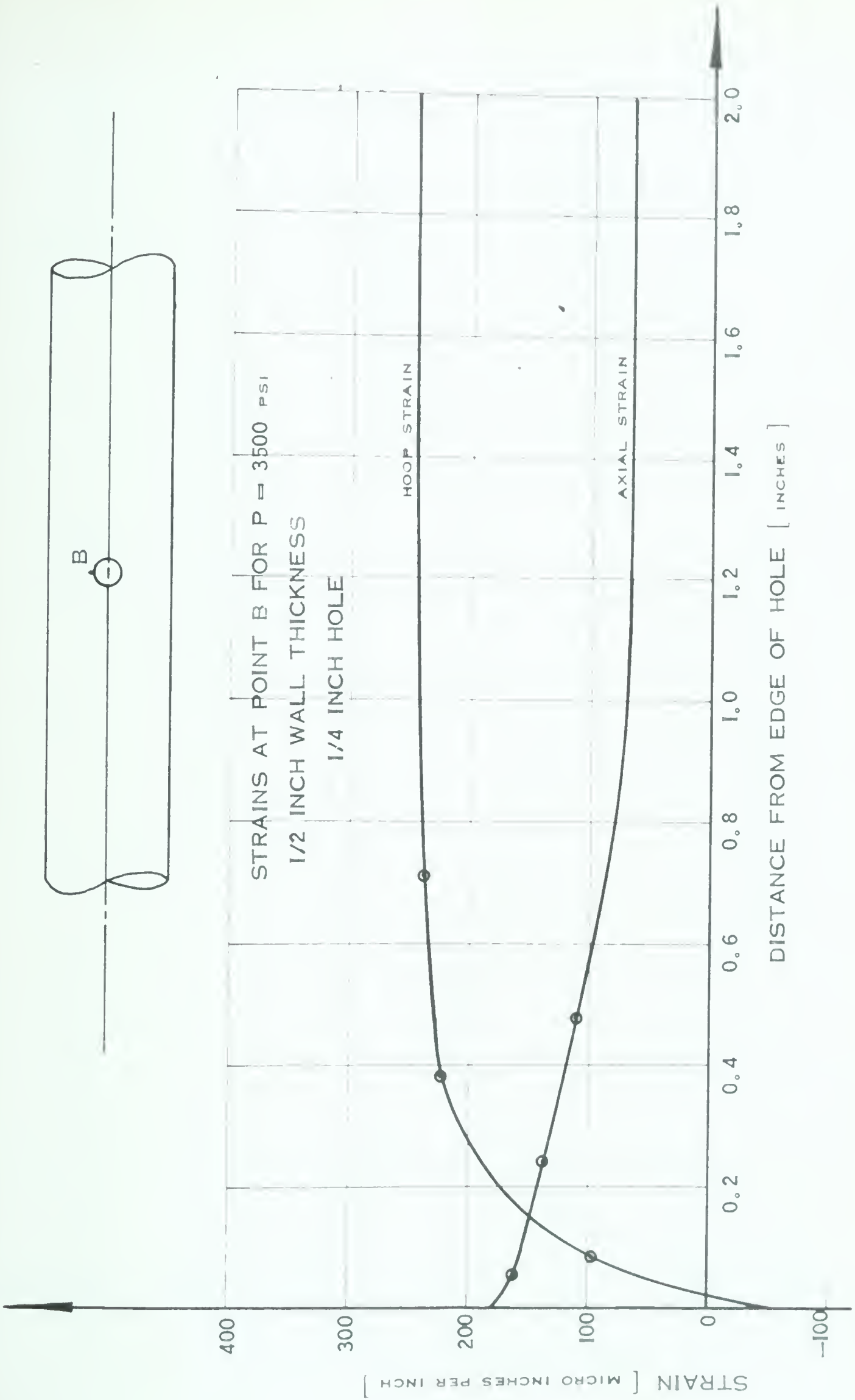


FIGURE 97.

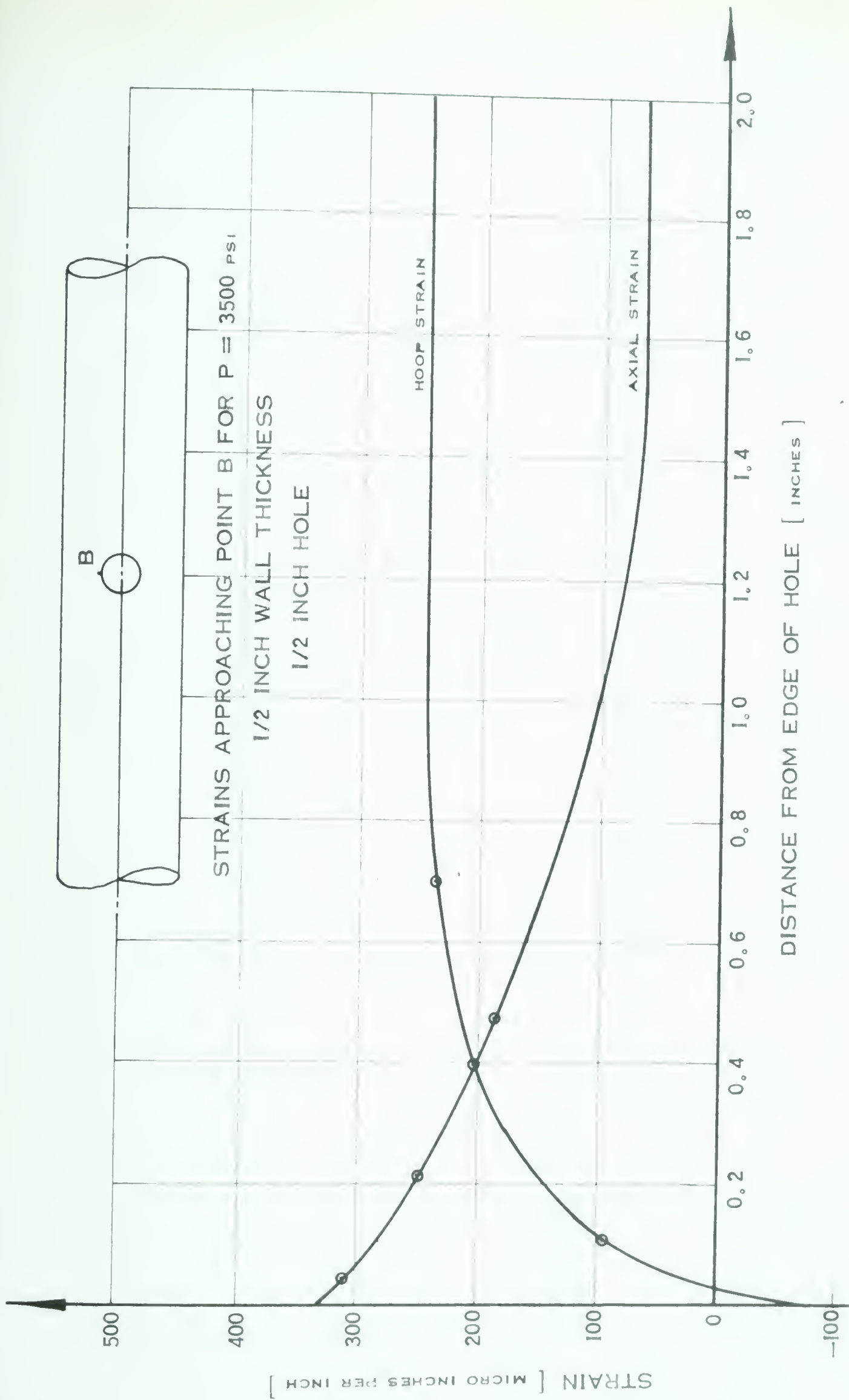


FIGURE 98.

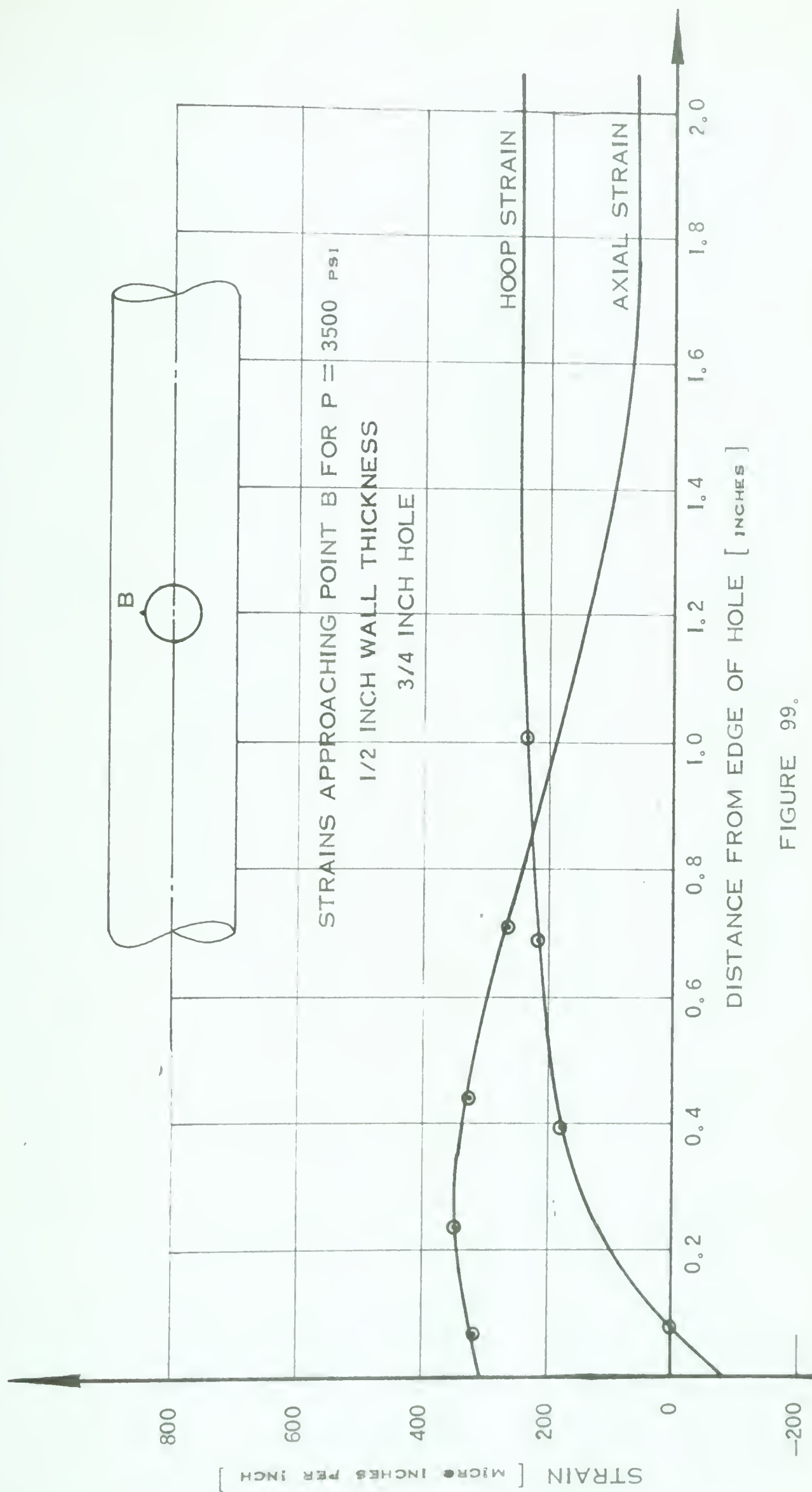


FIGURE 99.

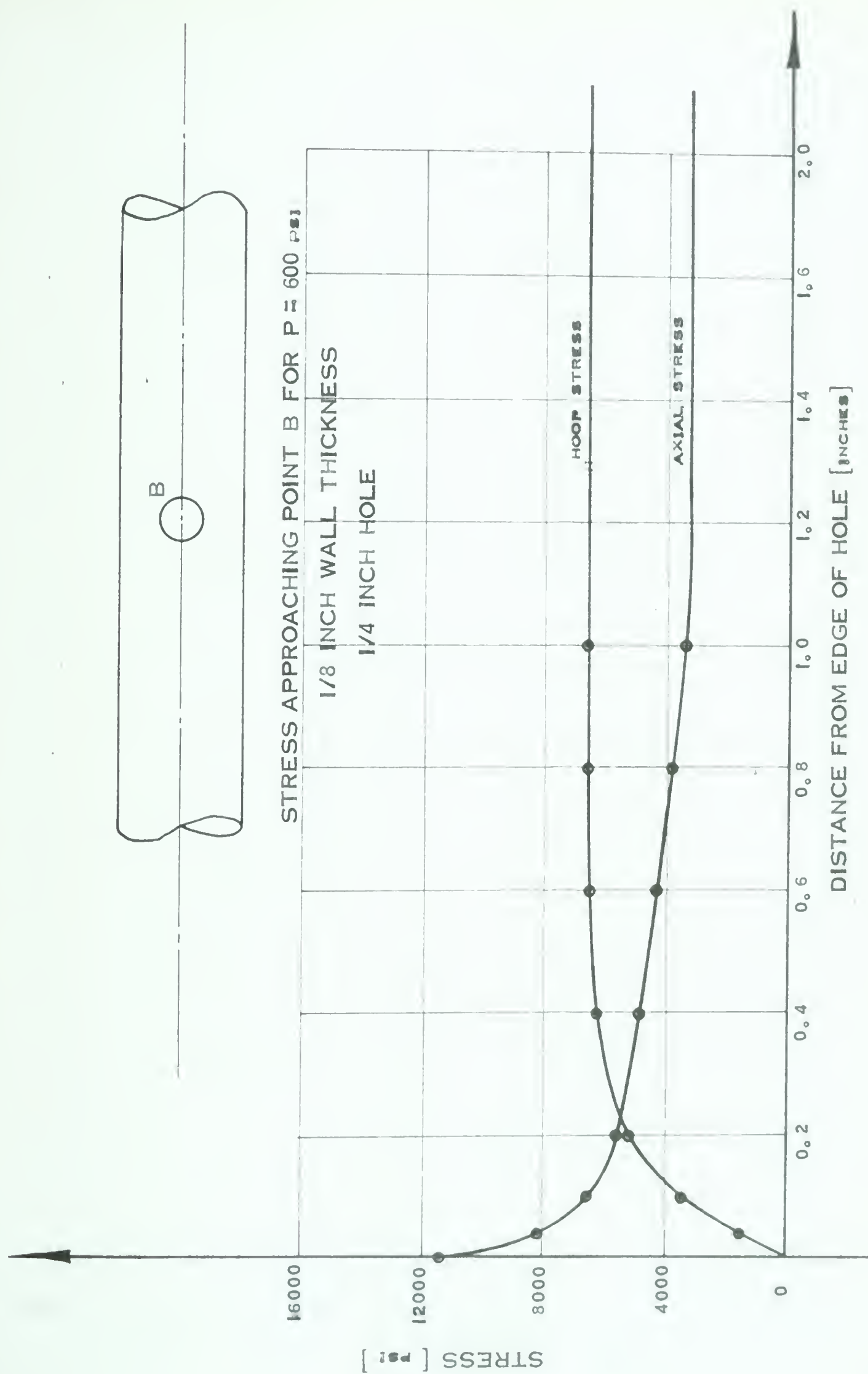


FIGURE 100.

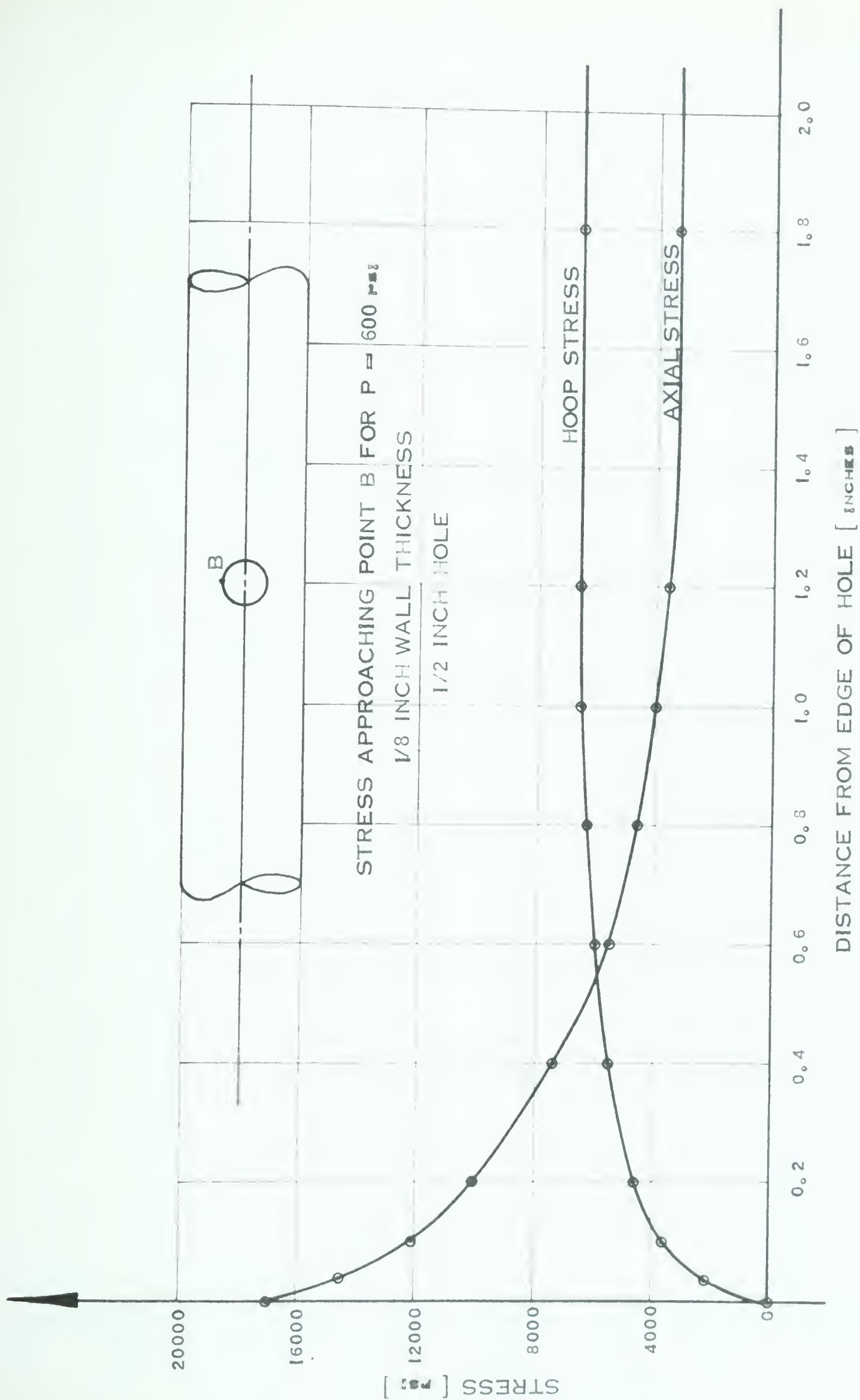


FIGURE 101.

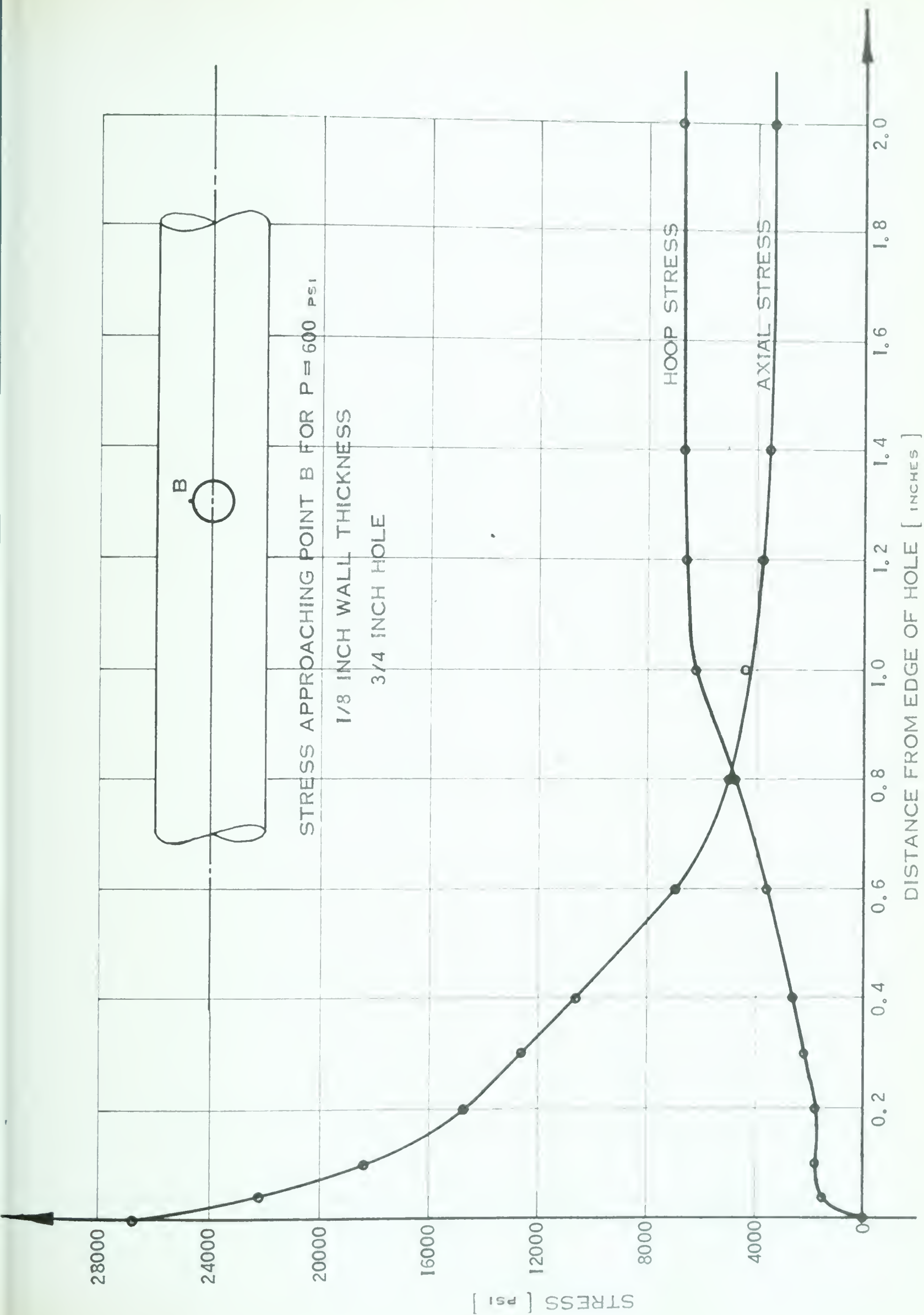


FIGURE 102.

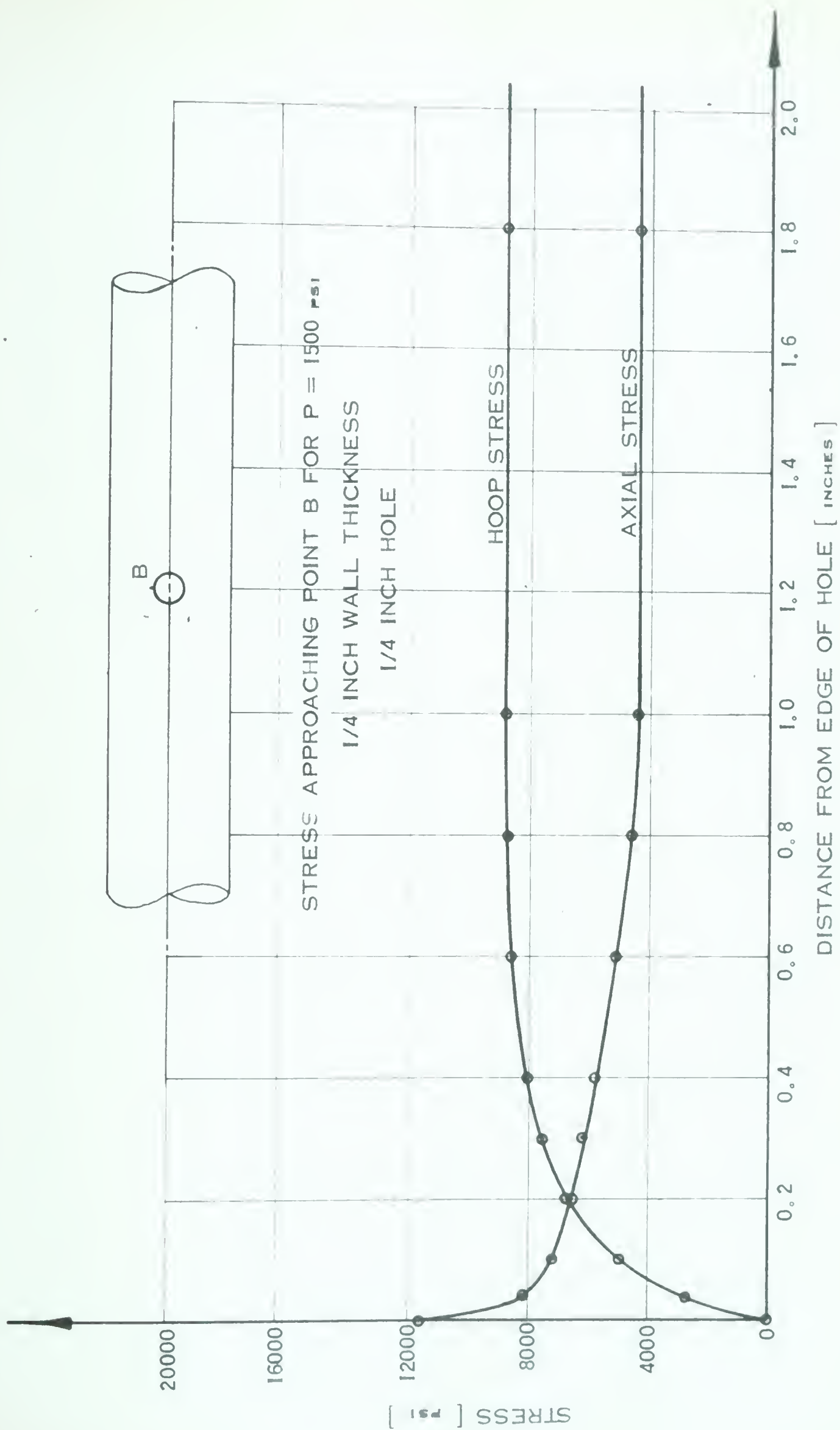


FIGURE 103.

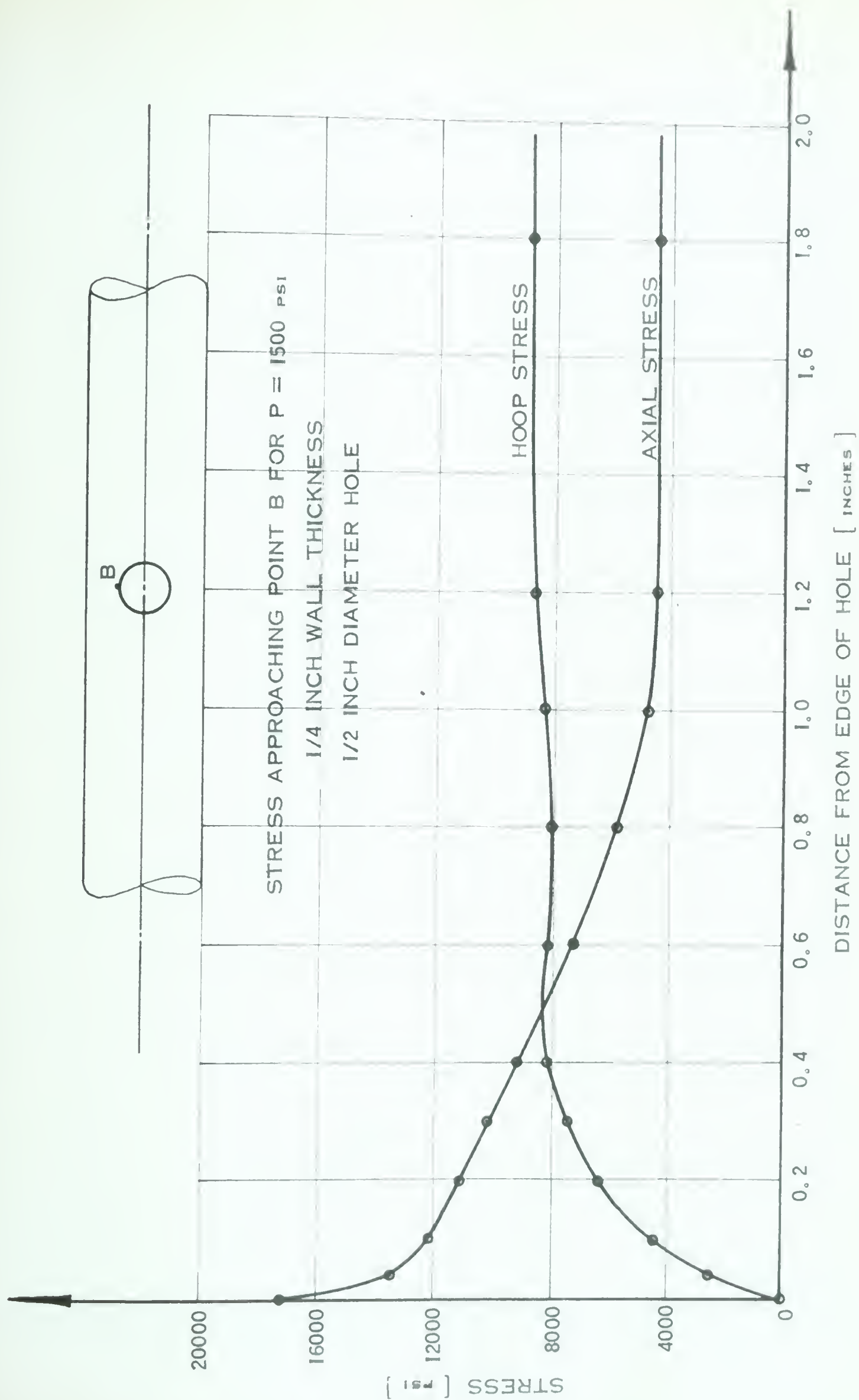


FIGURE 104.

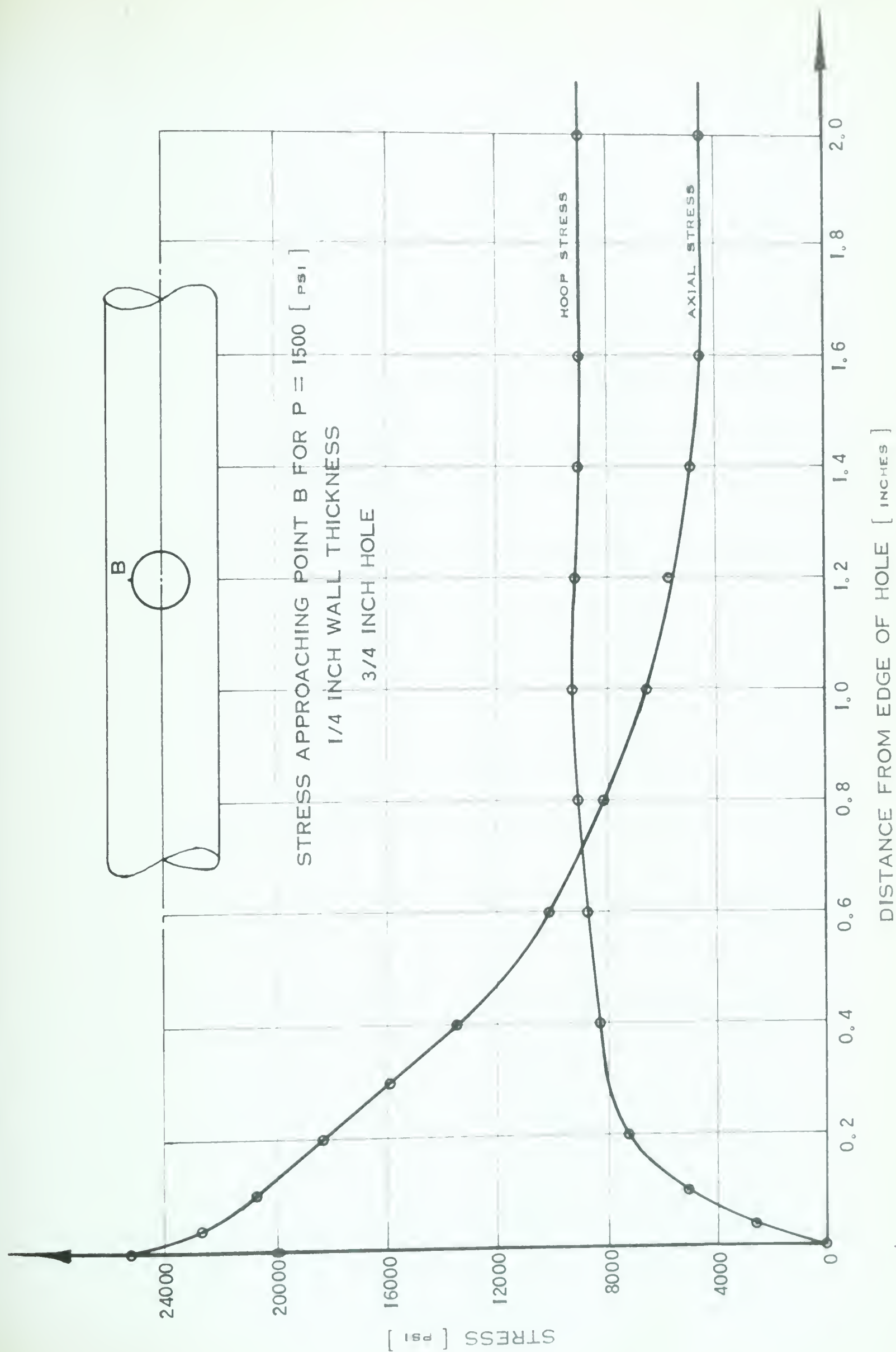


FIGURE 105.

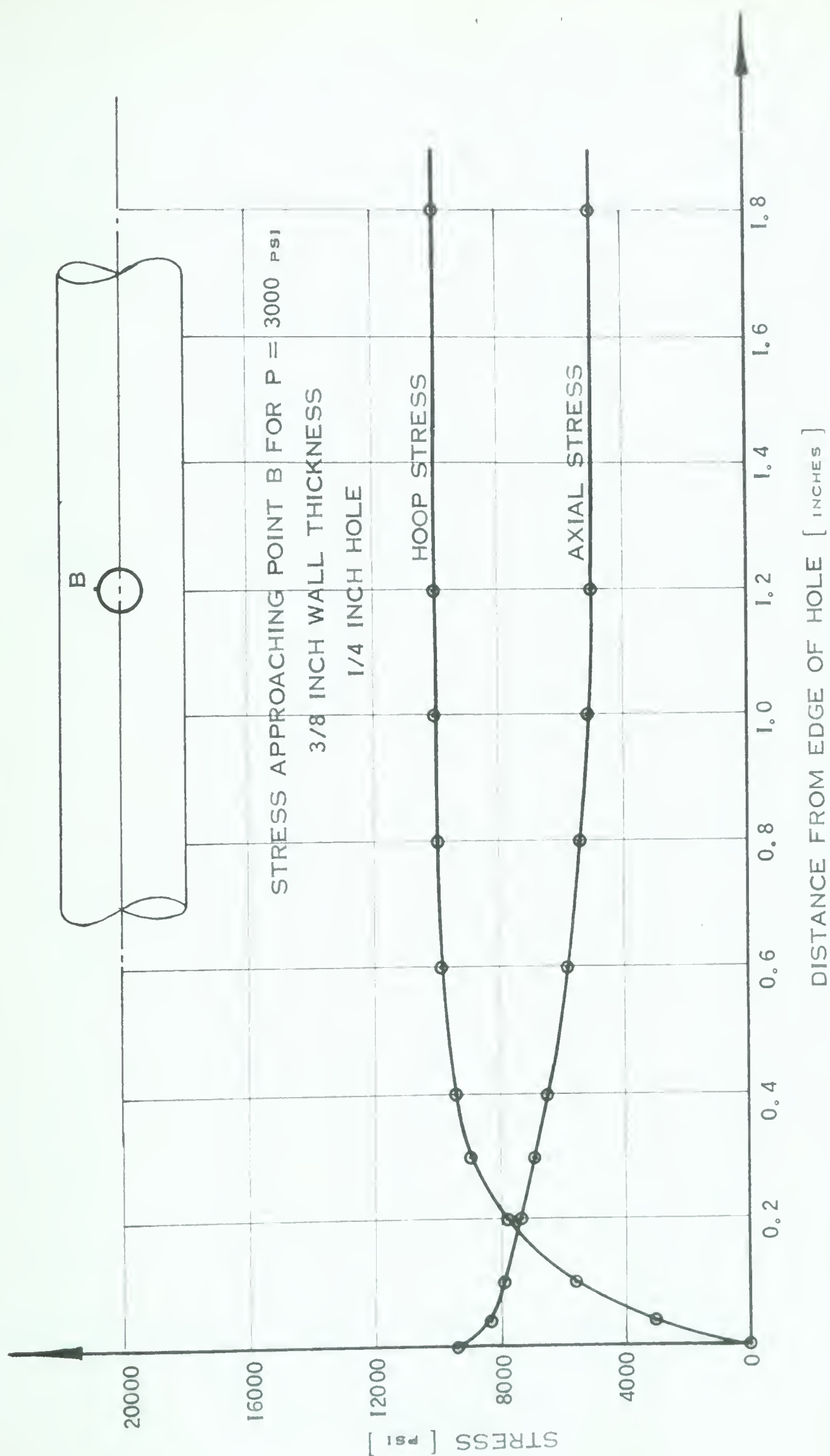


FIGURE 106.

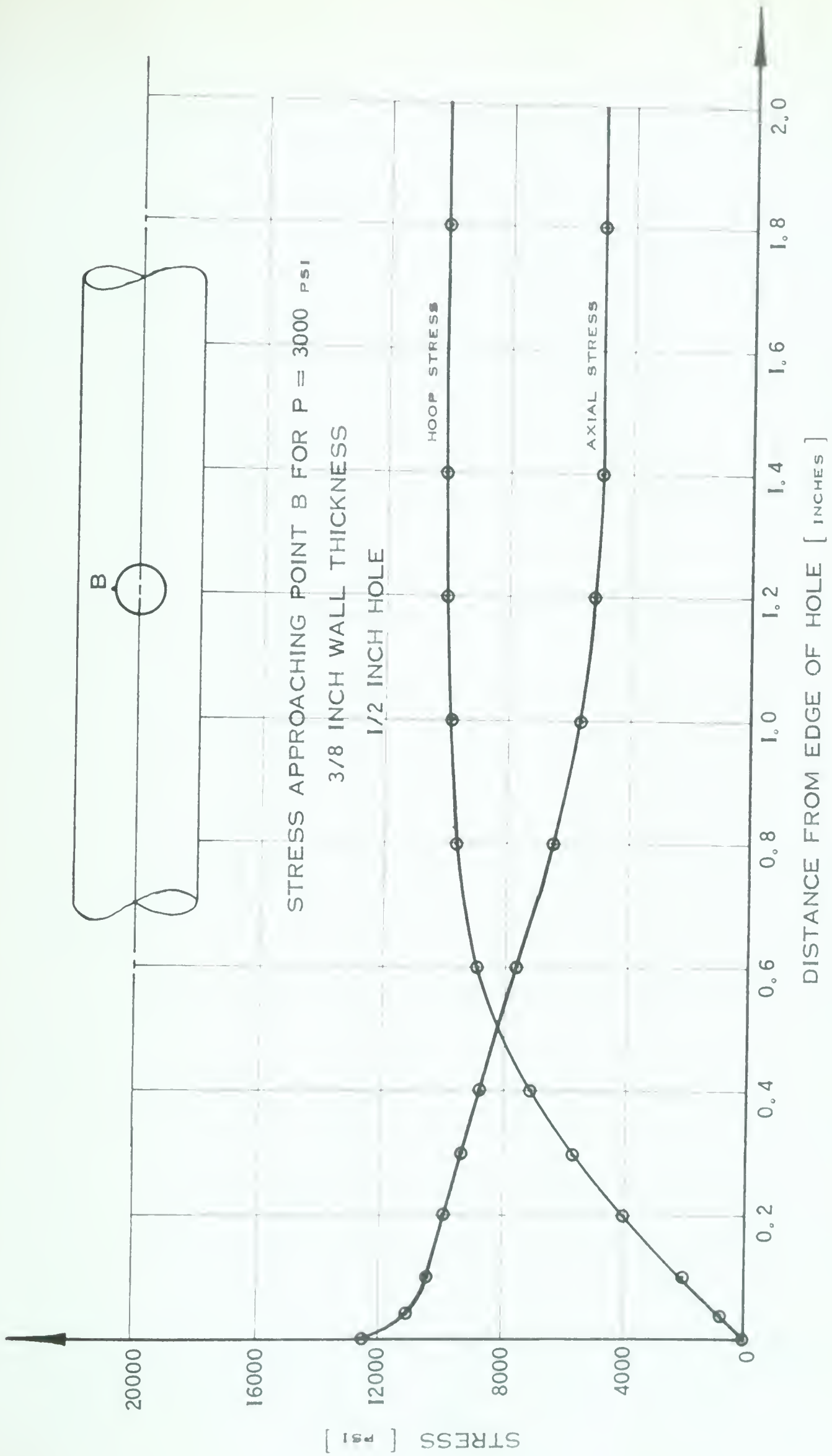


FIGURE 107.

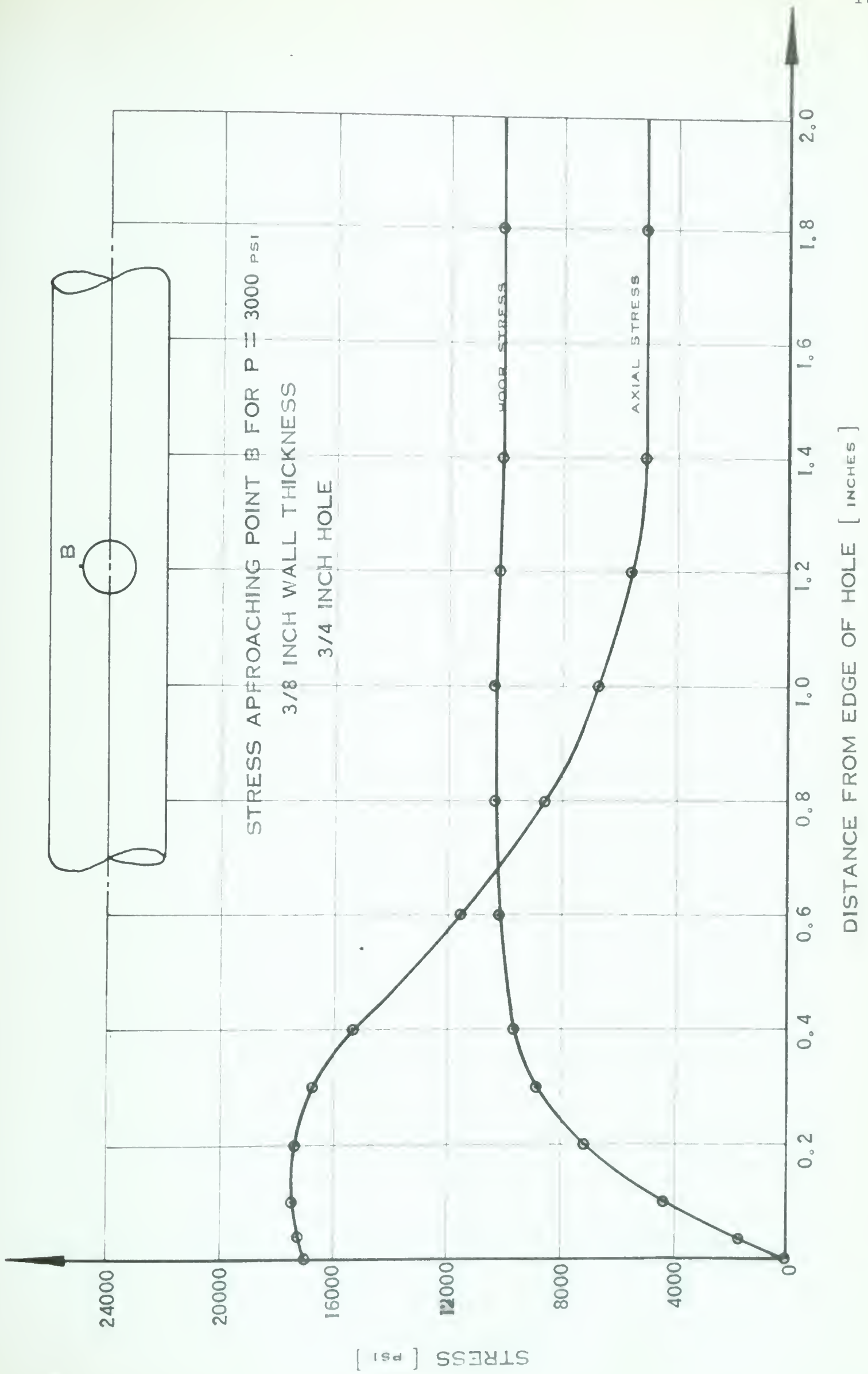


FIGURE 108.

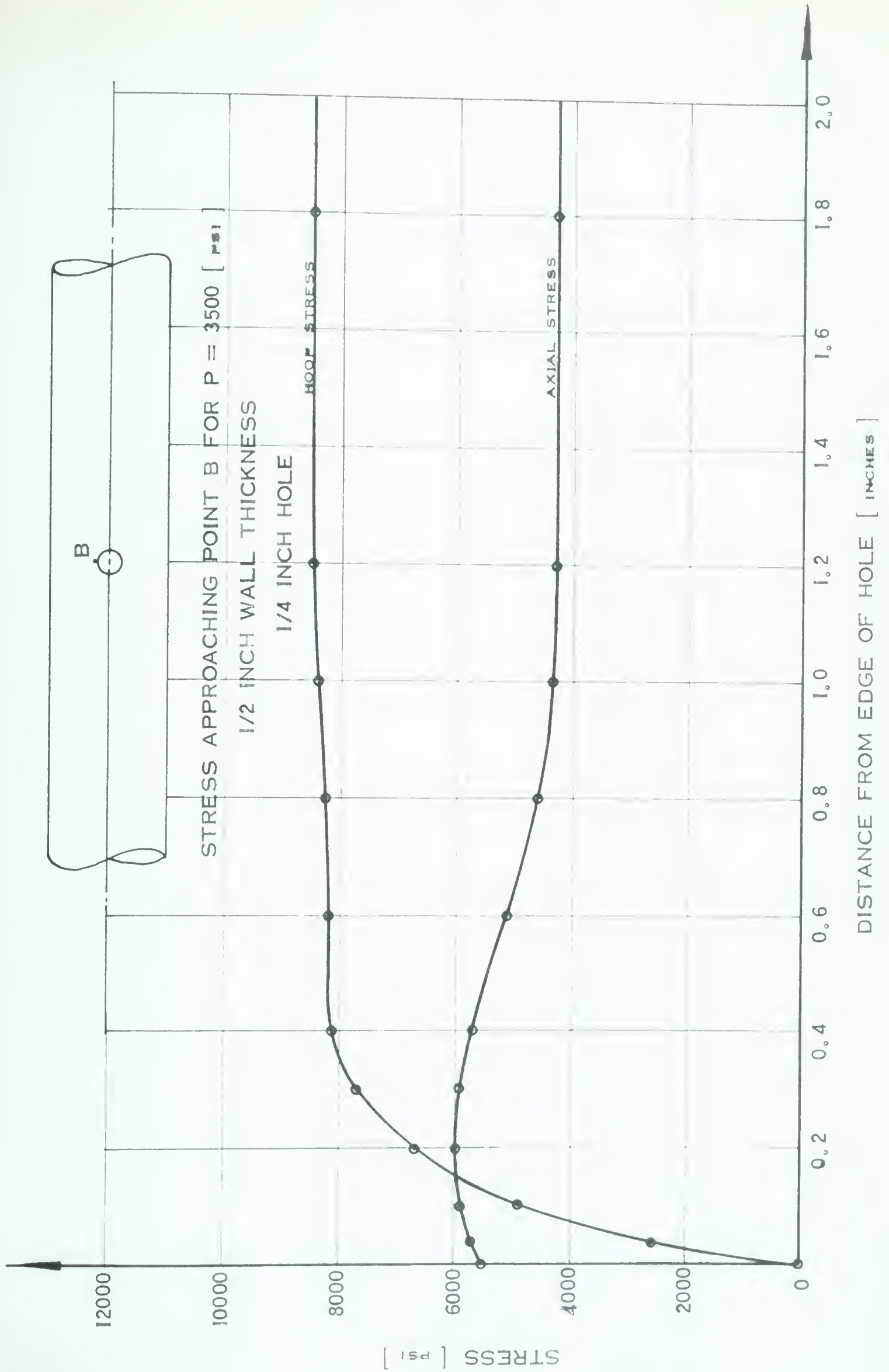


FIGURE 109.

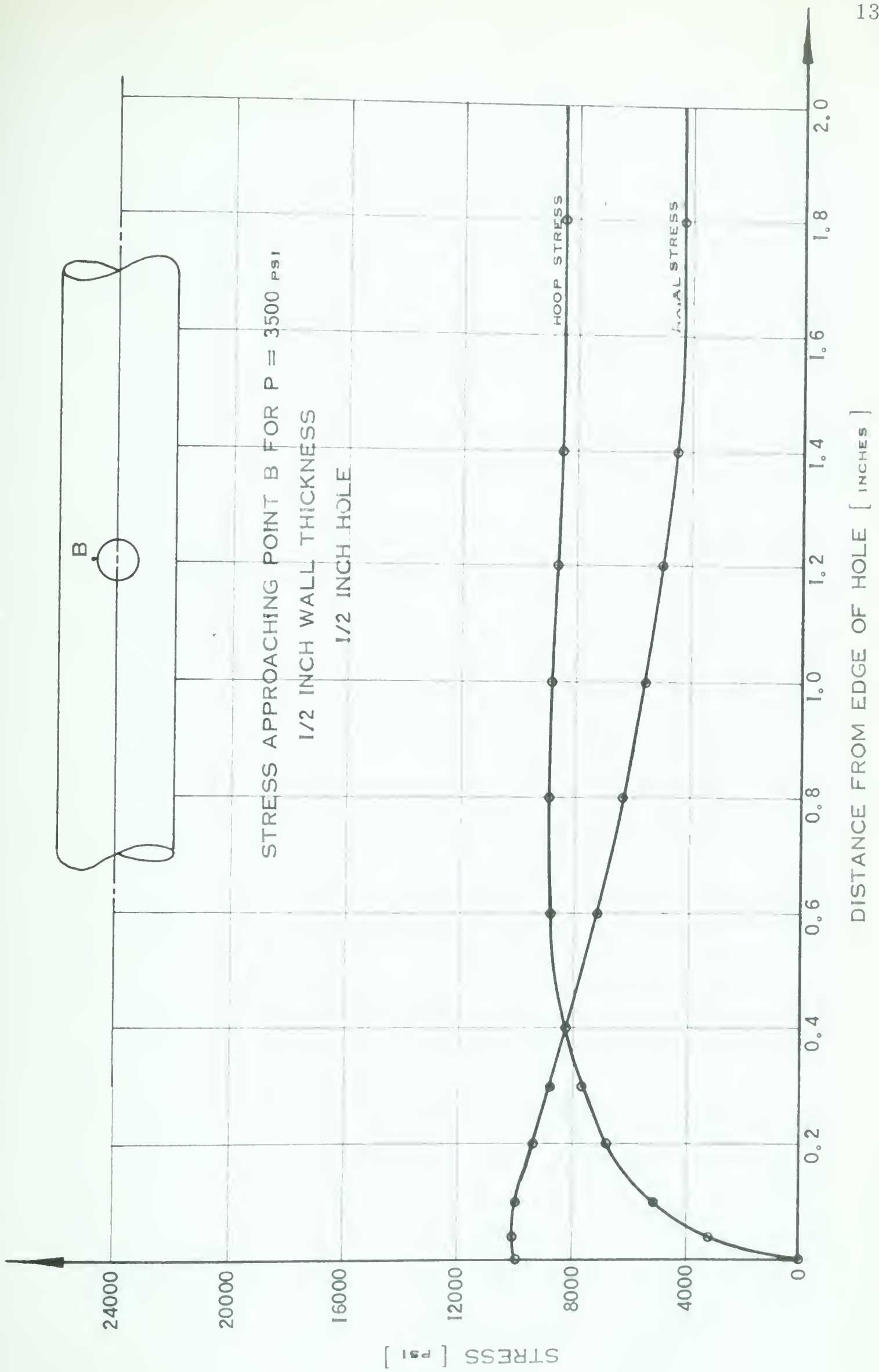


FIGURE 110.

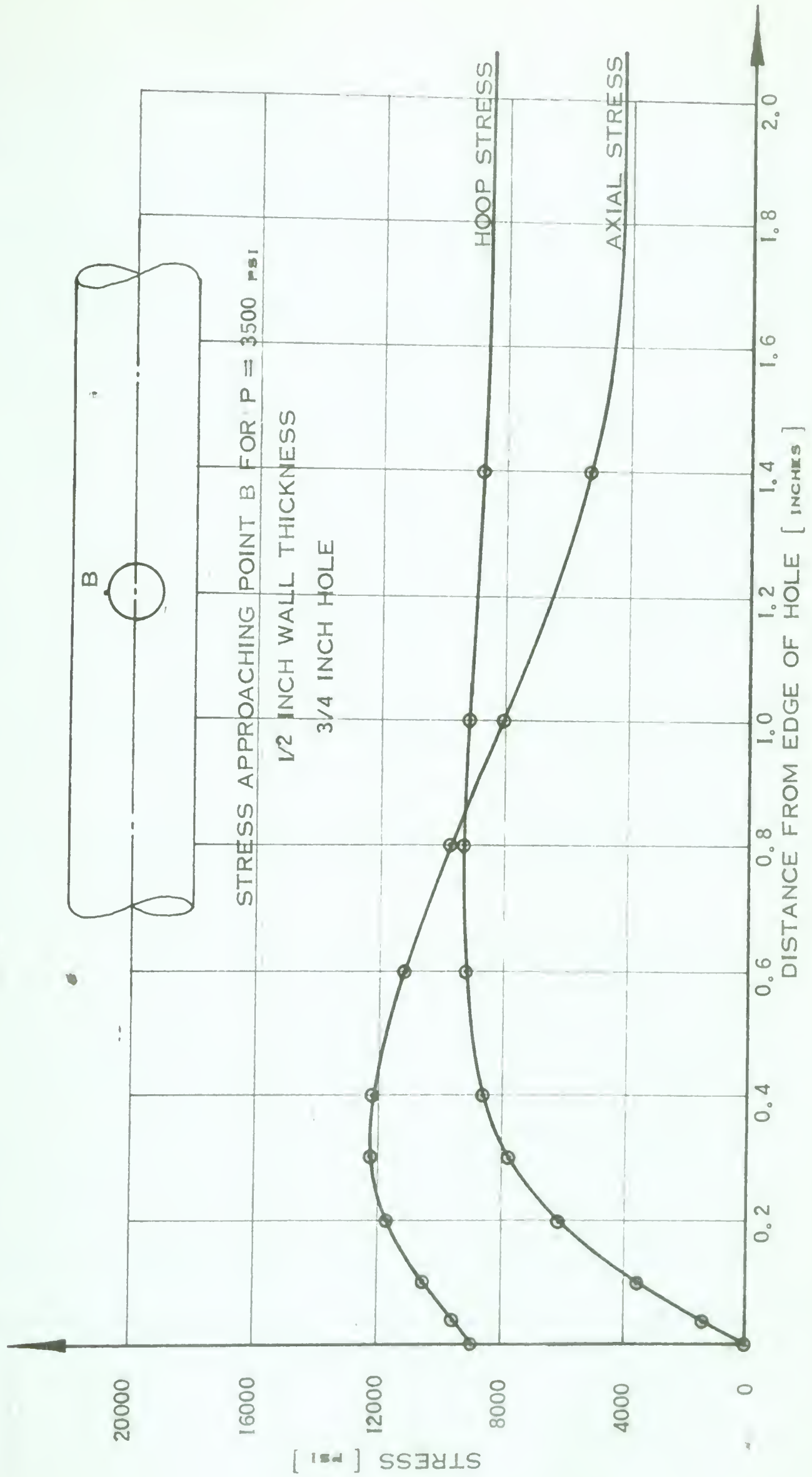


FIGURE III

7.5 Stress Concentration Factor Curves

The stress concentration factor curves at points A and B are given in Figs. 112 and 113 respectively. These curves were plotted from results of the previous diagrams of stress vs. distance from the edge of the hole.

The stress concentration factor in this case is defined to be the ratio of stress tangential to the boundary of the hole to hoop stress in an undisturbed region of the cylinder. This definition was used to compare the amplitude of the stress at the edge of the hole to the hoop stress at the same point on the cylinder without a hole. It should be noted that the maximum stress in a cylinder without a hole occurs at the inside surface and this investigation has only analyzed stresses on the outside surface of the cylinder.

For the thin cylinders tested the difference between stress at the outside surface and stress at the inside surface in the undisturbed region is relatively small as calculated using Lamé's solution¹⁰, so the stress concentration factor derived may be considered to be valid for all points through the wall of the cylinder. However, the stress at the inside surface of the thicker-walled cylinders is considerably different from the stress

at the outside surface. Although the stress concentration factor derived is correct when comparing stresses on the outside surface of the cylinder, there is no data available to support an assumption that the stress increases proportionately at the inside surface. However, this stress concentration factor may be used as an indication of the magnitude of the maximum stress in the cylinder.

As noted previously the accuracy of stresses found at the edge of the hole for smaller hole diameters is questionable, however, the results are sufficiently correct to give a quantitative indication of the magnitude of the stress concentration involved.

From Fig. 112 it is seen that the stress concentration at point A increases with increasing wall thickness, as well as increasing size of hole. This agrees with the findings of Loshkarev⁵. For the cylinder dimensions tested the rate of change of stress concentration factor at point A was not too great, the stress concentration factor varying from 2.5 to 3.0 for the whole range analyzed. The stress concentration factor at this point for a small hole in a thin cylinder was 2.5 as expected from flat plate theory.

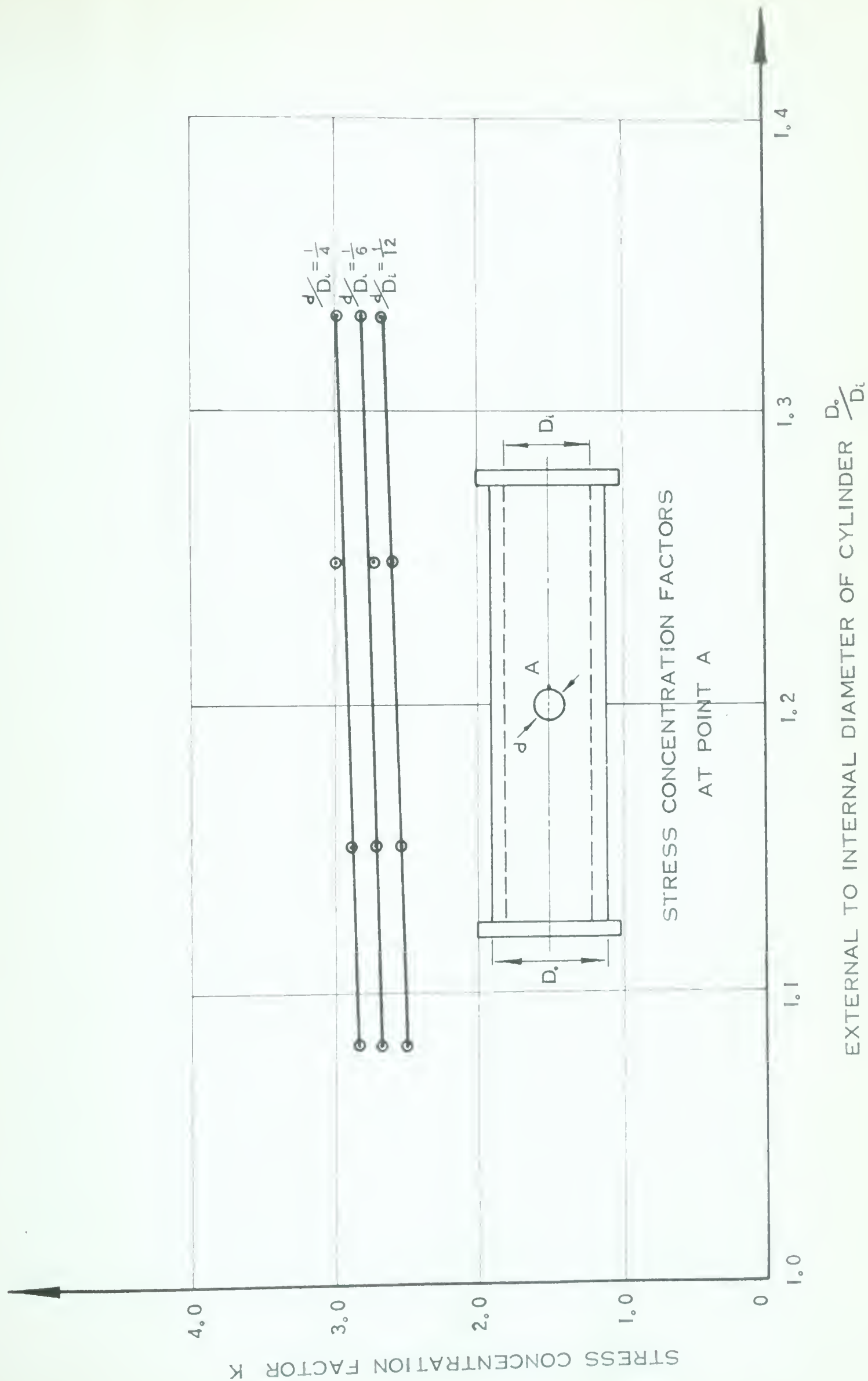


FIGURE 112.

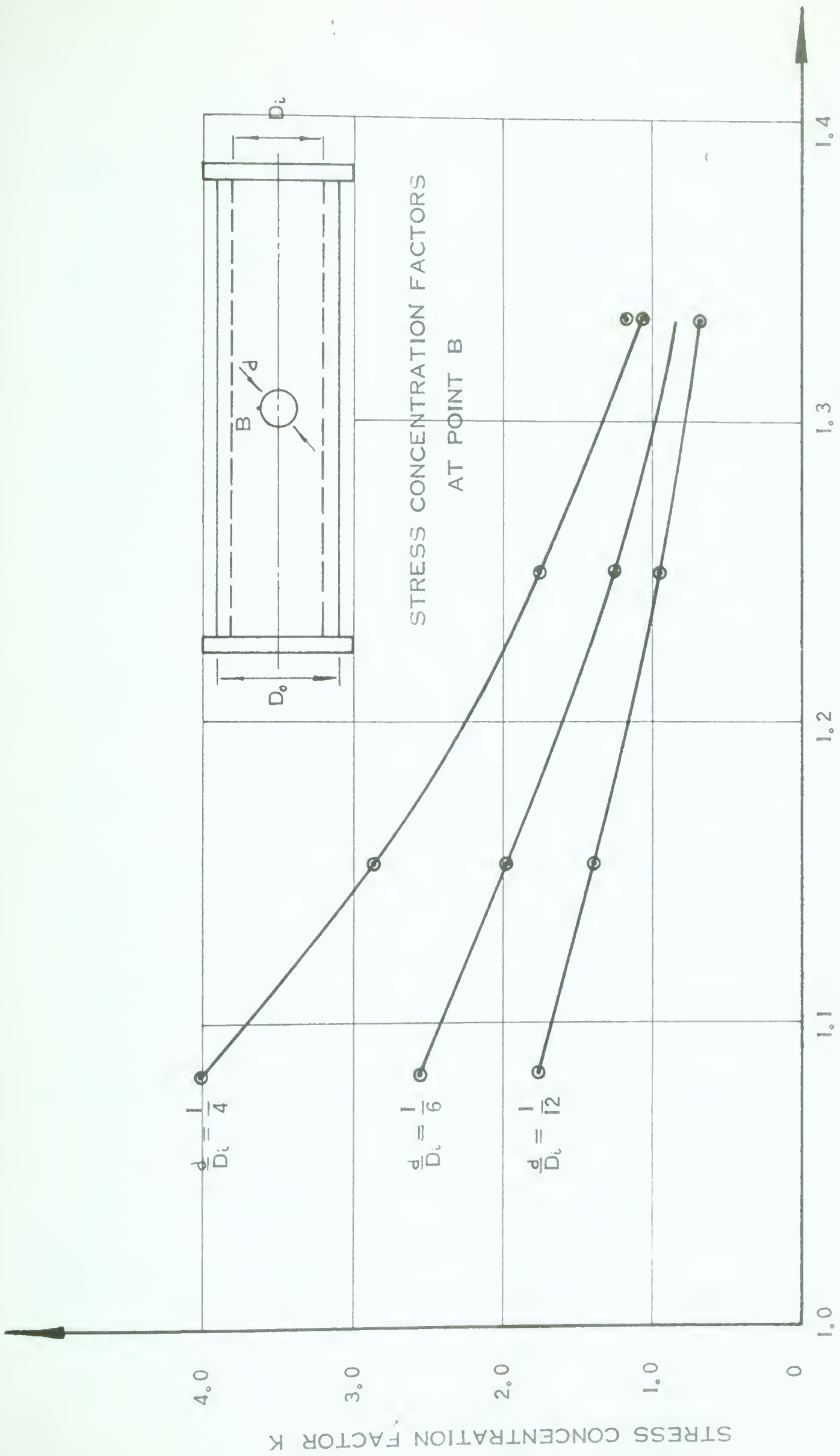


FIGURE 113.

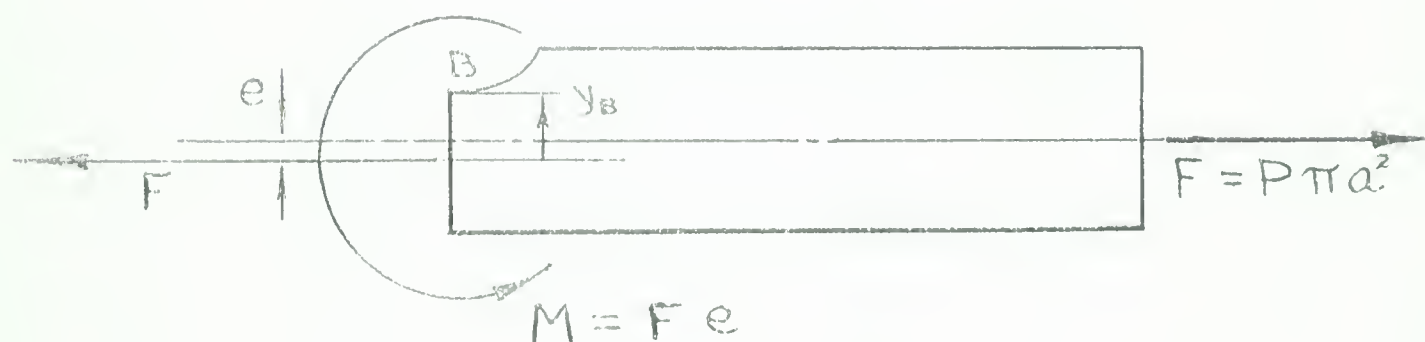
The stress concentration factor curves at point B shown in Fig. 113 are in general much different from what would be expected using flat plate theory. According to flat plate theory the stress tangential to the hole would be one half the hoop stress, or, the stress concentration factor as previously defined would be 0.5. Fig. 113 indicates that this value is valid if the diameter of the hole is very small compared to the diameter of the cylinder. The stress concentration factor approached 0.5 for a small hole in the thick cylinders, but for the thin cylinders, where flat plate theory was expected to have close agreement the stresses were much higher than those found using flat plate theory.

The reasons for this deviation cannot be fully explained by the results of the tests conducted in this investigation, but some suppositions can be forwarded. The dimensions of the cylinders may have had an effect on the stress at this point, in that the hole may not have been far enough from the ends of the cylinder to eliminate end effects. If further investigations are continued, it would be advisable to check this.

The hole in the side of the cylinder introduces bending stresses in the longitudinal direction at point B.

Consider the statical equilibrium of one half of the cylinder, taking a section through the centre of the hole. A force due to the internal pressure $F = P\pi a^2$ acts on the closed end of the cylinder and there is a stress in the longitudinal direction opposing this force.

To find the distribution of this stress, the section through the hole may be considered to have a force and a moment acting on it as shown below. The force acts through the neutral axis of the section.



The stress in the longitudinal direction at point B is given by:

$$\sigma_z = \frac{F}{A} + \frac{F e y_B}{I} \quad \dots\dots\dots 8$$

where A and I are the cross-sectional area and area moment of inertia for the cross-section at the centre of the hole.

Figure 114 shows the magnitude of the longitudinal stress at point B as calculated using Eqn. 8 compared, as previously, to the hoop stress in the cylinder without a hole.

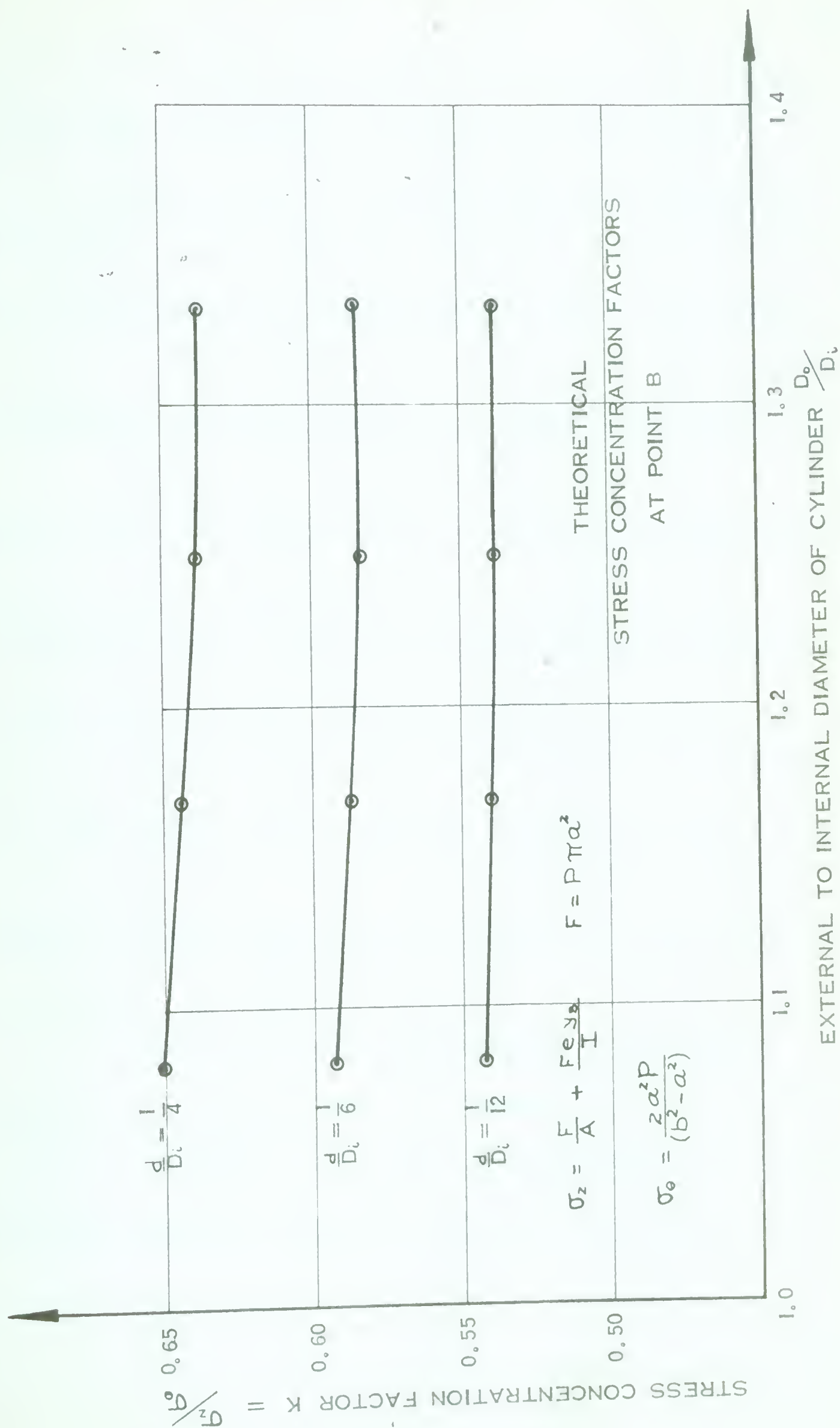


FIGURE 114.

This diagram has the same general shape as Fig. 113, although the magnitude of the stress concentration is much smaller.

This grossly oversimplified calculation indicates that bending does contribute toward the high stress at point B, and a more detailed theoretical analysis should consider this condition.

It also appears that the curvature has a greater effect on the stress around the hole than was assumed previously.

Whatever the reason for the increased stress at point B, the experimental results are consistent and have shown a definite trend. From Fig. 113 we see that the stress concentration factor at point B increases with increasing size of hole and decreasing wall thickness. Further, the rate of increase is rapid regarding both size of hole and wall thickness. For a thin cylinder with a large hole, the stress at point B becomes greater than at point A, and, if the curves can be extended, it appears that point B is critical for a hole which is not too large in an extremely thin shell.

Most of the previous investigations of the stress around holes in cylinders have not considered the stress at point B, however, Houghton, in his work using photoelasticity, analyzed the stress tangential to the hole at this point and found it to be

compressive, which agreed with the theoretical predictions of Lurie². This, of course, is in direct disagreement with the findings herein and with the flat plate theory. No reason for this discrepancy is evident from the results presented.

The stress concentration factors reported in this investigation were obtained using strain gauges, and the pressure-strain relationships for the specimens were very nearly linear. Consequently, the results should be interpreted as elastic stress concentration factors. There is some re-distribution of stress due to the yielding of the material, if the stress is taken into the plastic region. A plastic stress concentration factor may be more appropriate for some applications, but that is beyond the scope of the present work.

CHAPTER 8

CONCLUSIONS

The stress concentration factors at the edge of unreinforced holes in a cylindrical pressure vessel were found to vary between 0.6 and 4.0 for the cylinder dimensions tested as shown in Figs. 112 and 113.

From the results of this investigation it may be concluded that flat plate theory is not a good basis for analysis of the stress around holes in cylinders. This experimental analysis has shown that the stress tangential to the hole at point A agrees with that predicted by flat plate theory, but the stress tangential to the edge of the hole at point B is much greater than that predicted by flat plate theory and is not always smaller than the stress at point A. For large holes in thin shells it has a greater amplitude than the stress at point A.

The disturbed area extends further from the hole in the hoop direction than in the axial direction, the stress decreasing to the magnitude of the stress in the undisturbed region within four hole diameters from the edge of the hole in the former case, and one and one half hole diameters from the

hole in the latter case. The disturbed area, although larger than assumed by some authors is still of a relatively local character.

CHAPTER 9

REFERENCES

1. S. P. Timoshenko and J. N. Goodier, "Theory of Elasticity", McGraw-Hill, 1951, pp. 78-81.
2. A. I. Lurie, "Statics of Thin Walled Elastic Shells", Ogiz, Moscow, 1947.
3. D. S. Houghton, "Stress Concentrations Around Cut-outs in a Cylinder", Journal of the Royal Aeronautical Society, Vol. 65, 1961, pp. 201-204.
4. J. H. Faupel and D. B. Harris, "Stress Concentration in Heavy-Walled Cylindrical Pressure Vessels", Industrial and Engineering Chemistry, Vol. 49-#3, 1957, pp. 1979-1986.
5. M. A. Loshkarev, "An Investigation of the Stress Condition of a Thick-walled Cylinder with a Lightening Hole", (In Russian), Vopr. Prochnosti v Khim Mashinostr, Moskva, Mashgiz, 1958, pp. 44-53; Ref. Zh. Mekh. No. 7, 1959, Rev. 7924.
6. Applied Mechanics Reviews, Vol. 15, No. 1, 1962, p. 14.
7. C. E. Taylor and J. W. Schweiker, "A Three-dimensional Photoelastic Investigation of the Stresses Near a Reinforced Opening in a Reactor Pressure Vessel", Proceedings of the Society for Experimental Stress Analysis, Vol. 17, No. 1, 1959, pp. 25-36.
8. G. N. Savin, "The Stress Distribution in a Thin Shell With an Arbitrary Hole", Problems of Continuum Mechanics, Society for Industrial and Applied Mathematics, 1961, pp. 382-405.
9. D. V. Vainberg and A. L. Siniavskii, "Approximate Analysis of Shells with Holes by the Methods of Potential Theory", Problems of Continuum Mechanics, Society for

Industrial and Applied Mathematics, 1961, pp. 570-581.

10. S. P. Timoshenko and J. N. Goodier, "Theory of Elasticity", McGraw-Hill, 1951, pp. 59 and 60.

APPENDIX A

Typical Calculation

As an example of the procedure used to analyse the strains read from the strain gauges, the calculations for the cylinder having a $1/8$ inch wall thickness and a $1/2$ inch diameter hole will be presented here.

Three tests were run on the cylinder and the results of these tests were averaged. The average results were then used to plot the diagrams of strain vs. pressure shown in Figs. 28 and 29. From the "best-fit" straight line for each gauge in these figures, the strain was read for a pressure of 600 psi. These strains are presented in the table below.

GAUGE NO.	1	2	3	4	5	6	7	8	9	10	11	12
STRAIN micro inches per inch	380	195	174	-20	21	54	410	239	118	12	130	179

STRAINS AT 600 psi.

$1/8$ Inch Wall Thickness $1/2$ Inch Hole

The positioning of each of these gauges relative to the

hole is shown in Fig. 27.

Using the above strains and the dimensions shown in Fig 27 the diagrams of strain vs. distance from the edge of the hole were plotted approaching points A, and B. These diagrams are shown in Figs. 65 and 89.

The strains in the hoop and axial directions were read from these curves at regular distances from the edge of the hole, and Eqns. 3 were used to calculate the stresses at these points. A value of 29.8×10^6 psi. was used for the modulus of elasticity and, as previously described, Poisson's ratio was found to be 0.27. Eqns. 3 reduced to:

$$\begin{aligned}\sigma_{\theta} &= \frac{29.8}{[1-(0.27)^2]} (e_{\theta} + 0.27 e_z) = 32.1 (e_{\theta} + 0.27 e_z) \quad \dots\dots\dots 9 \\ \sigma_z &= \frac{29.8}{[1-(0.27)^2]} (e_z + 0.27 e_{\theta}) = 32.1 (e_z + 0.27 e_{\theta})\end{aligned}$$

where e_z and e_{θ} are in micro inches per inch.

The calculation of σ_{θ} and σ_z approaching points A and B using Eqns. 9 were set up in tabular form and are given in Tables 2 and 3 respectively.

The stresses found from these tabular calculations were used to plot the diagrams of stress vs. distance from the edge of the hole shown in Figs. 77 and 101.

The stresses found at the edge of the hole were then

used to calculate the stress concentration factors of 2.69 and 2.56 for points A and B respectively. These values were then plotted as points on the stress concentration factor curves, Figs. 112 and 113.

TABLE 2
CALCULATION OF STRESS AT POINT "A"

FOR $P = 600$ psi.

1.8 Inch Wall Thickness 1.2 Inch Hole

	①	②	③	④	⑤	⑥	Hoop Stress	Axial Stress
Distance From Edge of Hole Inches	Hoop Strain μ in in	Axial Strain μ in in	① x 0.27	② x 0.27	① + ④	② + ③	⑤ x 32.1	⑥ x 32.1
0	600	-160	162	-43	557	2	17,890	60
.04	500	-64	137	-17	492	73	15,790	2,340
.10	400	-22	108	-6	394	85	12,630	2,760
.20	285	-9	77	-2	284	68	9,110	2,180
.40	125	15	51	4	134	66	6,220	2,120
.60	175	40	47	11	185	87	5,940	2,790
.80	180	53	49	14	194	102	6,220	3,270
1.00	170	53	51	14	204	104	6,550	3,340
1.20	160	50	52	14	207	105	6,640	3,370
1.40	150	50	52	14	207	105	6,640	3,370

TABLE 3

CALCULATION OF STRESS AT POINT "B"

FOR $P = 600$ psi.

1/8 Inch Wall Thickness 1.2 Inch Hole

	①	②	③	④	⑤	⑥	Hoop Stress	Axial Stress
Distance From Edge of Hole Inches	Hoop Strain μ in./in	Axial Strain μ in./in	① x 0.27	② x 0.27	① + ④	② + ③	⑤ x 32.1	⑥ x 32.1
0	-150	570	-40	154	4	530	130	17,000
0.04	-55	471	-15	127	72	456	2,310	14,630
0.10	10	380	3	102	112	377	3,600	12,100
0.20	62	299	17	81	143	316	4,590	10,130
0.30	95	244	26	66	161	270	5,170	8,670
0.40	120	199	32	54	174	231	5,580	7,410
0.60	152	131	41	35	187	172	6,000	5,520
0.80	173	96	47	26	199	143	6,390	4,590
1.00	188	74	51	20	208	125	6,680	4,010
1.20	193	60	52	16	209	112	6,700	3,590
2.00	193	53	52	14	207	105	6,650	3,370

B29806